Large Scale Testing of Drystone Retaining Structures

Mundell, Chris

Award date:
2009

Awarding institution:
University of Bath

Large Scale Testing of Drystone Retaining Structures

submitted by

Chris Mundell

for the degree of Doctor of Philosophy

of the

University of Bath

Department of Architecture and Civil Engineering

August 2009

Mending Wall

Something there is that doesn't love a wall,
That sends the frozen-ground-swell under it,
And spills the upper boulders in the sun;
And makes gaps even two can pass abreast.
The work of hunters is another thing:
I have come after them and made repair
Where they have left not one stone on stone,
But they would have the rabbit out of hiding,
To please the yelping dogs. The gaps I mean,
No one has seen them made or heard them made,
But at spring mending-time we find them there.
I let my neighbor know beyond the hill;
And on a day we meet to walk the line
And set the wall between us once again.
We keep the wall between us as we go.
To each the boulders that have fallen to each.
And some are loaves and some so nearly balls
We have to use a spell to make them balance:
"Stay where you are until our backs are turned!"
We wear our fingers rough with handling them.
Oh, just another kind of outdoor game,
One on a side. It comes to little more:
He is all pine and I am apple-orchard.
My apple trees will never get across
And eat the cones under his pines, I tell him.
He only says, "Good fences make good neighbors."
Spring is the mischief in me, and I wonder
If I could put a notion in his head:
"Why do they make good neighbors? Isn't it
Where there are cows? But here there are no cows.
Before I built a wall I'd ask to know
What I was walling in or walling out,
And to whom I was like to give offence.
Something there is that doesn't love a wall,
That wants it down!" I could say "Elves" to him,
But it's not elves exactly, and I'd rather
He said it for himself. I see him there,
Bringing a stone grasped firmly by the top
In each hand, like an old-stone savage armed.
He moves in darkness as it seems to me,
Not of woods only and the shade of trees.
He will not go behind his father's saying,
And he likes having thought of it so well
He says again, "Good fences make good neighbors."

Robert Frost, 1915

Acknowledgements

The work in this thesis was carried out in the Department of Architecture and Civil Engineering at the University of Bath between July 2006 and July 2009.

The author would like to thank the Engineering and Physical Sciences Research Council (EPSRC) for the funding to conduct this research. Also thanks go to the associated partners of the project, those being Bradford Metropolitan District Council, Cornwall County Council, Gloucestershire County Council, Surrey County Council, Wiltshire County Council and Network Rail Ltd.

On a more personal note, the author would like to thank all those who have been instrumental in helping to make it to the finish line. Pete Walker, Andrew Heath and Paul McCombie have all been outstanding supervisors, with each adding their own unique (and usually opposing) perspective to any given problem. Throughout the course of this thesis, the friendship and patience exhibited by these three individuals has made the whole experience infinitely more interesting and enjoyable. The author would like to thank Paul McCombie in particular, who has provided continual support throughout the project, whether or not the particular crisis in hand was related to drystone walls.

Mention should be made to all of the laboratory staff at the University of Bath, who have also spent countless hours on various aspects of the project. Sophie - the project technician - has been involved in every aspect of the project, including the less glamorous tasks such as digging fence post-holes, ramming earthen walls and digging through tons of gravel looking for (gravel coloured) ball bearings. Soph has become a great friend, and as with so many of the author's colleagues, will remain so after the completion of this thesis. The same must be said of Eddie and Andy, with whom the author has shared an office for the past two years. Thanks to Ed, Andy and the rest of the the postgraduates, a day spent in the office could never be considered dull.

The author would also like to thank his family - Mum, Dad and Mark - not only for the support during the last three years, but for the last 26 years. Throughout school, university and this PhD, the author's family have always been there to give whatever needed to be given, whether it be asked for or not.

Last but by no means least, thanks go to Anna, whose love and belief has made it all worthwhile.

Abstract

Drystone walls have been used extensively around the world as earth retaining structures wherever suitable stone is found. Commonly about 0.6m thick (irrespective of height), there are about 9000km of drystone retaining walls on the UK road network alone, mostly built in the 19th and early 20th centuries, with an estimated replacement value in excess of £1 billion[1].

Drystone wall design is traditionally empirical, based on local knowledge of what has worked in the past. Methods vary from region to region, driven by both custom and the nature of the materials available. Design is not necessarily optimised, and includes unknown margins of safety. There is a recognised need for guidance on the assessment and maintenance of dry stone retaining walls, as no such documents currently exist.

This thesis documents the construction of a series of full-scale tests designed to provide sufficient information to validate current theoretical and numerical analysis techniques. The development of a unique test rig is detailed, in addition to the testing regime and results from a programme of five 2.5m high drystone retaining walls. The walls were subjected to localised surcharging and foundation movements, recreating the conditions that many in-situ walls are subject to. Movements such as toppling, bulging and sliding were observed, and recorded using a broad range of instrumentation. This has provided high quality, quantitative data relating to the factors which influence these mechanisms, and their affect on wall stability. Also documented are the associated laboratory tests which have been conducted to determine the mechanical properties of backfill and the walls themselves, as well as the manner in which they interact together.

To assist in the analysis of these full-scale tests, a limit equilibrium program has been developed. This package allows the rapid generation of a wall of any size and constructed with any materials. The limit equilibrium program has then been used in conjunction with the data from the full-scale and laboratory tests to analyse observed drystone wall behaviour. These include the phenomena of toppling, bulging, bursting, sliding and individual block rotation. In each case, the underlying causes of such movements have been determined, and the critical parameters identified.

Contents

List of Figures

List of Tables

List of Symbols

B	thickness of wall block, width of foundation
B_c	distance to centre of mass
e	eccentricity of thrust line
F_g	internal safety coefficient for sliding
h	height of wall or block
H	horizontal forces within the system
K_a	coefficient of active earth pressure
n	batter of external face
n_1	batter of internal face
N_c	bearing capacity factor
N_q	bearing capacity factor
N_γ	bearing capacity factor
p	weight of surcharge
P_a	resultant force from backfill
P_V	vertical component of P_a
P_H	horizontal component of P_a
q_{ult}	ultimate bearing capacity
R	resultant force
t	thickness at top of wall
V	vertical forces within the system
W	self weight of wall block
α	angle of repose of the earth from vertical ($\alpha = 90^o - \phi$)
γ_{stone}	weight of masonry
γ_{soil}	weight of earth
δ	angle of wall friction
η	angle of tilt for each course of the wall
θ	angle of failure plane
Θ	rotation of blocks from initial postition to failure
σ_v	vertical stress
ϕ_m	internal angle of friction

Chapter 1

Introduction

1.1 Introduction

This chapter introduces the subject of drystone walling and both its historical and current use by the construction industry. The benefits and potential concerns of drystone walling as a modern building material are discussed, along with the problems faced by many of the existing structures in the UK. This leads on to the subject of this thesis, and the issues that the project will address.

1.2 Drystone construction

1.2.1 Origins of drystone construction within the UK

Drystone walling is an ancient construction form where walls are built by stacking stones without mortar or other binders. It has been used throughout history to build buildings and enclosures, freestanding structures and retaining walls. Examples of drystone walls have been found dating back to the Iron Age and even some to the Stone Age (fig. 1-1), although most of the walls found around the UK today date back to the 14th century and onwards [1].

Between the 15th and 18th centuries, a large number of drystone walls were constructed by villagers and farmers as society moved away from feudalism and individuals sought to enclose their own lands and properties (fig. 1-2). Further building was encouraged by the Enclosure Acts of the late 18th century, which were private Acts of Parliament and could be engineered by the wealthy and more prosperous landowners[2]. The Acts allowed these individuals to commission long stretches of wall and partition the land, denying its use to the local villagers.

Previously, retaining walls had only been constructed as part of fortifications. However with the industrialisation of the country, it was becoming affordable to travel between towns and cities more rapidly. To reduce journey times straight roads with minimal gradients were constructed, requiring retaining walls to support the necessary cuttings and embankments[3]. Many of these retaining walls and

Figure 1-1: Mousa broch: Iron Age structure in the Shetlands, UK[1]

Figure 1-2: 17th century drystone wall at Muchalls Castle, Scotland, UK[2]

bridges were of drystone construction, and remain standing today.

With the dawn of the railway in the 19th century, many of the existing transport routes became redundant, and so fell into disrepair. However, new routes were still constructed in response to increasing populations and also to act as feeder roads to the rail network[1]. The construction of new roads and railways through the 19th and early 20th centuries, combined with the increasing network of canals, required many kilometres of retaining walls, of which a large portion were drystone

[1]Photo courtesy of Wikipedia
[2]Photo courtesy of Wikipedia

structures[4]. At the beginning of the 20th century, fewer new drystone retaining walls were being constructed, as brickwork and reinforced concrete became more frequently used. Despite this, it is estimated that 50% of the UK's retaining walls are drystone in nature[5, 6], and remain in use today.

1.2.2 Typical construction techniques

A large issue with drystone walls is that each is unique, with the bespoke nature of wall construction ensuring that no two structures are ever identical. However, there are many similarities which are carried through most of the construction styles, allowing for assumptions and generalisations to be made.

The regional differences are diverse; the style of a wall greatly depends on local traditions and on the material itself as shown by figure 1-3[2]. For example, where slate is the most readily available material, the construction method accounts for its low inter-stone friction, placing the stones in a herringbone or vertical fashion (figs. 1-3(a) and 1-3(b)). Where the stone is more regular and easy to work with, a coursed wall is often produced (fig. 1-3(d)), although the courses are not always horizontal and some walls are traditionally built with diagonal courses. In some areas the locally available stone is in the form of rocks and spherical stones. In these cases it is not practical to shape each stone, and so instead the wall is constructed of round stones, and coursing is not applicable (fig. 1-3(c)).

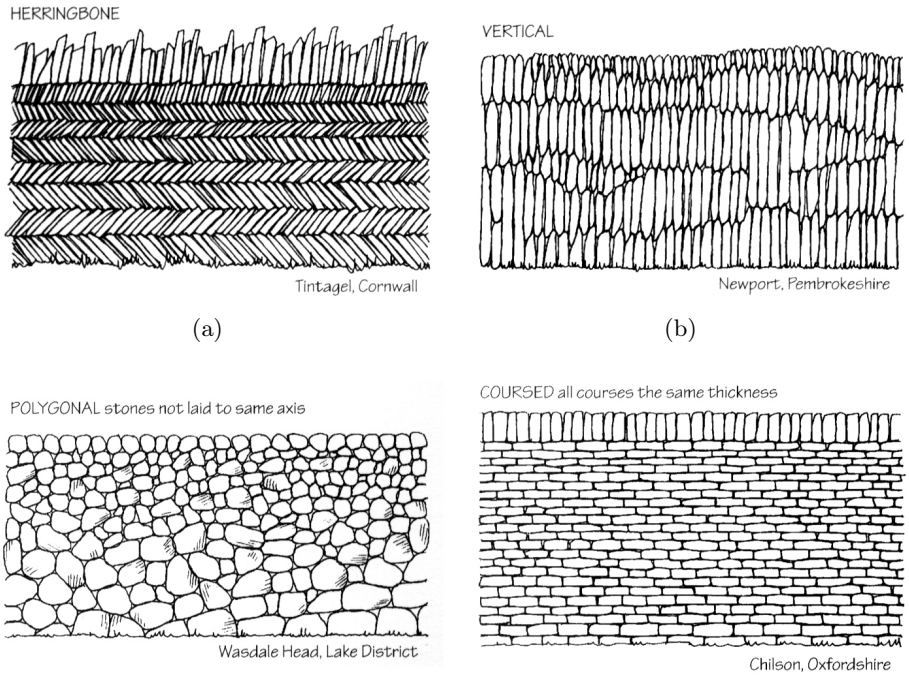

Figure 1-3: Regional styles: a)herringbone; b)vertical; c)polygonal; d)coursed

For free standing walls where lateral loads are not usually severe, aesthetics

may form a large part of how a wall is constructed, depending on the nature and location of the wall. However, for the purpose of retaining structures, it is necessary to construct a wall which will withstand large overturning forces, making the configuration of the wall much more critical.

Most drystone retaining walls are built using horizontal layers in the style of figure 1-3(d). Figure 1-4 shows a typical section through a double-faced retaining wall. The wall itself is constructed of coursed stone, which may be shaped to a high standard for ease of construction. There are both an internal and external face, often called the 'double', with an infill of courser and smaller material between these faces. At regular intervals, 'through stones' or 'tie stones' are placed, consisting of long blocks which span from the internal to the external face and bond them together. These are normally at 600mm vertical intervals[2], although this may depend on both the size of the wall and the mason. At the top of the wall, coping stones are laid, again spanning the entire width of the wall. This performs the same job as the through stones and also adds extra mass to the wall, improving stability. Figure 1-5 shows the internal make-up of these types of walls.

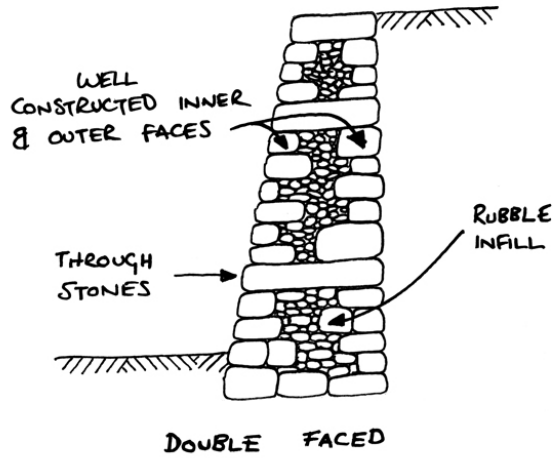

Figure 1-4: Typical cross section of a retaining wall

(a) (b) (c)

Figure 1-5: Internal wall configuration: a)face and fill; b)tie stones; c)coping stones

A slightly simpler construction technique uses only an external face, with the infill blending into the backfill. Through stones may still be used, anchoring the wall into the retained fill. Figure 1-6 shows a typical section through a wall of this nature.

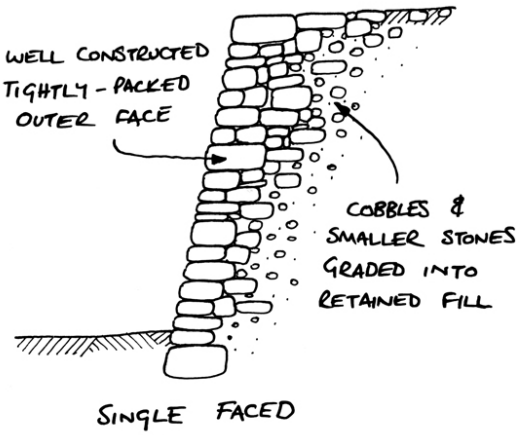

Figure 1-6: Single faced retaining wall

When placed, each block within the wall should ideally be in contact with several other stones, and pressure upon any part of a freshly placed stone should not cause any rocking or lifting at the opposite corner. In practice it is usually necessary to wedge in small shards of stone known as 'pins' to prevent rocking. The unavoidable presence of these pins presents a weakness for all drystone structures, especially as weathering of these smaller elements will occur more quickly than with the larger stones. Pins are often used to allow a more even appearance to the face by tilting stones so that their outer surface is in the plane of the face, or to improve drainage. Thus the face of a structure can often give the misleading impression of a very tight well-ordered construction, whilst behind the face there are substantial voids held open by a large number of small pins.

The build up of water pressures behind a retaining wall can often be catastrophic. However a significant advantage of drystone walls is that they are porous by nature, allowing water to flow through unimpeded. Should the walls require additional drainage, weep holes may be included, allowing the egress of excess water. These are only usually needed for walls which have been pointed or mortared, and can become fouled over time and limit the flow of water.

It is often the case that stable cuttings have been faced with a drystone wall. In these instances the wall may be contributing little to the stability of the cutting, and as such may behave more in the manner of a freestanding wall. It may be difficult to determine whether a wall is simply a facing or a functioning retaining structure, however this is a critical piece of information should movements be detected and

remedial works required.

1.2.3 Sustainability and environmental impacts

In today's climate, where sustainability and carbon footprints are driving factors in the construction industry, drystone walling could be a particularly attractive method for building modern walls and retaining structures. As previously discussed, a drystone wall can utilise almost any type of stone, and be built in any location. All that is required is a mason and a supply of stone to hand. The use of local stone can cut down the cost of material transportation against other forms of construction, and requires no plant or extensive formwork. The potential to reuse existing material on a site can also reduce the cost of construction, both financially and environmentally.

Where new material must be quarried, dry stone walling again is advantageous over most other forms of construction. The walling material necessary does not have to be regular or shaped, and so may be used as soon as it has been excavated from the ground. Assuming the material is broken up into sufficiently small pieces during the excavation process, no further processing is required, saving both time and money.

In aesthetic terms, drystone walls are a part of the heritage of the UK, and are generally more visually pleasing than more advanced materials like concrete. In addition, the voids within drystone walls may provide additional natural habitats for local wildlife, whereas the construction process of other structures is likely to damage the surroundings and destroy habitats.

1.3 Modern uses and structural issues surrounding drystone walls

1.3.1 Modern uses

Although there are numerous drystone walls around the UK, few new builds are commissioned, with new drystone retaining structures being fewer still. However, it is estimated that there are over 9000km of existing drystone retaining walls in the UK, mainly built in the 19th and 20th centuries. These are walls which vary in height from less than 1.5m to over 15m, and are used to support the road, rail and canal networks across the country[7].

1.3.2 Factors affecting drystone behaviour

There are several factors which may alter the stability of a drystone retaining wall. Many of these are common to all retaining structures, however some are unique to drystone walls. These include:

- Geometry and build quality of the wall
- Aging and weathering of the wall
- Changes to the retained fill
- Changing load conditions
- Build up of water pressures
- Damage to the wall (this may include inappropriate repairs)

Geometry and build quality

The geometry and build quality are all determined before the wall is fully operational, however they are critical factors. The geometry should be determined such that the wall has a sufficiently wide base and a mass large enough to resist both sliding and overturning. Several guidance documents advocate a base width of half the overall height, although many walls in the UK are commonly 600mm wide irrespective of height[8].

The quality of the wall can affect both its longevity and its ability to deform and bulge. Several factors are of combined importance when considering a wall's quality. This includes the density of the wall, and the care which has been taken to create a tightly-knit structure throughout. The mason is predominantly responsible for this, ensuring that the individual stones are laid such that they are locked into place in the most efficient way. Running joints should also be avoided, and may easily be identified when examining the external face of a wall. These occur when the joint between two adjacent stones is in line with a similar joint in the courses above and below. Running joints of two to three courses are common and not usually problematic, however joints which span several courses create a significant weakness in the wall (fig. 1-7). These joints limit the capacity for longitudinal restraint in-plane, where the adjacent sections of wall may otherwise provide some stability to an ailing portion of wall.

Aging and weathering

Depending on the material used to construct a wall, weathering and aging may have a varying impact. However, even the most durable of stones will eventually degrade due to continual exposure to the elements, whether it takes decades or centuries.

A highly visible form of weathering is due to the constant erosion of the face stones by the elements. This will cause a rounding of the blocks, which may in turn reduce the area of contact or the number of contact points of the individual stones. Alternatively, freeze-thaw action may crack the stones, and create weaknesses that lead to destabilisation of the wall.

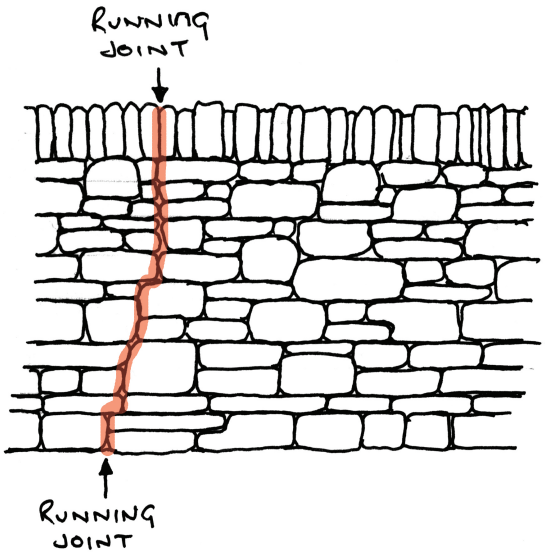

Figure 1-7: Running joint within the external face

Rainfall has the potential to wash material both out and into the wall joints. The small pins used to hold individual blocks in place may become loose, and eventually washed out of the wall. This allows the blocks to rotate more freely, and may be detrimental to stability. Conversely, if the retained material is granular, and water may flow from the backfill and through the wall, material may be washed into the wall. This becomes problematic if the joints become totally filled with soil. In this instance, the friction between the bedding planes becomes dependent on the friction angle of the soil, which may be substantially lower. A similar problem may occur with the growth of moss and other vegetation over a wall and through the joints.

The growth of trees, plants and other vegetation may be both advantageous and detrimental to a wall's stability, and so should be handled with care. Even small trees may have substantial root networks, which may easily dislodge or crack wall stones as they grow. On the other hand, vegetation may remove a large quantity of the moisture from the retained backfill, and prevent failures that may occur due to increases in water pressure. The presence of vegetation may also cause problems for even the most basic of inspections, should the wall be covered with plant growth. In these cases the walls must first be cleared of the excess vegetation before even a cursory inspection may be made.

Changes to the surrounding area

It is often necessary to make changes to the retained fill behind a wall, either due to new development behind the structure or through the depositing of excess material from work done elsewhere. This will cause an immediate increase of the loads upon the retaining structure which may also increase further should the material become

saturated with water. This may either cause a collapse of the wall itself, or it may instigate a rotational slip failure in the backfill, with the wall failing along with the retained material.

Excavations in front of the toe of the wall may also cause similar failures. The internal friction angle of most drystone walls is generally fairly high, and not usually the cause of failure. However, should the material near the toe be removed, it is possible that the whole structure could translate and collapse in response to the removal of the passive soil pressure which was previously helping to oppose the loads from the retained backfill. Alternatively, any excavations near the toe of the wall could initiate a rotational slip failure, and should be considered carefully.

Changes to external load conditions

As previously discussed, the majority of the retaining walls in use today were constructed in the 19th and early 20th centuries. As a consequence, the loads that they were designed to carry were much less than the loads applied by modern traffic and structures. In the 19th century, a maximum load of two tons was allowed along roads, which has now increased to an 11.5 ton allowance for axle loads on lorries and 25.5 tons for train axles on railways[1]. This is also combined with a steady increase in the volume of traffic causing large cyclic loading.

Water pressures

The presence of water behind a retaining wall can significantly increase its likelihood of collapse. With drystone walls, this is generally avoided, as the walls themselves are relatively free-draining. This means that whilst the soil may become saturated, there is no build-up of pore water pressures. However, saturation is still an issue, as it may eliminate any soil suction if the backfill material is cohesive. This in turn will increase the active pressures applied by the backfill, and potentially induce a failure.

Although most drystone walls are free draining, it is possible in some cases for pore water pressures to build up. This is most likely when the joints have been pointed in an effort to stabilise the wall, although the effect of vegetation or soil filling the voids may have a similar effect. Where weep holes have been inserted to drain the walls, these must be checked for clogging and be free flowing. It has previously been mentioned that soil infilling of joints may decrease a wall's safety against sliding failure between the courses. This issue could be made worse by heavy rain and excess moisture, as the shear resistance of the soil reduces as it becomes saturated.

Damage

Physical damage to drystone walls is generally only an issue when a road or transport route runs next to the base of the wall. In these cases vehicle impact may cause a small localised failure, however this could potentially undermine the foundations of a much larger section, which subsequently collapses.

The repair techniques used by some masons may also be detrimental to the overall wall quality. This may be due to a repaired section of wall being incorrectly blended with the existing wall, or a repair technique which reduces the stability.

1.3.3 Beneficial structural attributes

As discussed in the previous section, drystone walls have the significant advantage over other types of retaining structures in that they are free draining. This is particularly useful as climate change causes more extreme weather conditions, and higher amounts of rainfall in short periods of time.

Equally useful is the ability for drystone walls to bulge in response to applied loads. This is often perceived as a negative asset, and that bulging is merely a precursor to failure. However, bulging may in some cases merely be a redistribution of the wall's mass to better withstand the applied loads, allowing higher loads to be withstood. Where a failure mechanism is developing, the displacements that are seen prior to failure are often relatively large. This gives an obvious warning of the wall's distress, and a potential chance to rectify the situation. At the very least it may give an indication that the wall is on the verge of collapse, and may avert injury and damage to people or property. Conversely, where walls have been pointed or grouted (often as an attempt to stabilise a wall deemed unsafe), they have little opportunity to move, and the failures that occur are often rapid and with little warning.

1.3.4 Analysis issues

Assessment of existing drystone retaining wall is a difficult task, made more difficult by a lack of guidance or standards. The main difficulty arises in having few details regarding most of the country's stock of retaining walls. Whilst the external face of the wall may be assessed in most cases with little difficulty, the profile of the wall cannot easily be determined. The age, density, thickness, stone depth or the existence of through stones or an internal face cannot be verified without intrusive testing. The ground conditions behind the wall may sometimes be examined through borehole testing of the retained fill, however the plant required to do this may again be disruptive to the stability of the wall.

Where analyses of existing walls have been conducted, it is possible for the calculations to suggest that the structure is very close to collapse, or in some cases should not even be able to stand up[9]. The analysis methods adopted in most cases

are perfectly valid, however due to onerous or unrealistic parameters or factors of safety, the results may be misleading. This highlights the need for further research to allow the correct assessment techniques to be developed, ensuring that realistic assumptions regarding their stability may be made.

Currently, the replacement costs for all of the UK's drystone retaining walls is in excess of £10 billion[10]. This is a significant drain on local councils where there are a large number of drystone walls and no conclusive way of assessing their stability. As a consequence, many walls which are bulged but otherwise stable are deemed unsafe, and replaced with more modern equivalents. With more accurate assessment procedures, the walls in danger could be identified and dealt with, and fewer walls replaced because they are perceived to be on the verge of collapse.

1.4 Further reading on drystone walling

It should be noted that drystone walling is a complicated subject, reliant upon the skill of the mason to ensure that the build quality is adequate to the needs of the structure. This chapter gives a basic introduction to the subject, and highlights the important features that are critical to understanding the mechanics of the subject. There are empirically evolved methods for constructing walls in almost any circumstances; these are covered in much more detail in the documents highlighted in section 2.5.

1.5 Objectives of PhD study

As discussed both in this chapter and chapter 2, the available information relating specifically to drystone retaining walls is limited. In particular there is almost no data pertaining to physical tests on full-scale walls, which is required to identify the unique mechanisms which occur during deformation and failure of heavily loaded walls. This data is also required to verify any assumptions, analysis techniques or numerical models that are developed for industry use. The following objectives have been identified to address these issues within this thesis:

- Design and build a bespoke test facility with capable of housing full scale drystone walls and a retained fill. The laboratory should be designed to allow a variety of tests to be performed, allowing flexibility in the testing regime. Future use of the test laboratory beyond the scope of this project should also be considered.

- Conduct four full-scale tests, recreating commonly observed phenomena relating to drystone retaining walls (e.g., bulging, sliding, bursting etc.).

- Carry out laboratory testing in parallel to the full-scale testing. This should focus on the material properties relevant to the full-scale tests (e.g., material

densities, friction angles etc.).

- Develop an analysis package to allow stability assessments of drystone retaining walls. This will likely be based on the code originally written by McCombie as part of the work reported by Walker et. al.[11]. This program is intended to be used by design engineers to carry out rapid stability analyses of in-situ walls, and so should be flexible and easy to use. This program is to be updated and validated as the full-scale tests progress, incorporating any observed phenomena where possible.

- Combine each of the above objectives to further understanding of the behaviour of drystone walls. This should draw upon data and observations gathered throughout the various tests, as well as using the validated analysis package to confirm these findings. This should include investigating the mechanisms behind the phenomena particular to drystone walls (e.g., bulging and bursting), as well as the important criteria that should be considered when investigating the stability of these structures.

Although not specifically an objective of this thesis, one of the eventual goals of the project and those that follow is the creation of guidelines or codes of practice for the assessment of drystone retaining structures. This would ideally include assessment procedures to identify walls in danger of collapse, and also advice on the most effective remedial procedures for such structures. It would also include best practice procedures for new constructions, and give detailed design guidance. However, before such a document may be produced, further work beyond the scope of this project must be conducted, particularly focussing on repair techniques for deformed or failing walls.

1.6 Layout of thesis

This thesis comprises nine chapters (not including appendices). The introduction chapter is followed by a literary review, which describes the relevant work which has been conducted to date relating to drystone retaining walls. Chapter 3 contains the laboratory tests which have been carried out on the various materials used during the full-scale tests. Also included are the results from a series of small-scale tests, as well as a study into the voids within full-scale drystone walls. The limit-equilibrium program is described in chapter 4, including its validation using the previous work from chapters 2 and 3. Chapters 5 and 6 respectively concern the design and construction of the full-scale test site, and the proceedings of the tests themselves. An analysis of both the full-scale tests and laboratory work is given in chapter 7, using data from the limit-equilibrium package to support arguments. The implications of this work, as well as the recommendations for future work are discussed in chapter 8, with overall conclusions given in chapter 9.

Chapter 2

Literature Review

2.1 Introduction

Comparatively little research has been conducted on drystone retaining walls. Numerical studies attempting to recreate real drystone behaviour are difficult due to the absence of in-depth physical tests against which the models may be validated. In turn, physical test data are scarce due to the necessity to conduct the tests at full-scale. This is to ensure that all of the mechanisms associated with drystone behaviour are replicated, and consequently these tests are difficult and costly to set up and analyse fully.

This chapter begins by discussing the limited number of full-scale tests which have been conducted to date, and the analytical and numerical work which has been subsequently conducted. There are currently no formal standards related specifically to the design and analysis of drystone walls, but the guidance that has been published to date is presented and summarised.

2.2 Previous full-scale testing

Owing to the complex nature of drystone retaining walls, there is often difficulty in predicting their behaviour with current assessment techniques. For this reason, full-scale testing of these structures is of great importance, as methods like numerical modeling or small-scale testing cannot be assumed to accurately represent drystone behaviour. With sufficient full-scale tests, numerical modeling techniques may be verified against these test data, impoving confidence in their results. At present, there is little full-scale testing data available, due to both the expense and difficulty of testing to the standard required.

2.2.1 Kingstown full-scale tests

In 1834, a series of tests were carried out by Lieut-General Sir John Burgoyne, commissioned by the Board of Public Works in Ireland. These tests, conducted in

Kingstown - now Dun Laoghaire - consisted of four full-size drystone walls which were gradually backfilled until either full retention or failure. The observations of these tests, together with a paper entitled "revetments or retaining walls", were published posthumously by the Corps of Royal Engineers in 1853[12].

Wall geometries

Burgoyne's four walls were all 6.1m in length and height, constructed from squared granite blocks and founded on solid rock. Whilst the walls had identical mean thicknesses, each had a varying wall profile, as shown by figure 2-1. Wall 'A' had parallel sides with a batter of 1 in 5 and a mean thickness of 1.01m ($\frac{1}{6}$ of the height). To prevent this first wall from falling inwards, it was constructed in tandem with the placement of the backfill. Walls 'B' and 'C' had identical cross-sections, but were mirror images of each other. Wall 'B' had a sloping external face - again battered at 1 in 5 - with a vertical internal face, whilst wall 'C' had a counter-sloped internal face and a vertical external face. Thicknesses for both walls ranged from 1.63m at the base to 0.4m at the crest. Wall 'D' was parallel sided similar to wall 'A', although both faces were vertical with no batter, giving a constant profile thickness of 1.01m. Each wall was constructed in a bay 6.1m wide (the length of the walls), adjacent to one another and separated by 760mm thick stone dividing walls.

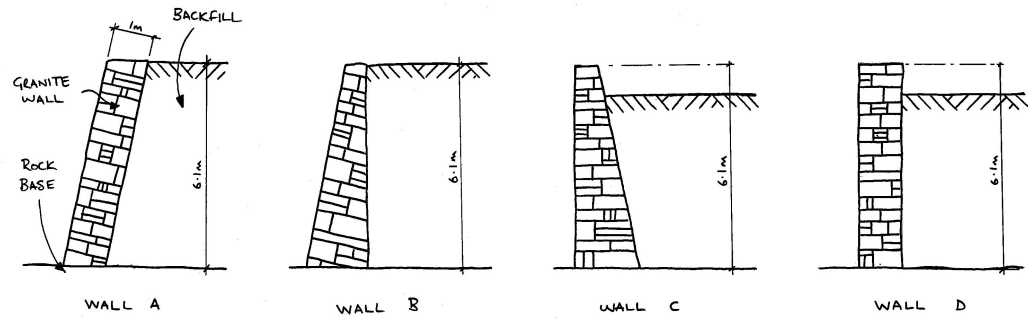

Figure 2-1: Burgoyne's wall geometries

Taken from Burgoyne's figures, a notable difference of walls 'A' and 'B' to walls 'C' and 'D' is the internal gradient of the courses. Although not mentioned within the text of Burgoyne's paper, the diagrams detailing the test walls show a negative gradient on the first two walls, being perpendicular to the external batter. Walls 'C' and 'D' have vertical external faces, and hence are shown to have horizontal bedding planes.

Test procedure

Testing was conducted between the 20th of October and the 7th of December 1834 (inclusive of the wall construction), with the timings of the backfilling detailed in

table 2.1 (Burgoyne's original imperial measurements have been converted to metric). The backfill was introduced in lifts, however as noted by Burgoyne, "...the deficiencies from subsidence...were made good from time to time"[12]. Deformations and cracks were recorded by the overseer present, including measurements and general observations.

Table 2.1: Backfill heights of Burgoyne's test walls

Dates	**A**		**B**		**C**		**D**		**Weather**
	am	pm	am	pm	am	pm	am	pm	
	All readings in metres, (m)								
Oct 20th	...	...	...	...	...	...	...	...	
Nov 7th	...	1.52	...	...	...	...	...	...	Dry
Nov 8th	...	2.13	...	...	...	...	...	...	
Nov 19th	...	3.35	...	...	...	...	...	...	Rain
Nov 20th	...	4.27	...	...	...	...	...	...	
Nov 26th	...	...	0.76	0.86	1.22	1.93	1.22	1.68	Dry
Nov 27th	...	...	0.91	1.44	2.13	2.23	1.83	2.13	
Nov 28th	...	...	1.83	2.44	2.36	2.44	2.13	2.54	
Nov 29th	...	...	2.44	3.35	2.44	2.97	2.54	2.54	
Nov 30th	...	...	3.24	...	2.90	...	2.64	...	
Dec 1st	...	...	3.24	3.51	2.95	3.01	2.64	2.97	Rain(night)
Dec 2nd	...	6.10	3.58	3.66	3.15	3.45	3.10	3.20	Rain(night)
Dec 3rd	...	...	3.66	3.96	3.45	3.35	3.20	3.96	Dry
Dec 4th	...	...	3.89	3.81	3.35	4.17	3.81	4.67	
Dec 5th	...	...	3.84	4.11	4.04	4.47	4.47	4.67	
Dec 6th	...	...	4.72	6.10	4.65	5.18	4.65	5.18	
Dec 7th	6.10	...	6.10	...	failure		failure		Rain(night)

Testing results

Burgoyne's report describes each of the four walls and their response to the loading. Wall 'A' retained a full height of backfill without undue distress, showing no visible movements or cracks at full height. Wall 'B' also retained the full height of backfill, however there was some slight fissuring and a movement of 64mm at the coping level.

Wall 'C' failed upon placement of 5.18m of backfill. Prior to failure, this wall exhibited an overhang of 127mm in the first 1.7m; 254mm at the coping level. In addition, the external face was "...greatly convex...and rending in every direction"[12]. Failure occurred via bursting at approximately 1.7m from the base, with the top $\frac{2}{3}$ remaining monolithic and falling vertically.

Wall 'D' also failed with a backfill height of 5.18m. This wall overturned, falling "...like a board"[12]. Convexity of 101mm was reported in the face, with an overhang of 457mm before collapse. 152mm of this movement occurred within the final half hour.

It was intended that further tests would be conducted based on geometries 'C' and 'D', building walls of similar profiles but with increasing thicknesses. However, these tests were never conducted.

Assessment of work

With this work, Burgoyne proved that geometry has an undeniable effect on stability and the type of failure mode that will likely occur. Assuming that the reported measurements are accurate, these data may be used to evaluate the effectiveness of various analysis techniques; indeed these tests and their results were used to check the validity of the limit equilibrium analysis program described in chapter 4.

The standard of Burgoyne's walls must be considered when comparing their behaviour to the in-situ walls in existence today. From the descriptions in the paper, the walls were constructed of squared granite blocks, giving very tightly interlocked structures. This is further supported by Burgoyne's measurements regarding the density of the wall. Granite generally has a density of approximately 26kNm^{-3}, however Burgoyne reported the wall to have a density of 22.3kNm^{-3}. Using these figures, the percentage of voids within the wall are estimated to be 14%. By comparison with the void testing carried out in chapter 3, this value is very low as would be expected for tightly packed and squared blocks (measured void ratios for the tested limestone and slate walls range between 21% - 50%). Finally, from Burgoyne's diagrams and notes, there is no mention of a course infill between the interior and exterior facades. It is indicated that the walls are of solid masonry construction throughout, as opposed to standard construction which would utilise a core of loose material. These factors would all cause the behaviour of Burgoyne's walls to be far more monolithic than a standard drystone wall. Hence, it is likely that should these tests be repeated with traditional drystone construction techniques, the results would be different. Whilst the final backfill heights may be similar, it would be expected that the bulging and deformation prior to failure would be much more pronounced.

Another criticism against this work relates to the setup of the tests. As each wall was built between dividing walls, the backfill pressures are somewhat resisted by friction along these partitions. Ideally, the full force of the backfill would be applied to the internal face of the test wall equally along its whole length. A further consequence of the partitions is that each wall segment acts independently and is unconnected at its ends; in reality the loaded sections of wall may gain some stability from adjacent portions. This may in turn alter the failure mode that occurs, and the amount of fill it is possible to retain. Burgoyne notes this fact in his paper, labeling it as an 'unfavorable circumstance' for the wall[12].

It is undocumented if any arching occurred between the boundary walls, or if the movements were uniform. It is unlikely, given the setup of the test, that identical deformations were observed along the length of each wall; it is more probable that

the central portions displayed much greater displacements than the end sections. If arching did indeed occur, it is again unclear if the drystone walls could have been braced between the boundary walls. This behaviour occurred during full-scale drystone retaining wall tests conducted by ENTPE in Les Cevennes, France[13]. In this particular case, a loaded wall arched between two steel boundary walls and was effectively locked into place and unable to fail, despite being subject to sufficient loads to do so. This condition arose due to the need to have the test wall tightly fitted between the boundary walls, so as to disallow any material to fall out around the sides of the wall. It was also further encouraged by the tightly-packed nature of the wall, allowing few individual block movements and causing the structure to behave particularly monolithically. In a similar manner, Burgoyne's test walls were tightly-packed, and must have been built up to the boundary walls to prevent a spillage of material at the sides of each wall.

It is possible that the proximity of the granite rock face to the back of the wall may have altered the results. In particular walls 'C' and 'D' appear close enough that this may have had some impact by reducing the wedge of soil affecting the retaining wall.

2.2.2 Lyon full-scale tests

In 2005, a series of full-scale tests were conducted by Villemus et. al. at ENTPE, in Lyon, France[14]. The aim of this work was to rationalise the structures, and quantify the safety factor for any given wall. Formulae were generated, considering both the internal and external stability of the test walls.

Wall geometries

Four drystone walls were constructed using a locally quarried limestone, with a fifth using schist from St. Germain de Calbert, France. The five walls ranged from 2m to 4.25m in height, each having a vertical internal face and varying external face batters of up to 15%, as shown in figure 2-2. Similar to Burgoyne's tests, these walls were relatively short sections, ranging from 2m to 4m in width. For each wall, sliding was inhibited by a 150mm stop-block in front of the toe. Further details of the walls' properties are shown in table 2.2.

Test procedure

To load these structures, hydrostatic pressure was applied through large PVC-lined bags located behind the walls. The PVC bags were slowly filled with water, and the movements of the walls recorded. In particular, the angles at which the internal movements occurred were focused on. Due to the nature of the loading, failure was predominantly by sliding, producing distinctive 'belly bulge' formations. Due to the manner of loading, total collapse was not possible, and so failure was defined as

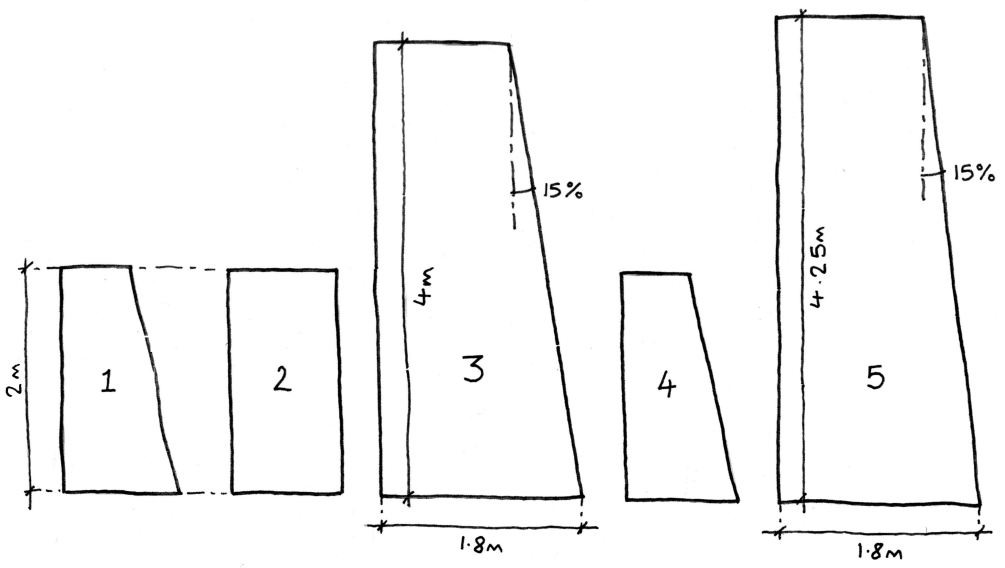

Figure 2-2: Villemus's wall geometries

Table 2.2: Villemus' wall properties

Property	Wall 1	Wall 2	Wall 3	Wall 4	Wall 5
Height(m)	2	2	4	2	4.25
Length(m)	2	2	4	2	4
Foundation width(m)	0.9	0.9	1.8	0.8	1.8
Crest width(m)	0.6	0.9	1.2	0.65	1.16
Batter(%)	15	0	15	12	15
Walling material	limestone				schist
Density(kNm^{-3})	15.4	15.0	15.7	16.0	18.0
Void percentage(%)	25	27	24	23	32
Stone friction anlge(^{o})	36	36	36	36	28.5
Inclination of courses(^{o})	0	0	0	4	8.5

occurring when a clear internal failure plane developed within the wall. However, at this point the walls were still upright and capable of resisting further loading.

The centre line of each test wall was monitored using up to 10 draw wire transducers, accurate up to ± 0.4mm[14]. In addition, a camera was set up to take a series of pictures of the side of each wall from a fixed point. These were then used to determine the direction and magnitude of any movements, using techniques adapted from stereo photogrammetry.

Assessment of work

Villemus' work examines the stability of each wall in terms of both internal and external stability, using a limit equilibrium approach[14]. External stability is determined by calculating the safety factor of applied forces against self weight. The resultant of these two forces must lie within the central third at each course

to ensure that no tensile forces are generated, however Villemus states that it may lie outside this area and still be stable, although this cannot be ensured.

Considering internal stability, Villemus gives a simple equation which includes the friction angle between the courses and the internal failure plane of the wall (equation 2.1). By assuming that when F_g=1 the wall is at the point of internal failure, the angle of the failure plane may be calculated, given that the forces in the system are known. In addition the rotation of the blocks may be calculated for these walls, using the initial tilt of the courses and the angle at which failure occurs (equation 2.2). The data gathered via the photogrammetry during the full-scale tests was then able to be compared with the theoretical values. Villemus' results are shown in table 2.3.

$$F_g = \frac{V \tan(\phi_m - \theta)}{H} \tag{2.1}$$

$$\Theta = \theta - \eta \tag{2.2}$$

Where:

F_g= internal safety coefficient for sliding
V= vertical forces within the system
ϕ_m= internal angle of friction
θ= angle of failure plane
H= horizontal forces within the system
Θ= rotation of blocks from initial postition to failure
η= angle of tilt for each course of the wall

From the table 2.3[14], it is shown that formulae 2.1 and 2.2 hold true for these tests. However, Villemus states that Θ must necessarily lie between 5^o and 11^o for these formulae to be valid. Whilst this may be consistent with results from the tests conducted in Lyon, this may not hold true for other wall geometries and materials.

Villemus' work makes the initial assumption that the two failure mechanisms considered - shearing failure and rotational failure - are independent events and that there is no interaction between the two. Also assumed is that once a shear plane develops failure is imminent. Both of these assumptions are not always valid for in-situ walls; a wall may develop a shear plane which may subsequently stabilise, or in turn instigate a failure via overturning. Similarly, these simple formulae do not account for the development of bulges, stable or otherwise.

Table 2.3: Comparison of full-scale and theoretical results

Value	Data source	Wall 1	Wall 2	Wall 3	Wall 4	Wall 5
Failure slope	theoretical	11.3	9.4	10.5	1.5	-0.5
$\theta(^o)$	photogrammetry	N.M.	N.M.	11.5	3.5	0 - 2.5
Stone rotation	theoretical	11.3	9.4	10.5	5.5	8
$\Theta(^o)$	photogrammetry	N.M.	N.M.	11.5	7.5	8.5-11

N.M. = not measured

The theories developed by Villemus' work highlight some of the crucial factors regarding drystone walls; namely that these structures are not monolithic and the internal movements are as critical as the external (and hence visible) deformations. The drive towards developing formulae which may provide a safety factor against various failure modes is required, however the interplay of these phenomena should not be ignored.

Villemus' full-scale tests in Lyon represent a great step forward in the understanding of drystone behaviour, providing a basis for further theory development. Especially useful is the ability to examine the ends of the walls during testing, which gives some indication of the internal behaviour - information which is otherwise extremely difficult to obtain. However, the side-effect of the use of short sections is that these walls do not behave in the three-dimensional manner of most walls, and the deformations identified may not be entirely representative. Hydrostatic loading is also unrepresentative for in-situ walls, despite allowing a precise knowledge of the loads applied. Due to the inherently rough internal faces which a retained fill rests against, both vertical and horizontal forces are applied through friction. These vertical forces have significant effects on the behaviour of a wall, and the manner in which deformations occur, as discussed in chapter 7.

2.3 Theoretical assessment techniques

There are few theoretical approaches in common use for assessing the stability of a drystone wall. An equilibrium approach is perhaps the simplest, although has the scope to include many of the factors critical to drystone walls. An alternate approach developed by Colas et. al.[15] applies yield design theory to drystone walls. This more complicated method allows the determination of the ultimate loading conditions, in addition to the failure mode generated. Numerical analyses are potentially the most sophisticated approach, providing a vast amount of data at the cost of significant run-times.

2.3.1 Static equilibrium

In 1874, Casimer Constable presented a paper which identifies the need for stability against overturning[16]. Although the formulae used were not new at the time, the

manner in which he employed them was not conventional. Constable noted that in observed overturning failures that the entire wall does not fail, instead shearing off at approximately 45^o from the toe. He thereby bases his formulae on the fact that the 'prism of pressure' which provides the overturning force does not begin at the heel of the wall, but instead at some point above this. The geometries of these assumptions are demonstrated in figure 2-3.

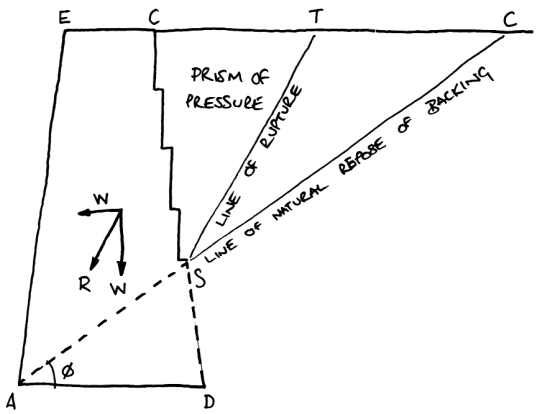

Figure 2-3: Example of Constable's assumed geometries

Constable's observed findings are that the angle of internal rupture within most walls (diagrammatically represented by ϕ in figure 2-3) is approximately 45^o. However, for the basis of his calculations, a conservative angle of 37^o is assumed (0.75 $\times$ the height of the wall). From equation 2.3, the given geometries are then used to determine the thickness of wall required to ensure safety for the given height. This formula may be simplified for walls which do not have surcharging or battered faces. Although the equation gives an allowance for a surcharge to be added, there is no method of determining the footprint or even the position of the load. This is a particularly important oversight, as this would greatly affect the stability of the wall and the associated thickness given.

$$t = h \times \left[-\left(n + \frac{n_1}{2}\right) \pm \sqrt{\frac{2\tan^2\frac{\alpha}{2}}{7\gamma_{stone}}\left(\gamma_{soil} + \frac{8}{3}p\right)} + \frac{n^2}{3} - \frac{n_1^2}{12} \right] \tag{2.3}$$

Where:

t = thickness at top of wall
h = height of wall
n = batter of external face
n_1 = batter of internal face
α = angle of repose of the earth from vertical ($\alpha = 90^o - \phi$)

ϕ = angle of rupture of stone
γ_{stone} = weight of masonry
γ_{soil} = weight of earth
p = weight of surcharge

Equation 2.3 was validated by Constable with small-scale testing using model walls up to 318mm in height. Small pine blocks were used as a walling substitute, and oats in place of the backfill, with each test being conducted in a glass-sided container. The results obtained proved both that the formula held true for these tests, and also that it produced a more efficiently sized structure than existing practice would give. Constables states that the agreement between his small-scale thicknesses and calculated thicknesses is attributed to his use of α being assumed at $0.75 \times h$. Although Constable's larger scale tests using squared masonry blocks did not fully verify these findings, Constable's work still raises many valid issues. Particularly important is the observation regarding the failure plane, which begins at the toe and continues through the backfill.

To test the validity of equation 2.3 against modern design practice, the specifications and parameters from the full-scale tests described in this thesis were used. A wall height of 2.5m was used, with a 4^o external batter and a vertical rear face. The backfill height was assumed to be the full height of the wall (2.5m). The material properties were as described in chapter 3, using limestone for the walls and the single-sized aggregate for the backfill. The equation was completed assuming no additional surcharging, giving a height at the peak of the wall. The associated base width was then calculated given that the external batter was 4^o. The base width calculated for these parameters was 500mm, tapering to 200mm at the coping. This is very close to the geometry of the second full-scale wall test, which was 500mm at the base and tapered to 300mm at the coping (although this wall was more slender than the masons would normally work). A simple hand calculation of this wall was undertaken, using the Coulomb[17] equation for the earth pressure co-efficient to determine the forces from the backfill. Based on the same geometries, a safety factor of 1.67 against overturning was calculated. This is outside the permissible values for modern practice, however it is still stable with a substantial margin of safety.

The thicknesses given by equation 2.3 may go some way to explaining the situation regarding the drystone walls that exist today. If the walls which were built before the advent of modern codes of practice used this equation (or similar), all such walls would have similar factors of safety. Despite the fact that these walls have stood for decades undisturbed, they would not meet the requirements demanded by current codes of practice. This is a critical point, and should be remembered during the analysis of any walls built in this period.

In 1986, Cooper used a limit equilibrium approach to address the issues of

drystone walling in a much more detailed manner than Constable[18]. Cooper dealt with the unbonded nature of drystone walls by examining these structures as a series of segments, each subject to both self weight and backfill pressure (figure 2-4). It is also assumed that the blocks are perfectly flat and completely rigid. The internal and external forces are balanced, with the backfill pressure resolved into a point load using Coulomb's analysis[17].

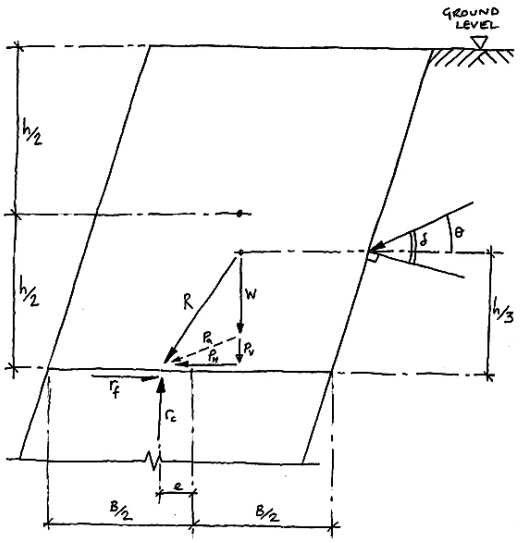

Figure 2-4: Idealised section of wall

The resultant force, denoted by R in figure 2-4, may be determined in terms of W (weight of segment) and the force from the backfill P_a, which can be split in to components P_H and P_V. The angle of the resultant from the point of application gives the size of the eccentricity(e), and in physical terms the distance between the line of thrust and the neutral axis. The system is then assumed to be held in equilibrium by the frictional resistance along the contact point (r_f) and the compressive resistance of the block below (r_c). According to Cooper, if e is greater than $\frac{B}{2}$ and the line of thrust moves beyond the boundaries of the wall, then rotation of this segment will occur. However, this boundary may not always be the exact limit, as due to aging and weathering the corners may become rounded, consequently lowering the value of e required before movement. Also, the segments may become compressible over time, again reducing the maximum value of e allowable without movement.

It should be noted that for Cooper's calculations the vertical component of P_a (P_V) is assumed to be acting at the same point as the centre of mass of the block (as figure 2-4 shows). Although this simplification allows a slightly simpler calculation, it underestimates the magnitude of the moment from the restoring force P_V, consequently indicating a lower safety factor against overturning. In

addition, the horizontal loads are applied at a distance of $\frac{h}{3}$ above the base of the segment. This is true only for the first segment below the retained fill, as a triangular distribution is used for the soil pressures. Below this first segment, the pressure distribution is trapezoidal rather than triangular, and hence the height of the applied load changes to suit.

The various behavioral aspects displayed by drystone walls are described by Cooper in terms of the equilibrium of forces and the position of the line of thrust. Bulging is a consequence of the line of the thrust reaching the extremities of the wall boundaries, as shown for both an idealised wall and a more realistic, compressible wall in figure 2-5[18]. Overturning occurs when the thrust line moves outside of the wall at the toe, causing the bottom block to rotate forwards.

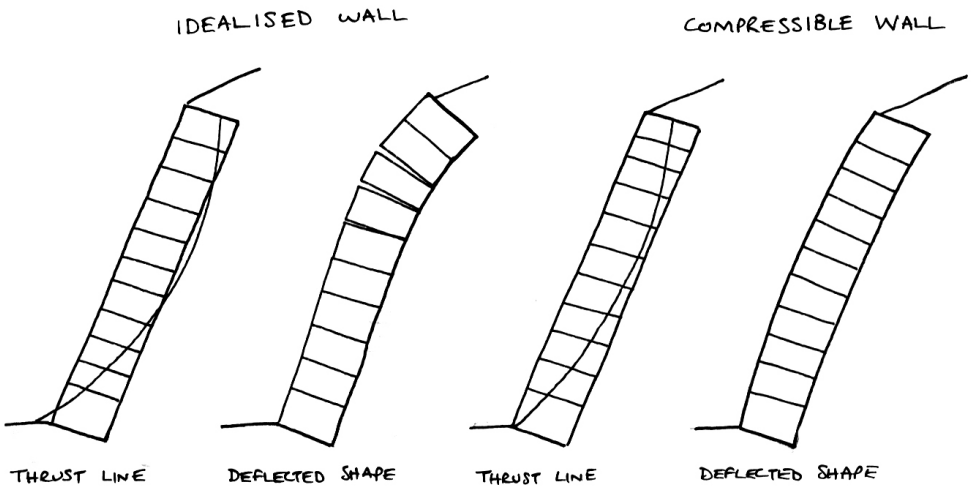

Figure 2-5: Bulging failure modes on a rigid base

Cooper also applies the limit equilibrium approach to foundation failures. As any eccentricity of the thrust line will induce a differential loading along the base, differential settlement may occur. This in turn would be likely to cause deformation of the wall above. If the eccentricity is large enough, or the foundation capacity particularly low, then the subsequent movement may be enough to destabilise the wall and initiate failure. It is noted that both inadequate bearing resistance and compressible bases can produce wall shapes which could easily be mistaken for other types of failure.

This work is highly important for the development of assessment methods for drystone walls. The use of the thrust line to identify a particular failure mode can also be adapted to give a safety factor against this event. The use of the segmented structure is also appropriate for drystone walls, allowing for the effects of bulging and deformation.

Arya and Gupta also presented work using a limit equilibrium approach in a similar manner to Cooper, dealing with the stability of hill roads in India[19]. This

work pays particular attention to the issue of sliding in drystone walls, checking the applied forces against the sliding resistance between the bedding planes. Although the work does not use the segmented approach demonstrated by Cooper[18], it does account for internal sliding in walls with bedding planes tilted to varying degrees. Arya and Gupta illustrate mathematically the importance of tilting the courses away from the external face, so that should sliding occur, the blocks are moving up an inclined slope. In the example given in this paper, a wall with bedding planes angled at 15^o has over double the safety factor of a wall with horizontal beds. Conversely, tilting the bedding planes forwards would lower the safety factor, as gravity is assisting the applied forces to initiate a failure by sliding.

Although a negative batter seems entirely logical to aid a wall's stability against sliding, it is not always employed by masons, particularly in the UK. In some instances this is due to the difficulty of attaining tilted bedding planes which are parallel - it is much simpler to ensure this with horizontal planes. Secondly, some masons use a slight positive batter to ensure water run-off. The work presented in Arya's paper relates to designing drystone retaining walls able to withstand earthquake loadings, and in these instances the maximum possible resistance to sliding should be attained. However, sliding is generally not a critical issue in the UK, as earthquakes are rare and most walling materials used have relatively high friction angles (limestone, granite, etc.), causing bulging or overturning to be of greater concern. Further research using a limit equilibrium approach to assess a wall's safety against sliding was conducted by Villemus et. al.[14], as discussed in section 2.2.2.

In 2006, Walker, McCombie and Claxton developed a computer program to generate a thrust line for any given wall profile, using the original principles proposed by Cooper[11]. The wall profile, which was segmented into a series of stacked blocks, could be deformed and bulged and the effect on the thrust line instantly viewed. The program is used to show how a wall may initially have a thrust line which exits the wall (indicative of failure), but through the development of a bulge the resultant force can be moved back within the boundaries of the wall. The code of this program was modified by Mundell[20], and further expanded upon for use within the project described in this thesis. Details of the work that has been conducted to date using this program, as well as its operation, are discussed in chapter 4.

2.3.2 Yield design theory

The use of yield design theory provides an upper-bound answer for the load capacity for a structure, based on the resistance of the constituent materials[15]. Originally used for soil mechanics problems, Colas et. al. have adapted yield design theory in order to model drystone retaining walls[15]. In Colas' calculations, the wall is assumed to remain generally monolithic, with the exception of a shear plane which

passes through both the wall and backfill when failure occurs. The backfill height which causes failure to occur are determined by the formulae, as are the angles of the failure plane within the wall and backfill. The model also accommodates the inclination of the bedding planes, and will identify the ultimate load at which sliding will occur.

Colas used the physical test data gathered by Villemus et. al.[14] to verify the yield design theory, comparing her results with both the in-situ results and a simple limit equilibrium approach. The results of these comparison studies are shown in table 2.4[15]. For sliding, yield design and limit equilibrium approaches give identical results. This is due to the fact that they both utilise the same calculation, with both models assuming that sliding will take place at the foundation level, using the same frictional values. For overturning, the simple limit equilibrium analysis method adopted by Colas requires the entire weight of the wall to be overturned by the applied loads, and so gives a more higher failure load than the yield design analysis.

Table 2.4: Comparison of yield design, limit equilibrium and full-scale results

Model		Wall 1		Wall 2		Wall 3		Wall 4		Wall 5	
		S	O	S	O	S	O	S	O	S	O
YD	H_{max}(m)	**1.75**	1.82	1.90	**1.86**	**3.62**	3.75	1.97	**1.87**	4.04	**4.00**
	ϕ(deg)	0	16.0	0	15.6	0	16.0	0	16.1	0	17.1
LE	H_{max}(m)	**1.75**	1.85	1.90	**1.89**	**3.62**	3.81	1.97	**1.92**	**4.04**	4.14
EX	H_{max}(m)	**1.59**		**1.75**		**3.22**		**1.84**		**3.48**	
	ϕ(deg)	N.M		N.M		11.5		7.5		8.5	

S = sliding; O = overturning
YD = yield design
LE = limit equilibrium
EX = experimental
N.M. = not measured
H_{max} = maximum height
ϕ = angle of internal shear failure

Although table 2.4 indicates that a yield design approach gives a more efficient design, this is not altogether accurate, as both models in this instance assume a monolithic structure. The limit equilibrium approach initially proposed by Cooper[18], and later adopted by Walker et al.[11] and Mundell[20], allows the model to incorporate a bulged and deformed profile, hence giving a more realistic analysis.

Overall, Colas' model presents a potentially viable alternative to limit equilibrium and numerical approaches. Colas' formulae provide the ultimate loading conditions for a structure with minimal known quantities, and are somewhat more accurate than the standard limit equilibrium approach. At the same time, it is a much simpler technique to use than numerical packages such as UDEC or

VISAGE^{TM}, which use either the Distinct Element Method or the Finite Element Method. However, a serious limitation of yield design for drystone walls is that it currently requires a monolithic, straight-sided, structure. This is especially critical for the analysis of in-situ walls, many of which have deformed to the point where this assumption is no longer representative. This work has also been used to provide a simple design guide, based on the height of the wall required, and the friction angle of the backfill. These guidelines are discussed in section 2.5.

2.3.3 Numerical analysis techniques

There are various numerical packages available for both finite and discrete element analysis of structures. Drystone retaining walls are complicated to assess with numerical packages as they require a meeting of distinct elements (the wall blocks themselves) and a continuum (the retained backfill). The Universal Distinct Element Code (UDEC) is the tool most predominantly used, originally developed by Cundall to assess blocky rock systems[21]. UDEC allows a two-dimensional structure to be analysed, involving joint characteristics and block properties[22]. In the case of the papers discussed in this chapter, UDEC uses the Mohr-Coulomb plasticity model to model dynamic behaviour of the elements until equilibrium is reached. The process is completed over notional time-steps. The significant advantage of numerical modeling is that once a simulation has been completed, a full cross section of the wall can be viewed at any time step during the test. This allows velocity vectors, stress distributions and displacements to be known throughout the simulation - information which is otherwise very difficult to ascertain.

UDEC was initially used on drystone structures by Dickens and Walker, to assess the behaviour of free standing sections of walls[22]. This work recreated physical models which were themselves replicas of the drystone national monuments of Great Zimbabwe. The monuments have been under great scrutiny for some time, as they have been found to bulge outwards under their own weight. To attempt to recreate this process both in UDEC and the physical tests, the central portion of the foundations were slowly lowered, creating a void within the core of the wall. It was theorised that this causes the internal wall material to arch over the void, hence inducing additional lateral loads and causing the observed bulging.

Dickens and Walker proved with this work that UDEC could recreate the observed deformations and failures of in-situ walls. Once the validity of this approach had been proved the program was used to assess the impact of other factors on stability. Variations in block and void sizes were tested, in addition to different material properties and the inclusion of through-stones. Finally, the program was used to simulate the behaviour of drystone retaining walls, and compared with those at the Great Zimbabwe monument.

Between 2000 and 2002, two papers were published regarding the use of UDEC to model the geometries tested by Burgoyne in 1834. In the first paper, Harkness et

al. used UDEC to model Burgoyne's test walls for comparative purposes[8]. This was followed in 2002 by a similar group comprised of Powrie et al., using UDEC to do a more in-depth study on Burgoyne's first two test walls[23].

One of the issues with numerical modeling is the computational time involved; the UDEC tests for Harkness et al.'s paper were carried out in 1996 on a RS6000 workstation, and took approximately seven days per run[8]. Intuitively, it can be seen that the processing time is proportional to the number of elements involved, and that the size of these elements governs the accuracy of the results. A careful balance is then required by the programmer to ensure a feasible run time, whilst retaining enough elements of a fine enough size to guarantee useful data.

Whilst Dickens et al. used rigid blocks to model their freestanding walls, the work conducted by Harkness et al., and Powrie et al. both used a mesh of compressible blocks, with a constant stiffness. An example of the generated mesh is shown by figure 2-6[8]. The walls, foundations and backfill were all modeled as a series of discrete elements, and allowed to reach equilibrium. The test process (with the exception of the model of Burgoyne's Wall 'A'), was to recreate each of Burgoyne's walls, and then systematically increase the backfill and allow the system to come to rest.

Two separate series of tests were conducted, attempting to recreate the exact material properties used by Burgoyne. The first series is the more stable, using a wall density of 2650kgm^{-3} (the typical density of granite) and friction angle of 25^o for the backfill. The second uses a much lower wall denisty of 2270kgm^{-3} (as measured by Burgoyne), but with a slightly higher angle of friction in the backfill (28^o). The results as obtained by Harkness et al. are shown in table 2.5[8].

Both series of results give the same backfill heights at failure that Burgoyne reported, with the exception of the runs which used 1700kgm^{-3} as the density of the fill. In these instances, the higher density of the backfill caused larger pressures to be applied to the wall, hence causing an earlier failure. It is also noted from Harkness et al.'s work that the second series of wall tests were more unstable than the first, by virtue of having higher deformations prior to failure[8]. Again this is understandable, as the lower wall density would provide a smaller resistance to the active pressures from the backfill.

The work subsequently published by Powrie et al. used UDEC to link the numerically calculated movements with a factor of safety. This was attempted by undertaking parametric analyses of Burgoyne's walls 'A' and 'B', to see which elements of the structure were most critical for stability. The following factors were investigated:

- block rounding
- lateral extent of backfill
- wall joint inclination

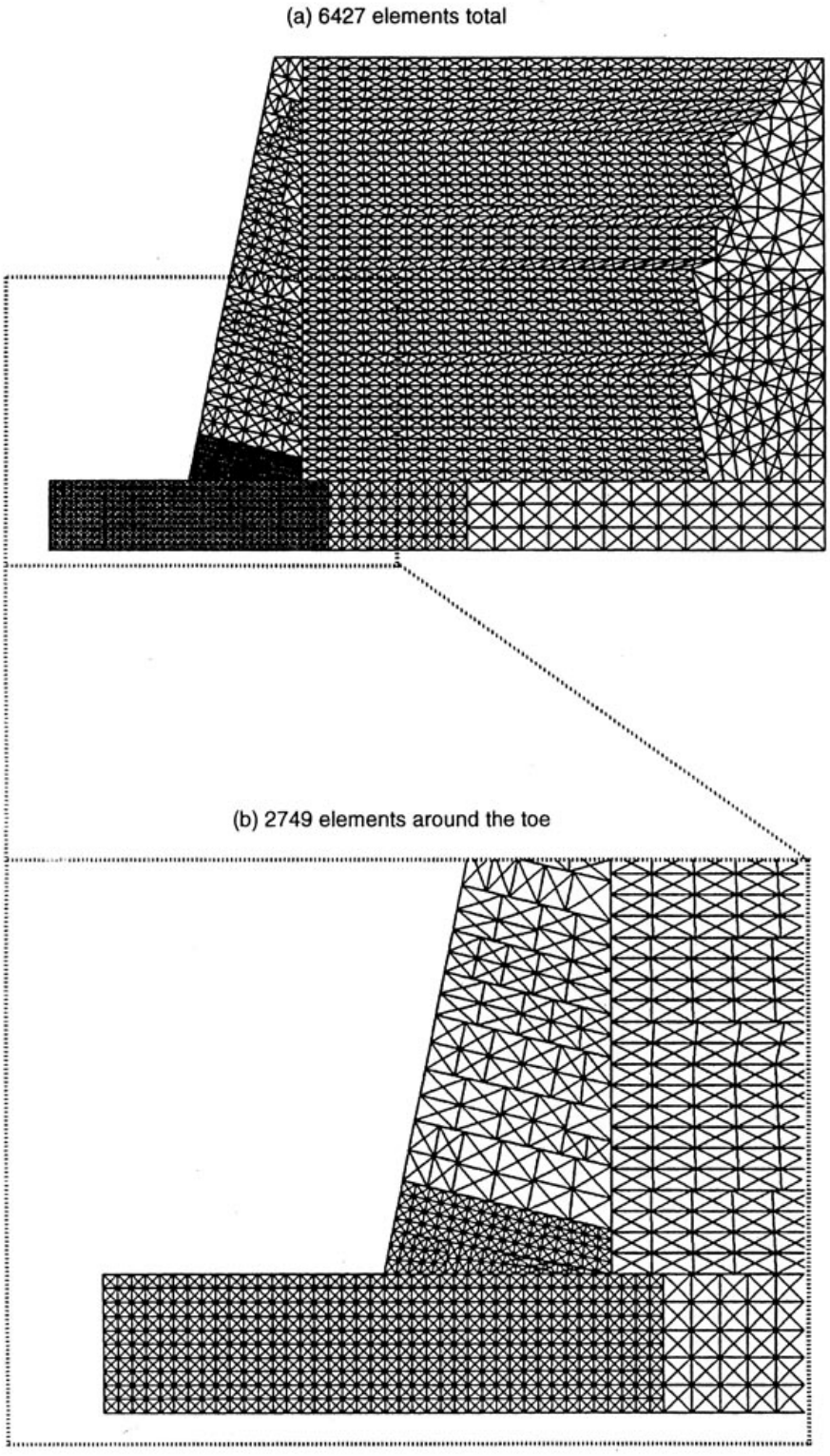

Figure 2-6: Typical mesh as used by Harkness et al.

Table 2.5: Harkness et al.'s analysis of Burgoyne's test walls using UDEC

Series 1

Soil height (m)	Wall A			Wall B			Wall C			Wall D		
	Soil dens (kgm^{-3})			Soil dens (kgm^{-3})			Soil dens (kgm^{-3})			Soil dens (kgm^{-3})		
	1400	1500	1700	1400	1500	1700	1400	1500	1700	1400	1500	1700
6.1	NF			NF								
5.49	NF			NF								
5.18	NF			NF			F	F		NF	F	
4.88	NF			NF			NF	NF	F	NF	NF	F
4.27	NF			NF			NF	NF	NF	NF	NF	NF

Series 2

Soil height(m)	Soil dens (kgm^{-3})			Soil dens (kgm^{-3})			Soil dens (kgm^{-3})			Soil dens (kgm^{-3})		
	1400	1500	1700	1400	1500	1700	1400	1500	1700	1400	1500	1700
6.1	NF			NF								
5.49	NF			NF								
5.18	NF			NF			F			F		
4.88	NF			NF			NF			NF		
4.27	NF			NF			NF			NF		

NF = No failure
F = Failure

- effective friction angle of backfill
- effective friction angle and stiffness of the joints
- compressibility of the sub-base

Powrie et al. make many valid observations from both this work and the earlier work by Harkness et al.[8]. The variation of parameters allowed different failure mechanisms to be observed, and the extent to which each factor influences them. It was found, for example, that small changes in sub-base strength and stiffness have a much higher effect than previously thought, whereas joint strength requires a vast reduction before any significant differences are noted.

The friction angle of the backfill is also a critical factor. Powrie et al. show that by lowering the friction angle by as little as 1^o, the factor of safety on the soil may reduce by 4%. As there is usually a great uncertainty of this value in practice, this has large implications for the stability of existing in-situ walls. This observations is made from simple calculations based on the soil strength; Given that $\tan 27 \div \tan 28 = 0.96$, this indicates a drop of 4% in the strength which is related to the tangent of the soil's angle of friction.

Powrie et al. acknowledge the fact that this work is based on two-dimensional analyses, and that by increasing the scope of the project to incorporate three-dimensional movements that the possible deformations may be greater. As part of the project discussed in this thesis, a three-dimensional analysis package has been developed by John Harkness of Southampton University (results yet to be

published).

In a parallel study conducted by Claxton et al., UDEC was again used to model Burgoyne's field studies[7]. In these simulations, the walling material was assumed to be comprised of rigid blocks, and not subject to failure (although the joints between the stones may still fail).

Claxton et al.'s work successfully reproduced the tests conducted numerically by Harkness et al.[8], although the deformations recorded prior to failure were much smaller. This is to be expected, as with Harkness et al.'s model, the wall blocks themselves could deform, causing additional movements, whereas in Claxton et al.'s work deformations may only occur at the joints. It was attempted to reconcile these differences by allowing a degree of block overlap, however it was found that this reduced the accuracy of the model.

An important goal of Claxton et al.'s work was to produce a tool which could potentially be used to assess existing walls. The use of UDEC for this purpose had previously been limited due to its significant run-time. However, by adopting rigid blocks and reducing the elements in the backfill mesh, much shorter simulation times are obtained (60-80 minutes). This is obviously met with a reduction in the accuracy of the data obtained, but the results are still in general agreement with the more detailed analyses.

Similar to Powrie et al.'s work[23], a parametric analysis was also undertaken, using Burgoyne's wall 'D' as a template. The results of this study were again consistent with Powrie et al.'s work, identifying the crucial factors such as the friction angle of the backfill and the wall thickness.

Although most of the numerical studies involving drystone walls have used UDEC, it has also been attempted within other program environments. For example, Zhang et al. used VISAGE^{TM} to study Burgoyne's 'wall D'[24]. VISAGE^{TM} is a finite element code, which models the separate elements (wall, foundations and backfill) as continuums.

Zhang et al. experiment with two methods of modeling the wall. Firstly, the wall was modeled as an equivalent continuum, with a lower stiffness and weaker strength accounting for the presence of wall joints. In the second, joint elements were used to simulate the wall[24]. The test procedure was carried out by initially modeling the wall without any retained fill, then incrementally increasing the retained fill. Although this is similar in principle to the original process carried out by Burgoyne[12], the incremental fill heights are not the same, instead using 1m and 0.5m lifts.

Figure 2-7 shows a comparison between the finite element models and the UDEC analysis of 'Wall D'[24]. Although it is clear that the equivalent continuum model does not model the final deformations in a similar manner to UDEC, the joint element model does. Moreover, all three models provide almost identical deflections up to 5m of backfill.

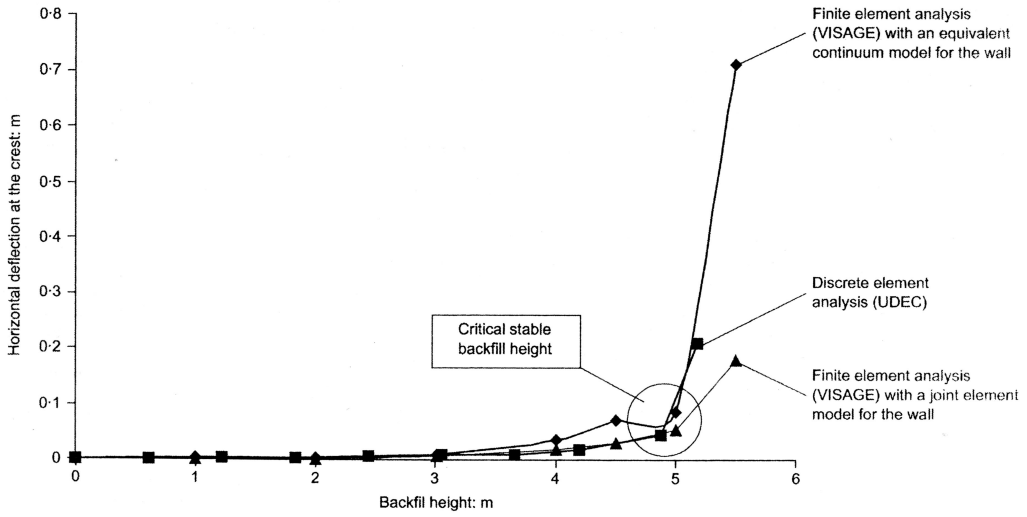

Figure 2-7: Comparison of simulated wall behaviour of VISAGE^{TM} & UDEC

In addition to the failure heights being similar to those reported by both Harkness et al. and Burgoyne[8, 12], the exact mode of failure was also similar. The finite element model described a tensile stress developing on the internal face of the wall, peaking at 1m above the base. As the real wall would be unable to carry such tensile stresses, it is likely that movement and cracking would occur at this point, potentially creating a failure plane within the wall. If this crack extended through the wall to the overturning point (which in this case is the toe of the wall), a failure plain at an angle of 45^o to the horizontal would be created. This replicates precisely the findings of Burgoyne, and the reported failure mode of the original 'wall D'.

The numerical work based on Burgoyne's work[7, 8, 23, 24] generally provides close agreement with the original tests. However, in all the studies mentioned, the wall models were all comprised of tightly-fitted blocks, with no voids or spaces between them. This is not the case within real walls, which have a large percentage of voids between the blocks. This has the effect of not only lowering the overall density of the wall, but also allowing rotation of the component blocks. The possibility of rotation within the wall blocks was briefly discussed by Powrie et al.[23], although only in reference to blocks with rounded edges being detrimental to stability. It is these voids, coupled with the unmortared nature of drystone walls, which provides the ability to bulge and deform without necessarily becoming destabilised.

To address the issue of internal voids, Walker et al. conducted a UDEC study which utilised a more realistic model of drystone walls[11]. Instead of modeling the Burgoyne field trials, this work focused on recreating the typical walls found along the UK's highways and infrastructure routes.

The representative wall section, shown in figure 2-8 had an internal and an external skin, with a core material running through the middle[11]. Each wall

block was not tightly fitted to the adjacent stones, but placed such that there was a gap between. In addition, the wall was not modeled and subsequently backfilled until failure as with previous numerical studies. Instead, as shown in figure 2-8, the wall is given a predetermined fill height to retain, which is covered with a stiff layer representing a road base. To deform the wall, a surcharge is applied to the backfill area, simulating heavy traffic loads.

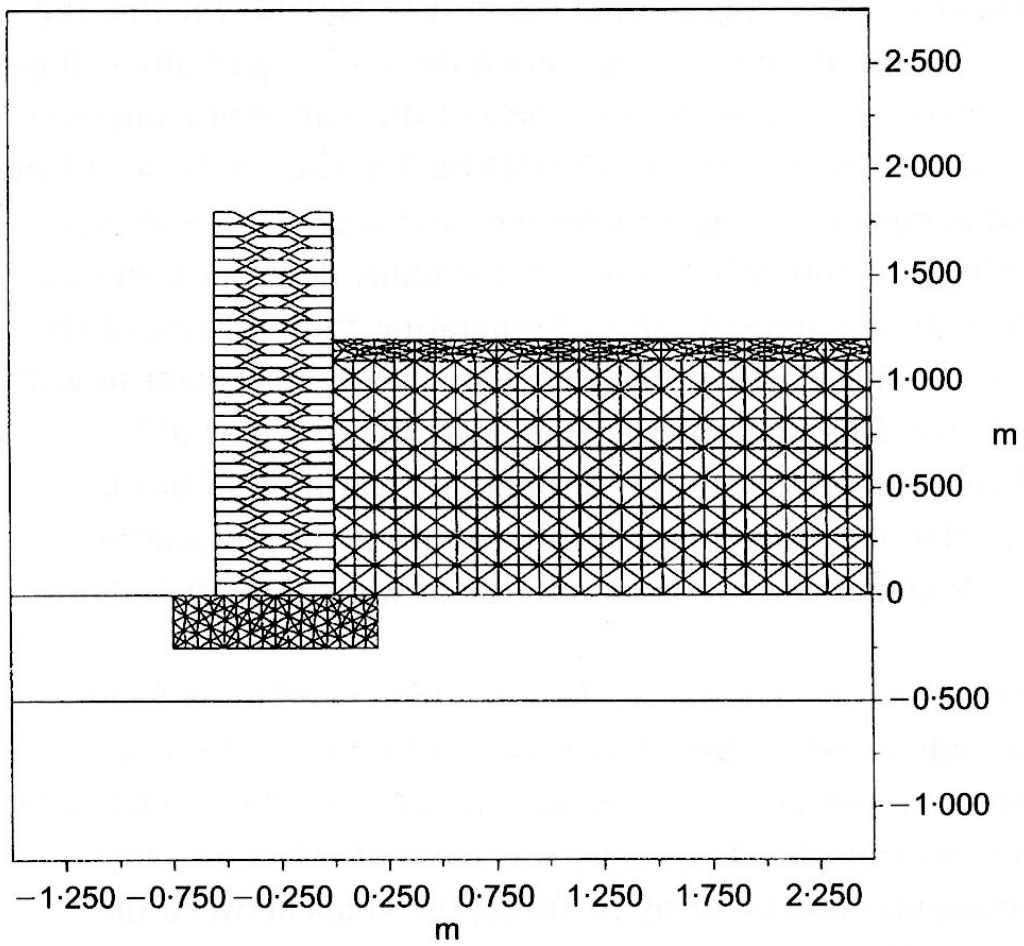

Figure 2-8: Wall model with incorporated voids

It was found that with the combination of this model and type of loading, bulging of the wall occurred. In particular, stable bulges formed, which allowed the walls to withstand the applied surcharges in their deformed shape without further movement (figure 2-9[11]). The final wall position shows that the blocks have both rotated and translated to achieve the bulged position - a phenomenon which was similarly noted during the full-scale drystone tests described in this thesis.

Following these initial tests, a parametric study was undertaken to determine the general validity and robustness of the structure. This included varying the wall and backfill density and friction angles, wall thicknesses, joint stiffnesses and the

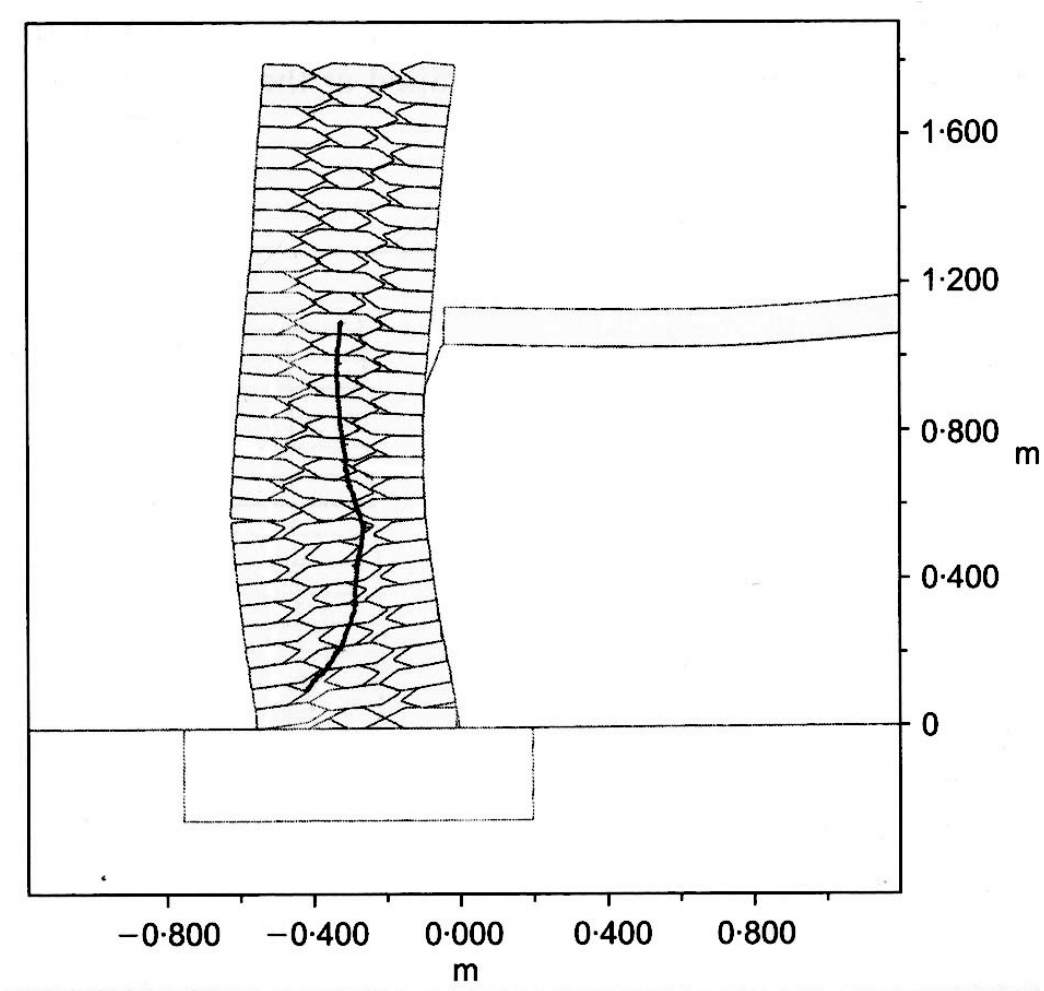

Figure 2-9: Wall model with stable bulge

bulk modulus. Results are similar to those already ascertained in other numerical studies; i.e., wall thickness and backfill friction angle are major factors, whereas the material densities and joint stiffnesses require large changes before the failure conditions vary.

Walker et al.[11] also used this approach to analyse existing walls. A 2.5m high Cotswold limestone wall which had recently collapsed was modeled and subjected to patch surcharging. The wall bulged in a similar manner to the original wall, and eventually collapsed.

Of all the numerical models reviewed in this chapter,the final model by Walker et al. is perhaps the most useful. The modeled walls contain perhaps fewer elements than in previous studies, but the arrangement gives more realistic behaviour. However, it is likely that should this model be used to recreate the Burgoyne field walls, the results would not be as close to the original as those produced by the numerical studies previously discussed. This is due to the fact that Burgoyne's walls were carefully squared and laid granite blocks, and as such are more closely modeled by the tight-knit arrangements demonstrated by the earlier models[7, 8, 23, 24].

Despite the many advantages of numerical modeling, the drawbacks of numerical modeling still cause many difficulties for UDEC to be used as a common engineering tool. First, there is the issue of the necessary hardware and software required, and the need for a skilled operator to use them. The run-time, whilst significantly faster than the first simulations, is still more than a simpler limit equilibrium analysis. Finally, many of the numerical packages require that all of the mechanical properties of the materials to be used are known. Much of these data may be difficult to ascertain, particularly if conditions behind the face of the wall are unknown.

There is no doubt that numerical analysis techniques will always have a place in the analysis of structures such as drystone walls. The information that may be obtained from these assessments has the potential to be highly accurate, as demonstrated by the work described in this section. Undoubtedly their role in assessing drystone structures will increase as the models get closer to representing the real behaviour of the wall, and the run times decrease due to improvements in processing power. However, at present these models are generally too expensive and specialised to employ for the majority of cases, which are more suited to simpler means of assessment. As a consequence, numerical assessments are currently reserved for walls of important heritage or those that could cause significant enough damage if they failed to warrant it.

2.4 Laboratory tests

To effectively determine the behaviour of drystone walls, the mechanical properties of the materials involved must be known. The laboratory tests conducted to date focus mainly on the behaviour of the stone within the wall, and the forces required to induce sliding between the courses.

2.4.1 Great Zimbabwe monument shear box testing

As discussed in section 2.3.3, Walker and Dickens conducted an investigation into the National Monuments of Great Zimbabwe[25]. Over the course of these investigations, they also measured the friction of the walling material through simple sliding tests and shear box testing.

Walker and Dickens conducted 105 separate sliding tests, using blocks approximately 220mm to 185mm by 50mm to 80mm. Friction angles ranging between 22.5^o and 48.6^o were gathered, giving an average value of 34.1^o and a standard deviation of 16.1%[25].

In addition to the sliding tests, shear box testing was conducted on four pairs of mismatched joints. These tests were performed to assess the relationship between shear stress and deformation. Walker and Dickens discovered that after an initial increase in shear stress with little movement, there were substantial fluctuations

in stress accompanied by horizontal displacement. The shear stress was found to drop by up to 73%, although the variation was generally limited to 20% - 40%. This was attributed to a slip-stick movement pattern, as demonstrated by figure 2-10[25].

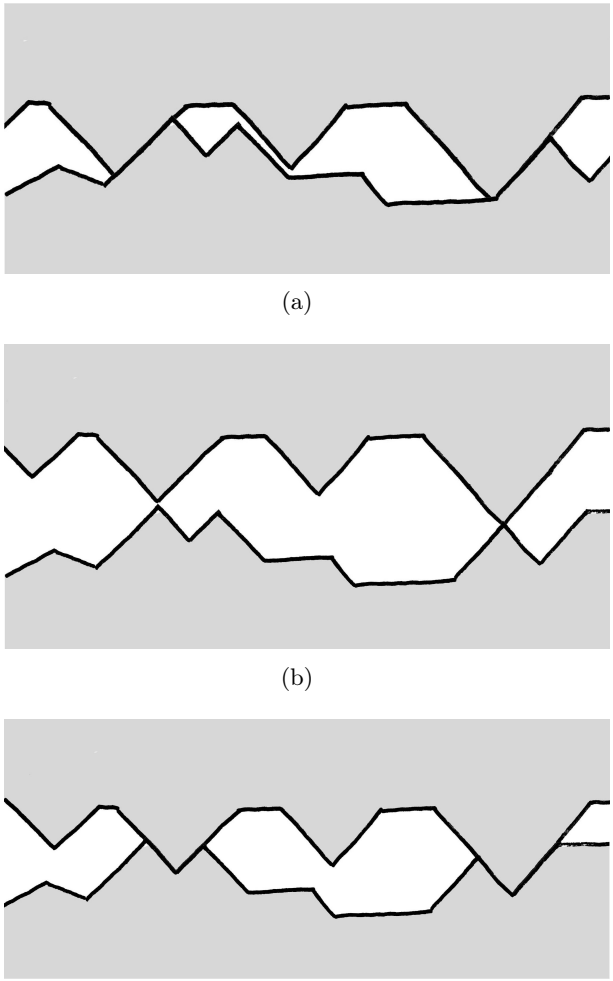

(a)

(b)

(c)

Figure 2-10: Representation of joint shear behaviour

Initially good contact is made by the opposing halves of the joint (fig 2-10(a)). Increasing displacement is accompanied by an increase in shear stress until an unstable equilibrium is reached (fig 2-10(b)). Upon further displacement, the joint shear stress will suddenly decrease as the joint is able to move more freely. This continues until the pair lock together in a similar manner to the initial condition (fig 2-10(c)).

The friction angle of these joint tests provided a range of values between 27.2^o and 39.6^o, giving an average of 34.2^o, being almost identical to the result obtained by the sliding tests.

Walker and Dickens also experimented with saturated joints and soil infilled joints. It is reported that whilst saturation alone made no difference to the joint

stiffness, when the joint was both saturated with water and soil infilled there was an average drop of 13% to the strength of the joint[25]. This has implications which must be acknowledged when assessing in-situ retaining walls. Due to the actions of rain and erosion, it is likely that particles of the backfill material will be washed into the joints of the wall. This may not always be visible from the external face, as it originates from the internal. In such cases, heavy rain may then significantly reduce the sliding resistance, causing a failure which was not otherwise anticipated.

2.4.2 Villemus shear box testing

Villemus et al. also conducted shearbox testing as part of an investigation involving full-scale drystone walls[14]. For their tests, three sizes of shear tests were used; 60mm by 60mm, 300mm by 300mm and 1000mm by 1000mm.

Both the 60mm and the 300mm shear box tests used samples with cut faces, whereas the 1000mm shear box was a more realistic setup, using uncut stones as might be found in an in-situ wall. The vertical loads applied during testing were consistent with those found at the base of a wall 7.5m high, with shearing rates of under 3mm/min[14]. The results are shown in table 2.6[14].

Table 2.6: Friction angle measured by shear box testing

Material	60mm shear box cut sample	300mm shear box cut sample	1000mm shear box uncut sample
Limestone	37 ± 2^o	37 ± 1^o	38 ± 2^o
Limestone of St. Gens	36 ± 1^o	36 ± 1^o	not measured

Perhaps surprisingly, the results from the smaller shear boxes with cut samples give very similar results to the large 1000mm shear box which used more realistic samples. This result makes the measurement of friction angles within drystone walls much easier, as it shows that small, cut samples may be used to give representative values of much larger and more complicated structures. This also has cost implications, as the smaller tests are much cheaper and simpler to conduct.

2.5 Existing guidelines

2.5.1 Design guidance

There exist several papers and documents regarding the design of drystone walls, with many dating back to the 19th Century when construction of drystone walls was common. Burgoyne's work is notable as it was accompanied by the full-scale tests which he conducted in 1834. Burgoyne's report on his field trials (section 2.2.1) also included a discussion on the merits of various walling styles. This did not relate solely to the geometries of his full-scale tests, but also to the use of offsets in the internal face, which reportedly aid stability[12] (fig 2-11[12]).

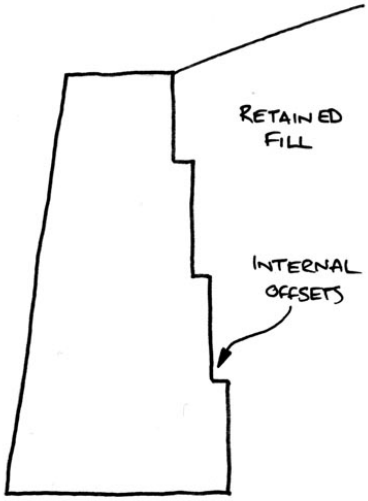

Figure 2-11: Wall design with offset internal face

Burgoyne also notes that it is often newly constructed walls which display movement and bulge, and that temporary shoring may sometimes be necessary. In his paper he gives anecdotal evidence of a freshly constructed wall which began to bulge shortly after completion[12]. The wall was shored up with timbers for several months, at which point the supports were removed and the wall remained stable. A primary reason for this is due to settlement of the retained fill. Upon placement, the backfill is likely very loose, and so applying a relatively large horizontal force upon the wall. However, over time the backfill would consolidate, reducing the resultant horizontal force on the wall. In addition, the subsequent settlement will cause a vertical force to be applied to the internal face of the wall, which further aids stability.

Several documents and papers published in the late 19th Century give recommended dimensions for the construction of drystone walls. These recommendations include verticality of the faces, the use of offsets (or counterforts), inclination of the bedding planes and typical thicknesses for any given height. Some of the notable documents include "Road making and maintenance" by Aitken[4], "Retaining walls - an attempt to reconcile theory with practice" by Constable[16], "Useful formulae & memoranda" by Molesworth[26] and "The civil engineer's pocket-book" by Trautwine[27]. These papers were all published between 1876 and 1900, and give detailed notes for the construction of drystone walls for most situations. Several include design charts which allow engineers to determine the required thickness for walls with a particular batter, or vice-versa.

The modern design guidance takes on a remarkably similar appearance as that produced in the 19th Century. "Pierre seche", published by the Ecole National des Travaux Publics de L'Etat (ENTPE), gives design charts detailing specific height

to thicknesses ratios for walls of varying batters (figure 2-12)[13]. Each chart shows the design curves for walls between 1.5m and 6m tall, in 0.5m steps. The specific chart in the series required is determined by the batter on the internal and external faces (e.g., 10% gradient on the external face, 0% on the internal face). Finally the minimum base thickness required is given by reading the value on the Y-axis at the intersection of the desired wall height and the angle of friction of the backfill.

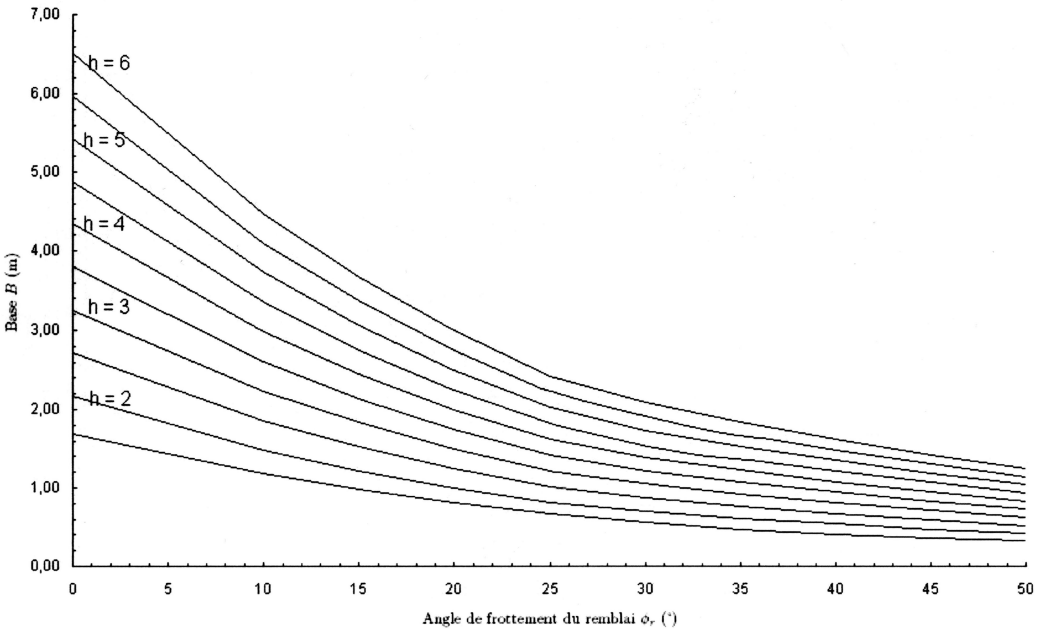

Figure 2-12: Example of a design chart from Pierre Seche

The design charts shown in figure 2-12 were created using the basic limit-state theory discussed in section 2.3.1. That is to say that the wall is assumed to resist both sliding and overturning as a monolithic structure and with a sufficient factor of safety.

With regards to the actual details for the construction of drystone walls, there are several published works. These are not recognised standards, however many are endorsed or written by groups such as the Drystone Walling Association of Great Britain (DSWA), or the British Trust for Conservation Volunteers (BTCV). For example, "Drystone walling: A practical handbook" by Agate and Adcock [2] and "Building and repairing drystone walls" by Tufnell [28] are endorsed by the DSWA and the BTCV respectively, and written by practising masons. In these books, traditional building methods as described in section 1.2 are given, aimed at both professionals and beginners alike. Historically, these practices would have been passed on to masons during apprenticeships. Although it is still possible to apprentice as a drystone mason and work under the tutelage of an experienced waller, this has become far less common. As a consequence, the aforementioned books become of much greater importance, providing key details for novice masons. They are, however, mainly focussed on free-standing walls rather than retaining

structures.

2.5.2 Current assessment guidelines

There are few specific documents dealing with the assessment and monitoring of drystone walls. BS7370 part 2[29] - which concerns grounds maintenance - states that "...stone walls should generally be treated in the same way as concrete structures." By these recommendations, cracking and spalling are highlighted as major problem areas and should be treated with epoxy mortar and resin based cements[29]. However, as drystone walls are unmortared, it is often difficult to differentiate between developing cracks and construction flaws. Also, it has not been proven conclusively that pointing of the external face with mortar is beneficial to drystone structures, and it may even reduce the wall's capacity by limiting drainage (as discussed in section 2.5.3). With regard to bulging and deforming, only vague guidance is given in BS7370, stating that, "If retaining walls show signs of movement, expert advice from a structural engineer should be sought to ensure that they do not constitute a safety hazard." It should be noted that in many cases, problems surrounding the stability of a retaining wall are the result of the soil conditions, and so geotechnical advice may be of more use.

Currently, most drystone walls are assessed using the guidelines relating to their location. E.g., for those drystone walls along the UK's highway network, documents such as "Management of highway structures: A code of practice" [30] and "Inspection manual for highways structures" [31] are used. Whilst neither of these documents specifically mention drystone walls, the guidance is often used to determine the frequency of inspections and the criteria to be assessed.

The inspections advised by the various infrastructure documents generally consist of routine inspections, with periodic principal assessments. For roads and railways, these principal assessments should be conducted every six years irrespective of size, whilst for canals they may be as infrequent as once every 20 years (depending on quality). All of the codes advise that the engineers conducting the routine inspections be vigilant for developing structural issues, such as:

- water flow and seepage
- evidence of movement, sliding, bulging deformation and cracking
- ground movements
- increased surcharging above the wall
- wall or backfill settlement
- growth of vegetation
- missing or deteriorating masonry

In the recent CIRIA guide "Drystone retaining walls and their modifications"[1], the relative benefits of these assessment guidelines are discussed and elaborated upon. It is suggested that the nature and frequency of the principal inspections should be weighted with regard to the potential risk of the structure. This includes both the size of the wall, and the potential for loss of life or damage to surrounding structures should failure occur (table 2.7[1]).

Table 2.7: Risk categories for drystone walls

Category	Height of wall	Location
A	Exceeding 3m	Walls above or supporting locations frequented by people such as infrastructure, habitations, footpaths etc.
B	3m or less	
C	All heights	Walls abutting agricultural land not frequented by people

When wall failure is not an immediate concern, but the stability of structure is in question, careful monitoring is often employed. The CIRIA guide provides some guidance on this topic, stating some of the methods which may be used, and their frequency. It advocates reviewing the stability of the structure in question either weekly or monthly as appropriate, at the simplest level involving visual inspections and photographic documentation. Details of the current condition and critical aspects of the structure should be noted and compared with previous records.

When a more detailed study of the progression of deformations or cracks is required, or long term monitoring of a wall is necessary, more advanced inspection methods may be employed. These may consist of simple telltales, which can be used to monitor crack widths and movement of adjacent stones. A more precise version of this would be to employ demountable mechanical extensometers (demec guages) over points of interest. For larger deformations and movements, standard surveying techniques may be employed, e.g., through the use of theodolites, taping and electronic distance measurement (EDM). However, the use of surveying techniques is reliant on having a static reference point.

Case study: Great Zimbabwe National Monument

The National Monuments of Great Zimbabwe are free-standing drystone walls, ranging from 1.5m to 10m in height. These walls are in various states of decay, and several sections have previously collapsed[25]. In order to determine which areas were in greatest need of repair and replacement, a monitoring system was set up by Walker and Dickens to record the walls' movements[25]. Around 650 individual points were monitored using demec gauges in 43 locations, measuring both in-plane and out-of-plane movements over a period of five years. Walker and Dickens collected the movement data in addition to rainfall and temperature records, in an attempt to identify any external changes during periods of instability.

This work is an example of effective use of relatively simple monitoring techniques to identify the critical locations in a vast series of structures (the walling covers an area of of 70 hectares). The collated data indicated that roughly a third of the 43 locations were displaying movements. Furthermore, the majority of these movements occurred after periods of heavy rainfall, as the frictional resistance of soil infilled joints was dramatically reduced. From the gathered data, three sections were determined to be in immediate danger of collapse and were rebuilt.

Case study: Kwun Lung Lau landslide

On the 23rd July 1994, a landslide occurred in the Kwun Lung Lau housing estate in Hong Kong, killing five people and injuring three more. The incident involved the collapse of a pointed masonry wall over 100 years old, and was investigated by the Geotechnical Engineering Office (GEO)[32].

The wall itself was 10.6m at its highest point and battered at 15^o from vertical. The thickness was measured to be between 700mm and 800mm, causing it to be extremely slender. Above the wall, the ground was 2.5m to 6m high, sloped at an angle of 20^o to 50^o to the horizontal and covered with chunam[3][32]. It was also discovered through historical photographs that several changes were made to the surrounding area after the wall was constructed, including the development of a housing estate and an excavation of the natural slope above the wall.

The landslide occurred after record amounts of rainfall in the previous two days, totalling 915mm. In this time, eye-witness reports stated that muddy water was issuing from the weepholes near the toe. In the hours prior to failure, further reports stated that a 1m hole in the chunam had appeared and that the muddy water was seeping through both the weepholes and the masonry joints. This seepage rapidly increased to cover the entire area which then collapsed. Failure occurred almost instantaneously and in a brittle manner with no obvious movements prior to collapse[32].

The failed section of wall had been part of a routine inspection process between 1980 and 1994, whereby it was reportedly in good condition and displaying no signs of distress. The only recommendations made were the removal of unplanned vegetation and clearance of weepholes. In the inspection during the year of the collapse, some signs of distress were recorded, including localised settlement near the crest, cracking in the chunam cover, unplanned vegetation and leakage from a nearby manhole cover[32].

The GEO inquiry following the collapse included a detailed geotechnical investigation of the site, investigating seepage, ground-water and foul-water pathways and material tests on both the fill and walling material. A numerical study using UDEC was conducted based on these data, modeling both the wall failure itself

[3]Chunam is a mixture of cement, hydrated lime, non-organic soil and water, and used to form an impermeable barrier on a surface

and the potential seepage patterns of the surrounding area.

It was concluded that the failure was due to the saturation of the ground, which caused a loss of soil suction, and reduced its shear strength. The subsequent increase in the active earth pressure then caused the brittle failure of the wall. This saturation was potentially due to a combination of unseasonably high rainfall combined with major leakage of the foul-water sewer running near to the site[32].

The work conducted by Wong and Ho highlights the need to have a thorough understanding of all the facts before assessing any masonry structure. The historical additions to the site occurred 25 years prior to failure, and so although not directly responsible for the failure they would have undoubtedly decreased the structure's stability or its susceptibility to other influences. The seepage patterns of the various water flows were deemed a critical influence on the wall, channeling the rainfall behind the wall. Once this was combined with the presence of a damaged water pipe, collapse occurred.

Failure occurred in a brittle fashion, and was perhaps due to the fact that the wall was pointed. Pointing of the wall may perhaps have caused the wall to be slightly more stable, however as a consequence it did not allow any movements to occur prior to collapse. Had the wall been unmortared, it may have deformed as the stability was reduced, giving an indication of the failure to come. Moreover, had the wall been left unmortared it is possible that the collapse may have been averted as the structure would likely have been more permeable, dissipating any build up of pore water pressures rapidly.

2.5.3 Maintenance and repair

Drystone walls have the capacity to remain stable for decades without interference. However, due to either the natural aging process, or increases in traffic loads, it is inevitable that some walls will be pushed close to or beyond their tolerances, requiring either maintainace or repair. The CIRIA guide displays a graph which demonstrates the need for maintenance and renewal (fig 2-13[1]).

General maintenance procedures as advised by the CIRIA guide, consist of occasional pointing and clearance of weep-holes or drainage[1]. Generally, drystone walls should be free draining, and as such drainage should not be an issue. However, if the wall has been pointed or grouted, or if the joints should become infilled with soil, drainage may be necessary to prevent the build-up of pore water pressures, and as such should be kept free of any blockages or debris. The issues arising from pointing or grouting are discussed in the next section.

Pointing and grouting

Pointing and grouting are techniques commonly used to repair or increase the stability of drystone walls by limiting rotation of the stones and providing additional

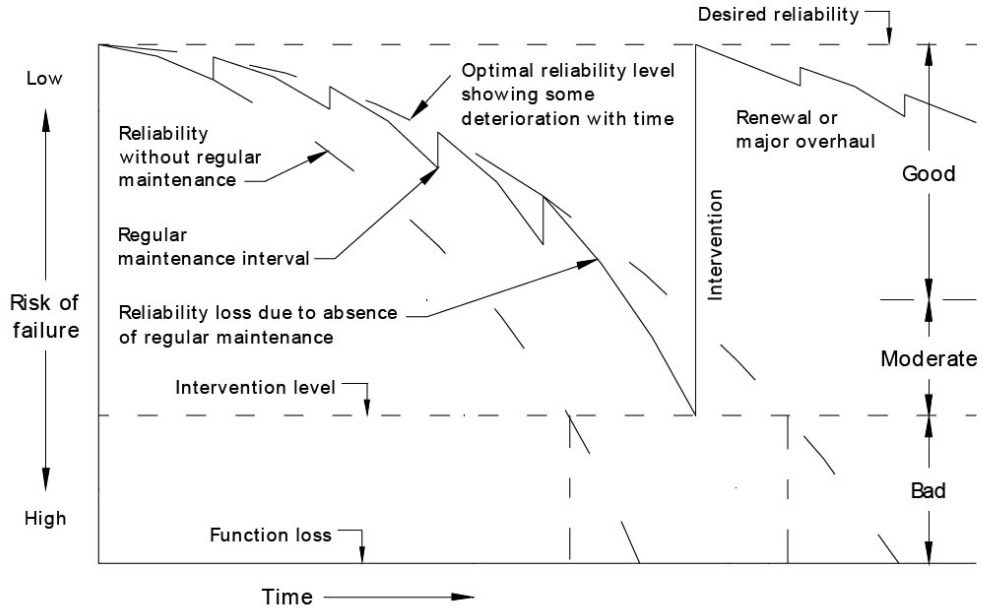

Figure 2-13: Maintenance and repair of drystone walls

shear resistance. The CIRIA guide acknowledges the issues which arise due to filling the joints and essentially creating an impermeable barrier for water, stating that alternative arrangements should be made for the drainage. One option suggested is to point alternate joints, thereby leaving many free draining areas in the structure[1].

Pore water pressures are undoubtedly critical factors causing instabilities within drystone walls, even over localised areas. This is highlighted by anecdotal evidence given in the CIRIA guide[1]. A section of drystone wall along the Macclesfield canal at Richmond Hill, Cheshire, was seen to be in distress, and was pointed as a remedial measure. This portion subsequently collapsed, and was replaced with new, mortared masonry. This section again collapsed, owing to the build-up of water pressures which could not dissipate quickly enough.

The second factor to consider with pointing and grouting is the lack of flexibility within the repaired section. As discussed in chapter 7, bulging within a wall may increase stability, therefore pointing may initiate a failure prematurely. More importantly, deformations within a drystone wall can be used as indicators of stability; bulging may be monitored over time to determine if it is progressive or merely adjusting to the applied loads (as demonstrated by Walker et al.[25]). As a consequence of pointing or grouting, the wall behaves monolithically, and so may give little or no indication if a failure is imminent.

Soil nailing and anchoring

Soil nailing has become an established method of strengthening existing retaining structures. Soil nails are used to anchor unstable slopes into the more unstable

ground behind. With soil nailing of drystone walls, both the wall and the potentially unstable slope behind the wall are anchored in place.

A case study is given by Whyley[33], whereby an old masonry retaining wall was anchored with both glass reinforced plastic (GRP) and Ischebeck Titan nails, which were grouted into place. Spacings of 0.75m vertically and 1.5m horizontally were used over the structure, which varied from 2m to 5m in height. Following this remedial action, it was determined that the movements which had previously been occurring had been halted. Whyley's work indicates that soil nailing may in the correct circumstances prevent failure, however without thorough site testing it is unclear just how effective soil nailing is[33].

For soil nailing to be effective, the wall must be be able to transfer load into the inserted nail. This will only occur if the wall moves after the soil nails have been inserted, creating a reinforced soil block behind the drystone wall. Although only a small number of blocks will be physically restrained by the soil nail, the loads on any adjacent stones will also be relieved through joint friction. If required, each nail may restrain a larger number of blocks with a larger head plate, however these are unsightly and not ideal for preserving the wall from a heritage point of view. The alternative is to use more nails, at a consequently higher cost. As previously mentioned, the lack of specific test data is a significant issue, and must be rectified before this method of stabilisation can be adopted for drystone walls efficiently and with confidence.

Modification of wall geometry

Rebuilding a damaged wall like-for-like can often be the most valid solution, assuming that the reasons behind the initial deformations are known and that a potential repeat of the circumstances can be avoided. There are many advantages to a simple rebuild, one of the largest reasons being cost. Where a section of wall has collapsed, it may be possible to reuse the collapsed stone. Although some small site equipment may be required to restore the backfill to its previous height, this on the whole eliminates the need for plant, equipment or materials to be brought to site and requires only a mason to rebuild the wall. This is particularly appropriate for walls in inaccessible locations. There is limited environmental impact from the rebuild or associated carbon footprint and it maintains the natural heritage of the original structure. Finally, there are fewer bonding issues between a rebuilt section and the surrounding walls, as it is often difficult to knit different materials into existing walls.

The CIRIA guide recommends rebuilding in addition to other remedial options like thickening the wall or adding buttresses. All of these solutions may be valid for distressed or collapsed portions of wall. Buttressing may help to stabilise sections of the wall and add sufficient mass to prevent failure, although it may be possible for the panels between buttresses to deform and bulge. Overall thickening can often

be an excellent solution, as it both adds mass and also gives the retaining wall's restoring moment a larger lever arm and hence may increase the safety dramatically. However, the typical thickening measures adopted by many agencies and county councils involve a mass concrete filling between the existing wall and a drystone facing; in these cases adequate drainage must be ensured as the mass concrete fill will otherwise allow the build-up of pore water pressures.

2.6 Conclusion

Until recently, much of the work regarding drystone walls has been related to the use of static equilibrium techniques to determine the optimum geometry for walls of various heights. With the development of numerical packages such as UDEC, more advanced studies have been carried out, mainly with regards to Burgoyne's field trials. From this work - in particular the parametric studies - some of the more important aspects of drystone structures have been ascertained. Packages such as UDEC are extremely useful, however they are not ideal for the analysis of in-situ walls were cost and time are issues. Conversely, the more simple static equilibrium and yield design approaches - which consider the wall to be a monolith - are perhaps too simplistic, and may not give an accurate indication of the stability of the wall. The three-dimensional behaviour of drystone walls is currently an area where very little research has been conducted to date. Through the research in this thesis it has been proven that modelling drystone walls in two dimensions can lead to an underestimation of a wall's capacity and a misinterpretation of its stability. However, it is very difficult to model these effects, as they currently require either realistic physical recreation of in-situ walls, or advanced numerical models which are expensive to create and run. Despite these issues, the three-dimensional nature of drystone walls cannot be ignored, and future research should consider this aspect of their behaviour.

The main issue with the research conducted to date is that very little involves full-scale physical testing. These tests are critical, and can be used to validate any current or proposed assessment techniques. This is doubly important in the development of wall stabilisation techniques. Many products are now used to stabilise distressed or deforming drystone walls, however there are no purpose-conducted tests into the effectiveness of these measures, particularly in long-term use. The difficulty in gathering data of this nature is that it is generally expensive to conduct full-scale drystone wall tests. This is particularly true if modern scientific techniques are used to monitor the walls, but without such data many walls perceived to be in danger will be rebuilt with modern building techniques rather than simply stabilised.

One of the goals of this project was to develop techniques that may be used to assess the stability of walls of any age and condition - preferably at a low cost.

It has been found through this thesis and other work (e.g. that of Cooper[18]), that it is possible to use a basic static equilibrium approach to give a realistic assessment of a drystone wall. Factors such as the three-dimensional nature of in-situ walls have not yet been successfully incorporated into a static equilibrium model, however with sufficient testing this may happen in the future. It is unlikely that any analysis technique will be developed to model every aspect of a particular drystone wall, but with sufficient test data it is possible for a model to focus on the critical elements, and therefore be of most use.

Chapter 3

Laboratory testing

3.1 Introduction

This chapter covers the various laboratory tests which have been conducted in conjunction with the full-scale tests. This includes the material testing on the elements of the full-scale tests, as well as small-scale tests which investigate the repeatability of drystone wall behaviour using much simpler and smaller walls. In addition, a series of voidage tests were conducted using full-scale replicas of wall sections. These data were all then used in conjunction with the full-scale test data to analyse drystone wall behaviour and highlight the critical factors.

3.2 Materials testing

3.2.1 Test materials

The primary walling material was supplied by the Cotswold Natural Stone Ltd. The company specialises in providing different grades of material for different applications, and is obtained from Grange Hill quarry in Naunton, Gloucestershire. The stone type utilised by the project was an oolitic limestone, which is approximately 165 million years old and was formed in the Jurassic period[34].

The quarry offers three types of limestone, differentiating in both strength and colour. The grey variety is generally considered the hardiest, with the creamier coloured stone being weaker and more susceptible to damage and weathering. As it was planned that each subsequent test wall built during this project would reuse the material from the previous wall, the grey variety was selected for use.

Over 35 tonnes of walling material were delivered to the project site, with approximately 30 tonnes used per wall (varying depending on the sectional depth). The stone was delivered undressed, and consisted of generally large, plate-like slabs. Sizes of 300mm by 300mm to 400mm by 400mm were common, with thicknesses of approximately 100mm(fig 3-1).

The fifth wall test described within this thesis utilised Mort Slate throughout

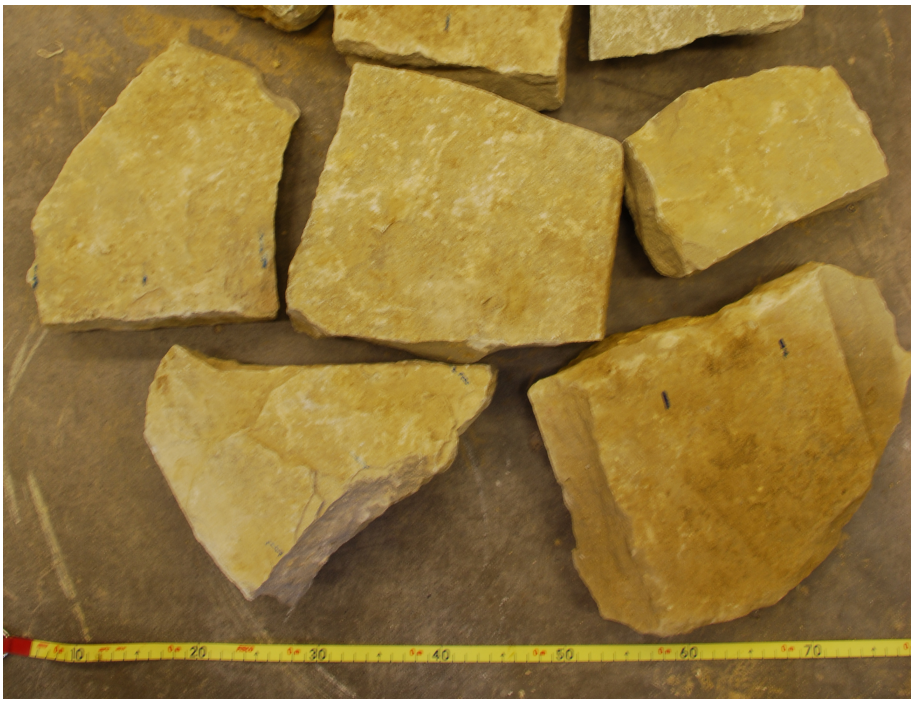

Figure 3-1: Samples of quarried limestone

the main central portion of the wall. This slate was quarried at Combe Sydenham, in Taunton, Somerset. Approximately 20 tonnes were used for the construction, some of which consisted of very large slabs (some with dimensions in excess of 1m) which had to be broken into smaller pieces before use. As each slate block was made up of several thin layers, the stone was highly susceptible to delamination if shaped. The wing walls for this test were constructed with limestone, merely providing sufficient mass to retain the backfill at each end of the test.

Ideally, each wall would have been backfilled with a cohesive material, as this would be more representative of the county's existing in-situ walls which retain earthen banks. However, the use of a cohesive material gives rise to a number of problems, mainly regarding the effects of water. As the test area was recessed into the ground (see chapter 5), a cohesive fill may have encouraged the development of a water table given enough rainfall. This would then cause additional loads to be applied to the wall, which would have to be monitored and accounted for. However, more important are the effects of soil suction and the saturation of the fill. Where the soil is completely saturated, soil suction will not be able to occur, and will consequently have a lower shear strength. Had the tests utilised a clay-like backfill material and been subject to heavy rainfall, it would have been impossible to assume uniform behaviour throughout the backfill. This would lead to problems in their analysis, and make the verification of assumptions and theories much more difficult.

To counter the effects of water on the full-scale tests, a free draining granular

backfill material was adopted. Ideally, a rounded aggregate would be used, providing an angle of friction similar to that of a loose cohesive backfill (30^o-40^o). However, the cost implication of procuring an aggregate of this quality was considered excessive. Instead, a 14mm single-sized limestone aggregate is used. This material, although angular, provided the free-draining behaviour necessary to eliminate the build-up of water pressures. Approximately 110 tonnes of the aggregate was used to completely fill each retaining wall to the required level.

Although the use of a granular material is not representative of many existing in-situ walls, it does not reduce the usefulness of the results obtained in this project. This is due to the research being focussed more on the behaviour of the wall, and its reaction to pressures exerted from the backfill, rather than on the behaviour of the backfill itself. A granular backfill is more predictable than a cohesive soil, and therefore the interaction between the wall and the backfill may be assessed with greater reliability. The complications arising from cohesive soils and the presence of water were not to be addressed by the physical testing described in this thesis, but instead in the previously mentioned numerical testing conducted by John Harkness of Southampton University (results yet to be published).

3.2.2 Limestone walling material tests

Initially, the density of this material was determined. As the stone was very durable, it was possible to accurately produce several small samples using a stone cutter on some of the larger slabs of rock . The samples were dried in an oven until consistent mass readings were ascertained and then measured using a digital caliper to determine their volume. The results are displayed in table 3.1. The limestone was relatively variable, with the six samples having a mean of 24.6kN/m^3 and a standard deviation of 0.33kN/m^3.

Table 3.1: Density determination of limestone samples

Sample	Dimensions(mm)			Volume	Mass	Unit weight
	Width	Length	Height	($m^3 \times 10^{-4}$)	(g)	(kN/m^3)
1	102	152	61	9.46	2343	24.3
2	103	104	33	3.53	904	25.1
3	101	099	58	5.80	1427	24.1
4	038	273	42	4.30	1091	24.9
5	090	094	84	7.09	1768	24.4
6	076	076	81	4.68	1178	24.7
Mean						24.6

The angle of friction of a limestone joint was then ascertained using a series of shearbox tests. This involved a 100mm x 100mm shearbox as demonstrated in figure 3-2. Cut samples of limestone were then subjected to varying normal stresses and increasing shear stresses until shearing occurred. It should be noted that the analysis assumes that the normal and shearing stresses are applied evenly over the

joint, as shown in figure 3-2. However, in reality it may be the case that the vertical distance between the horizontal applied load and the joint may induce a moment, hence giving a variation in the stress distribution over the joint. In an attempt to eliminate this effect, the shearing load is applied as close as feasibly possible to the joint, hence reducing this effect. The results are shown in figure 3-3, with a calculated friction angle of 24.5^o.

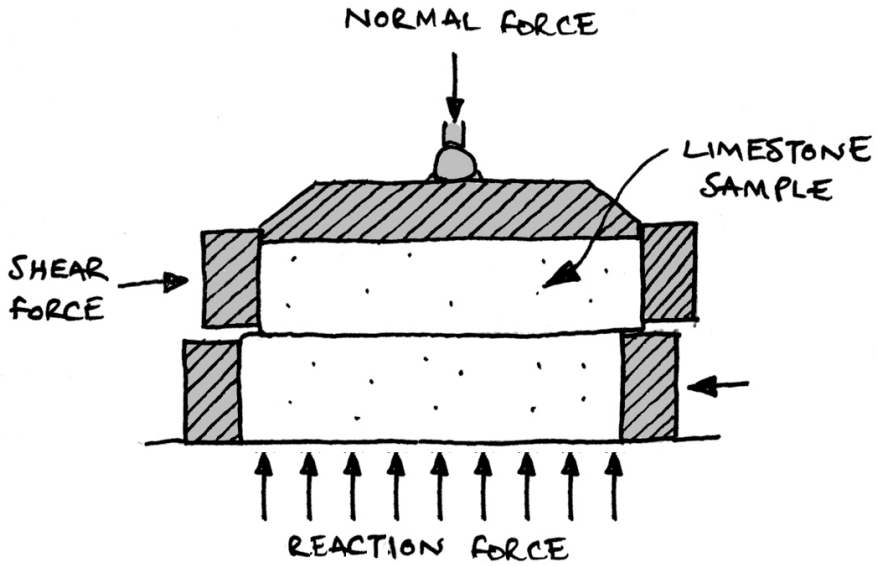

Figure 3-2: Test setup for limestone shearbox tests

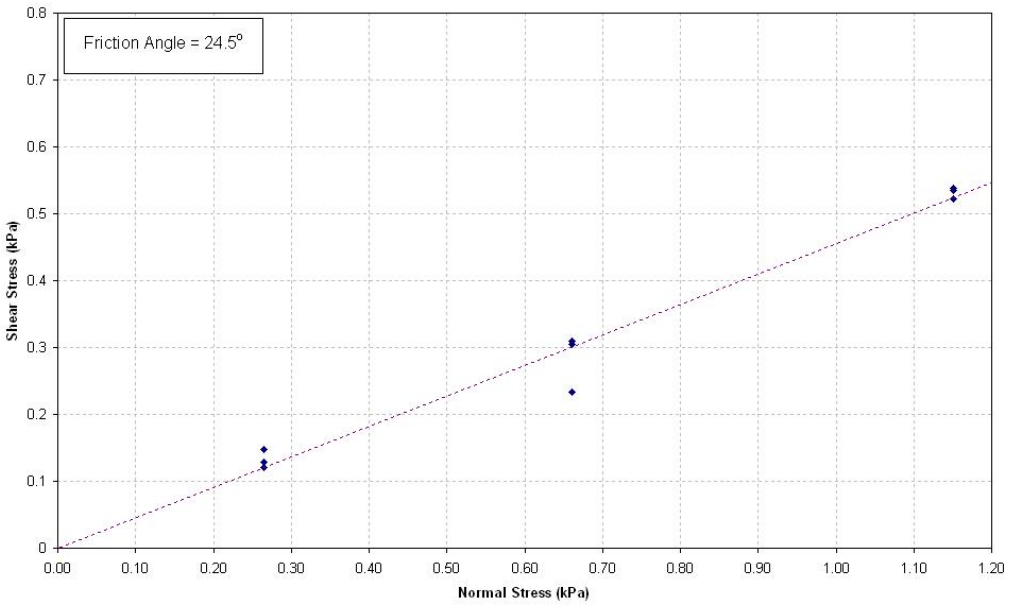

Figure 3-3: Results for limestone shearbox tests

As the shearbox tests utilised cut samples of stone, it may not be representative

of the behaviour of the real stones due to imperfections and uneven surfaces. Also, the cutting of the stone causes a fine layer of grit and sand on the sliding surface. Despite extensive washing and drying, this was still in evidence during testing. As a consequence, the failure occurs along this plane of sand and dust, rather than between stone-on-stone contact. To compare, a series of simple tilting tests were conducted, using samples of the limestone as quarried. Three large stones were selected as bedding planes, with six smaller samples used in conjunction. Each of the bedding stones was fixed in turn to a wooden board for ease of handling, with a smaller stone resting on top. The bedding stone was gradually inclined until the smaller stone began to slip, and the inclination recorded (fig. 3-4). The mass of each sample is known, and the inclination at failure is used to determine both the shear and normal stresses at work. Each of the six sample stones was tested six times on each of the three bedding stones, giving 108 individual sliding tests. The results are shown in figure 3-5. The test uses the self weight of the stone being tested to provide both the normal and shearing force. As a consequence, an increase in the inclination of the bedding stone simultaneously increases the shearing force whilst reducing the normal force. This is shown in figure 3-5 as the results from each series of stone tests forms a group which is inclined in the opposite direction to the overall angle of friction.

The friction angles obtained range from 39.9^o to 52.9^o, with an average of 46.4^o. These friction angles are higher than those obtained by Walker et. al.[25] and Villemus[35], who determined friction angles of 34^o and 36^o-38^o respectively, although this was for samples of granite. As the tilting test closely represents the real ineractions that would occur within a wall (i.e. involving uneven surfaces and potential interlocking elements), these results were used when assessing the full scale tests. This also negates the potential innacuracies caused by the previously discussed uneven stress distributions inherent in a shearbox test.

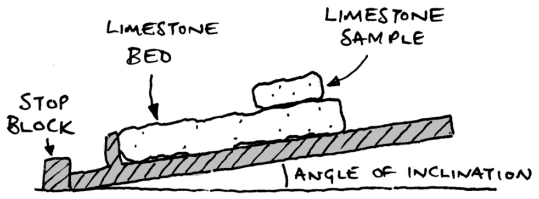

Figure 3-4: Test setup for limestone friction tests

Subsequent tests involved measuring the unconfined compressive strength and the flexural strength. The unconfined compressive strength was measured using a Controls Automax 2000kN compression testing machine on 11 samples of various sized samples of oven-dried limestone. The results are shown in table 3.2, and give a mean compressive strength of 70.1N/mm^2 (70,100kN/m^2). The sample strength

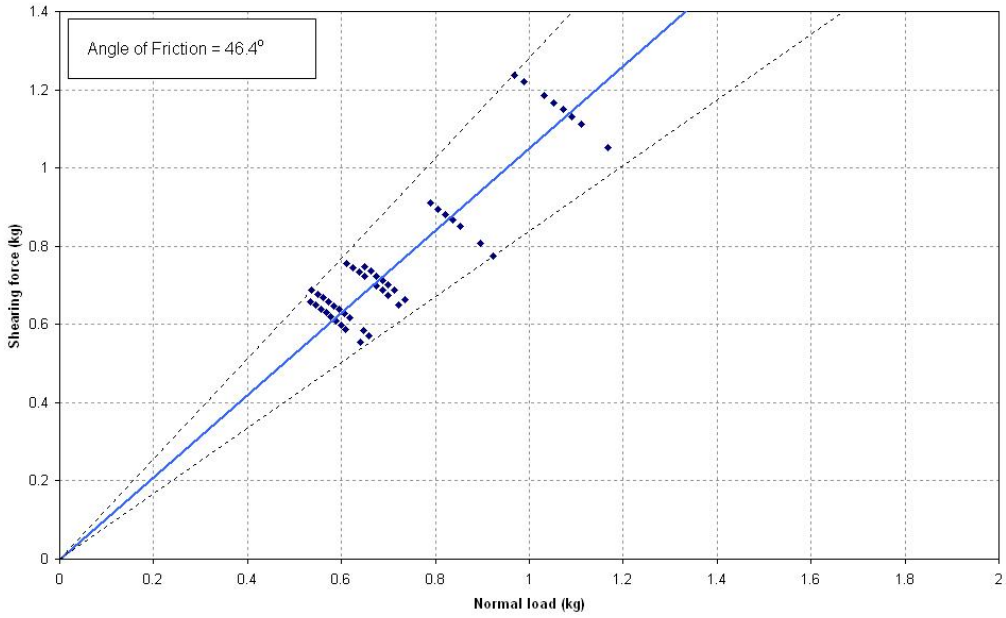

Figure 3-5: Results for limestone friction tests

was again variable, ranging from 44.3N/mm^2 to 101.3N/mm^2. By comparison with the limestone's unit weight, it is very unlikely that a wall of this material would ever fail due to crushing of the stone regardless of the total height of the structure.

Table 3.2: Unconfined compression strength of limestone samples

Sample	Dimensions(mm)			Peak Load	Peak Stress
	Length	Depth	Height	(kN)	(N/mm^2)
1	41	40	44	97.9	59.4
2	36	40	44	64.1	44.3
3	35	40	42	96.0	68.4
4	37	40	44	73.3	48.9
5	40	37	41	104.9	72.3
6	40	38	43	115.6	76.1
7	97	103	92	704.4	70.7
8	99	101	100	721.1	72.7
9	98	92	93	913.2	101.3
10	76	76	81	505.3	86.9
Mean					70.1

Finally the tensile strength was determined by subjecting samples of limestone to three-point bending tests in a Dartec 1000kN loading frame with an Instron 88 control unit. The results are shown in table 3.3, giving a mean tensile strength of 19.1N/mm^2. The supports were 100mm apart, with the load applied at the midpoint. It should be noted that all of the samples were tested with the bedding horizontal.

These results were then compared with the typical rock parameters for limestone[36].

Table 3.3: Tensile strength of limestone samples

Sample	Dimensions(mm)		Z	Peak Load	Moment	Peak Stress
	Width	Height	(mm^3)	(N)	(kNm)	(N/mm^2)
1	34	44	10582	7.7	0.19	17.8
2	39	46	13319	10.0	0.25	18.9
3	41	38	10000	8.2	0.21	20.6
Mean						19.1

The results are shown in table 3.4, with the values obtained by the material testing falling in between the typical values. It is indicated that the stone is a fairly strong limestone, although there is some variation between the samples.

Table 3.4: Comparison of test results with typical parameters

	Compressive Strength MPa	Tensile Strength MPa	Density kN/m^3
Limestone (Typical)	30-250	5-25	22-26
Limestone (Tested)	70.1	19.1	24.6

3.2.3 Mort slate material testing

The same parameters were tested for the slate as for the limestone; friction, density, compression strength and tensile capacity. Due to the fissile nature of the stone, it was difficult to produce samples without damaging the material. However, sufficient samples were cut and dried such that the material characteristics could be tested and compared to typical values for slate and shale. Initially, the dry density of several samples was determined (table 3.5).

Table 3.5: Density determination of slate samples

Sample	Dimensions(mm)			Volume	Mass	Density
	Width	Length	Height	($m^3 \times 10^{-4}$)	(g)	(kN/m^3)
1	99	97	16	1.57	403	25.3
2	97	98	7	0.68	180	25.8
3	97	97	8	0.73	194	25.9
4	40	43	245	4.23	1116	25.9
5	43	45	243	4.75	1250	25.8
6	42	41	246	4.31	1128	25.7
Mean						25.71

A 100mm shearbox was set up as for the limestone tests to measure the friction angle. Repeat tests with varying normal forces were conducted, using different samples of the mort slate. The faces were not cut, as it was not possible to cut the stones parallel to the direction of the bedding without causing them to delaminate. However, the natural surface of the stone was very smooth and would not have

been significantly changed should it have been cut. Figure 3-6 shows the results from the 15 individual tests, giving an average friction angle of 19.3^o.

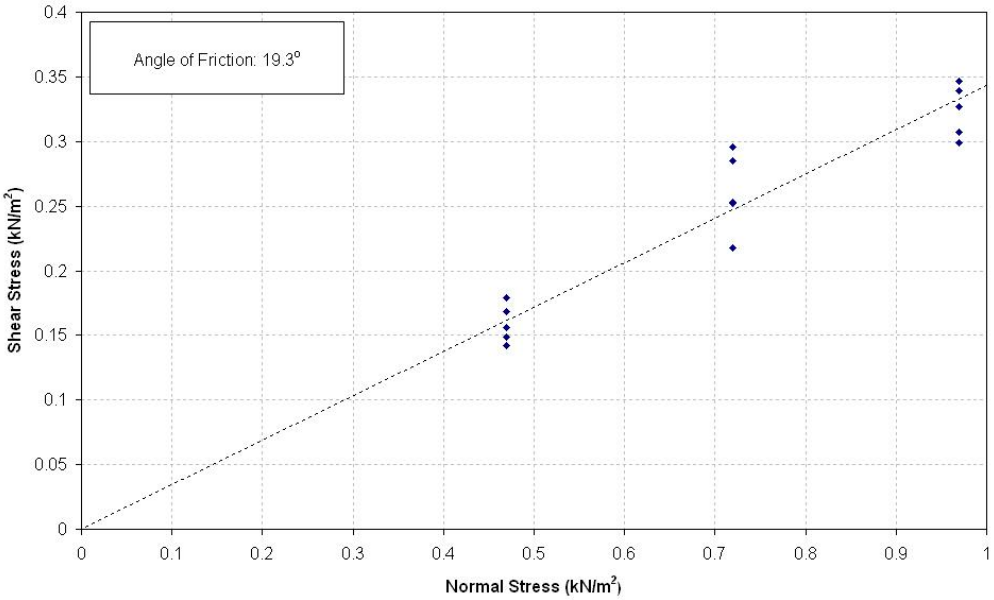

Figure 3-6: Slate 100mm shearbox test results

Compressive and flexural tests were also conducted in the same manner as for the limestone tests. The data are shown in tables 3.6 and 3.7 respectively. The mean compressive strength was found to be 82.1N/mm^2, with a dry tensile capacity of 7.74N/mm^2 (tested in three-point bending perpendicular to the bedding plane of the stone).

Table 3.6: Unconfined compression strength of slate samples

Sample	Dimensions(mm)			Peak Load(kN)	Stress(N/mm^2)
	Length	Depth	Height		
1	102	104	85	902	85.2
2	103	103	90	855	80.7
3	101	98	96	792	80.4
Mean					82.1

Table 3.7: Tension strength of slate samples

Sample	Dimensions(mm)		Z	Peak Load	Moment	Peak Stress
	Width	Height	(mm^3)	(kN)	(kNm)	(N/mm^2)
1	40	43	12415	3.92	0.98	7.89
2	43	45	14744	5.28	1.32	8.95
3	42	43	12792	3.78	0.94	7.38
4	42	41	12083	3.26	0.81	6.74
Mean						7.74

Finally the results were compared with the typical values for both slate and

shale (table 3.8). The tensile strength and the unit weight are both in the ranges normally associated with slate. However, the compressive strength is slightly below the range of values for slate, and instead falls into the category of shale. Therefore, the material is shown to be a very weak slate, and may be justifiably identified as shale rather than slate.

Table 3.8: Comparison of test results with typical parameters

	Compressive Strength MPa	Tensile Strength MPa	Unit weight kN/m^3
Slate (Typical)	100-200	7-20	26-27
Shale (Typical)	5-100	2-10	20-24
Mort slate (Tested)	82.1	7.74	25.7

3.2.4 Aggregate

As part of the project described in this thesis, an investigation into the behaviour of the aggregate used was conducted by Readshaw[37]. This included shearbox and triaxial testing of the specific gravel used in this project, and so the findings and results are reproduced in this section.

The primary tests were conducted in a 300mm diameter triaxial test rig. The main components are sketched in figure 3-7. Varying confining pressures were applied in conjunction with an increasing deviatoric stress. Due to mechanical issues in using a large angular gravel within the triaxial rig, the results do not give a linear relationship between the shear stress and confining stress. This is mainly attributed to the gravel damaging the membrane of the triaxial rig during testing at higher confining pressures[37].

Readshaw's results are given in table 3.9. By combining the results from both the triaxial and the shearbox tests, it was possible to ignore some of the erroneous results and provide a more accurate result. An average of 51^o is indicative of a very stiff material, with the fact that both the triaxial and shearbox tests where highly compacted would only further add to this.

As part of the full-scale tests conducted as part of this project, on-site testing of the gravel via a plate compaction test indicated a friction angle of 53.1^o (see section 6.2.1). This is close enough to give some confidence in these results, particularly as the gravel tested on-site was heavily compacted using a vibrating plate compactor. However, later tests of a similar nature on the uncompacted gravel gave a result of 39^o. Further discussion of these tests is found in chapter 6.

Table 3.9: Measured angles of friction

	Triaxial Test	Shearbox Test
Angular Gravel	51.0^o	50.1^o

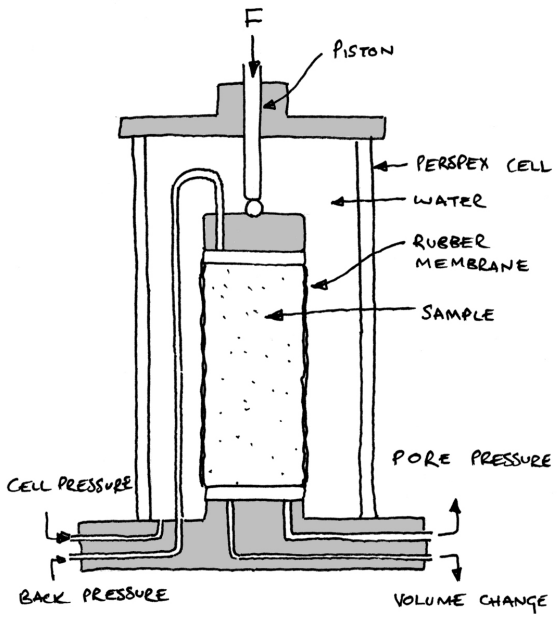

Figure 3-7: Triaxial test rig

The density was measured by filling a known volume with the gravel and measuring the mass. This was done both with the fill loosely placed and also with the fill introduced in thin layers and compacted. The results are shown in table 3.10, with a unit weight of 13.8kN/m^3 for the compacted gravel and 16.2kN/m^3 for the uncompacted.

Table 3.10: Unit weight measurements of gravel

Sample	Compaction	Volume ($m^3 \times 10^{-6}$)	Mass (kg)	Unit weight (kN/m^3
1	Uncompacted	5.96	8.30	13.7
2	Uncompacted	5.96	8.26	13.6
3	Uncompacted	5.96	8.49	14.0
Average	Uncompacted	5.96	8.35	**13.8**
4	Compacted	5.96	9.88	16.3
5	Compacted	5.96	9.93	16.3
6	Compacted	5.96	9.67	15.9
Average	Compacted	5.96	9.82	**16.1**

3.2.5 Limestone/aggregrate interface

The interface between an in-situ wall and a backfill material is an important boundary, as the friction on this interface has a substantial impact on the behaviour and stability of the wall. It is difficult to measure the friction generated for in-situ walls, as there are many factors which may alter the results; e.g., the loads measured during any shearing may indicate a greater or lesser than anticipated section of the wall, as the forces may be potentially shed into adjacent sections of the wall.

To examine as many of the variables as possible, a series of shear box tests were undertaken in an attempt to replicate this boundary.

A large 300mm x 300mm shearbox was used to replicate the behaviour of the full-size elements, as this would be difficult to recreate in a smaller test rig. The basic layout of the test is shown in figure 3-8.

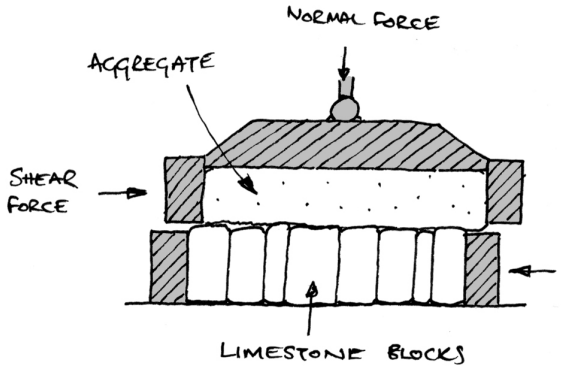

Figure 3-8: Shearbox rig for wall/backfill interface

The lower half of the shearbox was used to represent the backface of the wall. This was done by cutting several stones to fit the width of the box, and laying them in such a manner that recreated the effect of block coursing at the face of a drystone wall (fig 3-9). The individual stones were cut such that the face was flush with the lip of the shearbox, to ensure that shearing could occur without the stones resisting the movement. Pins were also used to wedge the blocks into place, ensuring that the blocks did not move in any direction during testing. Once the upper half of the shearbox was placed, it was filled with the aggregate used for the backfill of the full-scale tests and left uncompacted.

As the test is in effect a recreation of the wall interface tilted by 90^o, the normal stress in this case is equivalent to the horizontal pressure acting on the wall. Hence, the normal stresses were representative of the stresses found behind the proposed full-scale walls at varying heights. The maximum normal load applied was 150kg, equivalent to a stress of 1.27kN/m^2, which would be the horizontal pressure found at a depth of approximately 1m below the top of the fill, based on the material properties of the aggregate. This was the largest applied load that could feasibly be applied as a normal stress, as the load was applied using a static mass as opposed to loading via a jack or actuator. In this way, it was ensured that the normal stress was constant, and no errors could accrue from a fluctuating normal stress.

Four different normal stresses were applied, with each being tested six times to ensure an adequate amount of data was obtained. The friction angle was measured to be 45.9^o (fig 3-10). It is to be expected that there was a relatively large scatter of the results given the relatively unpredictable nature of the aggregate and its interaction with the wall, however sufficient data is present to justify some confi-

Figure 3-9: Recreation of stone coursing within the shearbox apparatus

dence in the results. Further support to these data is given by the closeness of this value to the friction angle measured for the limestone upon limestone tilt tests.

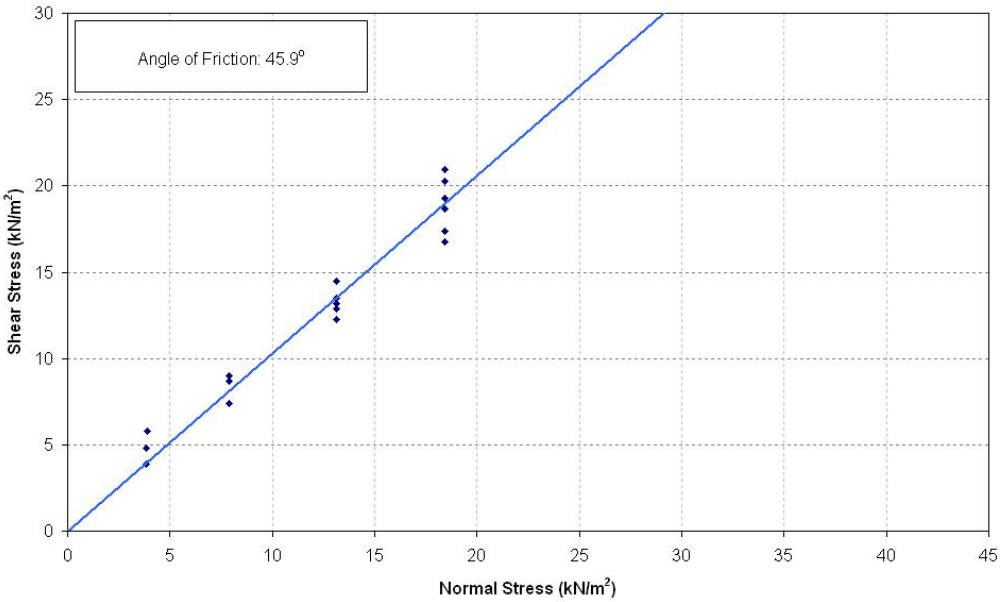

Figure 3-10: Wall/backfill interface friction

The obtained friction angle is consistent with the expected findings. Even with

the stones in a relatively level setting, there is sufficient surface roughness to ensure a high degree of friction. The value is lower than measured for laboratory tests on the gravel acting independently; again this is to be expected as a shear plane within the gravel-only tests would have a substantial amount of interlock due to its angularity. It should also be noted that the laboratory tests on the gravel involved a compacted material. For the full-scale tests - with the exception of wall 1 - the gravel was not compacted (although even with wall 1, as significant deformations took place during testing, the gravel would become loose at the contact plane between the wall and the fill). Due to this, the gravel had a lower angle of friction during the in-situ tests (39^o). Although the friction angle for the wall/backfill interface is higher than that for the loose gravel, the maximum value that could realistically be assumed at this point is that of the gravel alone. This is due to the fact that although the gravel in direct contact with the wall may have a higher friction angle, the fill directly behind this will only be in contact with gravel alone. Therefore, the horizontal and vertical forces transmitted from the backfill to the wall/fill interface are dependent on the gravel's properties, and may not exceed these values.

Should the experiment have been altered to vary the height of individual stones within the shearbox, there may have been a greater degree of friction obtained. However, this would likely be due to the staggered face forming pockets which would fill with aggregate. The shear plane would then form over a combination of both the prominent wall blocks and the gravel filling the pockets. As the non-uniformity of the wall increases, so would the angle of friction, until the shear plane is purely acting through the gravel and the friction angle at a maximum.

3.3 Small-scale test blocks

To attempt to recreate drystone wall behaviour on a small-scale, a series of tests were conducted by Bailey[38]. These were conducted within the umbrella of the project discussed in this thesis as part of a masters thesis, utilising the same equipment and resources. The main outcomes and results are reported here; a full account of the work may be found in the Masters thesis of Bailey[38].

3.3.1 Test setup

To house the tests, a steel box was constructed, with the capacity to hold scale walls 500mm in height and 500mm in width. The box was lined with a double layer of plastic sheeting, to help reduce friction at the edges and hence minimise end effects (fig. 3-11). Concrete or timber blocks of varying geometries were tested to recreate the wall material, with pellets of lead shot (2mm-3mm diameter) used as the backfill material.

Figure 3-11: small-scale testing rig

Lead shot was used due the scaling issues arising from the test setup; a standard fill would not be able to induce sufficient lateral pressures to overcome the stabilising forces generated by the scale walls. The lead shot had an internal friction angle of 31^o, with a unit weight of 50kN/m^3, generating large enough active pressures to cause failure purely by increasing the backfill height.

To ensure that the lowermost block did not fail by sliding on the surface of the steel box, a timber stopper was placed between the first block and the forward lip of the box. The calculations and results are all based on the assumption that the bottom course of the small-scale wall plays no part in the wall's behaviour, and simply provides a surface on which to base the wall.

3.3.2 Test procedure

Each test was conducted in the same manner. Initially, the wall was built up to the full height without the presence of any backfill material. Measurements were made initially by using marked points on the stiff sides of the box as references. Later tests involved the use of draw wire transducers as used in the full-scale tests (described in section 5.3.7).

The backfill was then introduced in layers and spread evenly behind the wall (fig. 3-12). As the volume of the space behind the wall was known, and the mass of the material introduced measured as it was placed, the exact backfill height - and

hence the active pressure applied - was known at all times. The backfill height was slowly raised until failure occurred, proceeding slowly to allow for any movements and the recording of the wall position.

Figure 3-12: small-scale testing procedure

3.3.3 Results

Several different wall block geometries were used, either using timber or concrete as previously described. The majority of tests utilised long wall blocks which spanned the full width of the box (500mm), but some initial tests utilised individual cubes. The block sizes for each test are given in table 3.11[38]. It should be noted that width relates to the span of the wall, whilst depth is the thickness. The results of the tests are also given in this table.

Table 3.11: Wall block geometries and fill heights of small-scale tests

Test number	Walling material	Friction angle(^{o})	Block geometry(mm)			Wall geometry(mm)		Fill height(mm)	Collapse Mode
			Width	Depth	Height	Depth	Height		
1	Concrete	29	100	100	100	100	500	NA	NA
2	Timber	24	500	50	50	100	500	185	Overturning
3	Timber	24	500	50	50	100	500	245	Overturning
4	Concrete	29	500	100	100	100	500	360	Overturning
5	Concrete	23	500	100	100	100	500	330	Overturning
6	Concrete	29	500	100	50	100	500	350	Overturning
7	Concrete	23	500	100	50	100	500	340	Overturning
8	Concrete*	29	500	50	50	100	500	355	Bursting
9	Concrete*	23	500	50	50	100	500	320	Overturning
10	Concrete* **	29	500	50	50	100	500	300	Overturning

*wall has 100mm deep through-blocks at 4th and 8th levels

**wall blocks given 10mm chamfer to all corners

3.3.4 Discussion of results

The initial tests used 100mm cubes of concrete. It was found that the blocks were arching between the sides of the steel box, and locking into place rather than failing. To overcome these three-dimensional effects, long blocks were used, each spanning almost the whole width of the steel box but with gaps at either end to allow small rotations of the wall elements. Both timber and concrete block walls were tested independently; the timber blocks were quickly discarded as their densities proved too low for realistic modeling of drystone behaviour (5.5 kN/m^3 as opposed to 24 kN/m^3 for the concrete blocks). However, this data still proves useful for comparison with the limit equilibrium program presented in chapter 4.

As a method for recreating large scale drystone walls these tests are of limited use. The small-scale tests adequately show overturning failures, however the more complicated mechanisms that occur within a full-scale drystone wall could not be replicated. Whilst wall 8 did fail by bursting, it was not apparent if the bulge was due to locking of the blocks between the sides of the steel housing box, and the results could not be repeated.

There are several issues with these tests, most relating to scaling issues. Full-scale walls comprise both very large and very small components (i.e., wall blocks and fill and pinning material), and whilst the larger blocks may be effectively scaled down, the smaller elements are then too small to model. The geometry of the wall blocks was also problematic, in that the rectangular blocks with flat planes of contact did not allow for any block rotation prior to failure. As will be discussed in chapter 7, this is of great importance in the development of more complex behaviour, and without more realistic block geometries this will not occur.

Despite the scaling problems which could not easily be overcome, this method of testing has some distinct benefits. Primarily, cost, space and time. The cost of performing these tests is fractional when compared with that of building full-scale retaining structures, requiring very small amounts of the materials to be tested, and no expensive equipment to set up each test. The spacial requirements are also much smaller, giving benefits in terms of practicality and also further cost reductions. Finally, the time and effort required to perform each test can be measured in terms of hours, rather than weeks and months. This is potentially the most advantageous feature of this style of testing, as it allows large amounts of physical data to be generated in a relatively small space of time, allowing for numerous repeat tests to confirm the results.

As the experiments progressed, each moved closer to replicating the behaviour of in-situ drystone walls. Due to the difficulty in recreating a representative drystone wall in miniature, the full range of movements required for bulge formation could not be achieved. However, this line of investigation bears the significant advantages previously mentioned, and should a suitable method be identified for overcoming the highlighted problems then it would become an extremely useful

source of data. Even in this case however, full-scale testing would still be required to ensure that the small-scale models are recreating the behaviour and failure mode found in in-situ walls.

3.4 Large-scale void-ratio tests

The percentage of void space within drystone walls is not a characteristic that has been heavily researched. Villemus et. al., measured the voids in their full-scale walls as a percentage of the overall volume of the wall[14], although there is currently no basis for comparison of these figures. Throughout the course of the full-scale tests described in this thesis, voidage measurements have been made where possible, and compared with benchmark data also gathered during the course of the project.

For the benchmark data, the masons were required to build small sections of wall within the confines of a timber frame. The internal dimensions of these frames were carefully measured (usually 700mm long and 500mm both in height and depth), so that the overall volume could be determined. Upon completion of each section, it was photographed and disassembled in layers. Each layer was graded and weighed, so that the sizes and total mass of the stones was known.

3.4.1 Limestone

The benchmark data for the Limestone tests consisted of two samples of wall built to the highest standard possible, and one wall built quickly and without care (fig 3-13). As shown by figures 3-13(a) and 3-13(b), the sections built to best practice were tightly fitted together, with each block being firmly pinned into place with smaller stones to eliminate any movement. Figure 3-14(a) shows the internal make-up of these sections to be equally well laid out, with the course infill material placed in such a manner as to reduce internal voids. The first and second samples, built using best practice procedures, were calculated to contain 21.3% and 22.3% voids per unit volume respectively. Considering the characteristic randomness of drystone walling, a 1% discrepancy shows a very high degree of consistency, and it is unlikely that identical results could ever be attained.

The poorer section, shown in figure 3-13(c), is of a much looser construction. The stones were laid with little regard for a structure of courses, and minimal pinning was used throughout. As a consequence, the blocks themselves were loose even after completion of the section, with large gaps visible between. Similarly, the internal make-up of the wall was poorly constructed (fig. 3-14(b)), with larger and more irregular fill stones being used, giving much greater voids. The voidage calculated for this sample was given as 37.4% - nearly double the value of the best practice sections.

Upon destruction of the first wall, a sample of undamaged and undeformed masonry was photographed and dismantled in a similar manner to the benchmark

(a) Limestone: Best practice

(b) Limestone: Best practice repeat

(c) Limestone: Poor construction

Figure 3-13: Benchmark void tests: Limestone sample faces

(a) Limestone: Best practice (b) Limestone: Poor construction

Figure 3-14: Benchmark void tests: Limestone internal view

samples. This section of wall, shown in figure 3-15(a), was taken from one of the wing walls, approximately 1m above the base layer. The section comprised of four courses of masonry, and was chosen such that the minimal amount of blocks crossed the sample's boundaries. Any stones which did cross the selected boundary were carefully cut at this intersection and added to the volume measured.

The difficulty with this work was in ensuring that the correct volume was obtained, as even with relatively good masonry there are undulations and outcroppings, which will alter the results. In an attempt to counter this, several readings were taken for each face of the sample, with the total volume incorporating these dimensions.

The internal configuration of the wall was shown to be somewhere between the ranges demonstrated by the benchmark tests; the fill generally consisted of small elements, filling the majority of the space, but placed without the care of the best practice samples. These observations are consistent with the eventual findings, as the voidage of this sample was found to be 28.6%, which is approximately mid-way between the best practice and poor sample voidages.

An identical procedure was carried out for the second wall. However, as the wing walls from the first wall were incorporated into the second wall to speed up construction time, the sample had to be taken from any surviving portion of the central part after testing. The maximum available section was approximately 230mm in height, enough for only two or three courses, and consequently does not give a reliable indication of the general quality of the wall. Furthermore, the sample was taken from the lowest layers, which are generally better constructed. The sample was found to contain only 23.5% voids, in addition to having a much higher percentage of rocks with dimensions over 100mm in length. With a higher percentage of large square blocks, the voidage would be naturally lower, regardless of the care of the build.

To test the third wall, timber frames were again constructed as per the benchmark tests. The masons built the sections to the same quality and speed as for the wall itself, allowing a more accurate measurement of the volume. Two frames were

(a)

(b)

Figure 3-15: Void testing: Test wall 1

used, one being 500mm wide (representing a section of the wall slightly above the foundation) and the second 300mm wide (similar to the coping level of the wall).

The style of the third wall was much looser and more quickly built than the first or second wall, and so was expected to contain a higher percentage of voids. In addition, the larger, plate-like blocks were replaced with smaller stones, giving more joints and therefore more voids, as shown in figures 3-16(a) and 3-16(b). The foundation representation was found to contain 38.3% voids - slightly higher than the poor construction benchmark section. The coping level was slightly lower with 32.3% voids (figs 3-16(c) and 3-16(d)). Again, this was expected, as due to the narrow width of the section, the same sized stones occupy a larger percentage of the volume, giving fewer joints and a lower voidage than the foundation.

3.4.2 Mort slate

As the full-scale tests also included a fifth wall constructed of Mort slate, small boxes were constructed to test the voids within walls of this material. This again consisted of two samples; one box was completed to the masons' highest possible

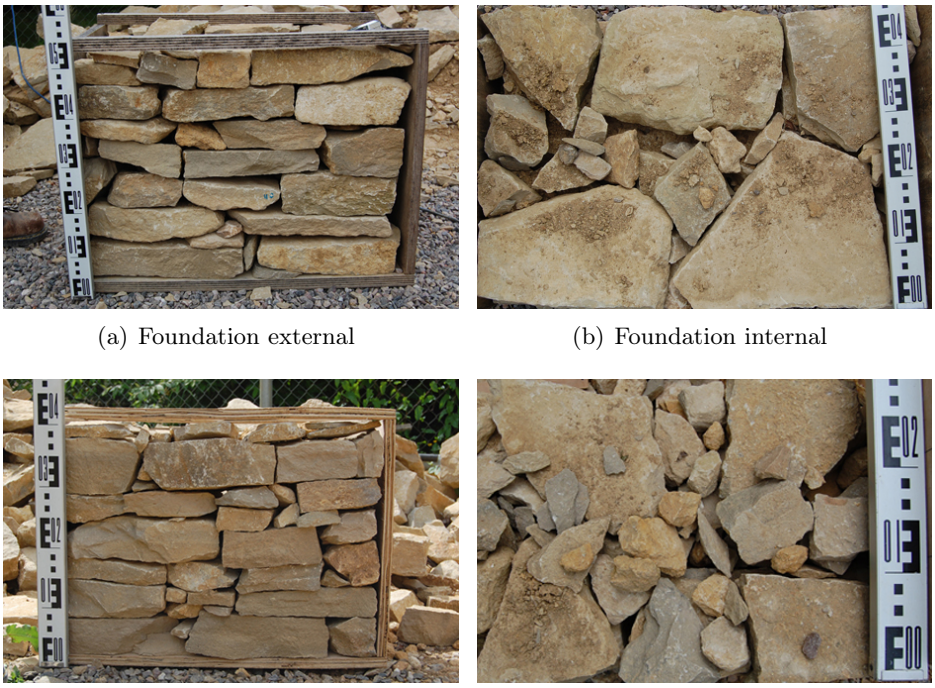

(a) Foundation external (b) Foundation internal

(c) Coping external (d) Coping internal

Figure 3-16: Void testing: Recreations of test wall 3

standard and the other was built quickly without excessive care. Figure 3-17 shows both of these samples along with an internal view.

When examining figures 3-17(a) and 3-17(c), there are not the same discernable differences that exist in the limestone samples. This is perhaps due to the quality of the stone and its tendency to split during working. However, there still exists a marked difference in the internal make-up of the walls, with the voidage of the best practice wall measured at 24.5%, with the poorer section containing 33.3% voids. Although this is a much closer spread than for the limestone, this is unsurprising given the geometry of the stones, which consist of predominantly flat blocks, rather the more rounded and uneven shapes found in the limestone. It should also be noted that the best practice wall could potentially have been constructed with a lower voidage, as each gap within the box could have been filled with the readily available slivers of slate which were created during shaping of the stones. However, this would have been much more time consuming, and not representative of a wall which would be realistically built.

3.4.3 Yorkshire stone

A final pair of test boxes was constructed using material from a limestone wall in Yorkshire which had collapsed. This material was similar to the limestone used for the full-scale tests, however the geometry of the blocks was slightly different, with several of the stones being much bigger than those of the quarried cotswold stone.

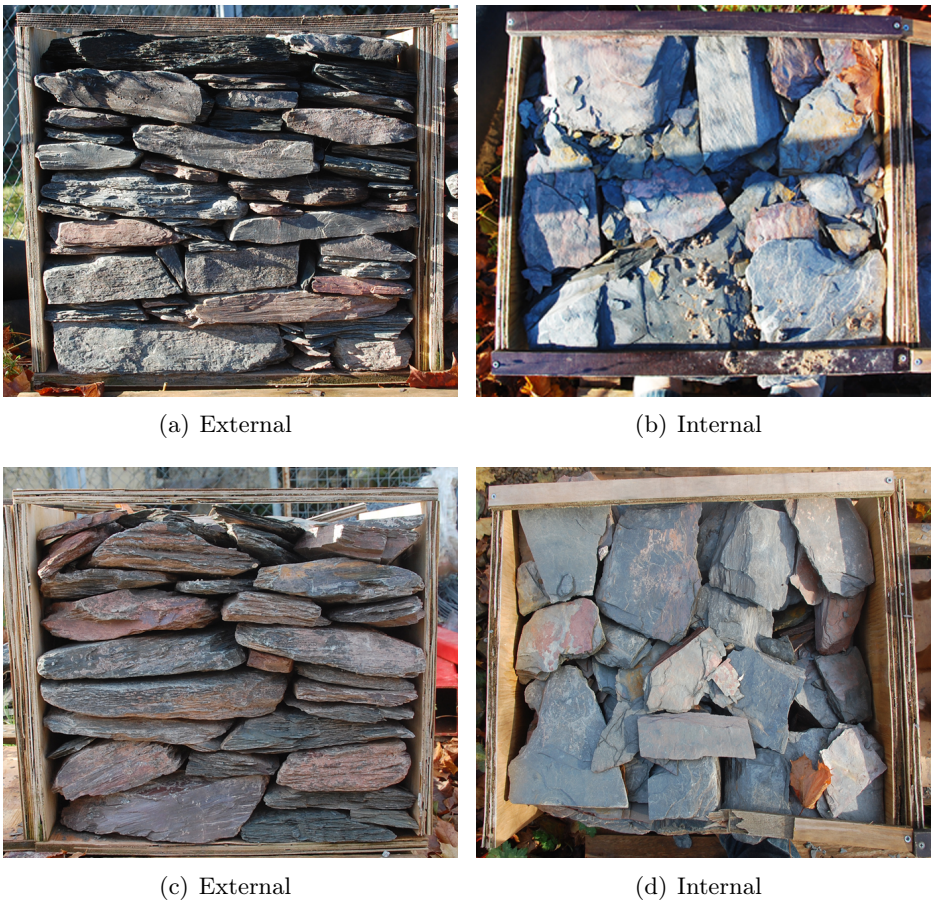

(a) External (b) Internal

(c) External (d) Internal

Figure 3-17: Void testing: Slate (a & b: best practice; c & d: poor construction

As the stones came from a wall which had been standing for some time, the blocks themselves were more weathered and irregular.

Figure 3-18 shows the internal courses and the external faces of both test sections. As with the Cotswold stone, it is easy to differentiate between the quality of the two walls, and there are many visible similarities between them. The best practice section contains more voids than the respective Cotswold box, having a voidage of 28.7%. The poorer section is similarly higher in voids, measured at 42.2%. This is likely due to the aforementioned weathering of the stones; had the blocks been freshly quarried, the stones would have straighter edges and would potentially fit together more tightly.

3.4.4 Comparison of internal and external voids

In an attempt to correlate the external appearance of a wall with the internal voidage, the limestone samples were analysed using an adapted program originally designed to produce stereo photogrammetric images from pairs of photos, written by Paul McCombie. This program allowed individual photos to be assessed, giving a ratio of the black to white spaces in the image. Each photo of the sample box

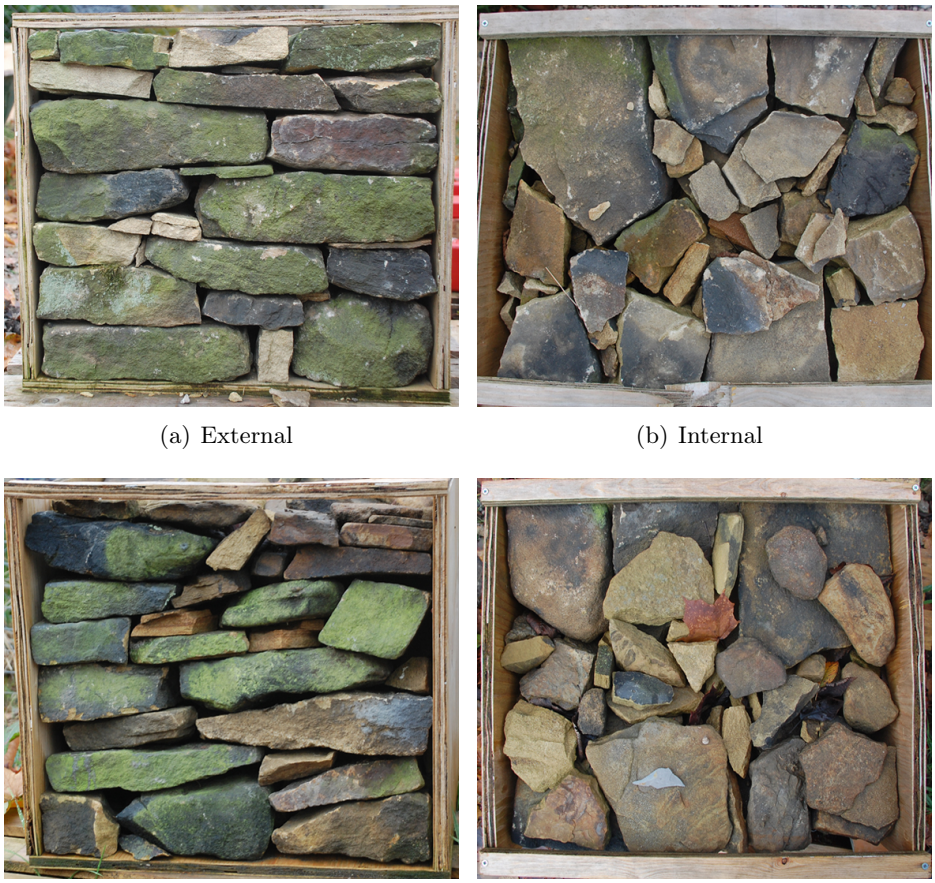

(a) External (b) Internal

(c) External (d) Internal

Figure 3-18: Void testing: Yorkshire stone (a & b: best practice; c & d: poor construction

sections was cropped so that a 400mm x 400mm section was left, and reduced to a black and white image (fig. 3-19). When reducing the image to a black and white image, it required a degree of judgement to determine where the threshold lies. For each image, a dark space may be a joint or it may be a shadow caused by overhanging blocks. In these cases a fine adjustment of the levels of the image was required to ensure that the best possible black and white representation was achieved.

Once processed, the stereo photogrammetry program was used to give a percentage of the black spaces in each image, in effect determining the voidage of the external faces. This was then plotted against the internal voids for each section, in an attempt to find a relationship between the two (fig. 3-20). This analysis was not performed on the slate or Yorkshire stone sections, as it was deemed that insufficient data were available to provide conclusive evidence of correlation.

Figure 3-20 shows a general trend, with the data set increasing linearly. Certainly at least for the samples of stone measured, there exists correlation between the voids visible at the face and the internal voidage of the wall. Although this

Figure 3-19: Black and white image of wall section

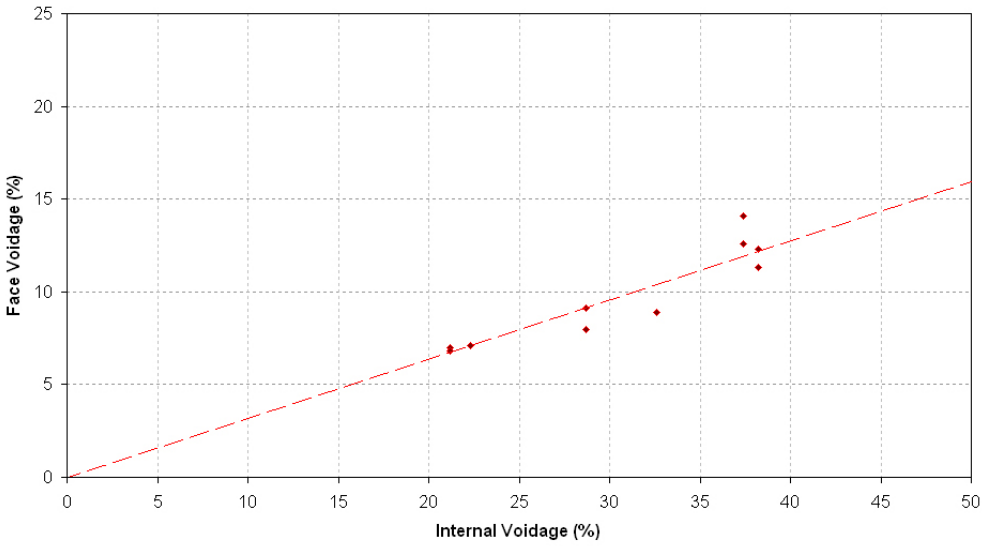

Figure 3-20: Comparison of external to internal wall voids

cannot be relied upon to give an exact answer, it may give a useful indication of the voidage of the internal structure of a wall. However, for the graph to be used at all, it is dependent on the wall being built of the same material and of the same construction style (i.e., twin leafed construction with a rubble infill).

3.5 Conclusions

Within the scope of the laboratory tests described in this chapter, all of the significant characteristics of the materials involved in the project tests have been

investigated. This includes both their individual mechanical properties as well as their interaction with one another. This data is crucial not only for the analyses conducted in this project, but also for any subsequent studies. In particular, this relates to any numerical studies, as they require values for a variety of mechanical properties for all of the materials involved for the cycles to be run.

The data obtained has also been compared with the standard values for the material as well as with similar tests which have been conducted to date. Generally the material properties have been within the standard ranges of values, except in the case of the Mort slate, which could technically be classified as a shale due to its low strength. For the limestone, although a discrepancy occurred between the shearbox and sliding tests, the higher angle of friction given by the sliding test was adopted. This was due to the inaccuracies of the shearbox testing (from grit and sand on the cut surfaces of the samples) as well as the comparative values obtained by both Villemus[35] and Walker[25].

Non-standard tests such as the interface friction angle between a drystone wall and a backfill have also been measured with success. This is generally a very difficult value to measure in practice, however through the shearbox experiments a peak value has been ascertained. As this is an important variable for drystone wall stability (discussed further in section 7.6), it is critical that this is known to allow the correct analyses to be made. Indeed, so important is this parameter to the wall behaviour that the full-scale test procedure includes steps which ensure that the peak interface friction angle is obtained.

Finally, several tests have been conducted on the wall construction as a whole. A series of sample sections were constructed, the dissection of which provided the overall mass of the walls as well as the percentage of voids within the structure. This is a quantity upon which very little research has been conducted, and in general was much higher than anticipated. For the best practice limestone sections, even given a free choice on the material used and taking exceptional care during the placement of each stone, there still existed 21% voids upon measurement. This is perhaps one of the major differences between drystone walling and standard masonry construction, and as discussed in chapter 7, one of the major reasons that allows bulges to develop.

This has been further expanded into a potential method of estimating the voids within a wall purely by examining its external face. From the test sections built by the project masons a linear correlation has be obtained, allowing a direct comparison given an image of a specific area of wall. Should this be verified with further tests and data, this could provide an excellent tool for engineers attempting to classify in-situ walls, as it could allow an insight into the internal structure of the wall without the requirement of intrusive testing. Although there is potential for significant variation from the trend line, this is perhaps not crucial, as will be discussed in section 7.6. It has been shown that the wall voidage (and hence the

density) requires substantial variation before it has a noticeable effect on stability. For this reason, even an approximate value for the internal voidage would be sufficient to give an indication of the wall stability. The major drawback of this line of investigation is that the masons cannot be relied upon to continue the same standard of workmanship throughout the wall. As it is only the external face which is visible to the observer, it would be possible for a mason to build a relatively poor wall with a high voidage, but then to pay extra care and attention to the external face for aesthetic purposes. In this case an under-estimation of the internal voids would be made, indicative of a more stable structure.

Chapter 4

Limit equilibrium program

4.1 Introduction

As discussed in chapter 2, there are currently three methods used for the analysis of drystone retaining walls:

- Static equilibrium calculations (chapter 2.3.1)
- Yield design theory (chapter 2.3.2)
- Numerical analyses (chapter 2.3.3)

Currently, the static equilibrium and the yield line approaches are the simpler options. However, due to the propensity of drystone walls to bulge and deform, a non-linear structure could become complicated to analyse with these techniques. In addition, these methods do not easily make allowances for the particulars of drystone construction, in particular that the walls are generally not monolithic, and bonded only with block friction and self-weight. Whilst numerical analysis techniques can more easily accommodate these aspects, numerical models require complex programs and an experienced operator. It may also take several hours or days to complete a single simulation. For these reasons there may be a high cost associated with numerical assessments, making them uneconomical in particular.

4.2 Program objectives

All of the options mentioned in section 4.1 are potentially viable solutions to analyse drystone structures. Currently, the main issues surrounding their applicability relate to the way that they are used or the factors of safety applied, rather than the theory involved. A basic static equilibrium assessment might assume that a drystone wall is a monolithic structure with very little interaction with the retained backfill. However, if the structure is broken down in to a series of much smaller elements, the same equilibrium equations can be used to give a much more accurate

model of the structure. Therefore, a computer program has been developed to explore efficient approaches to analysis and design which might be carried out by hand calculation or by a range of simple computing approaches. The program is designed to provide a rapid 2-dimensional limit equilibrium (LE) appraisal for structures of any size, with the ability to account for any deformations or bulges that might occur.

The focus of this program is to create a user-friendly package which can be used to quickly ascertain the critical issues relating to a drystone wall, and in particular be of use when assessing in-situ walls. As there is often some data which is unobtainable for an in-situ wall without using intrusive investigative techniques, the program has also been designed to run with minimal information. Also of importance was the capacity to allow rapid modification of the material properties, enabling parametric studies to determine the critical aspects of a structure.

4.3 Program coding

4.3.1 Programming language & workstation

The programming language used for the analysis code was Delphi, specifically through the use of Borland Delphi version 5. Delphi was used as it is a relatively fluent programming language, allowing rapid compiling, de-bugging and testing at almost any stage within the writing of the code. The workstation originally used was an AMD Athlon^{TM} XP 2500+ with a 1.83GHz processing speed and 512 Megabytes of RAM. Microsoft Windows XP Professional was the operating system (2002 version). The program concept is based on a similar piece of code originally written by Paul McCombie for research into drystone walls[7].

4.3.2 Geometry determination

As described in section 4.4.2, the geometry of the wall is determined by a string of data in a .csv file. This is then converted into co-ordinates, with each block having an x co-ordinate and a y co-ordinate for the front and back face of each block. An array captures these co-ordinates, beginning at the topmost block and progresses down the lowest block whose base is at $y = 0$. As in figure 4-1, the counter $[count]$ is used to denote which level of the wall is being examined, ranging from $[count] = 0$ to $[count] = N$, where N is the total number of blocks.

The area and the centroid of each block can be calculated from these four co-ordinates. The area is assumed to have a unit depth to give a volume, and is then multiplied by γ_{stone} to determine the block weight (W), and multiplied by the horizontal distance between the centroid and $xf[count]$ to ascertain the resisting moment against overturning.

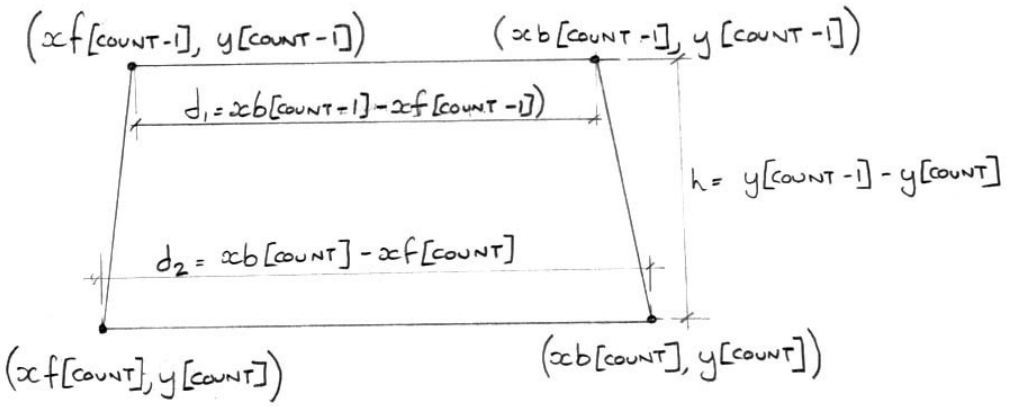

Figure 4-1: Calculation of block co-ordinates and area

4.3.3 Pressure coefficients

As the effects of wall friction have been demonstrated to be of great importance in this thesis, Coulomb theory is applied to calculate the active pressures acting due to the backfill and the surcharge force, as demonstrated by Cooper[18] and described in chapter 2.3.1. The Coulomb active pressure coefficient calculated in equation 4.1. It is then used to determine the resultant force, P_a, based on the weight of the soil and the retained height. For the first block below the retained fill, P_a is obtained by the equation 4.2, assuming a linearly varying stress distribution with depth. For each subsequent block, the resultant is the total force from the top of the fill to the base of that segment, minus the resultant at the base of the block above. This is shown in figure 4-2, where the active pressure being applied to each block comes only from a representative area of pressure directly adjacent to that block.

$$K_a = \left[\frac{\sin(\alpha - \phi)/\sin(\alpha)}{\sqrt{\sin(\alpha+\delta)} + \sqrt{\frac{\sin(\phi+\delta)\sin(\phi)}{\sin(\alpha)}}} \right]^2 \tag{4.1}$$

$$P_a = 0.5\gamma_{soil} K_a H^2 \tag{4.2}$$

The value for K_a is dependent on both the friction angle between the wall and the backfill (δ) and also the angle of the backface of the wall itself (α), shown in figure 4-3. Hence, K_a and the subsequent pressure P_a is different for each segment of the wall. As with Cooper's work ([18]), horizontal equilibrium is achieved by the frictional sliding resistance (r_f), and the vertical loads are taken by the block below (r_c). In the case of the lowermost block r_c is provided by the base of the structure.

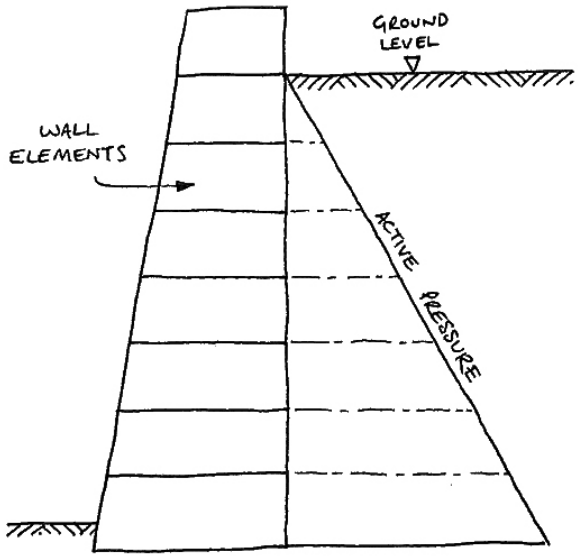

Figure 4-2: Active pressure distribution to each wall segment

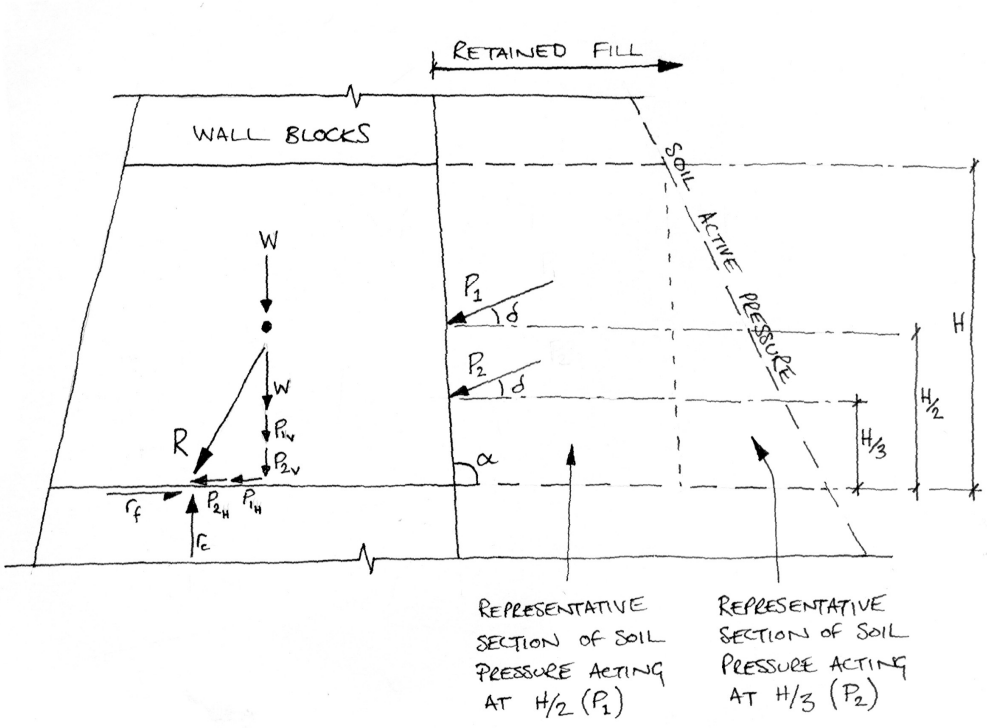

Figure 4-3: Backfill force & resultant force

4.3.4 Backfill pressures

From the earth pressure P_a, the horizontal and vertical components can then be calculated (equations 4.3 & 4.4), again dependent on α & δ (illustrated in fig. 4-3).

As shown in figure 4-3, the representative area of active pressure applied to each of the wall sections is trapezoidal (with the exception of the first block below the ground surface which has a triangular distribution). For this reason P_a is split into two parts, P_1 and P_2. P_1 represents the active pressure from the square area of the trapezoid, and hence acts at a height of $\frac{H}{2}$ above the base of the block. P_2 similarly represents the triangular area of active pressure, and therefore acts at a lower point of $\frac{H}{3}$ above the base of the block. Both P_1 and P_2 are then split into their vertical and horizontal components, which are then multiplied by their respective lever arms to determine their overturning and restoring moments.

$$P_H = P_a \cos(\alpha + \delta - 90) \tag{4.3}$$

$$P_V = P_a \sin(\alpha + \delta - 90) \tag{4.4}$$

4.3.5 Surcharge loading

In addition to forces arising from the self-weight of the backfill, patch surcharging may be applied. A user defined load is then applied to the backfill, which was initially assumed to spread out as the depth increses by a ratio of 1h: 2v. This is a simplification, as used for example in BS8006[39], when compared with the more rigorous approach of Bolton[40] as suggested in BS8002[41], but for the present purposes this approximation allows the combination of rapid calculation and reasonable accuracy. Further justification of this approach was given by Corte[42].

For this method, it is assumed that the surcharge will have no effect upon the calculated thrust line until the expanding area over which it is distributed crosses the boundary of the wall. At this point the additional vertical and horizontal forces present at this level are added to the applied backfill pressures. Although the analysis is two-dimensional, a three-dimensional load dissipation is assumed, with the force acting on the wall spreading in both horizontal dimensions (fig. 4-4).

A second method of surcharging was also investigated. This involves using the Boussinesq equations for stresses beneath a point load[43], describing a bulb of pressure in the material in which the stresses decrease as the bulb expands. As derived by Boussinesq, the vertical stress at a known distance beneath a point load is given by equation 4.5, where σ_v = the vertical stress, P = the applied load, z = the depth beneath the soil, and R = the direct distance between the point load and the location in question.

$$\sigma_v = \frac{3Pz^3}{2\pi R^5} \tag{4.5}$$

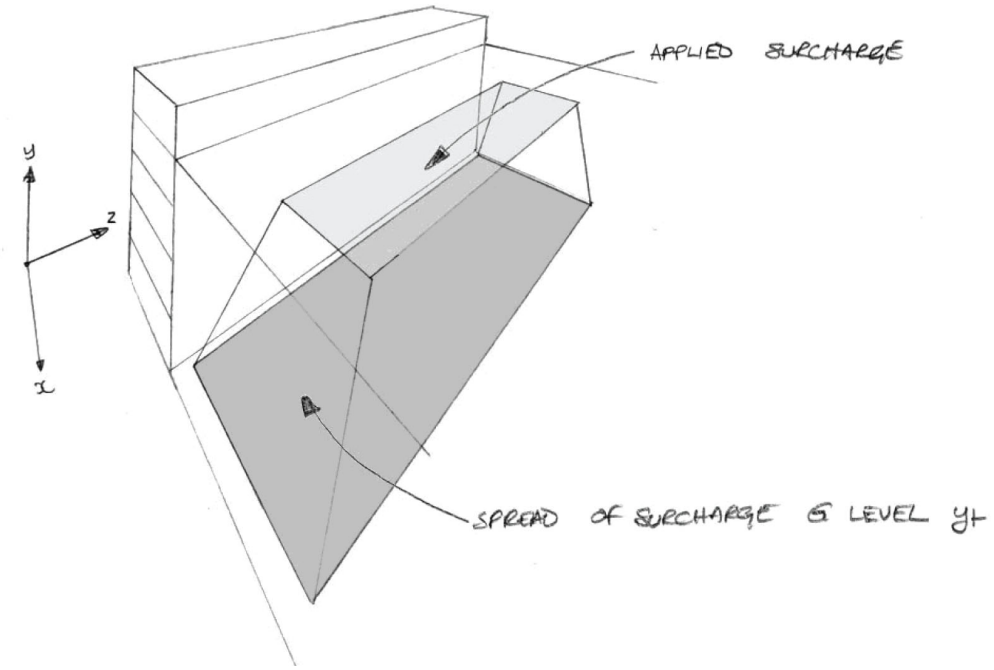

Figure 4-4: Surcharge spread in three-dimensions

Although the formula is applicable for point loads only, the program was adapted to split the user defined surcharging plate into a series of point loads. The stresses from each point load are then combined to give the total stress acting at any point. The mid-point of the internal face of each block is then taken as the point of action at each level, with the combined stress from the surcharge being multiplied by the height of this level to get a vertical force. Rather than use the radial stress as given by Boussinesq, the horizontal force is calculated by assuming that the vertical force is a component of an overall force, in the same manner that P_V is a component of P_a as shown by figure 4-3. This removes the need to know the Poisson's ratio of the backfill, which if incorporated could potentially cause problems as the backfill dilates in response to movements of the wall.

Although both methods are approximations to a relatively complicated process, it was found that the loads based on the Boussinesq theory gave better agreement with the observed results. Hence, this method was adopted in favour of the uniform load spread technique.

4.3.6 Thrust line determination

At each level, once the total overturning and restoring forces are known, the position of the thrust line can be determined. This is again calculated beginning with the topmost block, with the eccentricity of the resultant force derived as shown in figure 4-3. After the first level, the horizontal and vertical forces (including self weight, backfill and surcharging forces) are added to a cumulative total. For the

subsequent layers, the eccentricity is gained from a combination of the total forces from the previous blocks, in addition to the local pressures at that height.

4.4 Program operation

4.4.1 Program environment

Execution of the program generates a form in which all the data is entered and viewed (fig. 4-5). Initially, all the parameters are set to zero by default. Data entry is via either tick-boxes, labeled buttons or numerical entry boxes for the material properties.

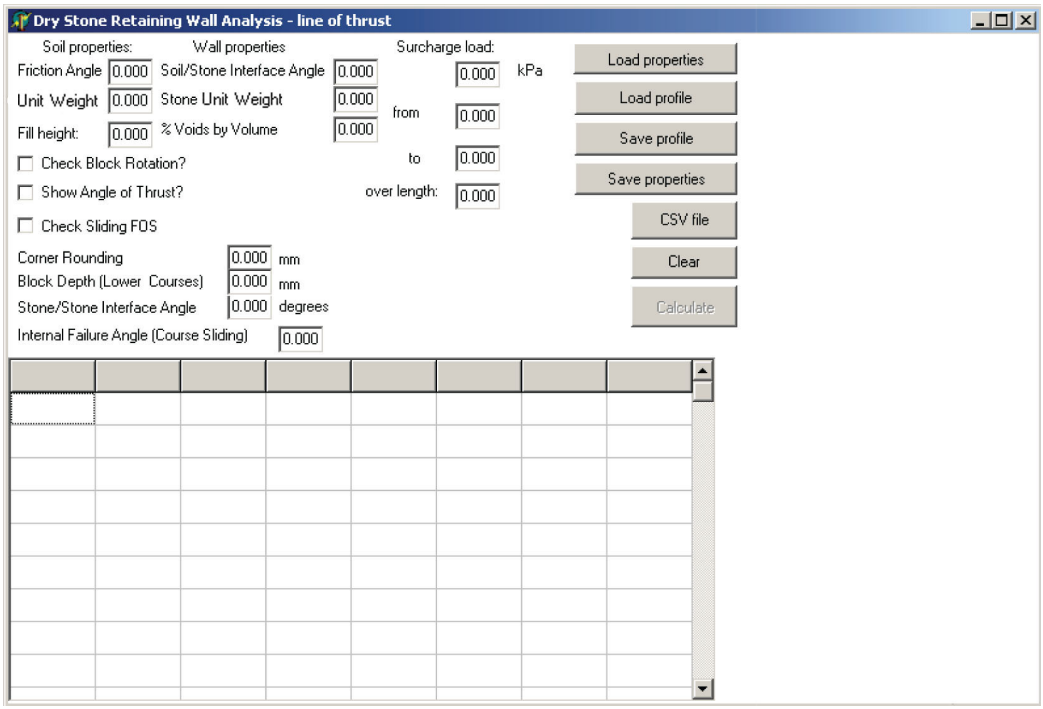

Figure 4-5: Blank program form

4.4.2 Wall geometry entry

The generated wall consists of a series of blocks, each representing a layer of the wall. The wall data is determined in a separate text file, saved as a .csv file. This file contains a string of data consisting of a series of numbers; each is assigned to an individual block describing its position and size. The height of the block is given in the first digits, followed by the horizontal distance between the front face of the block and a predetermined zero-point (identical for every block in the wall). The final digits indicate the width of the block. For example, a string of data for a wall block could be: "1 2 0.5". This would produce a wall 1m in height which is located 2m behind the zero position, and 0.5m in width.

The more complicated the wall face to be described, the more layers or courses are required. If the wall is particularly complex, then it may be necessary to model each course of the wall. There is also an advantage from having several courses in that the thrust line determined by the program will be more fully described. However, regardless of how many courses are present within a wall geometry, for identical profiles the resultant at the base will be in the same position.

Once created, the geometry may be entered into the program using the 'load profile' button and locating the .csv file. The data will then be transferred into the program form, as shown in figure 4-6.

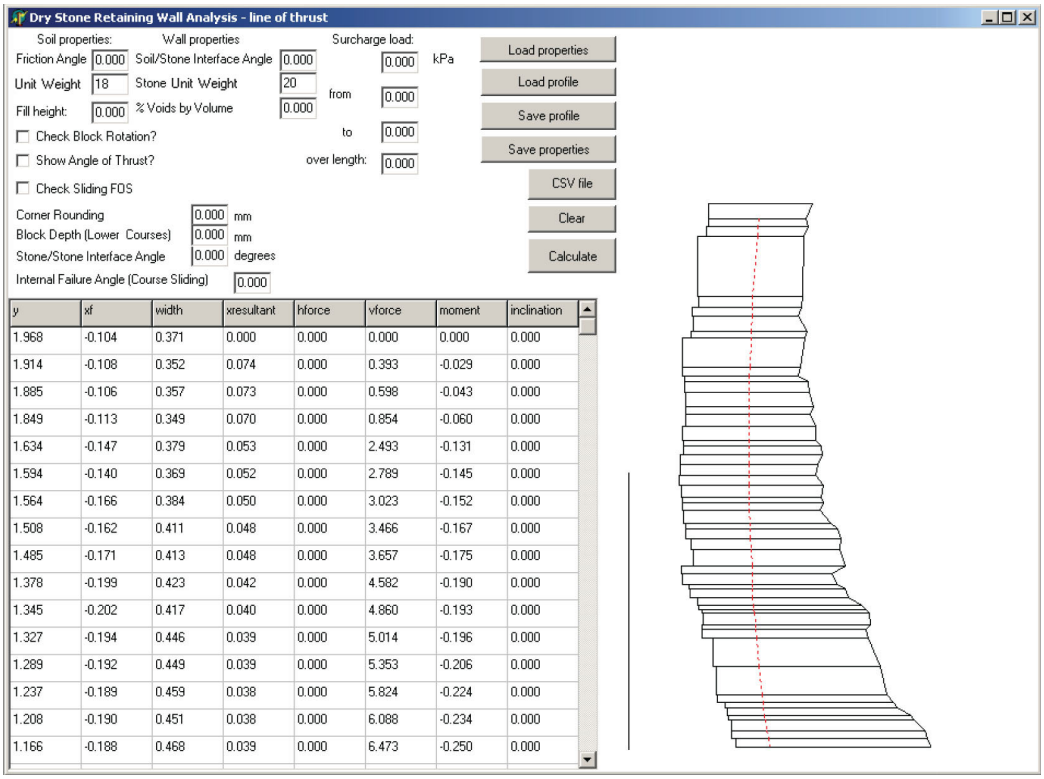

Figure 4-6: Form with wall geometry loaded

4.4.3 Parameter entry

Once the geometry is selected, the associated parameters may be entered into the form. With only the wall geometry loaded, the only numerical input required to run the program is the 'stone unit weight' value. If no value is assigned to this box, a value of 20kN/m^3 is assumed.

There are three main groups for properties during the standard use of the program: Soil & wall properties, and surcharging loads. The soil parameters section consists of the friction angle (ϕ), the unit weight (γ_{soil}) and the fill height (H). Wall parameters are the soil/stone interface angle (δ), the stone unit weight (γ_{stone}) and the % of voids by volume. There are four values defining the surcharging load -

the magnitude of the load in kN/m^2 and the size and position of the loaded area.

The parameter for 'corner rounding' allows the corners of the face of each layer to be chamfered by a user-defined amount. This influences failure modes and safety factors by reducing the effective width of the block (and hence the lever arm at which the restoring moment acts), allowing an approximation of aged and weathered walls to be incorporated. In addition to these parameters, there are three check-boxes with associated variables. The functions of these boxes and the additional required data are as follows:

- 'Show angle of thrust?'

  This causes the program to show the angle of the resultant force on each block due to the total horizontal and vertical forces at that point.

- 'Check block rotation?'

  The block rotation check-box attempts to identify a failure via individual block rotation, and is more fully described in section 4.5.3.

- 'Check Sliding FOS'

  This initiates a frictional sliding check between the courses, and produces the data as a factor of safety, described in section 4.5.2.

The task buttons provide the options of saving both the parameters ('save properties') and the wall profile ('save profile') as .wal and .csv files respectively. These may then be reloaded at any point should the model need to be recreated.

4.4.4 Generation of results

Once the correct geometry and parameters have been specified, the program is ready to analyse the structure. The 'calculate' button causes the generation of a thrust line for the system given, incorporating all of the variables entered (backfill heights & properties, surcharge forces etc.). In addition, if any of the check-boxes described in chapter 4.4.3 are marked, the relevant data will also be calculated (fig. 4-7).

In the form, the thrust line is visually represented by a red dotted line. The position of this line is also given in the 'xresultant' column. The forces being applied to produce this thrust are also given in the columns 'hforce', 'vforce' and 'moment'. The angle of the force from vertical is given in the column 'inclination', and is shown visually by a green dotted line should the 'show angle of thrust?' check-box be marked (section 4.4.3).

The data generated within the form can then be exported to a file entitled results.csv. This data may then be viewed in a suitable program (ideally Microsoft Excel), containing all the numerical data from the form without the image.

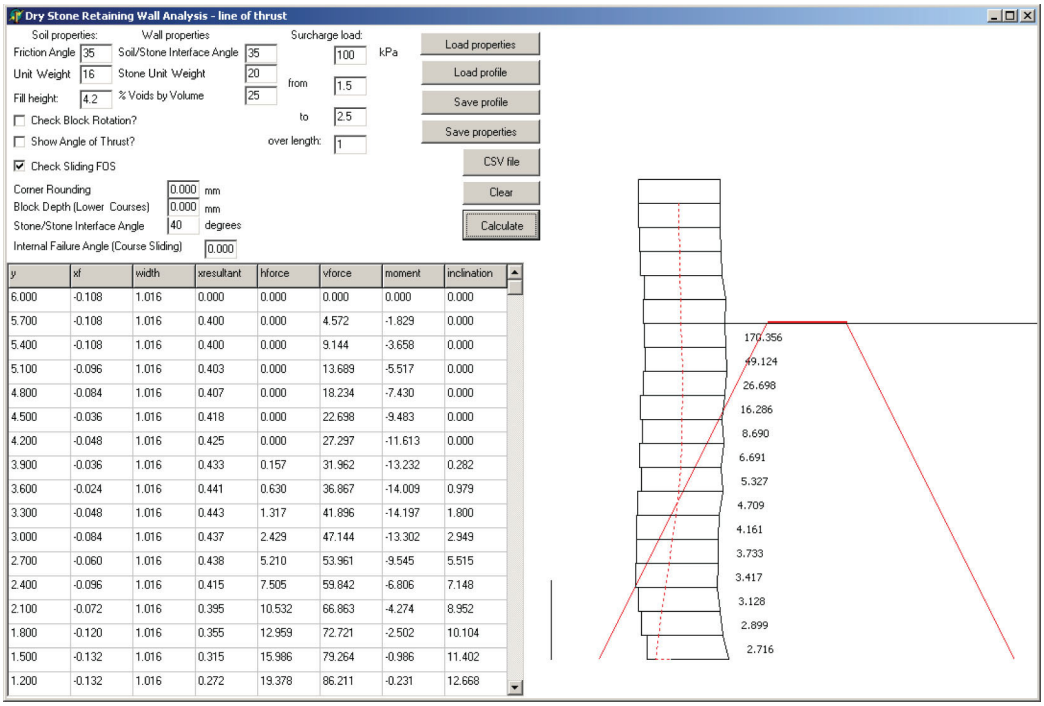

Figure 4-7: Form with thrust line generated

4.4.5 Manual wall deformation

Once a wall profile has been generated, the program allows the manipulation of the wall profile geometry. The numerical values describing the wall profile can be altered and the existing values replaced. Alternatively, there is also the option to 'drag' the individual blocks on the generated image of the wall profile. The co-ordinates of the wall are changed to conform with the altered image, and the thrust line is instantly recalculated. In this way, a generated wall with no deformations may be bulged to ascertain the effect of these movements on the static equilibrium.

4.5 Failure modes

The program assesses three failure criteria: overturning, individual block rotation and block sliding. Each of these is represented in the program via either a diagrammatic indication or a numerical safety factor. With the latter, a block with a safety factor of 1 is just stable, with any less identifying a failure. Often, a combination of these failure modes may happen simultaneously; in these cases the program will identify the initial failure mode, which may then instigate the others.

4.5.1 Overturning

Overturning (or toppling) is a failure mode often found in monolithic-behaving walls, although it can occur in walls of any condition. Toppling is initiated when the overturning forces within the system (backfill pressures and surcharge forces)

outweigh the restoring forces (self weight and any vertical loads on the backface of the wall). Within the program, this is indicated when the thrust line moves outside the boundaries of the wall, usually at the base level.

4.5.2 Sliding

A sliding failure occurs when the lateral forces overcome the friction between the block courses within a wall. Usually, this is not problematic as most common walling materials have a relatively high joint friction with block rotation being the greater issue. However, some materials may be more susceptible to this type of failure, e.g., slate walls. Sliding may also be initiated due to soil in-filled joints, tilted courses, heavy rain or frost, which may all lower the joint friction angle.

Within the program, sliding failure is indicated by a safety factor on the right hand side of each block (only applicable to courses below the backfill level). It should be noted that the safety factor for each block is different, and depends on the forces applied, the dead load of the wall above and the angle of the backface from vertical. In this way, it is sometimes possible for a block's safety factor against sliding to drop below 1, then with subsequent movement for the safety factor to become greater than 1 again, as the angle of the backface may allow for greater vertical forces to be applied (or conversely a drop in horizontal pressures). For this failure mode to be checked, the joint friction angle of the stone in question must be known and entered.

It is also possible to alter the angle of the bedding planes for each block from an assumed horizontal starting point. In this way, non-horizontal bedding planes may be examined. For example, the factor of safety against sliding would be increased with a negatively tilted bedding plane, as the sliding force is required to push the failing section of wall upwards as well as forwards. By comparison, should the planes be tilted forwards (i.e., given a positive angle), the sliding resistance will conversely reduce.

4.5.3 Block rotation

Block rotation is occurrence of overturning on a smaller scale. As the thrust line leaves the middle $\frac{1}{3}$ of the wall, the pressures are distributed over a decreasing area of the base of each layer. Towards the base, it is possible for the entire thrust of the wall to be passing through an area encompassing only the face stones. If the horizontal forces are great enough, the vertical forces may be overcome and the foremost block can rotate and fall out of the wall. This issue is made worse the closer the thrust line is to the face of the wall, and if the block in question is overhanging the stone below it the forces required are further reduced (figure 4-8. The shape of the stone in question is critical for this type of failure; thin, plate-line blocks which penetrate deep into the wall would be more resistant (although

susceptible to flexural cracking), whilst taller blocks with less depth would be much easier to roll on their forward edge.

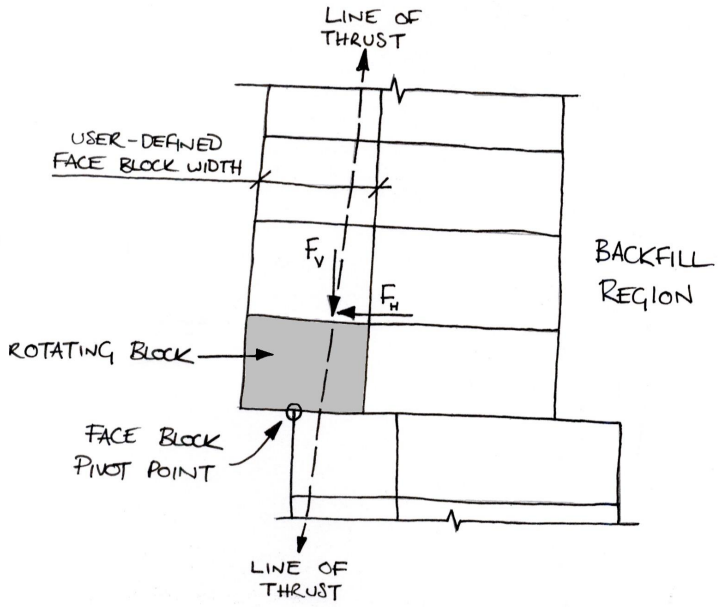

Figure 4-8: Rotational failure of individual face stones

The program allows for the checking of this failure mode, requiring only a depth for the individual face stones to be entered. This applies a uniform minimum depth for all face stones, and sets the ratio of height/depth at each level (as each course may have a different height this may be different at each level). If the eccentricity of the thrust line causes it to pass through the user-defined face stone, a safety factor against overturning is generated and displayed adjacent to the block.

4.6 Program verification

The program was tested and validated by comparison with simple hand-calculation checks. For the initial verification, a simple 2m wall was modeled, consisting of two blocks each 1m in height. A $1m^2$ patch surcharge of 10kN was applied 0.5m from the backface of the wall, as shown in figure 4-9(a). It should be noted that for this test, the 1h:2v load spread method was used to model the surcharge.

The forces are calculated by the same procedure as in the program, utilising Coulomb theory to determine the position of the resultant[18]. The values used for $\phi, \delta, \gamma_{stone}$ and γ_{soil} were 28^o, 30^o, $20kN/m^3$ and $18kN/m^3$ respectively. The method and calculations are found in appendix A. An identical wall was analysed in the limit equilibrium program, shown in figure 4-9(b). The hand calculations and program output for the forces acting at the base of the wall are compiled in table 4.1.

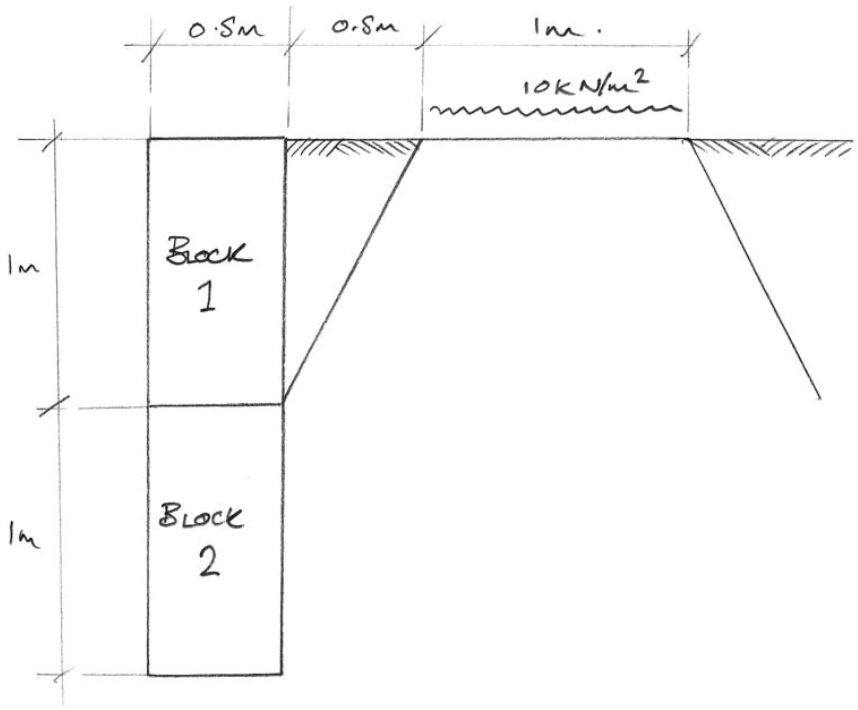

(a)

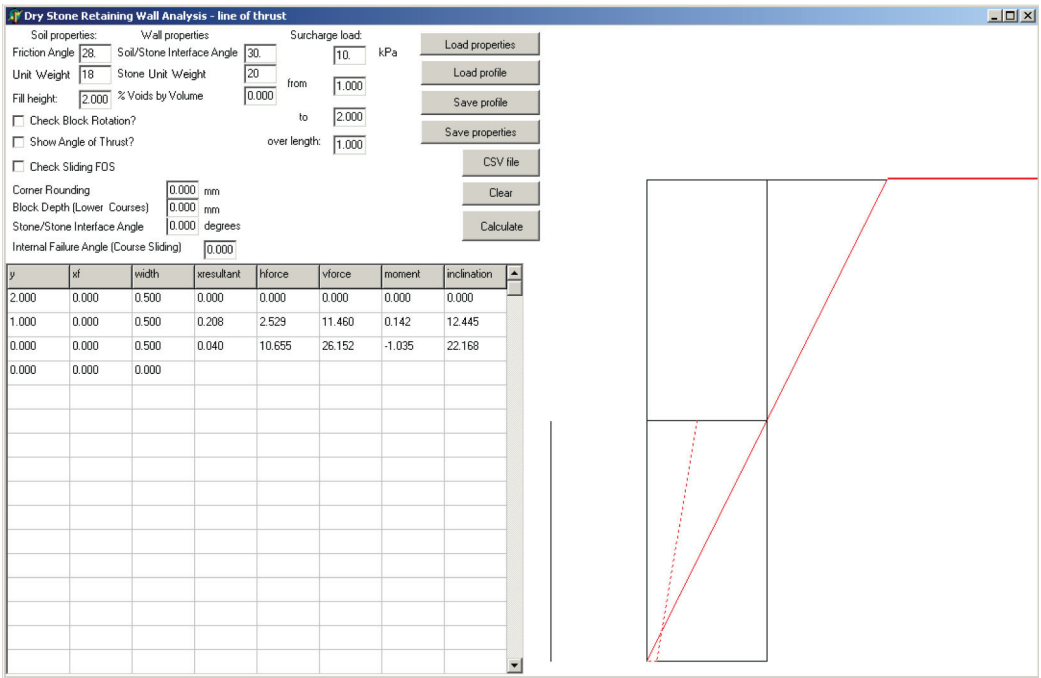

(b)

Figure 4-9: Program verification: a) geometry used; b) program output

Table 4.1: Comparison of hand calculation & LE program output

Output	**Hand calculation**	**Program output**	**Variation**
Horizontal force P_H,(kN)	10.5	10.7	1.9%
Vertical force P_V,(kN)	25.9	26.2	1.2%
Moment M,(kNm)	-1.08	-1.04	3.8%
Resultant xr,mm	42	40	4.8%
Angle θ_{RES},Degrees	22.1	22.2	0.5%

These values are within very close agreement; P_H, P_V and θ_{RES} are approximately within 2% of the program values, xr and M being within 3-5%. These discrepancies are due to the exact nature of the computational program and the degree of rounding within the hand calculations.

4.7 Recreation of Burgoyne's field tests

To test the validity of the program against real walls, the four tests conducted in Kingstown by Burgoyne[12](described in chapter 2-1) were recreated using the program. It should also be noted that Burgoyne's tests were conducted on a solid rock base, removing the possibility of foundation settlement as a potential failure mode.

4.7.1 Material properties

Although some of the material properties from the original wall tests were not determined at the time, they can be estimated from the Burgoyne's report[12]. The backfill was described as a 'loose mould' with a unit weight on placement of 13.6kN/m^3, although this would have increased as the fill height increased. It was also noted that the soil 'imbibed the rain and moisture readily', which would further increase the unit weight and potentially lower the strength of the material. Therefore, a value of 15kN/m^3 was used, which is also similar to the value used in the numerical studies described in chapter 2.3.3.

As described in chapter 2, the unit weight of the granite wall was measured to be 22.3kN/m^3, having approximately 14% voids by volume. This indicates a very tightly packed wall, which is also indicated by the relatively monolithic behaviour described in Burgoyne's report.

The angles of friction ϕ and δ were not measured and are estimated for the purposes of these tests. A value of 28^o was taken for ϕ, and 28^o for δ, assuming that δ reached the maximum value. This assumption is made based on Burgoyne's notes, which stated that settlement of roughly 200mm occurred during backfilling. This settlement, due to the dead weight of the soil above and general trafficking during construction, would cause a differential movement between the wall and the soil. By comparison with the full-scale tests conducted in this project, only 50mm

of differential movement was needed to ensure a full friction angle, indicating that this is an acceptable assumption in this case.

4.7.2 Testing procedure

In the original tests, the walls were fully constructed then backfilled in lifts of 1 foot, or 304mm. For the purposes of reconstructing the tests within the program environment, this same procedure was carried out, raising the backfill in lifts of 304mm. All the failure modes described in section 4.5 were checked.

4.7.3 Test wall 'A'

Burgoyne's first test wall was 6.1m tall, 1.01m thick and battered back at a slope of 1 in 5 (11.3^o). It is reproduced by the model shown in figure 4-10. Due to the batter on the rear face, this wall was built simultaneously with the backfill. The full height was attained with no visible signs of distress.

From the limit equilibrium model it can be shown that the theoretical resultant at the base is 246mm from the toe of the wall. This is outside of the middle third (338mm from the toe), however this would not necessarily be indicative of failure, only that a portion of the heel has become unloaded (assuming a linear pressure distribution across the base). Due to the high compressive strength of the foundations and the blocks themselves, this would not become problematic until the thrust line was much closer to the toe.

4.7.4 Test wall 'B'

Test wall 'B' was designed in the same manner as the other walls, having a mean width of 1.01m. However this wall has a varying cross-section, with the profile changing from 1.63m at the base to 0.4m at the crest. For this wall, the rear face was vertical, with an identical batter to wall 'A' on the front face (11.3^o).

As for wall 'A', the full backfill height was obtained without inducing failure. However, it was noted that upon completion, the wall had been subjected to slight fissuring throughout the face. In addition, there was an outward movement of 63mm at the top of the wall. In the undeformed position (without the 63mm movement), the wall reaches its full backfill height of 6.1m without the thrust line exiting the boundaries of the wall, being 280mm from the toe.

The recreation of this wall test in its fully loaded profile (as described in Burgoyne's report) is shown in figure 4-11. The deformation noted by Burgoyne has very little effect on the overall stability. As the centre of mass of the top of the structure is moved forward slightly, so too is the position of the thrust line. At the base level, the new position is 258mm from the toe - giving a theoretical movement of the thrust line of 22mm. At this point the wall is still stable, although the thrust is outside of the middle third of the wall.

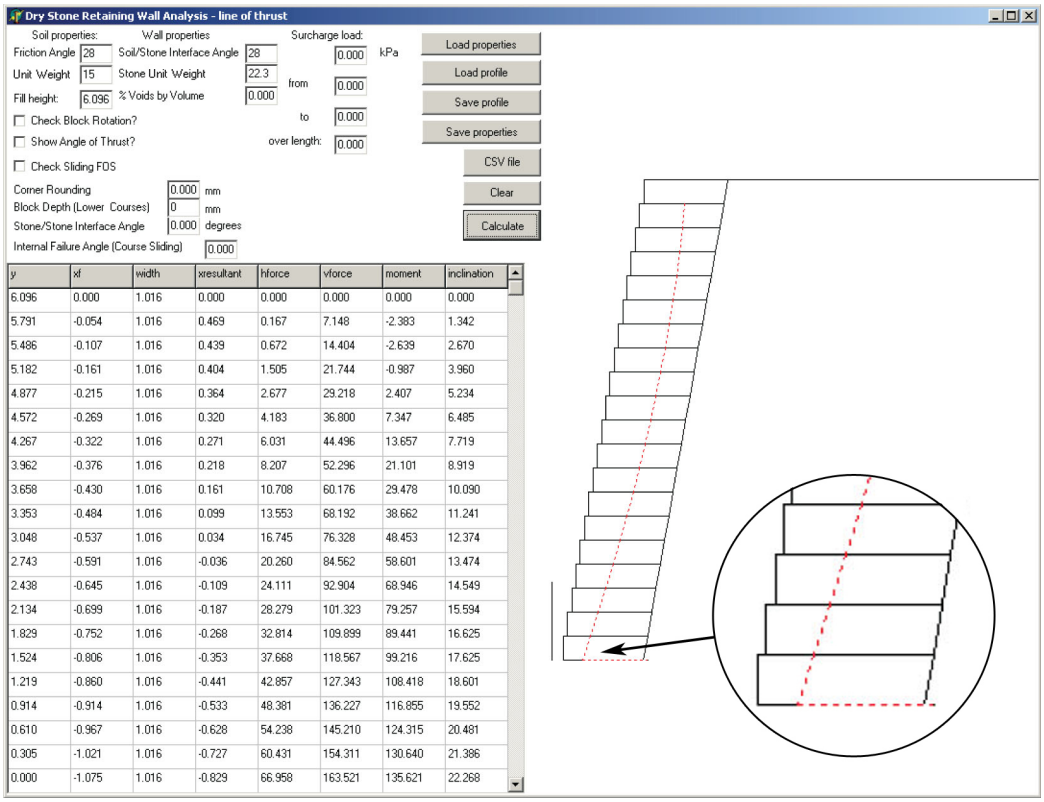

y	xf	width	xresultant	hforce	vforce	moment	inclination
6.096	0.000	1.016	0.000	0.000	0.000	0.000	0.000
5.791	-0.054	1.016	0.469	0.167	7.148	-2.383	1.342
5.486	-0.107	1.016	0.439	0.672	14.404	-2.639	2.670
5.182	-0.161	1.016	0.404	1.505	21.744	-0.987	3.960
4.877	-0.215	1.016	0.364	2.677	29.218	2.407	5.234
4.572	-0.269	1.016	0.320	4.183	36.800	7.347	6.485
4.267	-0.322	1.016	0.271	6.031	44.496	13.657	7.719
3.962	-0.376	1.016	0.218	8.207	52.296	21.101	8.919
3.658	-0.430	1.016	0.161	10.708	60.176	29.478	10.090
3.353	-0.484	1.016	0.099	13.553	68.192	38.662	11.241
3.048	-0.537	1.016	0.034	16.745	76.328	48.453	12.374
2.743	-0.591	1.016	-0.036	20.260	84.562	58.601	13.474
2.438	-0.645	1.016	-0.109	24.111	92.904	68.946	14.549
2.134	-0.699	1.016	-0.187	28.279	101.323	79.257	15.594
1.829	-0.752	1.016	-0.268	32.814	109.899	89.441	16.625
1.524	-0.806	1.016	-0.353	37.668	118.567	99.216	17.625
1.219	-0.860	1.016	-0.441	42.857	127.343	108.418	18.601
0.914	-0.914	1.016	-0.533	48.381	136.227	116.855	19.552
0.610	-0.967	1.016	-0.628	54.238	145.210	124.315	20.481
0.305	-1.021	1.016	-0.727	60.431	154.311	130.640	21.386
0.000	-1.075	1.016	-0.829	66.958	163.521	135.621	22.268

Figure 4-10: Program output for Burgoyne wall 'A'

4.7.5 Test wall 'C'

The profile of wall 'C' was a mirror image of wall 'B', having a vertical front face and a rear face battered forwards by 11.3^o. This wall failed before a full backfill height was achieved, reaching a height of 5.18m. This was accompanied by an overhang of of 254mm at the crest, with 127mm of this overhang occurring in the first 1.5m above the base.

With an undeformed shape, wall 'C' can attain a total backfill height of 5.79m (the penultimate lift before full retention is achieved) before a failure via overturning occurs. In its deformed shape as measured by Burgoyne (fig. 4-12), wall 'C' can achieve backfill lifts up to 5.49m with marginal stability, however a more dominant failure mode is via block rotation.

Although it is undocumented exactly how large the blocks comprising the walls were, estimations can be made based on the size of a granite stone which could feasibly be lifted by a mason. If the wall blocks were 200mm x 300mm x 150mm (breadth x depth x height), they would each be 24kg, allowing a mason to handle it unaided. For the purposes of this wall, 150mm x 300mm (height x depth) blocks were supposed in the front face. With 4.88m of backfill, the wall is still stable, with no rotational failure and the thrust line within the boundary of the wall. When the backfill is increased by a further 300mm, the thrust line remains within the boundaries of the wall, however the lower blocks have now failed by rotation, as

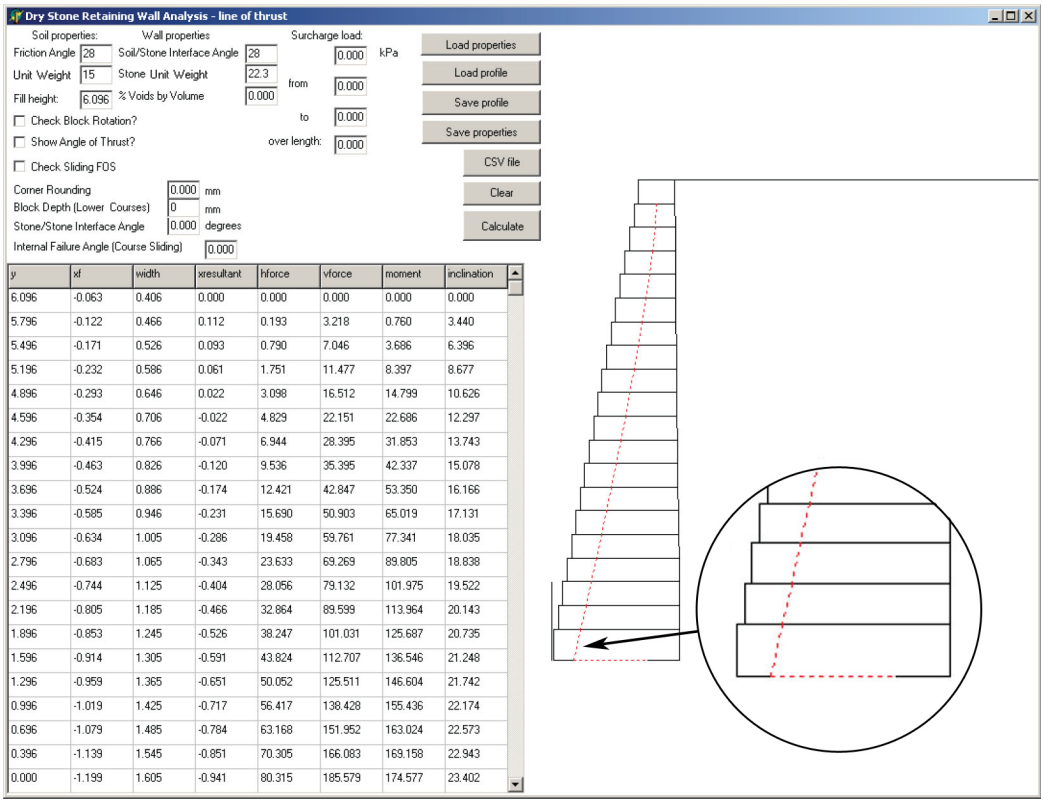

y	xf	width	xresultant	hforce	vforce	moment	inclination
6.096	-0.063	0.406	0.000	0.000	0.000	0.000	0.000
5.796	-0.122	0.466	0.112	0.193	3.218	0.760	3.440
5.496	-0.171	0.526	0.093	0.790	7.046	3.686	6.396
5.196	-0.232	0.586	0.061	1.751	11.477	8.397	8.677
4.896	-0.293	0.646	0.022	3.098	16.512	14.799	10.626
4.596	-0.354	0.706	-0.022	4.829	22.151	22.686	12.297
4.296	-0.415	0.766	-0.071	6.944	28.395	31.853	13.743
3.996	-0.463	0.826	-0.120	9.536	35.395	42.337	15.078
3.696	-0.524	0.886	-0.174	12.421	42.847	53.350	16.166
3.396	-0.585	0.946	-0.231	15.690	50.903	65.019	17.131
3.096	-0.634	1.005	-0.286	19.458	59.761	77.341	18.035
2.796	-0.683	1.065	-0.343	23.633	69.269	89.805	18.838
2.496	-0.744	1.125	-0.404	28.056	79.132	101.975	19.522
2.196	-0.805	1.185	-0.466	32.864	89.599	113.964	20.143
1.896	-0.853	1.245	-0.526	38.247	101.031	125.687	20.735
1.596	-0.914	1.305	-0.591	43.824	112.707	136.546	21.248
1.296	-0.959	1.365	-0.651	50.052	125.511	146.604	21.742
0.996	-1.019	1.425	-0.717	56.417	138.428	155.436	22.174
0.696	-1.079	1.485	-0.784	63.168	151.952	163.024	22.573
0.396	-1.139	1.545	-0.851	70.305	166.083	169.158	22.943
0.000	-1.199	1.605	-0.941	80.315	185.579	174.577	23.402

Figure 4-11: Program output for Burgoyne wall 'B'

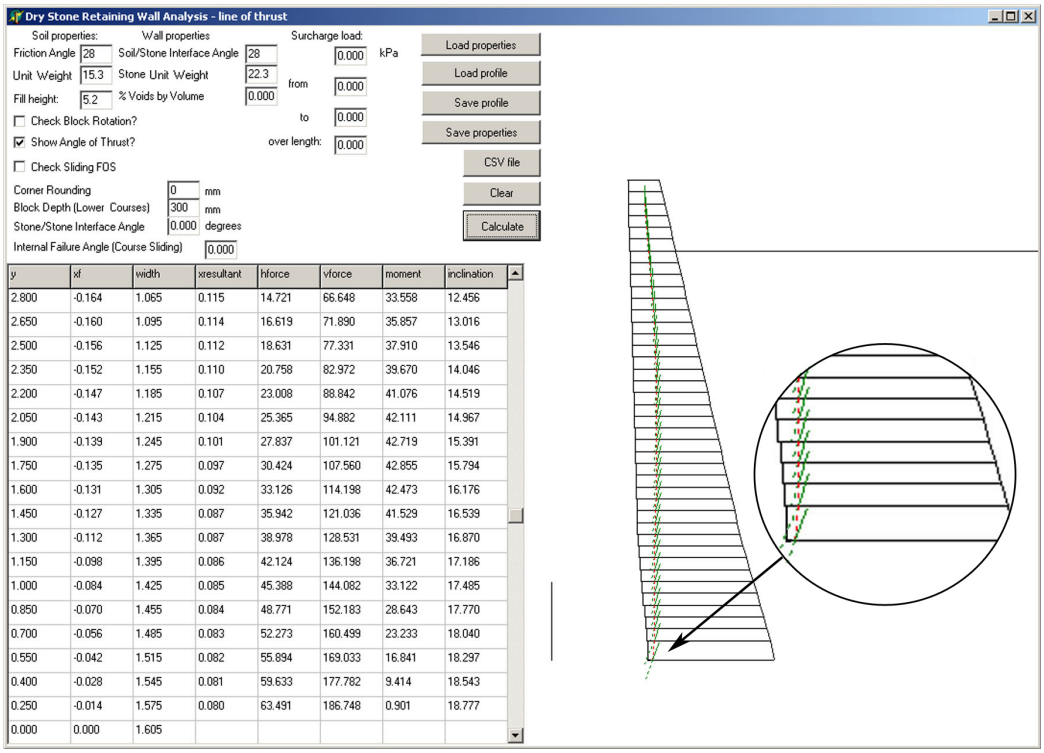

y	xf	width	xresultant	hforce	vforce	moment	inclination
2.800	-0.164	1.065	0.115	14.721	66.648	33.558	12.456
2.650	-0.160	1.095	0.114	16.619	71.890	35.857	13.016
2.500	-0.156	1.125	0.112	18.631	77.331	37.910	13.546
2.350	-0.152	1.155	0.110	20.758	82.972	39.670	14.046
2.200	-0.147	1.185	0.107	23.008	88.842	41.076	14.519
2.050	-0.143	1.215	0.104	25.365	94.882	42.111	14.967
1.900	-0.139	1.245	0.101	27.837	101.121	42.719	15.391
1.750	-0.135	1.275	0.097	30.424	107.560	42.855	15.794
1.600	-0.131	1.305	0.092	33.126	114.198	42.473	16.176
1.450	-0.127	1.335	0.087	35.942	121.036	41.529	16.539
1.300	-0.112	1.365	0.087	38.978	128.531	39.493	16.870
1.150	-0.098	1.395	0.086	42.124	136.198	36.721	17.186
1.000	-0.084	1.425	0.085	45.388	144.082	33.122	17.485
0.850	-0.070	1.455	0.084	48.771	152.183	28.643	17.770
0.700	-0.056	1.485	0.083	52.273	160.499	23.233	18.040
0.550	-0.042	1.515	0.082	55.894	169.033	16.841	18.297
0.400	-0.028	1.545	0.081	59.633	177.782	9.414	18.543
0.250	-0.014	1.575	0.080	63.491	186.748	0.901	18.777
0.000	0.000	1.605					

Figure 4-12: Program output for Burgoyne wall 'C'

shown in figure 4-12. This indicates that at this point the forces on this particular block are enough to cause the stone to rotate and fall out of the wall. This is turn would cause a cascade, with the wall above failing due to the absence of this key stone.

The description given by Burgoyne was that the wall fell due to bursting at 1.67m from the base, with the top $\frac{2}{3}$ falling in an upright position. The rotational failure of the lower blocks could conceivably cause this effect, as the wall splits into two distinct sections - an upper portion (1.5m - 6.1m), which has remained mainly monolithic; and a lower portion (0m - 1.5m), which has deformed by a comparatively greater amount (127mm deformation in 1.5m as opposed to the upper region which deformed 127mm over 4.6m). With the rotational failure of the block, the lower section would likely follow this movement and collapse in a similar manner. However, the upper portion of the wall would remain upright, and collapse vertically as the stability of the lower section was undermined.

4.7.6 Test wall 'D'

Wall 'D' was a parallel-sided vertical wall of width 1.01m. Similarly to wall 'C', this wall failed upon placement of 5.18m of backfill. Before failure, the crest overhung the toe by 457mm, with an overall convexity in the face of 101mm. Upon failure, the wall fell monolithically, toppling from the base.

In the undeformed state, the program-generated wall is marginally stable after the 5.18m backfill lift, with the thrust line 12mm behind the toe. However, in the deformed state (fig. 4-13), the wall has failed by overturning at this point. In fact in this deformed state, the wall is only stable with 4.28m of fill, with three further lifts required until the failure height obtained by Burgoyne is achieved. However, the deformations prior to collapse would not have occurred until the very final stages of the test. In the numerical tests conducted by Harkness et. al[8], only 38mm of overhang was present with 4.88m of backfill, with the same final backfill height and failure mode as reported by Burgoyne. Assuming this amount of deformation, the profile created by the limit equilibrium program is similarly stable when retaining 4.88m of fill.

During the backfilling from 4.88m and 5.18m, failure occurs. In this time it is probable that the majority of the deformation occurs, with the wall rotating as a monolithic structure. The program indicates that the failure is by overturning as the thrust line moves ahead of the toe at the base; again in line with Burgoyne's observations.

4.7.7 Comparison of results

The limit equilibrium program has been successfully used to recreate the tests conducted by Burgoyne. As described in this section, and highlighted in table 4.2,

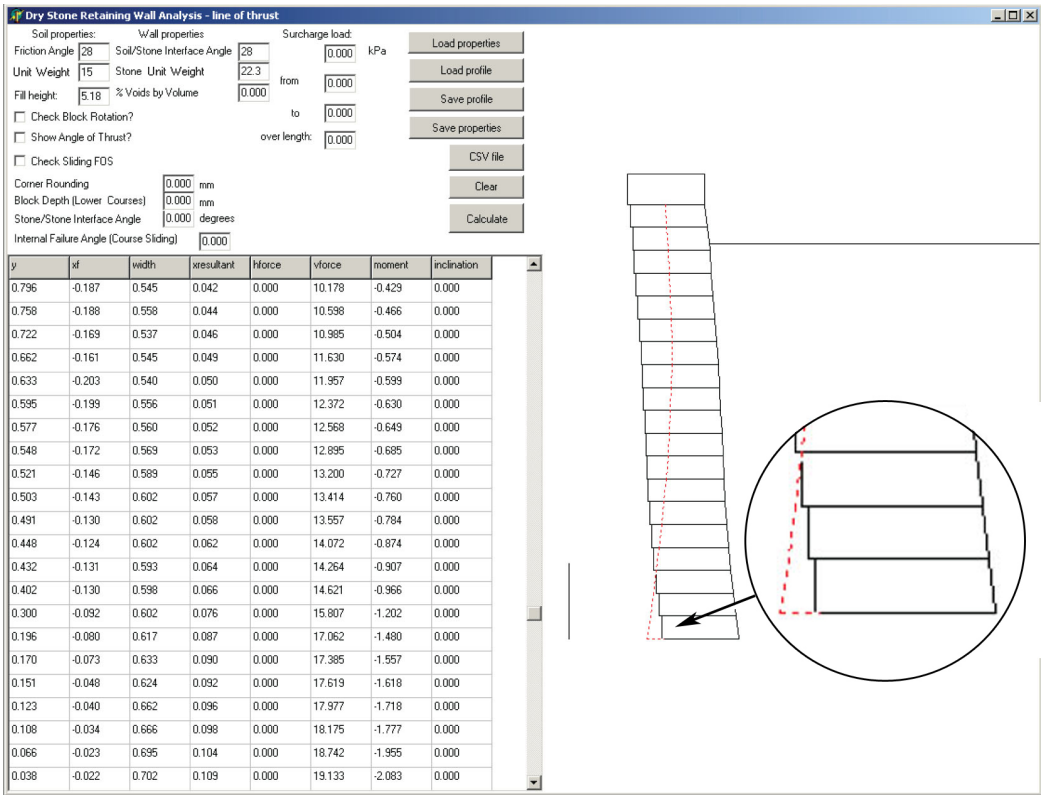

y	xf	width	xresultant	hforce	vforce	moment	inclination
0.796	-0.187	0.545	0.042	0.000	10.178	-0.429	0.000
0.758	-0.188	0.558	0.044	0.000	10.598	-0.466	0.000
0.722	-0.169	0.537	0.046	0.000	10.985	-0.504	0.000
0.662	-0.161	0.545	0.049	0.000	11.630	-0.574	0.000
0.633	-0.203	0.540	0.050	0.000	11.957	-0.599	0.000
0.595	-0.199	0.556	0.051	0.000	12.372	-0.630	0.000
0.577	-0.176	0.560	0.052	0.000	12.568	-0.649	0.000
0.548	-0.172	0.569	0.053	0.000	12.895	-0.685	0.000
0.521	-0.146	0.589	0.055	0.000	13.200	-0.727	0.000
0.503	-0.143	0.602	0.057	0.000	13.414	-0.760	0.000
0.491	-0.130	0.602	0.058	0.000	13.557	-0.784	0.000
0.448	-0.124	0.602	0.062	0.000	14.072	-0.874	0.000
0.432	-0.131	0.593	0.064	0.000	14.264	-0.907	0.000
0.402	-0.130	0.598	0.066	0.000	14.621	-0.966	0.000
0.300	-0.092	0.602	0.076	0.000	15.807	-1.202	0.000
0.196	-0.080	0.617	0.087	0.000	17.062	-1.480	0.000
0.170	-0.073	0.633	0.090	0.000	17.385	-1.557	0.000
0.151	-0.048	0.624	0.092	0.000	17.619	-1.618	0.000
0.123	-0.040	0.662	0.096	0.000	17.977	-1.718	0.000
0.108	-0.034	0.666	0.098	0.000	18.175	-1.777	0.000
0.066	-0.023	0.695	0.104	0.000	18.742	-1.955	0.000
0.038	-0.022	0.702	0.109	0.000	19.133	-2.083	0.000

Figure 4-13: Program output for Burgoyne wall 'D'

both the backfill heights and the failure modes reported in Burgoyne's report were obtained. These data are also supported by the numerical studies conducted by Harkness et. al.[8], who also obtained similar results (also presented in table 4.2).

Table 4.2: Comparison of Burgoyne's results using UDEC & limit equilibrium approaches

Geometry	**In-situ observations**		**UDEC analysis**	**Limit equilibrium analysis**	
	Maximum fill	Failure Mode	Maximum fill	Maximum fill	Failure Mode
'A'	Full height	No failure	Full height	Full height	No failure
'B'	Full height	No failure	Full height	Full height	No failure
'C'	5.18m	Bursting	5.18m	5.18m	Block Failure
'D'	5.18m	Toppling	5.18m	5.18m	Toppling

4.8 Physical test predictions

To ascertain the effectiveness of the program, a brief series of studies was conducted, analysing some of the recent physical tests conducted. Further to this, the proposed geometries for the full-scale tests of this project were briefly analysed, giving their initial factors of safety (with no deformations). This was primarily to check the safety of the structures, ensuring that the walls could be built and fully backfilled with no danger of collapse.

4.8.1 Full-scale Lyon wall tests

Initially the five full-scale tests conducted at Lyon by Villemus[35] were recreated. As the walls were loaded hydrostatically, the angles for both ϕ and δ were assumed to be zero. Failures of both sliding and overturning were checked for, using the sliding planes observed by Villemus where applicable (refer to section 2.2.2 for further test details). The results of the comparison study are shown in table 4.3.

Table 4.3: Comparison of Lyon full-scale tests with program output

Property	Wall 1	Wall 2	Wall 3	Wall 4	Wall 5
Height(m)	2	2	4	2	4.25
Walling material	limestone				schist
Level of water	1.74	1.90	3.37	1.94	3.37
Observed sliding	✓	✓	✓	✓	✓
Observed overturning	×	✓	×	✓	×
Program output assuming $\omega = 0$					
Max height of water(m)	1.84	1.94	3.71	1.84	3.53
Sliding safety factor	1.00	1.04	1.00	1.03	1.00
Overturning safety factor	1.16	1.00	1.16	1.00	1.62
Program output using observed value of ω					
Angle of ω (^{o})	N/A	N/A	11.5	7	2.5
Max level of water	N/A	N/A	3.15	1.67	3.38
Sliding safety factor	N/A	N/A	1.00	1.00	1.00
Overturning safety factor	N/A	N/A	1.31	1.62	1.85

ω = Internal sliding plane within the wall

Generally, very good agreement between the observed wall failures and the limit equilibrium output were obtained, with the program not only giving approximately the correct failure heights but also the modes of failure. The second set of data using the observed value of ω gave more correlation, however there are some discrepancies, particularly with wall 3. This may be due to the internal failure plane and the respective angle of friction. As the internal angle of failure was 11.5^o, this would cut through several courses of the wall. In this instance, a higher friction angle may be necessary, accounting for the the failure plane passing through multiple courses rather than along a flat surface.

4.8.2 Small-scale test walls

The small-scale wall tests described in section 3.3 were recreated using the limit equilibrium program to potentially predict the failure heights. A comparison of these predictions with the observed results are given in table 4.4. As the walls were relatively slender, failure was always through overturning rather than sliding.

Test number 1 was omitted as the test was halted before collapse. This was due to the setup of the test apparatus and wall, which used 100mm x 100mm x 100mm concrete cubes. As the backfill height was increased, the blocks rotated and

Table 4.4: small-scale tests with predicted failure heights

Test Number	Material	Friction angle	Fill height (observed)	Fill height (predicted)
2	Timber	24	185	240
3	Timber	24	245	240
4	Concrete	29	360	350
5	Concrete	23	330	350
6	Concrete	29	350	350
7	Concrete	23	340	350
8	Concrete*	29	355	350
9	Concrete*	23	320	350
10	Concrete* **	29	300	315

*wall has 100mm deep through-blocks at 4th and 8th levels
**wall blocks given 10mm chamfer to all corners

formed an arch between the metal sides of the test housing. Further deformation and failure was then resisted by the steel sides of the box, and therefore the results were not used in this comparison study.

The predictions of the program are very close to the observed results, with the exception of test number 2. However, in this instance, it was observed that the draw wire transducers used to measure the displacements of the wall were affecting the test. As the draw wires were sprung to retract into the housing of the instrument, when the end of the cable was attached to the wall blocks they exerted an additional load upon the wall. For the concrete walls, this effect was insignificant, however for the much lighter timber block walls, the effect was much larger and caused premature collapse. For this reason the draw wires were removed for test number 3, giving results that were much closer to the predicted failure heights.

4.8.3 Full-scale test geometries

Before the full-scale test walls were constructed, the limit equilibrium program was used to analyse the proposed geometries of the walls. Initially a proposed width of 1m was given, however, upon analysis of its potential safety against overturning and sliding (shown in table 4.5), it was reduced to 600mm wide at the base, with scope to reduce it a further 100mm. Both the limestone and Mort slate were tested as walling materials, based on the parameters obtained from the laboratory testing (section 3). The wall height was a constant 2.5m with a voidage of 25% for each wall, with 2.2m of backfill.

Table 4.5 shows that a wall 1m wide would be over three times more stable against overturning than a wall with a 500mm base width (based on undeformed wall profiles). From these initial predictions, a base width of 600mm was decided upon due to its general robustness, being unlikely to collapse during backfilling or whilst fitting any instrumentation. At the same time, a wall of this geometry was

Table 4.5: Analysis of possible full-scale test geometries

Wall configuration	Material	Base width(mm)	Crest width(mm)	Overturning safety	Sliding safety
1	Limestone	1000	700	6.68	5.84
2	Slate	1000	700	6.62	2.51
3	Limestone	600	300	2.57	3.56
4	Slate	600	300	2.54	1.46
5	Limestone	500	300	1.92	3.18
6	Slate	500	300	1.91	1.32

not beyond the capability of the test rig to initiate a collapse, as might have been the case had a larger wall been built.

4.9 Concluding remarks

In this chapter a limit equilibrium package has been introduced and successfully verified using hand calculations and a variety of physical tests. The package can identify the point at which failure occurs, and in many cases the type of failure itself. In the case of the Burgoyne tests, the program output has been validated by comparison with both the original observations and numerical analyses carried out by Harkness et. al.[8]. The advantages over numerical packages such as UDEC are that the package is extremely simple to operate, and requires minimal data regarding the structure to be analysed, providing answers almost instantaneously. These advantages also give this program enormous potential for use by engineers within the industry; its simplicity allows any engineer with a basic knowledge of any wall's geometry and material properties to obtain a reliable understanding of the factors influencing its stability, without the need for the detailed knowledge, advanced design parameters, time and expertise that are needed for reliable numerical analyses. The program's flexibility in use allows walls of any geometry with variable backfills to be analysed, and the application of surcharging can be applied to represent circumstances such as new constructions in the proximity of the wall or increased vehicle loading. However, the most problematic loading is wheel loading from a heavy vehicle, so it is important to model the three-dimensional distribution, even if crudely. A more sophisticated stress distribution calculation is simple to implement, but given the uncertainties in wall and backfill stiffness and anisotropy, this may overcomplicate the analysis without adding value.

A large drawback of the program is that it does not currently have the capacity to automatically deform a wall in response to a given loadcase. Therefore, where necessary, user-judgement is required to ensure that only realistic movements are applied to a wall. This has not raised any issues for its use within this project, as it has been used primarily to assess the stability of structures with known deformations. Similarly, as the program is intended to be used for the rapid analysis

of existing structures, the inability to automatically predict movements is not immediately problematic. However, where further movements are expected, or a new wall is to be constructed, an automated deformation function would be very useful. Whilst this remains outside of the scope of the program for this project, it should not be ignored as a potential avenue for further investigation.

This program is further utilised in later chapters of this thesis, aiding in the understanding of observed and recorded drystone behaviour. In particular, it will be used to assess large-scale testing conducted as part of this investigation.

Chapter 5

Development of full-scale test site

5.1 Introduction

The main focus of the work described in this thesis relates to the testing of full-scale drystone retaining walls. The importance of conducting full-scale tests stems from the difficulty of recreating every aspect of drystone behavior in either small-scale or numerical environments. In the case of small-scale testing, it is impossible to recreate an accurate representation of drystone construction in miniature. This is due to the fact that each wall is a careful interlocking of small items - such as pins, wedges and rubble infill - with the comparatively large walling stones. Attempts have been made to simplify the process and use miniature masonry blocks, however these do not allow for many of the inherent characteristics of drystone walls such as the ability of individual stones to roll and rotate without overly disturbing the structure. As a consequence, small-scale modeling may give an indication of some of the behavioral qualities of drystone walls, but certainly not all.

As the speed and quality of the various numerical analysis packages increase, it is becoming possible to recreate many of the important characteristics of drystone walls in a computational environment. However, as discussed in section 2.3.3, there are currently no models which recreate all of the nuances of drystone walls, and few which could assess the problem in three dimensions. These issues all lead to necessity of full-scale testing if theories and analysis techniques are to be validated with any certainty.

This chapter deals with the design and development of the laboratory used to house the full-scale wall tests conducted in this project. Due to the bespoke nature of the tests, every element of the testing procedure has involved in-depth planning and consideration. This includes the design and development of the test laboratory itself, the materials to be tested and the manner in which the tests themselves were conducted. A series of photographs detailing the construction sequence can be found in appendix B.

5.2 Laboratory design & construction

5.2.1 Location

The test site was located on the University of Bath campus, being approximately 160m^2 in size. Prior to the project described in this thesis, the site was used to house site offices (fig. 5-1).

Figure 5-1: Site prior to construction of test laboratory

5.2.2 Test specifications

Initial specifications required that the laboratory be able to house full-scale walls up to 14m long, and 2.5m high through the central 6m section to be tested. Each end of the walls was initially intended to gradually taper to the ground over 4m. Although drystone walls have been constructed several times larger than this, a wall 2.5m high was large enough that it represented many of the walls commonplace in the UK. The wing walls were required to induce the behavior of a much longer walls, however by tapering them to the ground, less material would be required, reducing construction time, storage space and material costs.

Each wall was required to be fully backfilled along its entire length, allowing enough material to ensure that any failure plane may develop unimpeded by the boundary walls of the test. Hence it was decided that the boundary walls should be

situated at least 4m from the test walls, with the backfill extending at full height from the drystone wall to the boundary wall.

It was necessary to be able to move the test section of the wall relative to the backfill at any time. In-situ walls are often subjected to foundation or backfill settlement, and to recreate these occurrences a large jacked platform was required under the wall. It was necessary for the platform jacks to be able to lift the wall, in addition to being able to tilt either forwards or backwards in the imitation of localised settlement at the heel or toe. In reality, any movement of the backfill due to settlement will be greater at the top of the wall, due to it being much less tightly packed in this region (the lower areas are compacted by the weight of the fill above). In the wall tests, the movement to imitate backfill settlement occurs at the bottom of the wall (by moving the wall upwards), and hence is not entirely representative of normal settlement. Despite this drawback, the effect of backfill settlement was critical enough that this drawback was ignored, particularly as it was not practical to wait for it to occur naturally.

A major cause of damage and deformation within drystone walls is the introduction of a surcharge force, either from a structure or vehicle load behind the wall. The test setup was designed to incorporate a hydraulic jack, which could apply loads simulating these surcharging forces over any part of the backfill.

As the walls would be built sequentially, each test must be decommissioned before the construction of the next. To allow this, it was necessary that the site plan incorporate storage areas to house the material while the testing bay is cleared.

The health and safety aspects of both the use of the site and the construction itself were carefully assessed throughout the design stage. The manner in which the tests would be conducted was also considered, with one particular outcome being the requirement for an area to monitor the test proceedings without being placed in danger during a wall collapse.

The option of using hydrostatic pressures, as demonstrated by Villemus et. al.[14] and discussed in chapter 2.2.2, was also considered. The benefits of using water pressure (the horizontal pressures may be known at all times) were outweighed by the lack of vertical forces which are generated by the friction between a wall and a granular material. Furthermore, the use of a PVC-lined bag would prove impractical due to the continuous nature of the test walls. Should the entire wall be loaded with water pressure, the wing walls (which were intended to remain relatively stable) would be under the same loading conditions as the central portion. This would likely result in their failure in addition to the central section, giving rise to the problems of end effects which are otherwise avoided. Finally, Villemus' tests were halted at the point when internal shearing of the wall occurs, whereas the tests conducted in this project were designed to be continued through to destruction. The extreme wall movement would cause difficulty in maintaining the water level at the required height, in addition to causing spillage of the water

when failure finally occurs.

5.2.3 Site layout

The initial specifications called for a relatively open site, as the wall required a large area and storage capabilities. However, the site eventually used for the project was smaller than initially anticipated, requiring some adjustments of the test setup. The wall was reduced in length to 12m, retaining the central 6m section to be tested, but with smaller wing walls. At the same time, it was determined that the test area would be recessed into the ground by 1m, allowing the tapering of the wing walls to be less severe, as shown in figure 5-2. Another significant advantage of this design is that it allowed the test observation area to be closer to the wall due to its comparatively elevated position, further saving space.

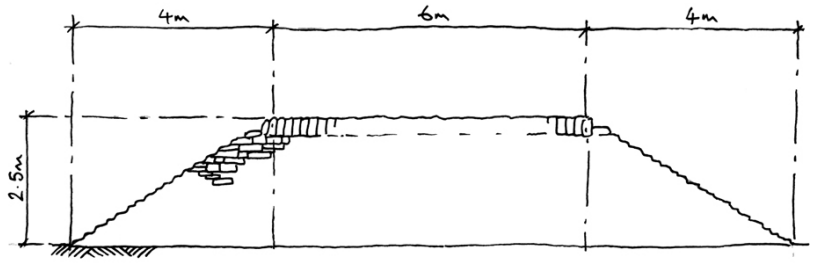

(a)

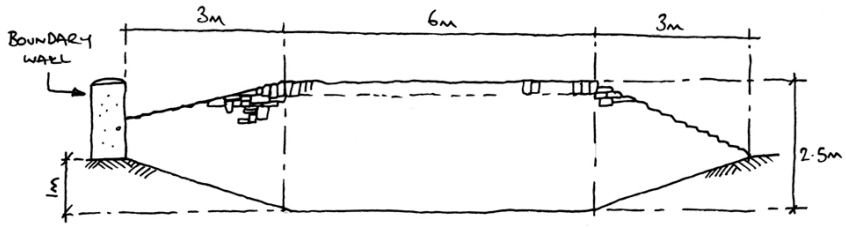

(b)

Figure 5-2: Wall geometry: a) initial specification; b) final design

After the final wall geometry was determined, the layout of the site was finalised. With estimates for the required sizes of the major test areas (test wall & observation area, backfill zone and storage zone) a basic plan was drawn up (Fig. 5-3). This considers the pre-existing vegetation around the site, in addition to allowing for the HGV access that would be required to deliver and remove materials.

5.2.4 Mechanical platform jacking design

As the specifics of each test had not been precisely determined during the construction of the site, the platform design had to account for many different potential

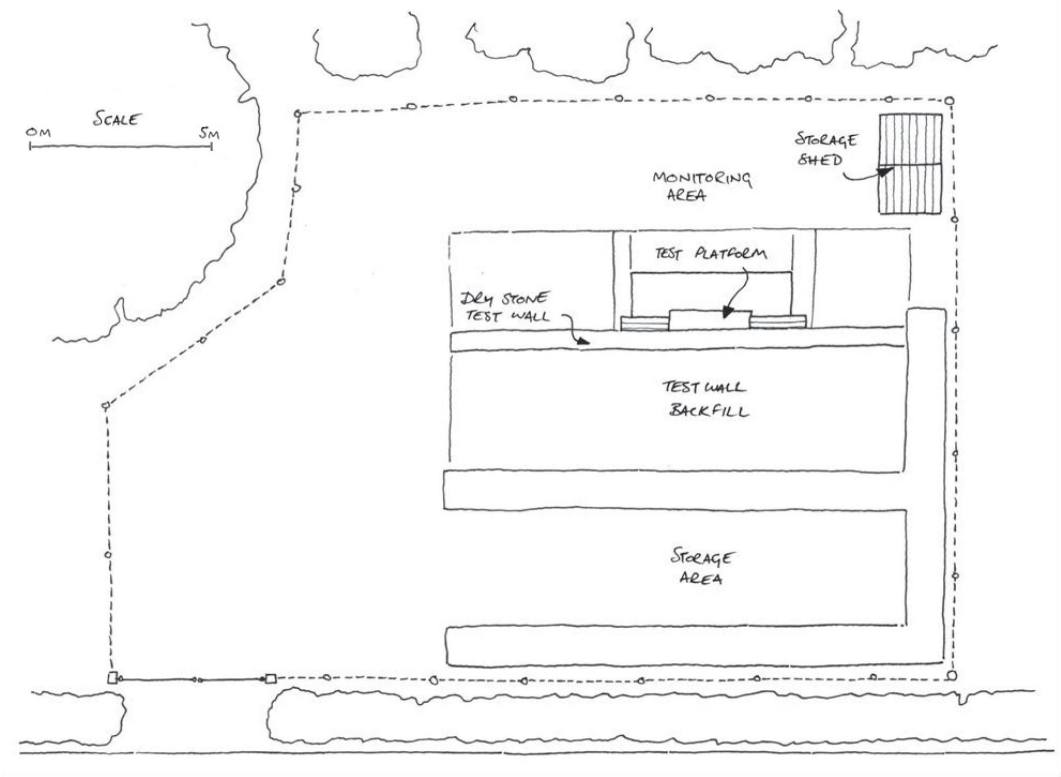

Figure 5-3: Site plan

designs. In particular, wall thicknesses between 500mm and 1000mm were anticipated, with the platform geometry and the member sizes designed to accommodate this.

When considering the actual platform mechanics, several factors had to be balanced to achieve the optimum design. The priority was that the platform deliver the full range of movements required, but this had to be incorporated into a design which was robust and safe. In addition, factors such as ease of construction and construction time, cost and flexibility were considered.

One possible design that was initially considered was the use of a system of jacks mounted away from the test wall, as shown in fig. 5-4. The jacks would move the platform in the required manner using a series of pivots and lever arms. This would have the benefit of placing most of the moving parts away from the underside of the wall, and as such be much more easily maintained. The jacks, by virtue of the pivots and lengthy lever arms would need to provide a much smaller force and hence be substantially cheaper. This in turn could potentially invite the possibility of a hand turned system once provided with the correct ratio of gears. This mechanism was eventually discarded for a number of reasons. Although several different arrangements of pivots and lever arms were possible, they utilised several moving parts, with some designs including sliding bearings. It was thought that reliance on such bearings in a system that would be permanently exposed

to the elements was unwise, as it could become fouled or corroded over time. In addition, the aim of the test is to take the walls to failure, which could potentially cause a failure of the platform should the lever arms and pivots be damaged by rockfall. Although an unlikely outcome - the workings would be covered by a protective case - this had to be considered as a cause for concern.

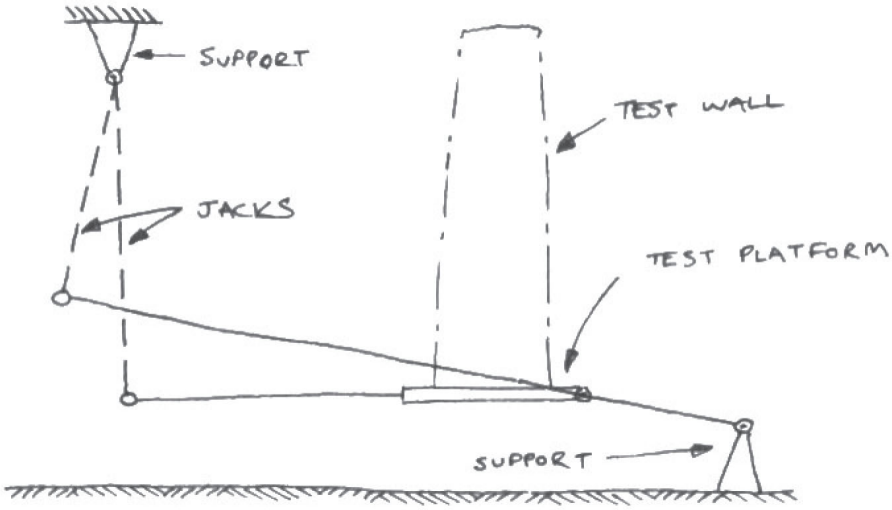

Figure 5-4: Initial jacking solution

The final design was a much simpler four-jack system, with each jack supporting a corner of the platform. However, there are still several drawbacks to this system. Firstly, the direct jack-to-platform connection requires that the jacks take the full load of the platform, without the mechanical advantage offered by the previous designs. This would also require four jacks, as opposed to potentially two for the pivoting system, and each must be of a substantially greater capacity, further increasing costs. Furthermore, this places the mechanical elements of the platform squarely underneath the wall. Should any mechanical problems occur during testing, it could be very difficult to fix them safely. Despite these issues, this direct-jacking system was decided to be the best option for the project, mainly due to its simplicity. From this decision stemmed many more issues - primarily, how the jacking itself should be performed. It became clear that one such method would have the main platform being moved purely vertically through four linked jacks, with a secondary platform on top which would be pushed by another two jacks mounted at the rear to produce the required tilt (fig 5-5). As the main platform would only move vertically, there would be many possible ways to restrain and monitor the lateral forces involved, which is a critical requirement of the design. One of the main disadvantage of this design is that it would necessitate six jacks, which would again increase the cost significantly. Extra driving mechanisms would be required for the operation of the four linked jacks, and it would also add a substantial amount to the overall depth of the platform. This greater depth

became a critical factor once ground excavation of the site was underway. The topsoil covered a very solid limestone bedrock, causing difficulty in excavating to the required depths.

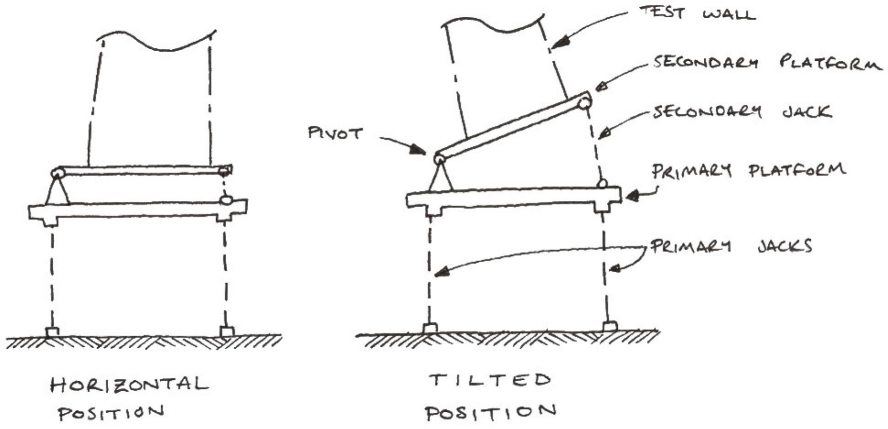

Figure 5-5: Initial jacking solution

The design was simplified to having just 4 jacks, with the front and rear pairs able to move independently, hence allowing the required movements and tilting (fig 5-6). The overall depth of the platform was reduced to an acceptable value, whilst also remaining a fairly simple design.

Once a jacking system was chosen, the platform deck design was completed, consisting of a series of large longitudinal rectangular hollow sections (RHS), braced with smaller sections. The platform was designed such that the main longitudinal beams at the front and rear of the platform could withstand the total applied load independently. The reasons for this are twofold; firstly, should the total applied load unexpectedly pass through the toe of the wall - as it might immediately prior to failure - it should still have adequate capacity. Secondly, the system has a considerable redundancy which may be required for unforeseen changes in the testing program (additional surcharging, larger walls etc). Calculations for the design of the platform may be found in appendix B.

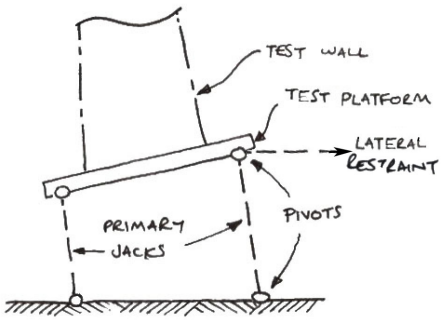

Figure 5-6: Initial jacking solution

5.2.5 Platform integration

Whilst the platform itself moves vertically and also tilts, the wing walls were to be founded on concrete. Between the platform and the concrete foundation exists a joint which could potentially affect the test results, as the central test section of the wall is being forced to move relative to the wing walls. To overcome this problem, a flexible joint was designed, capable of bridging the gap and eliminating the additional stresses that any platform movement would induce at this point.

The design selected consisted of hinges mounted at either end of the platform deck, from which six parallel box sections were mounted. The opposite end simply rested on a small, specially designed contact point, effectively creating a three-dimensional roller support. These 'transition beams' would move together in the event of pure vertical movement, giving a solid platform to carry the loads. In the event of tilting, the beams could move different amounts, but whilst each beam is at a different angle, the overall effect was still a solid bridge between platform and surroundings. This system works due to the magnitude of the movements. With a total travel of 400mm in the jacks, 14^o of rotation could be achieved. This translates into relatively small movements of the transition beams, such that whilst the individual beams may move independently, the difference from one beam to the next is slight - especially when compared to the general block size within the walls. A small-scale replica of the platform was constructed, shown in figure 5-7. This was built primarily to test the functionality of the platform, and ensure that the design could provide the movements initially specified.

5.2.6 Foundation design

The foundations for this project were initially designed to support all the loads within the system, including the platform and wall loads, as well as the surcharging frame and the surcharge load itself. Two strip footings would run under each side of the main platform, giving mounting points for the main jacks. The strip footings would also extend beyond these points in both directions, to allow anchor points for the surcharging frame columns, as shown by fig 5-8(a). The benefit of this closed system is that once the surcharging force is engaged, the loads are primarily kept within the system, and not transferred to the ground. This allows for potentially smaller footings, and hence a cheaper design. Another benefit of this is a reduction of any chance of ground settlement, which is critical to ensure the validity of the testing. The main flaw with this design was the location of the rear columns of the surcharging frame. The further back the columns are mounted, the deeper the strip footing would have to be below the fill, and the larger the forces within the concrete (hence, a more difficult construction, higher costs etc). Conversely, if the columns are closer to the platform, they run the risk of interfering with the interaction between the wall and the backfill, as well as limiting the flexibility of

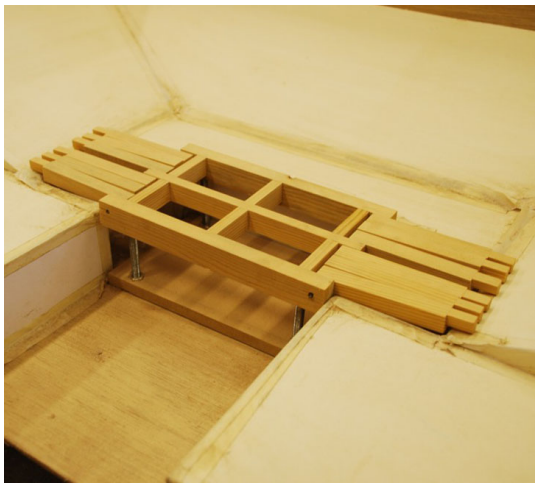

(a)

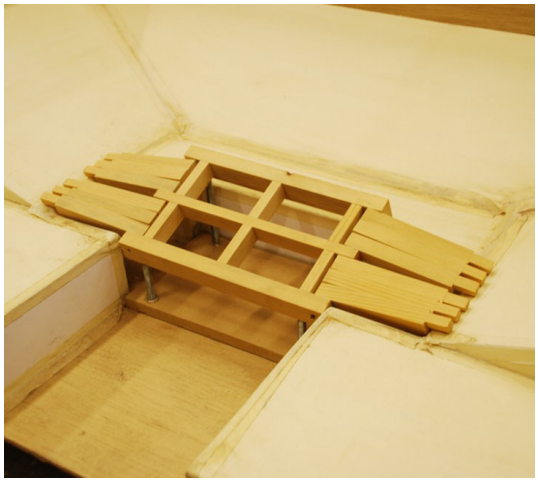

(b)

Figure 5-7: small-scale platform mock-up: a) untilted position; b) tilted position

the surcharge placement. Ideally, the columns would need to be at least 2m-3m away from the back face of the wall to ensure both that they do not interfere with the backfill and also to allow flexibility in the location of the surcharge plate.

Eventually the foundation design became a problem dictated by practicality rather than any other factor. As previously mentioned, the ground was discovered to be of extremely dense rock, making excavations very difficult. Hence, individual foundations were adopted for each component. Through a simple cost analysis, it was determined that the price of the additional volume of concrete required to provide enough dead weight to counter the force of the surcharge load was less than the potential cost of hiring the large plant required to excavate to the depth of the initial design.

The eventual design consisted of two large concrete anchors, to restrain both the front and rear columns of the surcharging frame. The rear pair was mounted at the very rear of the test bay - approximately 3m away from the backface of the

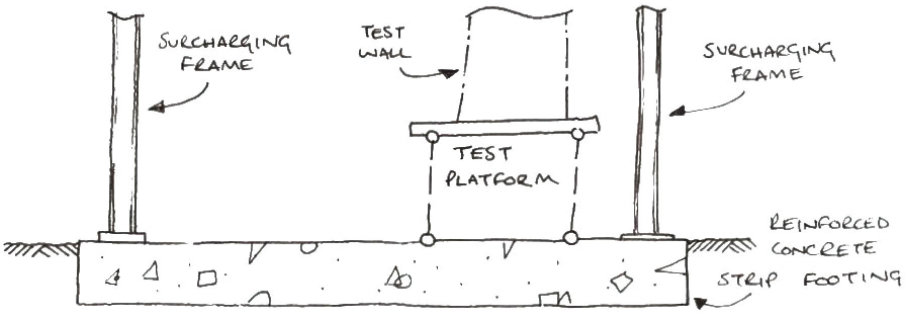

(a)

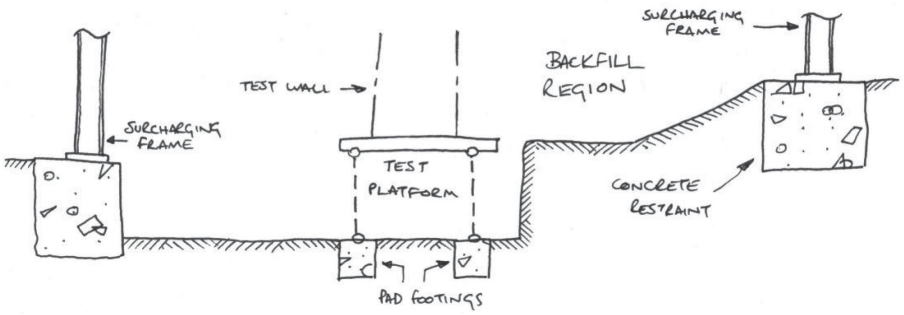

(b)

Figure 5-8: Foundation solutions: a) initial solution; b) final solution

test wall - so that the columns are far removed from the testing zone and have no impact upon it during testing. These were approximately 1.5m deep, 1m wide and 4m long.

The jack mountings were designed as four shallow pad footings. At the depth required to achieve the correct height of the platform, the ground was solid enough that the bearing capacity would exceed anything of the magnitude that the platform might impose. The pads themselves were approximately 300mm deep, 500mm square in plan and formed using C60 concrete to provide rigidity during testing (fig 5-8(b)).

5.2.7 Lateral restraints

Upon the construction of a wall and backfill, the active pressure from the retained material is transferred into the wall and hence into the platform. The jacks themselves are designed to operate axially, and so cannot be relied upon to resist the lateral loads. In addition there must be some means of recording the magnitude of this lateral force. The difficulty for this element of the platform arises from the versatility of the platform. Designs involving 'stop blocks' which the platform would rest against were ruled out due to the combination of vertical movements and the tilt of the platform. To reduce the movements that this restraint must be capable of accomodating, the focus shifted to the hinge between the rear jacks

and the platform. As any platform rotation will occur about this pivot, the lateral restraint could be connected here and only be required to move vertically, with any tilting having no effect.

The solution was only determined once the ground conditions and foundation design were set. The inclusion of a large concrete block to anchor the surcharging frame presented itself as an ideal place to also anchor the lateral loads. A pair of radial arms were designed to be connected by simple hinges anchored into the concrete via its reinforcement cage, with the free ends connected to the platform in line with the rear jacks (fig. 5-9(b)).

To ensure complete understanding of the system, a half-scale replica of the test platform was constructed (fig 5-10). In addition to proving that the system works as expected, this half-scale model also highlighted many of the difficulties that would be faced when installing the full-scale version, which would be made many times more difficult due to difficult ground conditions and little access for appropriate plant. Lifting points were added to the deck, allowing it to be safely suspended from all four corners. The construction sequence was designed to ensure that the steel surcharging frame was erected prior to the platform installation. The frame was then used to support the platform via chain hoists whilst it was safely lowered into place. Thick rubber sheeting was also detailed along the platform joints, where small gaps existed. These sheets allow movements and follow the profile of the platform, whilst creating a barrier for the backfill and wall material, preventing fouling of the joints.

5.2.8 Jack specification

For this application, mechanical screwjacks were chosen in favour of a hydraulic jacking system. The primary reason for this is that hydraulic jacks may creep over time, whilst the mechanical screwjacks may be locked off and will not change length unless driven by the motor. As the experiments depend on the platform remaining immobile during construction and loading, the hydraulic jacks were not a viable option. To ensure adequate provision for the platform loads, four mechanical screwjacks rated to 20 tonnes each were supplied by Power Jacks Group^{TM}, and mounted as described in figure 5-9. The jacks were also specified with lock-out switches to prevent movement beyond the safe maximum extensions, and bellows boots to avoid corrosion and fouling of the screws themselves.

The jacks move in pairs (front and rear), with each pair powered by a single 750W motor. The motor requirements are small due to the very slow movements of the platform (1mm/min), instead requiring a large reduction gearbox to achieve the necessary speeds. The motors themselves are mounted onto both of the northernmost jacks, with 50mm diameter drive shafts linking them to their respective partners. Both the jacks and attached motors are shown as installed under the test platform in figure 5-11. 400mm of stroke is possible from each screwjack, in turn

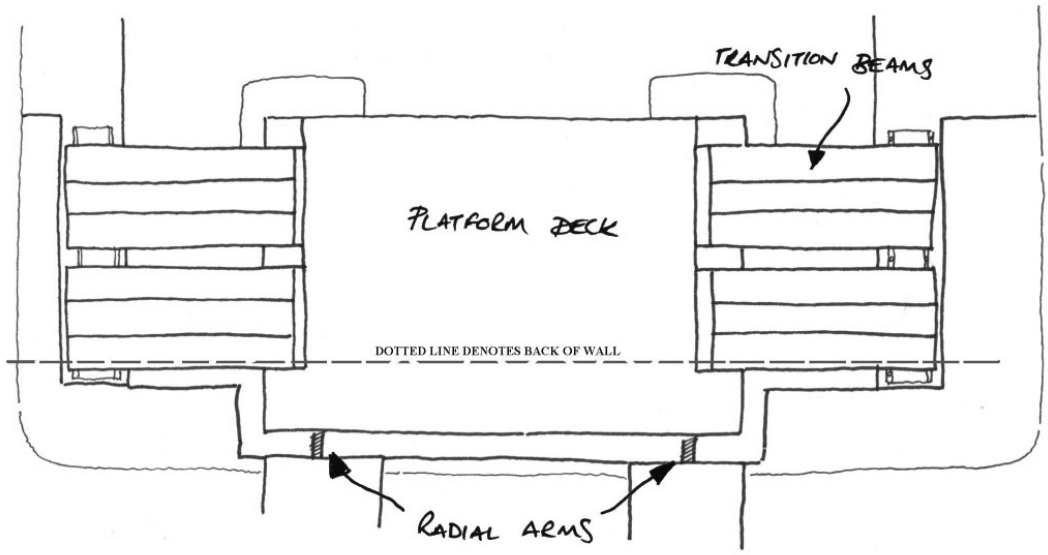

(a)

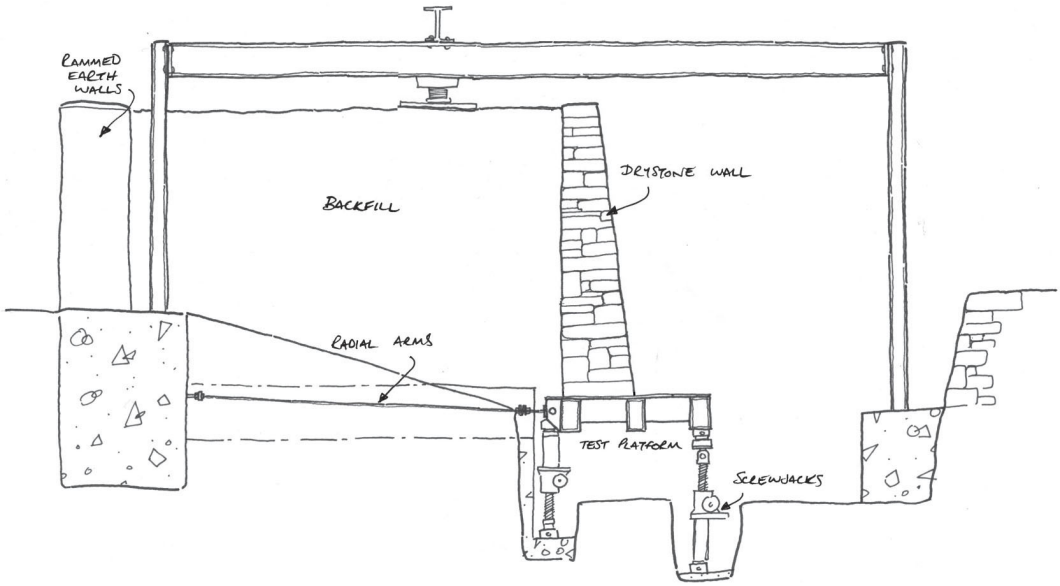

(b)

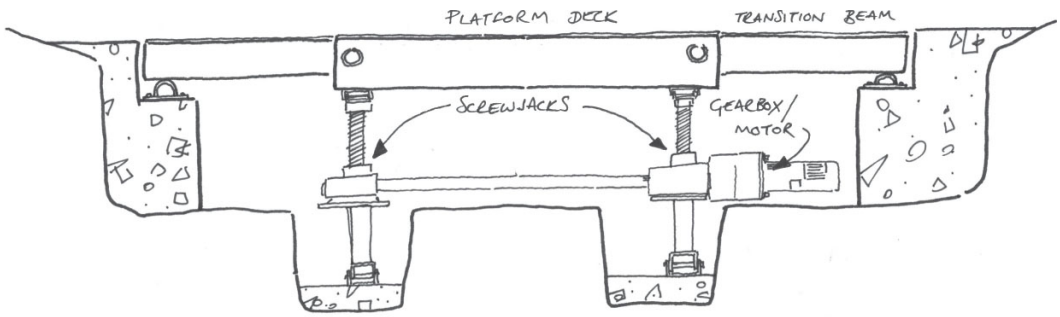

(c)

Figure 5-9: Mechanical platform details: a) plan; b) section; c) elevation

Figure 5-10: Half scale platform replica

allowing a platform tilt of up to 14^o.

The motors are single phase mains-powered, and controlled from a single control box unit, supplied and installed by Revolution Drives Ltd. The unit has movement buttons for each pair of jacks, as well as a tandem switch to move both pairs simultaneously. A LCD display shows current stroke positions of each jack pair, and allows selection of jack speed to 0.1mm/min resolution.

5.2.9 Platform sliding friction

As the wall was intended to be subject to large loads and tilting, it was crucial that the wall did not fail by sliding at the base. To ensure this, a wire mesh was welded to the platform deck, and a steel angle section was bolted to the platform's leading edge. With the beam in place, the lowermost course of stones for each wall would be unable to slide forwards.

5.2.10 Construction of rammed earth walls

As shown on figure 5-3, rammed earth walls were used as boundary walls at the perimeter of the tests. These were 1.2m high and 0.6m wide, constructed using the spoil from the initial excavation of the test area (fig. 5-12). Samples of the soil were graded, and after measuring the clay content it was determined that a small amount of cement was required to give a stable wall. The walls were constructed using Mabey formwork panels and a pneumatic earth rammer.

(a)

(b)

Figure 5-11: Jacking system: a) screwjack assembly; b) motor/jack coupling

Figure 5-12: Rammed earth boundary walls

5.3 Testing instrumentation

Throughout each test, several methods of monitoring wall displacements have been utilised. As the mechanics of drystone wall behaviour have not been thoroughly investigated via full scale physical testing, it was initially unclear how effective each technique would be. As each test was undertaken and the various data obtained, the instrumentation used has therefore evolved. In many cases, this involves the repositioning of a particular instrument to a more effective location. However, in some instances a particular technique has been abandoned in favour of another.

The layout of the tests calls for instrumentation to monitor three key areas; the wall, the backfill and the platform. The interaction between the wall and the backfill is also of great interest. This section describes the techniques used to gather the data in these various locations, along with their effectiveness and optimum positioning.

5.3.1 Platform positioning

Each pair of screwjacks was fitted with a limit switch. The limit switch has a twofold application; it ensures that the screwjack moves within a predesignated range and simultaneously monitors where within the stroke it currently rests, to a resolution of ± 0.1mm. This is relayed both to the screwjacks' control terminal and also as an analogue signal to a Grant Instruments DT505 Universal Data Logger, which is fitted with two additional channel expansion modules.

It should be noted that all load cells and transducers used in this project were connected to the Data Logger and its additional expansion modules, storing the data in real time at any intervals required (maximum of 1 reading every 5 seconds).

5.3.2 Platform loadings

Due to the pin joints at either end of the screwjacks, they attracted purely axial loading. By placing load cells between the jacks and the pins, these axial loads can be measured, hence determining the vertical forces within the system. 20 tonne capacity compression/tension button-type load cells were used, supplied by Vishay.

The radial arms resisted the lateral forces applied by the active pressures from the backfill and the surcharging forces. 20 tonne compression/tension S-type load cells were used to measure these forces, again supplied by Vishay.

In total six load cells monitored the global forces applied to the platform; two solely for lateral forces, and the other four for vertical loads. As the platform was made of relatively deep box sections, it had a large stiffness, so causing the loads to be distributed on to the jacks and radial arms unevenly. This was due to the fractional differences between the lengths of the radial arms and screwjacks and the fact that the platform only requires three legs and one radial arm to be stable. Consequently, at some points during testing (especially in the unloaded situation), one of the load cells could give a vastly different reading. At the time of installation, this was reduced as much as possible by making fine adjustments to the lengths of each of the screwjacks and radial arms, ensuring that each point of contact was bearing some weight from the platform. This error was further accounted for by combining the readings into pairs (front jacks, rear jacks and radial arms), rationalising the loads.

Although it is difficult to ascertain exactly how much of the wall and backfill was bearing down on the platform, these readings have been useful in understanding how the global loads change in response to the various test sequences. These data are explored in chapter 7.

5.3.3 Local backfill pressures

To monitor the changing pressures within the backfill, a series of small 250N and 500N capacity load cells were used. Each load cell was sandwiched between 100mm x 100mm steel plates, and placed at critical locations within the backfill (fig. 5-13). The load cells were orientated to record either horizontal or vertical pressures, with the aim of determining the distribution of stress within the gravel arising from the surcharge loading. The results were often inconsistent and erratic, mainly due to the size of the steel plates compared to the size of the gravel. Larger plates were considered, which would give more reliable readings, but these would have a greater impact on the test itself and possibly affect the wall behaviour. Due to

this, after the second test wall, these instruments were removed from the testing procedure. However, these load cells were still moderately useful. In monitoring the magnitude of the changes, and comparing them relative to one another, the impact of the surcharge force may be tracked.

(a)

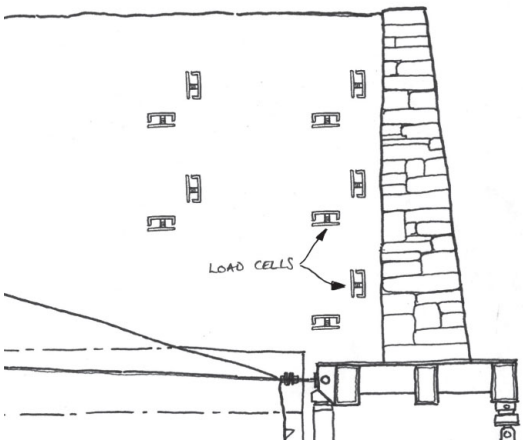

(b)

Figure 5-13: Backfill pressure monitoring: a) pressure cells; b) cell placement

5.3.4 Backfill monitoring

Monitoring of the backfill in real time is a difficult task using non-destructive means. Of particular interest within the backfill are the global and localised movements, including any developing failure planes.

Two methods have been utilised over the course of the tests, beginning with the use of 20mm steel ball-bearings within the backfill. The ball bearings were numbered and placed in a grid-like formation as the height of the backfill increased. Before the ball bearings were covered by the next layer of gravel, the position of each (relative to the site) was determined using a Total Station, operating in reflectorless

mode and accurate to ± 1mm. Upon destruction of each wall, the gravel was carefully unearthed and the ball bearings relocated using a metal detector. Using the Total Station, the final positions of the ball bearings were located, and the overall movements calculated.

An issue with this system of backfill monitoring is that it is time consuming to conduct. However, of more importance is the fact that the ball bearing positions can only be determined after total collapse. At this point, the gravel may have shifted due to the collapse of the wall rather than describing the gravel movements during testing, and hence inaccurately describing the development of a failure plane.

To this end, the final three walls incorporated rudimentary inclinometers, which could provide the angle and position of any failure planes as they develop. Long, very flexible plastic tubes were placed vertically into the gravel using a mandrel. At intervals during the tests, long marker poles were lowered down the flexible tubes until either the end or an obstruction occurred, such as kinks caused by developing shear planes (fig. 5-14). Through the use of multiple tubes, the kinks in the tubes can be correlated, giving a position and orientation of the developing failure plane.

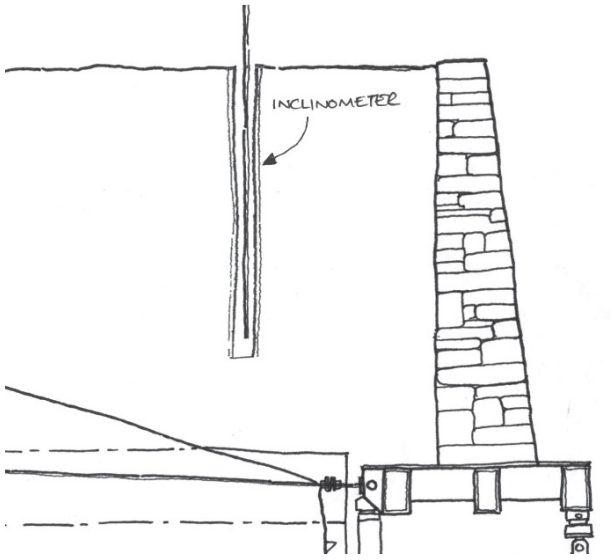

Figure 5-14: Backfill movement monitoring via dowel and flexible pipe

5.3.5 Total Station monitoring

Throughout each test a Leica reflectorless Total Station was used extensively to monitor the position of the wall. Two short concrete columns were cast into the observation area, with Tribrachs permanently attached (fig. 5-15). The co-ordinates of these Tribrachs were saved into the Total Station's memory, allowing the unit to be attached only when required whilst ensuring continuity of the results.

The total station was used in reflectorless mode, allowing data points to be recorded with a resolution of ± 1mm. At the loss of sub-millimetre resolution, this

(a) (b) (c)

Figure 5-15: Total Station mounting points: a) main mount; b) Tribrach mount; c) secondary mount

allowed the position of the walls to be investigated without disrupting the wall by mounting sophisticated and delicate reflecting prisms, whilst also ensuring that no persons were required to enter the vicinity of the wall during testing. Due to the relatively large displacements encountered, the accuracy of the Total Station in reflector-less mode provided acceptable results for the purpose of these tests.

Initially, the Total Station was used to monitor the walls during construction. After completion of each wall, a series of points were marked onto the face in vertical lines. Typically 5 lines were marked; a centre line, then at 1m and 2m intervals in either direction. Up to 350 points were marked in this fashion, allowing a full profile of the central portion of the face to be recorded. For the later walls, additional markers were added along the length of the coping stones.

The walls were monitored as the backfill was introduced, and then throughout the test procedures. Although this process provided a comprehensive survey of each wall, the major issue with this form of monitoring was that it was time consuming, requiring up to 30 minutes to perform a full survey. For this reason, the Total Station could not be relied upon to capture the final moments of each test.

5.3.6 Photography & video capture

Three Canon DX40 digital SLRs were used extensively throughout the project. During testing, two of these were used to mount onto brackets attached to the surveying post (figs. 5-15(a) & 5-15(b)), spaced 500mm apart. By taking simultaneous photos with these cameras, stereo pairs were created. The third camera was used as a roving camera, taking detailed images of bulges, cracks, movements etc., as well as documenting the final collapse mechanisms and the movement of the coping from behind the wall. It should be noted that although stereo images were taken for each wall test, these data were not used in the analyses. This was mainly due to the other forms of monitoring (video records, draw wire transducers and Total Station monitoring) providing sufficient information to conduct a thorough

analysis.

A fourth camera was used exclusively to capture images of targets fixed to the face of the wall (fig. 5-16(a)). These were then analysed at Southampton University using particle image velocimetry (PIV) techniques to accurately determine the monitored block movements and rotations (± 0.1mm).

(a)

(b)

Figure 5-16: PIV monitoring equipment: a) PIV targets; b) camera & mount

High definition (HD) video footage was captured of all of the test proceedings, including the final failure mechanisms on a Sony camcorder.

5.3.7 Draw wire transducers

As the monitoring of deformation and displacement were integral parts of the full-scale tests, displacement transducers were an important and effective instrument. Standard Linear Differential Voltage Transducers (LDVTs) were inappropriate for this site, as they generally do not have the stroke necessary and are not robust enough for use in an outdoor environment. Instead, Cable-Extension Displacement Sensors (CDS) transducers were used, supplied by Vishay. The CDS40 instrument has 1016mm of stroke, and by using a flexible cable, any vertical and lateral move-

ments could be easily accommodated. Sacrificial lengths of wire were connected between the wall and the ends of the draw wire cables, allowing a greater separation to further protect the transducer mechanisms from possible damage during collapse.

To mount the transducers, an L-shaped steel arm was attached to the platform and cable-tensioned to eliminate movement (fig. 5-17(a)). By attaching the arm to the platform, this ensured that the transducers recorded movements of the wall relative to the platform. In this way, any movements or rotations of the platform are automatically accounted for, with the draw wires giving only the wall displacements. The draw wire cables were susceptible to slight movements due to wind, vibrations etc., however, the effect of these was negligible.

(a)

(b)

Figure 5-17: Draw wire transducer mounts: a) initial mounting; b) multiple mounts

The second wall utilised five transducers in a single vertical line along the centre of the wall. These transducers proved very successful, and were crucial in particular for capturing the final moments of each test. For the third wall, additional lines

of monitoring were added (fig. 5-17(b)), allowing three vertical series of points to be monitored. Draw wires were also suspended from both the surcharging frame and the hydraulic surcharging jack, monitoring the vertical movement of the wall coping, the backfill and the loading plate. For the final tests, up to twenty five transducers were being used per wall, allowing the movements of the wall from construction to collapse to be recorded, and related to the loads and surcharge forces in real time.

Walls 3, 4 and 5 also incorporated draw wires to monitor the internal face of the walls. To achieve this, 100mm x 50mm rectangular hollow sections replaced selected face stones, allowing access to the internal face. The draw wires were then attached to the internal face block and the cable passed through the channel section and out of the face of the wall. It was ensured that the steel channel section was not in contact with internal face block, allowing sufficient space for the internal block to move freely (fig. 5-18).

(a)

(b)

Figure 5-18: Draw wire monitoring of internal wall face

5.3.8 Surcharge monitoring

As mentioned previously in section 5.3.7, a draw wire transducer was used to monitor the vertical position of the surcharging plate (relative to the steel frame supporting the hydraulic jack). In addition, a load cell was positioned between the

hydraulic jack and the plate, allowing the applied loads to be constantly recorded.

5.4 Testing procedure

To maintain continuity between the gathered test data, each wall was tested in a similar manner. Any changes that were made came in response to the outcomes of the previous tests, aimed at encouraging specific behavioural aspects. For each wall, there were several methods available for affecting the stability. These consisted of a platform movement - either vertical movement, a tilt or a combination of both - or a surcharge. Each action was designed such that it replicated an event which could occur to an in-situ wall.

5.4.1 Platform tilting

A localised bearing failure of the foundation is a possible failure mechanism for any retaining wall. If the loadings in the retained fill increase - either due to surcharging, water pressures etc. - the respective loads on the wall also increase. The higher overturning forces will cause a redistribution of the forces at the base of the wall, with higher loads at the toe. If the loads at the toe continue to increase, it is possible that differential settlement of the foundation may occur. Even should the settlement be minor, this would likely cause a drystone wall to deform, possibly to the point of collapse or failure by sliding.

For these wall tests, the foundations consisted of the mechanical platform. As the jacks and the platform are designed to accommodate much higher loads, the foundations will not be susceptible to any unwanted settlement. However, to mimic this phenomenon, the front jacks could be lowered, giving an approximation of localised settlement.

5.4.2 Vertical platform movement

Over time, it is common that both a drystone wall and its retained backfill will settle. However, due to the incompressible nature of most drystone blocks, the wall will not generally settle as much as the backfill. Indeed, this phenomenon was identified by Burgoyne during the backfilling of his full-scale tests, whereby additional fill had to be placed to account for the settlement which had already occurred[12]. Due to this differential movement, friction will be generated at the interface between the wall and the backfill. This in turn causes a redistribution of the active pressure so that a greater vertical force is applied to the wall, thereby aiding stability. As the differential movement continues, the friction also continues to increase (and hence the vertical component of the active pressure), until a peak value is reached (equal to that of the backfill's internal angle of friction).

From the limit equilibrium program, it has been ascertained that the friction

angle between the wall and the backfill has a large impact on stability, with even small variances being of importance. Therefore, to ensure that a correct analysis of the full-scale test walls in this project is possible, this friction angle must be known. The time constraints of the project do not allow enough time for each wall's backfill to settle naturally, in addition to the problem of the use of a stiff aggregate as a backfill material, which may limit the scale of the settlement. Instead, the platform was raised, giving the sane relative movement.

As the wall is raised, the differential movement will cause the interface friction to increase. Consequently, as the friction angle increases, so the vertical loads on the wall increase. The load cells attached to the screwjacks under the wall record these changes, and are monitored as the movement progresses. At the point at which the peak friction angle is achieved, the loads on the platform will plateau, despite the continuing vertical movement. It is at this point that sufficient displacement has occurred to produce the full friction angle between the wall and the backfill, and the vertical lift may be halted.

5.4.3 Surcharging

The third test procedure applicable to the test walls is localised surcharging. The steel frame shown in figure 5-9(b) allows the application of a maximum of 200kN at any point along the centreline of the backfill. As the concrete footings holding down the steel frame have a volume of approximately $12m^3$, this provides sufficient dead weight to easily restrain a surcharge of this magnitude. The load itself is applied to a metal plate via a hydraulic jack which is manually pumped at a safe distance from the wall.

The consequence of using a manually-operated hydraulic jack is that as the backfill and wall displace, the applied load reduces. For a more realistic simulation, the loading would not decrease once movement has began. This would likely cause the walls to collapse much more quickly and uncontrollably, and potentially in a more dangerous manner. Although less realistic, the use of a manually-jacked load is much safer as it does not allow the large amounts of energy to be stored in the system, which could lead to a more explosive failure. As each wall deforms beyond its optimum profile, the maximum load it can withstand drops.

This is highlighted in chapter 6, which shows the maximum applied load dropping as deformations occur, until finally the wall is destabilised and collapse occurs. This method allows for a much more controlled collapse, and allows more time to document the wall behaviour and obtain pictorial evidence.

It should be noted that for the purposes of the full-scale testing, the actual values of the surcharging loads are not as important as their effects. Whilst the maximum applied loads may be used to make comparisons between the various tests, the main function of the surcharging forces are to drive the deformations of the walls. Through these deformations, the mechanisms which cause such phenom-

ena as bulging, bursting, sliding and toppling may be better understood.

5.5 Concluding remarks

Initially, the scope of the full-scale testing was not fully determined, especially with regard to the final walls. The process of designing each test was a fluid process, with information from each successive wall feeding into the design, test procedure and instrumentation of the next. With this in mind, the laboratory was designed to allow some flexibility in the test design. The platform had the capacity to move vertically by 400mm, tilting in the plane of the wall by up to 20^o in either direction. In reality, only a fraction of these movements was required, however the possibility of additional movements was anticipated and catered for. Similarly, the capacities of both the screwjacks and surcharging frame were rated to much higher values than required, allowing for 200kN of surcharging and granite walls of up to 1m thick, compared with 100kN surcharge forces and limestone walls of up to 600mm thick that were used in actuality.

The shape of the test walls was a combination of design necessity and costing; each should be tall enough and long enough to avoid any end-effects and imitate a typical wall of a much longer length, but balanced against the cost requirements which are associated with a larger wall. The final design accommodated both of these needs, providing test walls capable of reproducing in-situ wall behaviour within the constraints of the project budget.

Chapter 6

Full-scale testing

6.1 Introduction

Five full-scale drystone wall tests were conducted during this project, carried out between June 2007 and February 2009. A variety of methods were used to instigate deformation and failure, as discussed in chapter 5. The tests themselves were primarily designed to induce phenomena specific to drystone walls - specifically bulging and bursting. This chapter is concerned with documenting the test procedures used to produce these effects, and the measurements and observations made during testing. The analysis of the underlying mechanisms behind the wall behavior, together with the theory which led to the progression of the test procedures, is discussed in chapter 7.

6.2 Wall 1

6.2.1 Wall construction

Wall 1 was constructed in June 2007 over five days. The wall dimensions were set at 600mm at the base, tapering to 400mm at the coping, totalling 2.5m in height, with a vertical internal face and a battered external face at approximately 4^o-5^o. Roughly 30 tonnes of limestone were required for each wall.

The first wall was constructed by the masons in the style and of the standard to which they would normally work. This incorporates full pinning where necessary, ensuring that there is no block which could rotate or rock before placement of the next stone. It was also ensured that running joints were not present where possible, and the stones were dressed to ensure interlock and a minimum of voids.

Tie stones were incorporated into the wall at 1m intervals when the height reached 1m, 1.5m and 2m. These stones were generally an unbroken length of stone which spanned from the internal to the external face and protruded slightly. In the cases where no suitable stones were available, two lapped stones were used instead. Figure 6-1 shows examples of the tie stones used.

(a)

(b)

Figure 6-1: Examples of tie stones used

Both the internal and external faces were finished to a high standard, with large, slab-like blocks being used where possible. As figure 6-2 shows, these stones protruded most of the way to the middle of the wall, with the remaining space being well packed with a core material.

Coping stones were used to provide the upper 300mm of the wall, placed upright and unmortared. These stones are shown in figure 6-3, and span across the length of the wall which was constructed to full height. The blocks generally chosen to be used as coping stones were generally 300mm - 400mm on each side, and 100mm thick.

For the first test wall, backfilling was carried out at the same time as the construction of the wall itself. The fill was placed in layers of approximately 300mm using a CASE 40XT skid steer loader (fig 6-4), then raked to ensure an even application. Finally, a 1kN vibrating plate compactor was passed over the surface in an attempt to provide a uniformly dense material throughout the backfill. This

Figure 6-2: Wall 1: Internal configuration

Figure 6-3: Wall 1: Coping stones

was particularly important as the location of the instrumentation buried in the backfill (ball bearings and pressure cells) were dependent on remaining unmoved until the start of the test.

Once a comfortable working height had been exceeded on the external face, a series of trestles was erected. This consisted of a materials bench for storing stone and equipment, with a slightly lower platform for the masons to stand on (fig 6-5).

Figure 6-6 shows the completed wall 1. As shown by the figure, the wall was

Figure 6-4: Placement of backfill

Figure 6-5: Trestle setup for upper sections of wall

extremely well constructed with tightly-fitted joints and few running joints. Care was also taken to maintain level, even courses to the extremities of the wing walls, where it tapered to the ground.

Upon completion, wall 1 was fully backfilled to 2.2m in height and then mon-

Figure 6-6: Wall 1: Prior to testing

itored for 4 weeks using a Total Station, to identify any developing movements. No noticeable movements were detected within the resolution of the Total Station, which is accurate up to ±1mm.

Each of the subsequent test walls described in this chapter were constructed with several commonalities. These include the material used, the general wall style (internal and external face with rubble infill), and the placement and location of both coping stones and through stones. The use of trestles to aid working at height was also repeated where required.

Prior to testing, a plate loading test was carried out on the retained fill to ascertain the approximate friction angle. A 100mm x 100mm plate was placed on the surface of the fill and hydraulically jacked into the fill whilst monitoring the displacement and applied load. When the bearing pressure exceeded 600kN/m^2, the displacements began to increase with a much smaller increase in bearing pressure, indicative of a shear failure. The Terzaghi equation [44] for shallow foundations was then used to determine the associated angle of friction for the material from this data (equation 6.1[45]). An ultimate capacity of 600kN/m^2 equates to an angle of friction of 53.1^o, which is extremely high, but unsurprising given the angularity of the backfill and the high level of compaction.

$$q_{ult} = p_c N_q + \frac{1}{2}\gamma_{soil} B N_\gamma \tag{6.1}$$

where:

q_{ult} = ultimate bearing capacity
$p_c N_q$ is due to surcharge and friction in the soil
γ_{soil} = bulk unit weight of soil
B = width of foundation
N_γ = bearing capacity factor as given by Brinch Hansen[46]:

$$N_\gamma = 1.5(N_q - 1)\tan\phi \tag{6.2}$$

6.2.2 Test procedure

Testing began on the 9th of July 2007, and was conducted over five days; each day of testing was followed by a day of monitoring until the fifth day when collapse occurred. On the first day of testing the wall was raised by 20mm to generate the full friction angle at the wall/backfill interface (see section 5.4.2). The loads on the screwjacks were monitored as the platform was raised, and after they were seen to plateau as shown in figure 6-8, the movement was ceased. The rest of the day, as well as the following day were given over to monitoring the wall for any changes. No further movements were recorded in this period.

The third day of testing (11th of July, 2007) comprised a combination of surcharging and platform rotation. Initially, a 400mm x 400mm surcharging plate was positioned such that the closest edge to the internal face of the wall was at a distance of 500mm. The plate was then slowly loaded up to 50kN, whilst the wall was carefully observed. It was found that the wall was rotating about the toe, mainly due to the fact that the surcharging force was being applied too close to the wall. For this reason the surcharging force was then moved back until the leading edge was 1m from the wall before reloading up to 96kN.

At this point, a localised bearing failure at the toe was simulated. The front jacks of the wall were lowered initially in increments of 2mm at a rate of 1mm/min. This later increased to increments of 5mm at the same rate (1mm/min), until a total vertical movement of 50mm had been achieved at the front jacks. This equates to a rotation of just 2.04^o from horizontal, and a theoretical outward horizontal movement at the top of the coping stones of 89mm. This was followed by a further surcharging at a distance of 1m, with loads reaching 80kN before the plate began to shear through the backfill and became difficult to load. As before, the fourth day was used to monitor the wall with no applied load.

The fifth day was again a combination of platform rotation and surcharging. Initially, the front jacks were lowered a further 25mm, causing a rotation of 1.02^o. At this point the jacks were stopped, and not moved again until failure.

Figure 6-7: Wall 1: Prior to failure

As the wall still appeared fairly stable and in good order, it was found necessary to increase the surcharging plate size, to allow a larger force to be applied and to reduce punching in the backfill. A stiff, steel box of dimensions 500mm x 600mm was used, again 1m from the internal face of the wall, with the longer side parallel to the wall. With this apparatus, a surcharge load of 110kN was reached. The wall was slowly loaded and monitored for 3 hours and 45 minutes, with the maximum load dropping off as the displacements increased. At this point, the wall was heavily distorted, with a slight convexity in the face and a measured overhang of 425mm at a height of 2m (fig. 6-7). Finally, the wall failed via toppling. Just prior to failure, the maximum load which could be applied was 40kN.

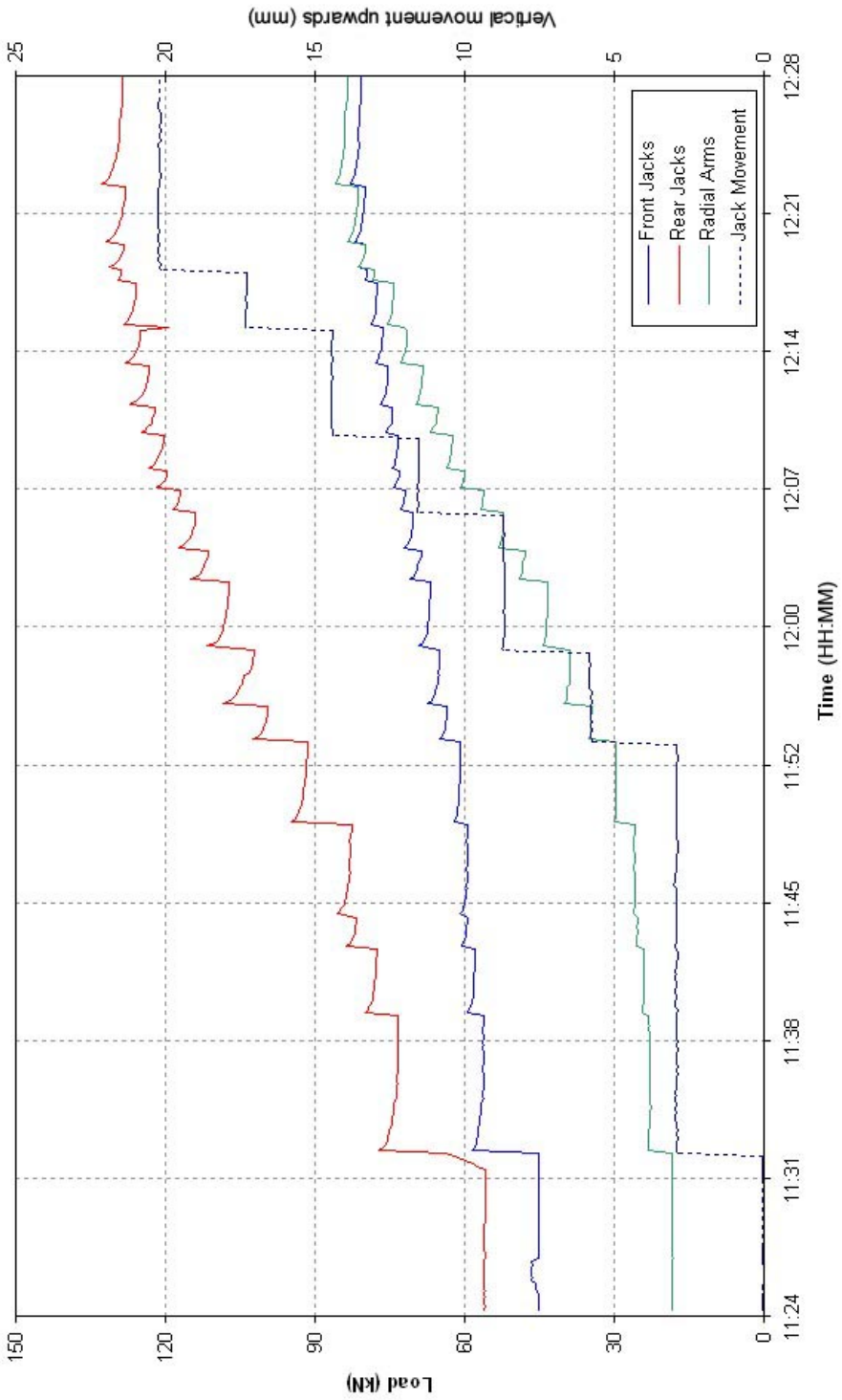

Figure 6-8: Wall 1: Generation of interface friction via platform lift

6.2.3 Recorded data & observations

Test wall 1 incorporated several methods of instrumentation, allowing many different aspects of the test to be examined. The behaviour of the wall is most obviously displayed by Total Station data, which measured the displacements of the external wall face. In figure 6-9, the horizontal movements of the wall are shown for the duration of the test. The legend indicates both the time at which the readings were taken in addition to the conditions imposed upon the wall prior to surveying (Platform raising, tilting or localised surcharging).

From the surveying measurements taken before and after the initial raise 20mm of the platform, it was found that the wall bulged slightly; 800mm from the base a horizontal movement of 10mm was recorded, whilst at a height of 2m an outward movement of 6mm was observed. It was accompanied by an increase of loads on the platform, both horizontal and vertical. The tensile forces in the radial arms increased by 54.4kN, whilst the vertical loads increased by 67.7kN, with 47.3kN of this directly from the rear jacks.

Rotation of the wall also caused additional movements. On the 11th of July when the platform was rotated by 2.04^o, the deformations increased rapidly, with horizontal deformations greatest at the crest of the wall, reaching 92mm at the highest recordable location (1.8m from the base). However, the pure rotation of the wall would only give a movement of 78.6mm at this point, indicating that the rotation has caused an additional displacement of 13.4mm. The additional deformations caused by the rotation are not linear, increasing from 5mm to 13.4mm in the first 1m of height, then remaining at approximately 13.4mm for the subsequent 1m.

Figure 6-11 shows the displacement at specific heights, plotted against the peak load applied via the surcharge. Although there were difficulties with the initial plate size and location, once the 500mm x 600mm plate was in use the system could carry loads over 110kN. The wall's response to these loads was continuing displacements in the form of a linear topple. This behavior is apparent in figure 6-11, with the deformations increasing at a faster rate for those points higher up the wall than those near the base. On the final day, prior to failure the peak load rapidly decreased from over 110kN until only 40kN could be sustained. At this point, collapse by toppling occurred.

Upon collapse of the wall, the gravel was carefully removed and the ball bearings within the backfill were located with a metal detector. Once unearthed, the new position of each ball bearing was determined with the Total Station. Figure 6-10 shows both the initial and final positions of the ball bearings that could be located. Many of the ball bearings within the failure zone were lost during collapse, however the position of those that remained give an indication of the critical failure plane, noted in the figure.

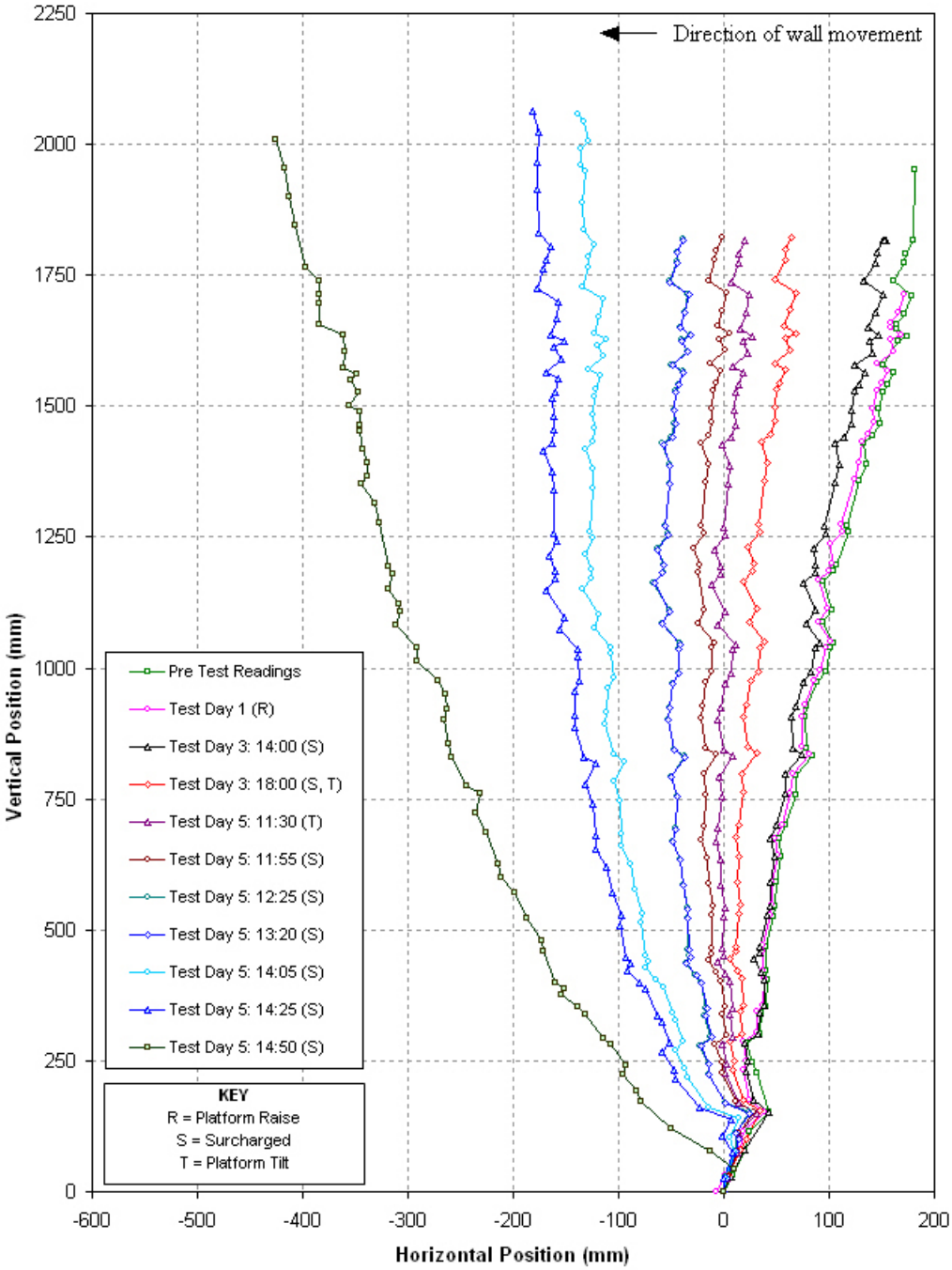

Figure 6-9: Wall 1: Measured displacements

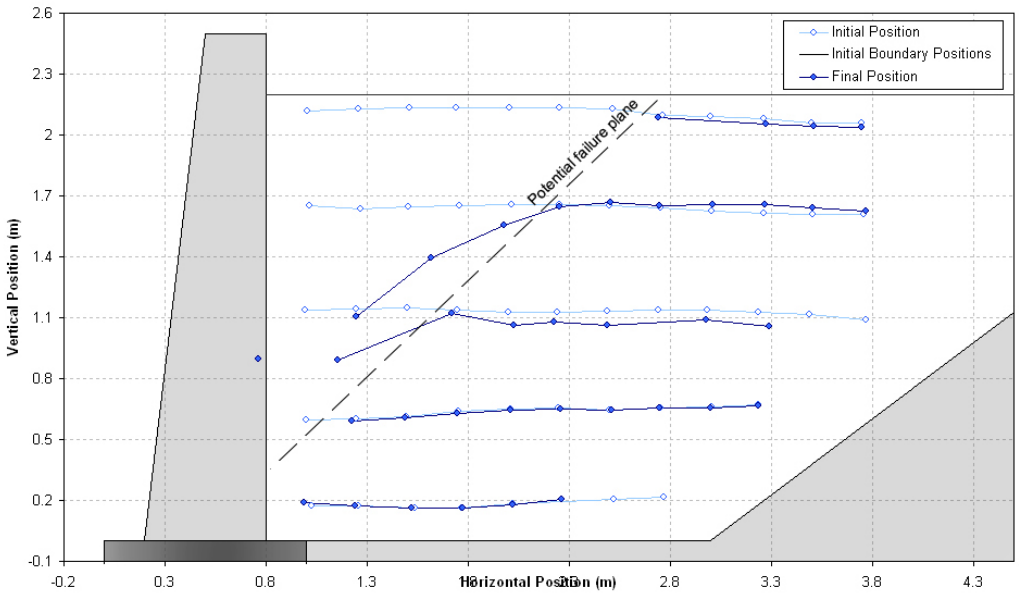

Figure 6-10: Wall 1: Displacement of buried ball bearings

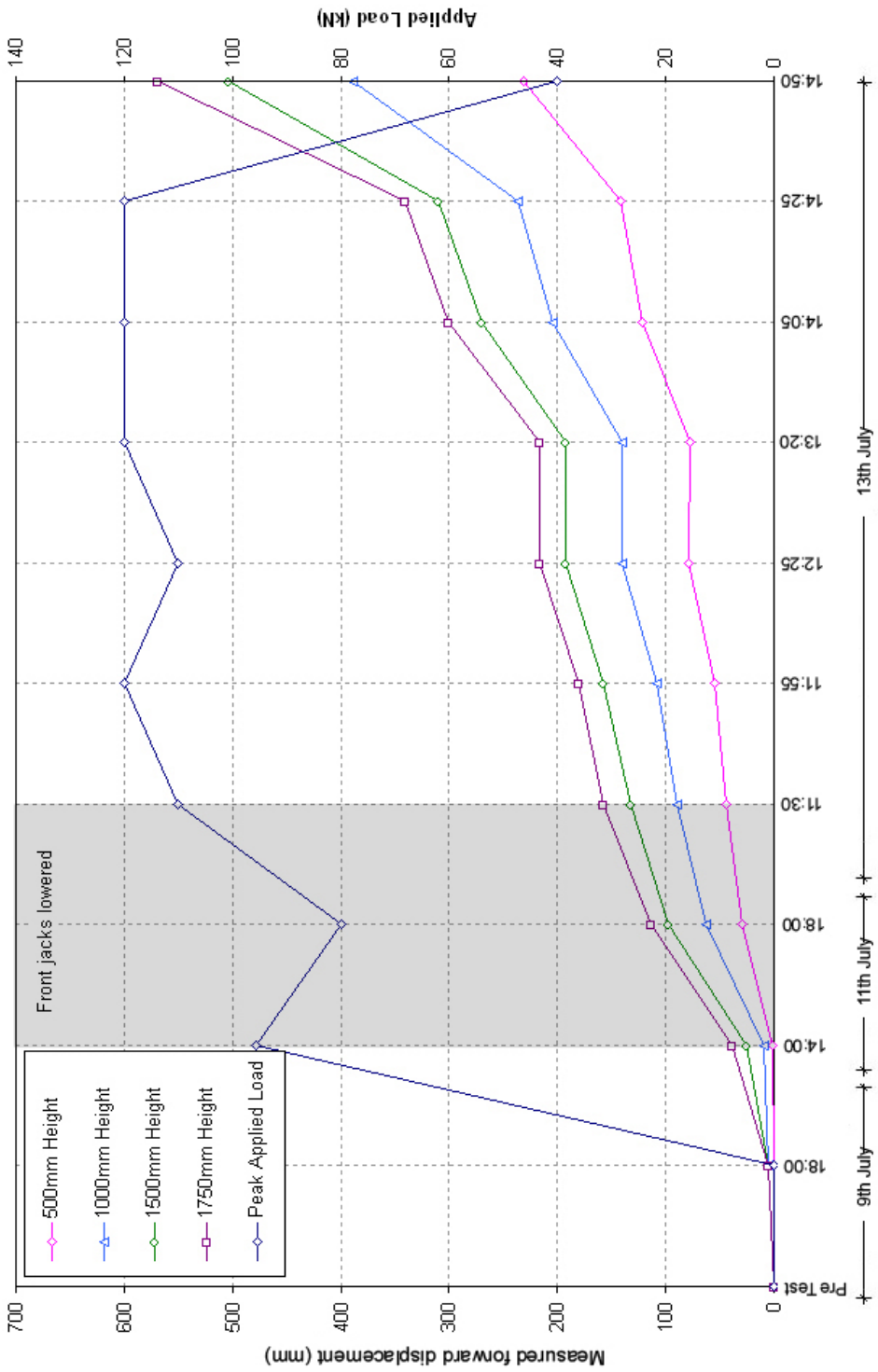

Figure 6-11: Wall 1: Applied surcharge vs wall displacements

6.3 Wall 2

6.3.1 Wall Construction

Wall 2 was constructed in November 2007 over four days. The base thickness was 500mm, tapering to 300mm at the coping, giving a profile 100mm narrower than for the first (as discussed in section 7.2). The wall was again 2.5m tall, extending 12m in length. The external face was battered at 3.4^o, with a roughly vertical internal face. As the wing walls were mostly unaffected after the first test, these were incorporated into the second wall, to reduce build time. As the wing walls were slightly thicker in profile, it was ensured that the sections to be reused were far enough away from the central test area so as not to interfere with the overall behavior of the second wall.

The build style of the second wall was similar to that of the first, however the overall quality of the wall was purposefully lower. Fewer pins were used to stabilise wall blocks, and the blocks themselves were worked less before placement. This is evident in figure 6-12, where the external face of the wall is shown.

Figure 6-12: Wall 2: Prior to testing

Vertical running joints were also built into the face. These were concentrated above the transition beams of the mechanically-jacked platform, effectively splitting the central test area and the wing walls. The joints ran through several courses, and became obvious features when loading occurred.

In a similar manner to the first wall, backfilling was conducted at the same time as the wall construction using the skid steer loader. However, due to the high

friction angle of the compacted backfill material, the vibrating plate compactor was not used for this or any subsequent tests. To ensure that no localised compaction occurred during construction, large timber boards were used to distribute the weight of both plant and construction materials.

A plate loading test was carried out in the same manner described in section 6.2.1 once backfilling was complete. Deflection was carefully monitored with respect to the applied load, and once a peak load was reached it was assumed that shearing of the backfill had occurred (fig 6-13). The associated angle of friction for the data gathered was 39^o. This lower value was expected due to the lack of any compaction and was consistent with the laboratory data gathered.

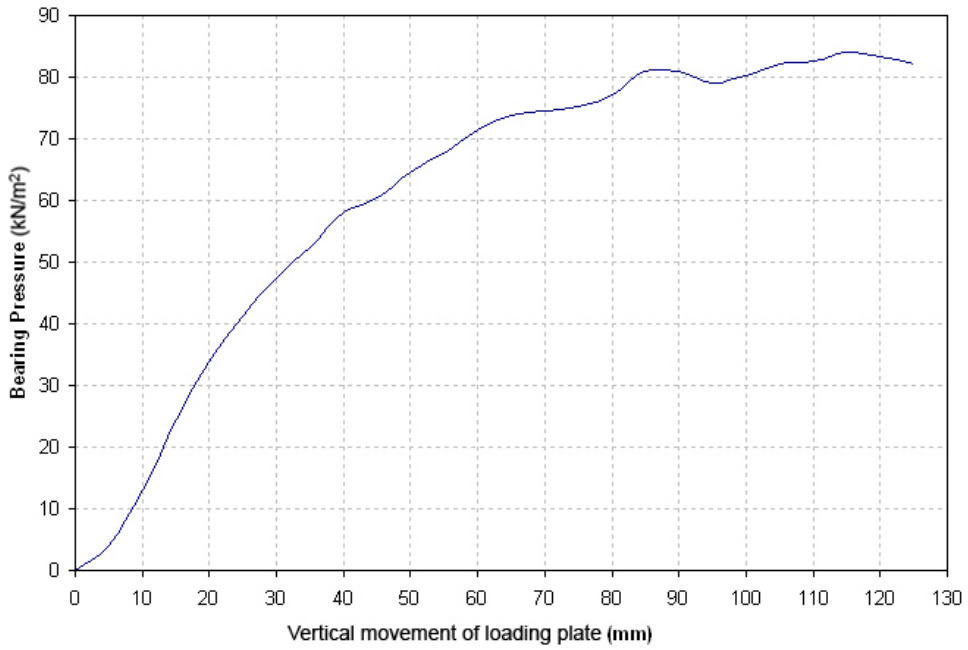

Figure 6-13: Wall 2: Plate loading test

6.3.2 Test procedure

As no movement occurred between each day of testing for wall 1, wall 2 was planned to be tested to destruction over three consecutive days between the 10th and the 12th of October, 2007. The general procedure was the same as for the first wall, however rotation of the platform was not employed. In addition, the surcharging was all conducted using one loading plate in a fixed location.

As per wall 1, the initial day consisted of a platform raise to generate the full friction angle. The platform was raised 40mm in total, after which the loadings were found to plateau (fig. 6-15). As the platform was moved, it was found that a hole in the rubber seal between the platform and the surrounding concrete was allowing some of the backfill to spill underneath the test area. This subsided once

the movement had finished and the aggregate had arched over the gap.

Surcharging began on the first day of tests after the platform raise, using the 500mm x 600mm plate at a distance of 1m from the wall. A load of 60kN was reached, however the loading plate was found to slip occasionally due to movements of the backfill. A slightly different loading arrangement utilising a pivot was introduced for the subsequent test days to accommodate these movements, however the loading plate size and position remained unchanged.

Testing on the 11th and 12th of October consisted purely of surcharging, with no further changes to the loading setup. A peak load of 75kN was reached and maintained whilst the deformations progressed. The wall movements were driven by the displacement of the backfill, which was caused in turn by the applied surcharge. In this way the wall test was carefully controlled using the surcharge, allowing for full measurements and observations to be made when required.

Figure 6-14: Wall 2: Prior to failure

Wall 2 failed on the 12th of October 2007, after the peak surcharge load had dropped from 64kN to 47kN. At this point the wall had been deformed to such a position that it was no longer stable and failed by toppling. Figure 6-14 shows the wall in its final state prior to collapse.

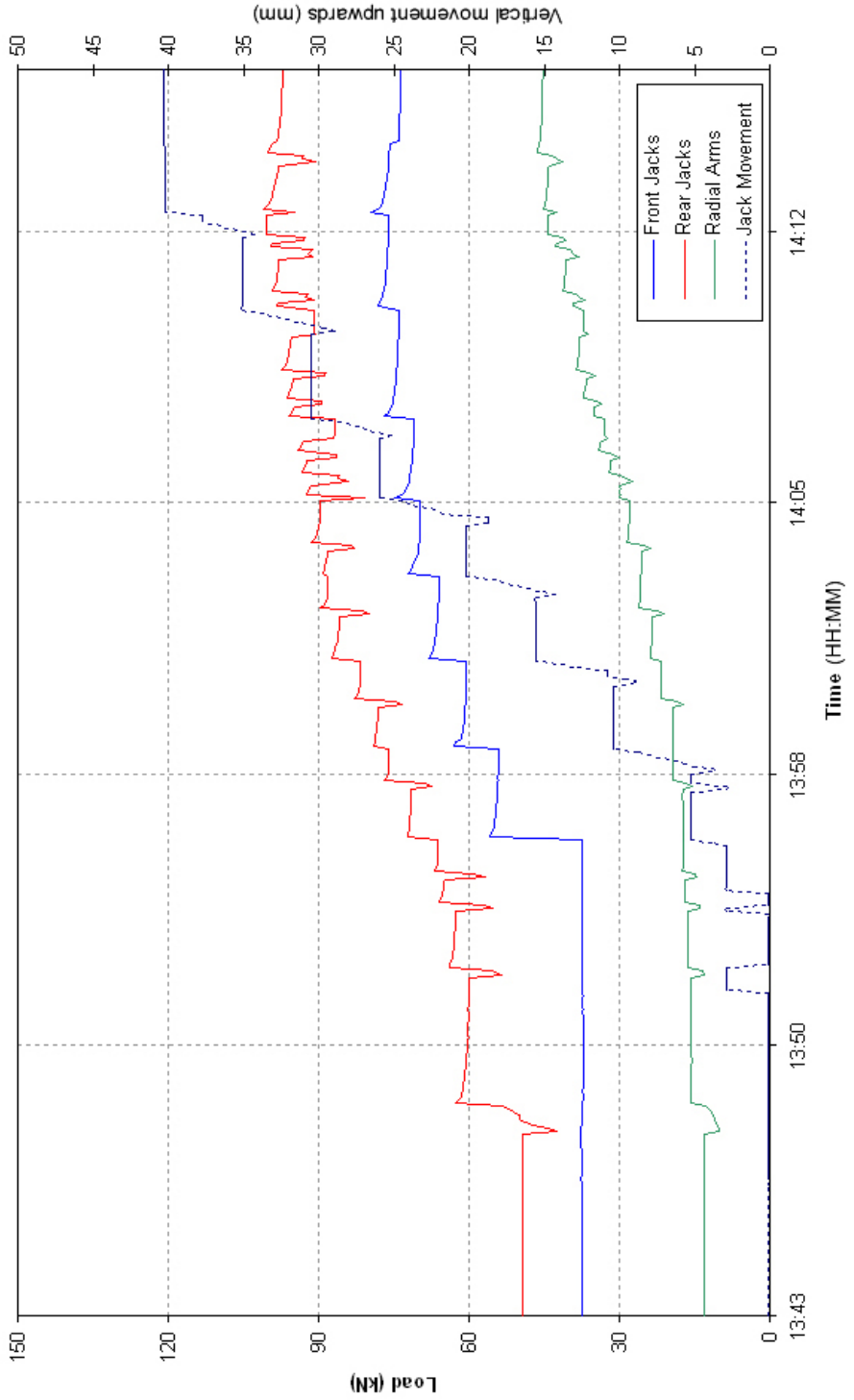

Figure 6-15: Wall 2: Generation of interface friction via platform lift

6.3.3 Recorded data & observations

Test wall 2 utilised the same basic instrumentation as wall 1, including the placement of ball bearings and pressure cells within the backfill, Total Station surveying measurements and the platform load cells. However, the second wall also used several draw-wire transducers, described in section 5.3.

Similarly to wall 1, the initial platform raise caused the loads to increase. The vertical loads upon the platform increased by 69.9kN (43.2kN from the rear jacks), with the radial arms subject to a 31.4kN increase in tensile load. The associated movements were also similar to wall 1, but of a greater magnitude. In the first 1m of the wall, the horizontal displacements increase linearly up to 20mm, above which no further movements occur, and the deformations remain at 20mm $\pm$ 1mm.

Upon surcharging it was found that the displacements continued initially in the same manner as for the initial platform raise. Each time the surcharge was applied, the deformations would vary within the lowest 1m, however above this point the movements were generally uniform. This is shown by figure 6-16, in which the plots for 1000mm, 1500mm and 1750mm heights are tightly grouped, with the displacements for the 500mm height increasing much more slowly. Towards the end of the test, the wall began to fail in an overturning manner, with the movements at the peak of the wall accelerating in comparison to the lower points.

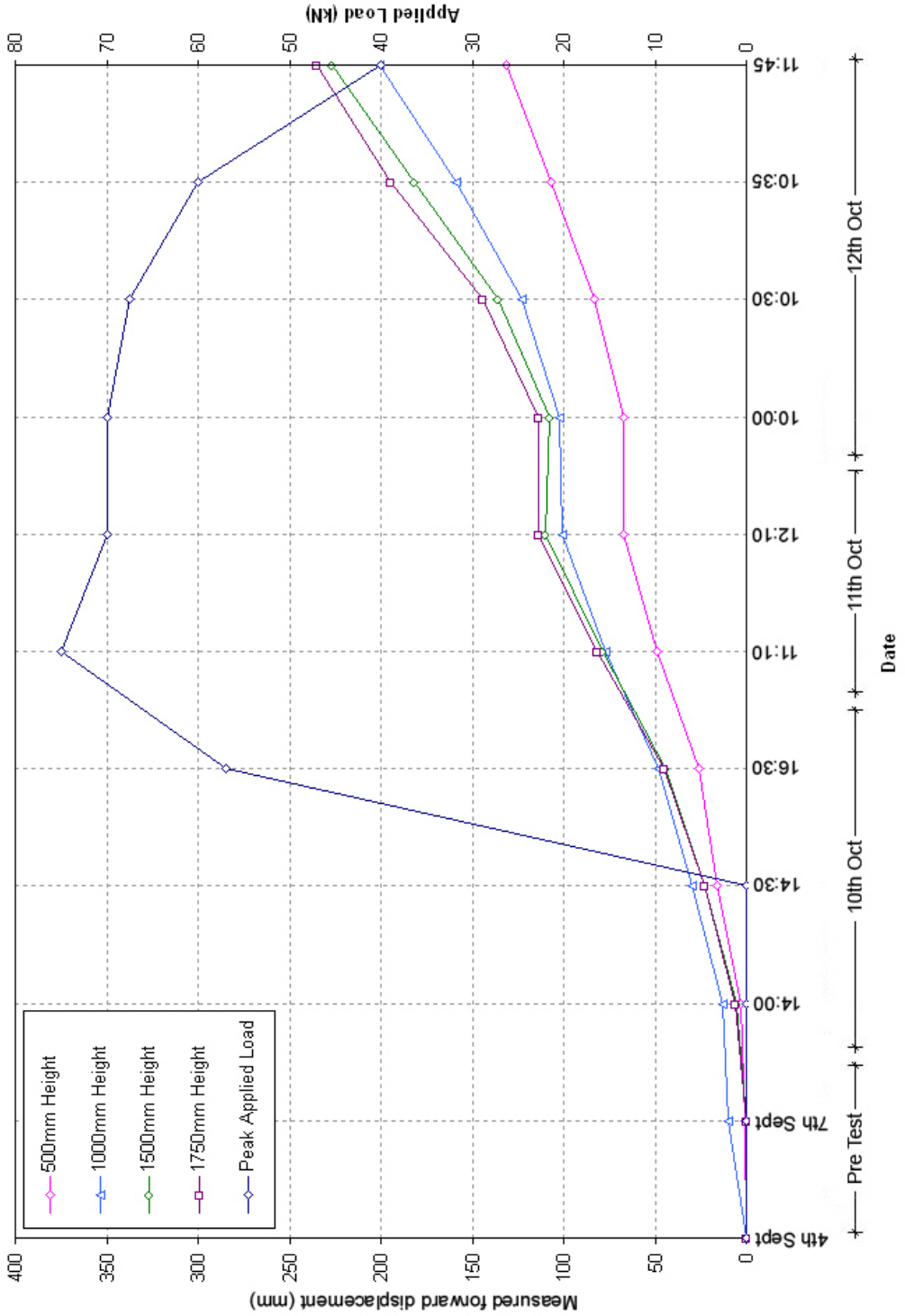

Figure 6-16: Wall 2: Load and displacement vs time

Further evidence of the non-linear behavior is found within the surveying measurements taken using the Total Station, shown in figure 6-17. The major movements occur under 1m in height, with the wall profiles above this point remaining generally parallel until the second day of testing. From photographic records, it is shown that these displacements found in the lower portion of the wall are due to a combination of translation and rotation.

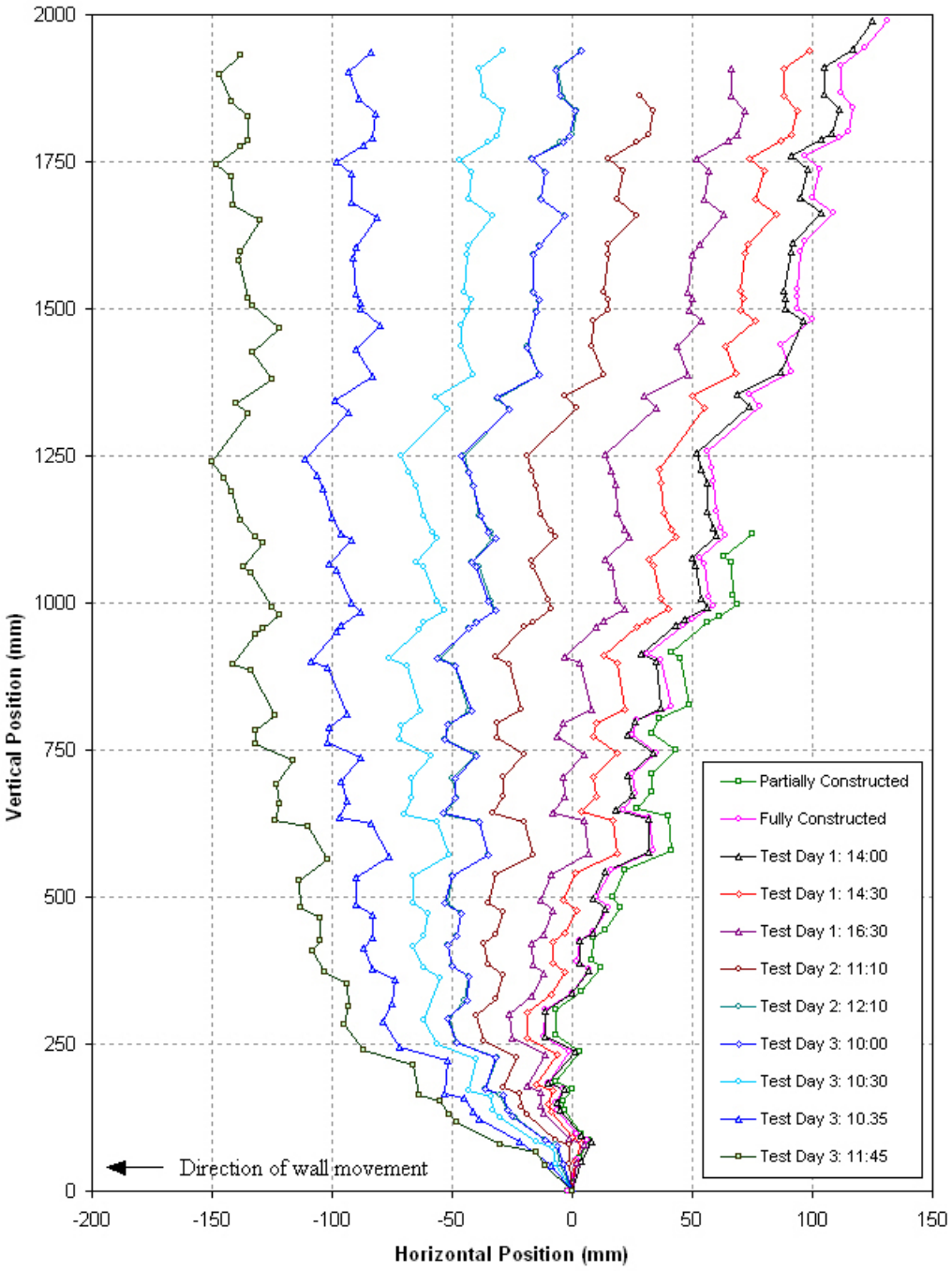

Figure 6-17: Wall 2: Measured displacements

On the third day of testing, an overall rotational movement occurred, with the top of the wall moving more rapidly than points lower down. At failure, the coping stones had moved over 300mm from their initial starting point, compared to 190mm as measured at 960mm above the base. However, although the overall displacements were much larger at the top of the wall, at the base of the walls the movements occurred over a much smaller distance. Prior to collapse, a horizontal displacement of 88mm was recorded at a point 240mm from the base. In the same set of measurements, the horizontal difference between this point and a point only 174mm lower is 72mm, giving a negative wall batter of 22^o from vertical (below this point the majority of the movements were inhibited by the concrete stop block attached to the platform). By comparison, over a distance of 984mm from the highest recordable wall position using the Total Station, only 20mm of horizontal movement occurred, giving a negative batter of -1.3^o from vertical.

Similarly to wall 1, the overall failure mode was via toppling. However, movements near the base of the wall at the moment of collapse suggest that the failure was instigated by individual block rotation. This in turn appeared to be a consequence of the comparatively large displacements and block rotations that occurred at this section of the wall, and will be discussed in chapter 7.

6.4 Wall 3

6.4.1 Wall Construction

For the third wall, the testing area was totally cleared prior to construction, including the still-standing wing walls. The wall was built over four days in June 2008, with proportions as close as possible to that of the first wall (600mm at the base, tapering to 400mm at the coping level). Backfilling was again accomplished with the skid steer loader, and left uncompacted prior to testing.

Although the overall wall geometry was similar to the first test, the internal make-up of the wall was much different (fig. 6-18). Wall 3 was constructed using using far fewer of the large slab-like stones found in the first wall. Although the masons were not instructed which particular blocks to use or how to employ them, the selection of material available to them was restricted to smaller, more rounded stones.

Trimming and pinning of the stones was mostly disregarded, causing the wall to be much rougher in appearance (fig. 6-19). The masons were requested to work quickly and with less care than for previous walls, and consequently construction was completed in significantly less time than both the first and second walls. Even once completed, some of the blocks had insufficient pressure applied to them to hold them in place, and could easily be moved by hand.

Also from figure 6-19, it can be seen that the courses do not maintain constant thicknesses, and there is some evidence that they are not horizontal at several

Figure 6-18: Wall 3: Internal configuration

Figure 6-19: Wall 3: Prior to testing

points. Running joints are also prevalent in this wall, occurring almost all the way along the wall face.

6.4.2 Test procedure

The third wall was tested over three days between the 10th and the 12th of October. The general test procedure was the same as for wall 2, consisting of an initial raise of the platform, followed by surcharging until failure. On the second day of testing (11th of October), no tests were performed and the wall was monitored for any

changes.

On the first day the platform was initially raised 40mm, after which it was found that the full friction angle had been mobilised (fig. 6-20). No other actions were taken this day. Surcharging began on the third day, using the same plate and setup used for wall 2. The wall was loaded until peak values between 75kN and 80kN were reached and shearing of the gravel began to occur. The wall was routinely unloaded to allow safe examination and full monitoring to take place. The peak loads attainable gradually decreased as the deformations increased, dropping to 45kN at collapse (fig. 6-21).

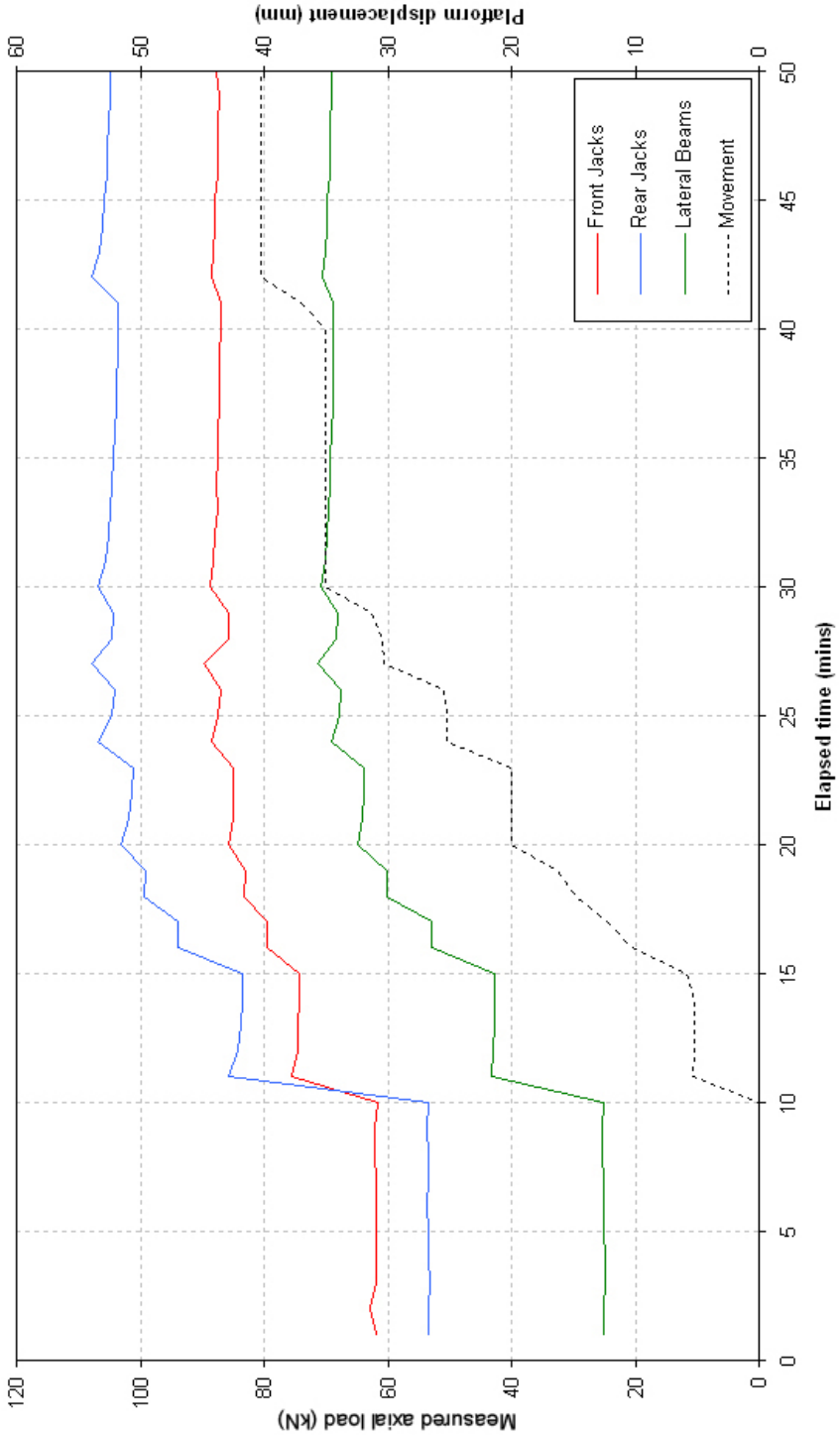

Figure 6-20: Wall 3: Generation of interface friction via platform raise

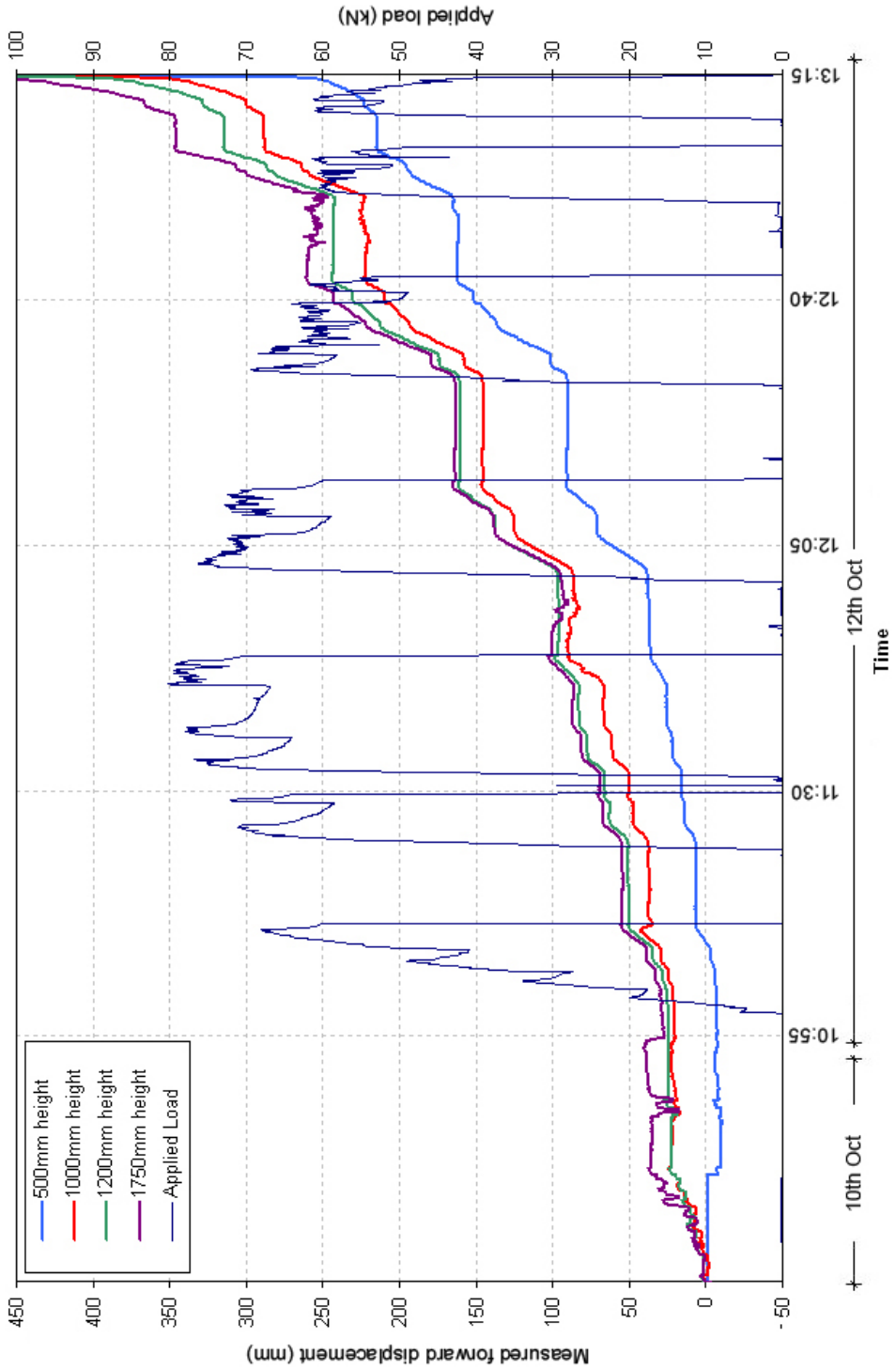

Figure 6-21: Wall 3: Applied surcharge vs wall displacements

6.4.3 Recorded data & observations

The instrumentation used for the third wall was slightly different from the previous tests, as the use of pressure cells and ball bearings within the backfill was discontinued. Instead, the buried flexible tubing and marker poles described in section 5.3 were employed, allowing any developing failure wedges within the backfill to be identified as they developed. In addition, several extra draw wire transducers were incorporated, allowing the wall face to be monitored in much more detail in 'real time'. These additional draw wires were also used to monitor the movements of the wall blocks of the internal face - also discussed in section 5.3.

Following the initial platform raise of 40mm, similar movements were recorded as for walls 1 and 2. Vertical loads increased by 77.6kN (51.7kN from the rear jacks), with the loads on the radial arms increasing by 43.2kN. As for wall 2, the deformations associated with this movement increase linearly with height from the base until approximately 1m, which moved a horizontal distance of 29mm (see fig. 6-22). Above this point the deformations are much smaller, with only 24mm horizontal deformation at 2m above the base. This gives a slight overall bulge, with the lower 1m inclined to give a negative batter of -1.7^o from vertical and the upper 1m battered at 0.3^o (the wall extended a further 0.5m, however Total Station readings are unavailable for these points).

The response of the wall 3 to the applied surcharge was the formation of a distinctly bulged shape, centred at roughly 1.2m above the base (fig. 6-23). As the loading progressed the bulge grew more pronounced, with the centre of the bulge moving a further 65mm than the highest surveyed point between 11:45am and 12:45pm. After this time the wall began to both topple and bulge, causing the deformations at the peak to be greatest (fig. 6-21).

In the final stages of the test once a prominent bulge had formed, a small section of wall collapsed independently without causing a total failure of the whole structure. Approximately five facing stones fell out near the base of the wall, with the stones above arching across the gap and causing the internal core material to be visible (fig. 6-24).

The use of draw wires to monitor the internal face of the wall proved successful, allowing the displacement of four points to be monitored (located at 200mm, 600mm 1100mm and 1600mm from the base). Through the course of the test, the deformations varied relatively linearly with respect to height, with the highest point moving forwards 422mm before failure. Overall, the rear face of the wall did not move parallel with the front face, causing the overall profile of the wall to widen as the test progressed. The greatest variation was at the lowest monitored point, where 140mm of relative movement occurred, causing the wall to become 742mm wide at this point. Increases in width of 85mm and 80mm were calculated at heights of 600mm and 1100mm, with the highest point showing an overall increase of 71mm. Despite this widening effect, there was no evidence of the inner

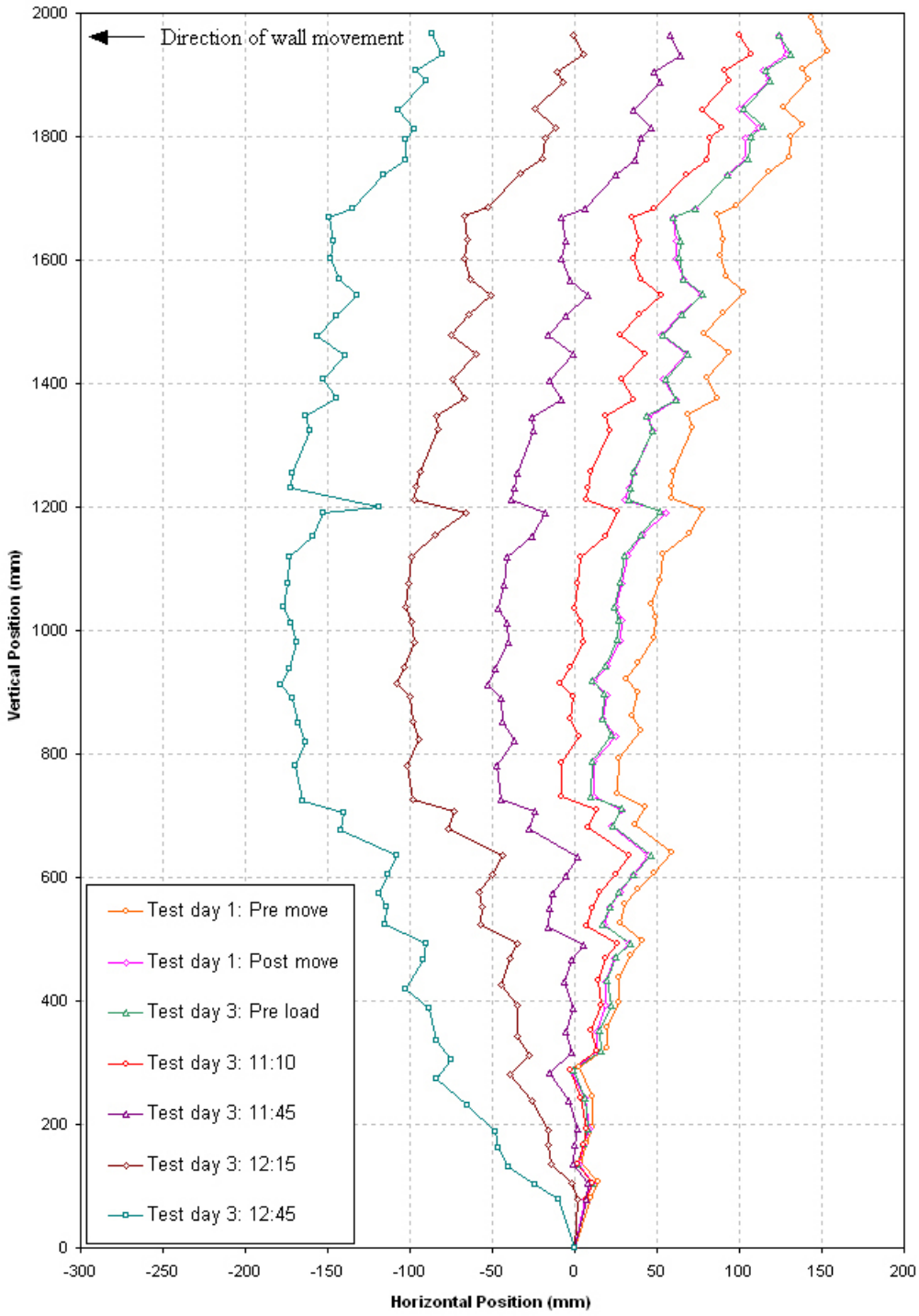

Figure 6-22: Wall 3: Measured displacements

and outer face of the wall separating. This was mainly a result of the regular through-stones spanning from the back face to the front.

Immediately prior to failure, the bulge protruded over 350mm in front of the toe of the wall, centred at approximately 1.2m above the base. The subsequent

Figure 6-23: Wall 3: Prior to failure

(a) (b)

Figure 6-24: Wall 3: Local failure

failure was at 13:15pm, via a combination of bursting and toppling, as shown by figure 6-25.

Figure 6-25: Wall 3: Bursting failure

6.5 Wall 4

6.5.1 Wall construction

Wall 4 was built and tested in October 2008, built to the same standards and procedures as wall 3 in an attempt to get a wall as similar as possible. The wall was inadvertently thicker at the base, being 700mm wide, however all other factors remained the same. The internal configuration again consisted of small, unpinned and roughly trimmed blocks, giving an overall appearance very similar to wall 3 (fig. 6-26).

Figure 6-26: Wall 4: Prior to testing

6.5.2 Test procedure

The test procedure for wall 4 was identical to wall 3, carried out on the 28th and 29th of October, 2008. On the first day of testing, the wall was raised 50mm to generate the full friction angle. The second day was given over to surcharging, using the same equipment in the positions used for walls 2 and 3. Peak surcharging loads of 85kN were reached and sustained for short bursts, with monitoring and observations in between loading. Prior to failure, a maximum surcharge of 61kN could be sustained, after which it reduced rapidly as the failure was instigated (fig. 6-27).

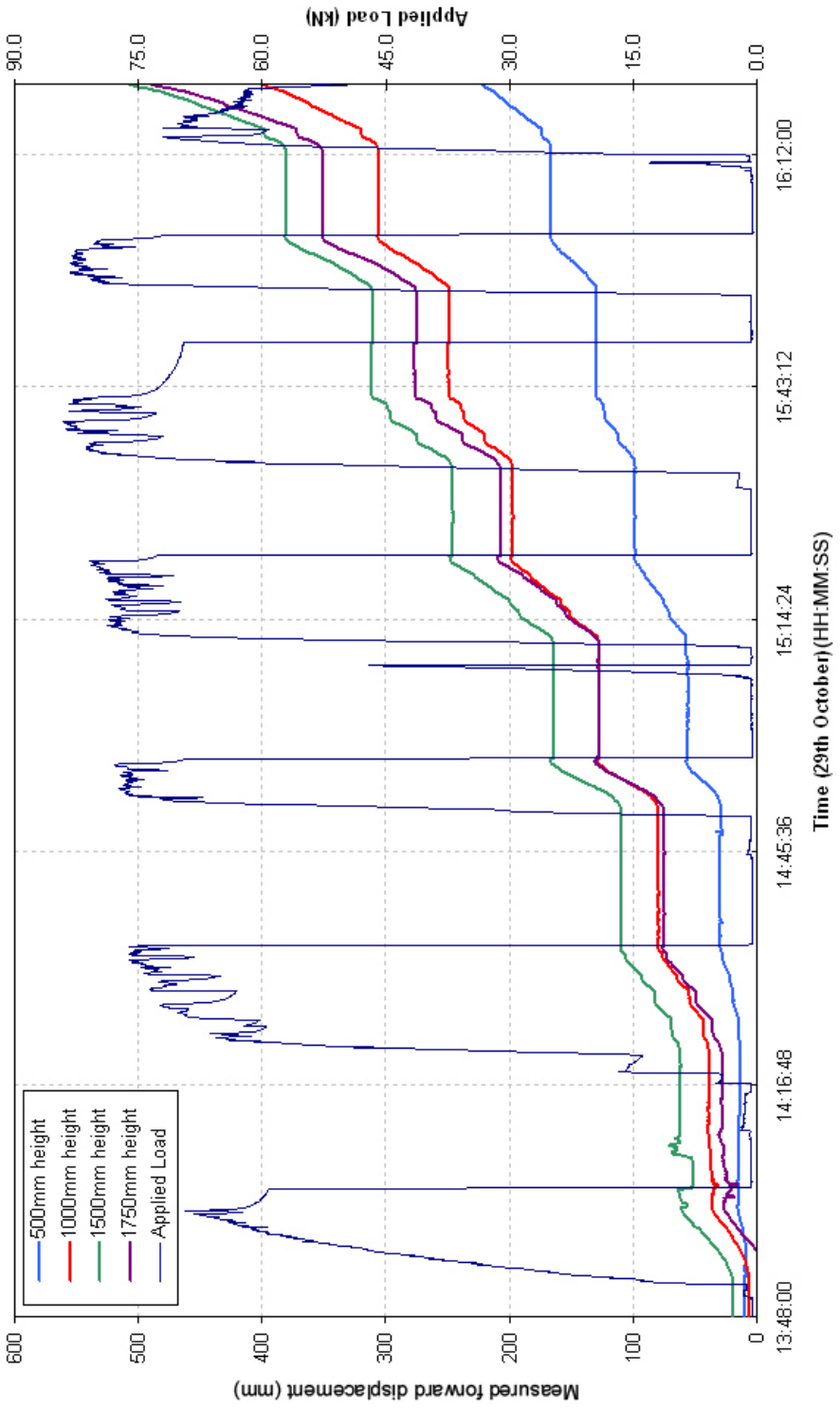

Figure 6-27: Wall 4: Applied surcharge vs wall displacements

6.5.3 Recorded data & observations

Wall 4 employed the same instrumentation as wall 3, using inclinometers rather than ball bearings in the backfill, with no buried pressure cells. Additional draw wires were purchased for this test, allowing the monitoring of almost 30 points with these transducers.

Deformations due to the platform raise on the first test day were very similar in magnitude to those observed for wall 3. At 1.1m from the base, there was a horizontal deformation of 22mm, increasing to 28mm at 1.5m and again reducing to 22mm at 1.9m, giving a slight overall bulge (fig. 6-28).

As with wall 3, surcharging caused the formation of a bulge. From figure 6-27, it is clear that the point monitored at 1.5m above the base is moving much more rapidly than the adjacent points. However, due to the initial batter of the wall, the most prominent point is actually between 1m and 1.5m above the base, shown clearly in figure 6-28.

The internal monitoring points were located at 300mm, 800mm, 1200mm and 1650mm above the base. The deformations measured were not linear as per wall 3. The greatest movement was still at the highest point (404mm), however the lowest point moved only 14mm prior to failure, giving an overall increase in the wall profile thickness of 128mm at this level. Above this point, the wall profile thickness increased by 16mm, 39mm and again 39mm respective to increasing height.

Failure was again via a combination of bulging and toppling. Immediately prior to failure, the centre of the bulge was 250mm in front of the toe, occuring between 1.1m and 1.5m above the base. Figure 6-29 shows the state of the wall in the final moments before collapse.

6.6 Wall 5

6.6.1 Wall construction

Wall 5 was built in December 2008, using Mort slate as the primary building material. The profile thickness was similar to wall 4, being 670mm at the base, tapering to approximately 400mm at the coping height, with a battered external face and a vertical internal face.

The construction of this wall was slightly more difficult than for previous walls due to the nature of the material, which was prone to delaminate, and fractured with ease. As a consequence, working of the material was impractical and usually resulted in the stone splitting into small fragments. Without being able to work the stones, each had to be used as quarried - often in large slabs which spanned much of the depth of the wall (fig. 6-30(a))

To minimise the additional material required on site, the wing walls were con-

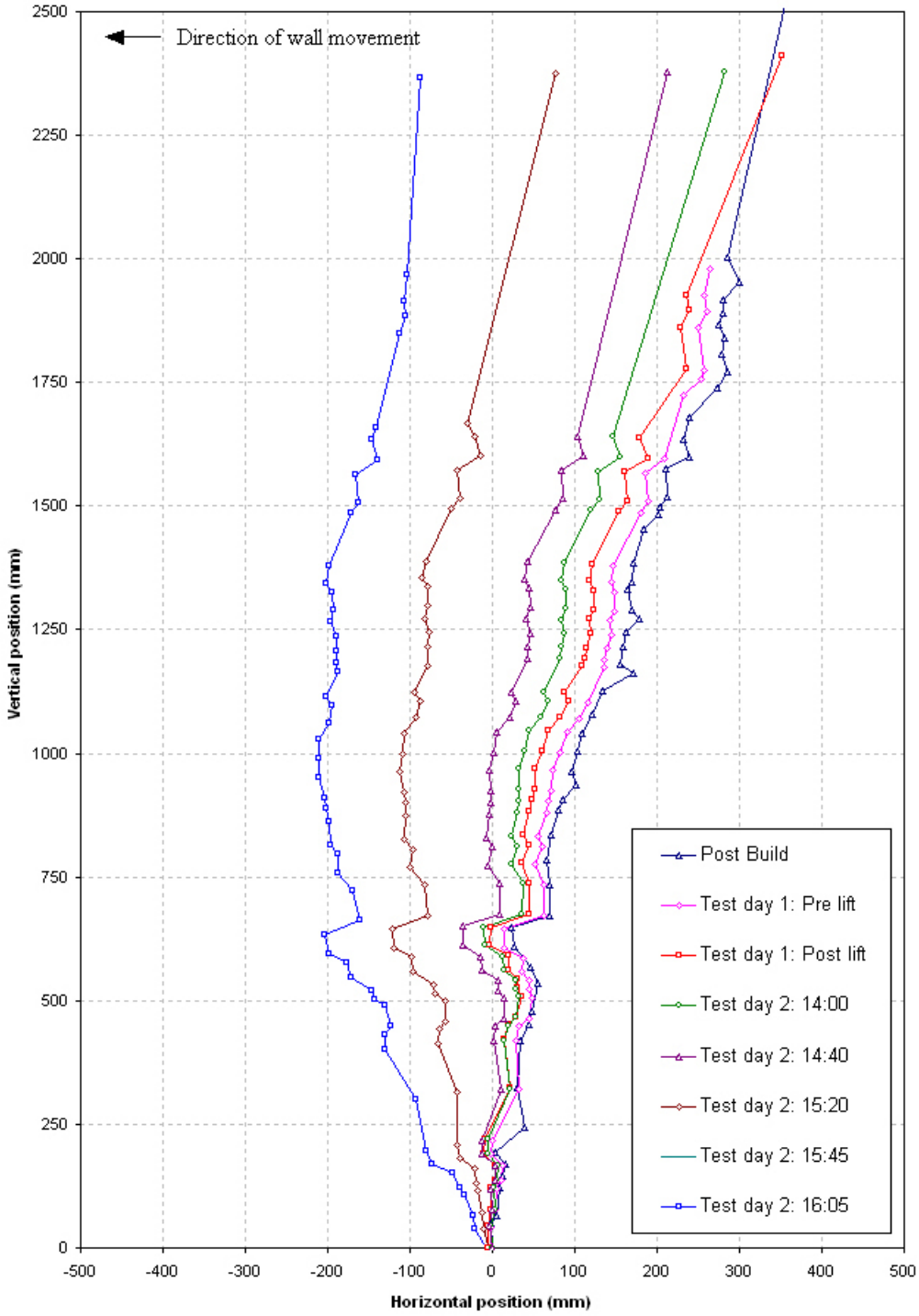

Figure 6-28: Wall 4: Measured displacements

structed using the original limestone. The boundary between the two materials was kept beyond the boundaries of the central test zone, ensuring that the limestone was not affecting the behavior of the tested section. A 'herringbone' style join was used, overlapping the slate and limestone at the boundary, eliminating

Figure 6-29: Wall 4: Prior to failure

the formation of a running joint (figs. 6-30(b) and 6-31).

As figure 6-32 shows, the wall was similar to walls 3 and 4 in that the build quality was relatively rough, allowing many gaps in the face. Due to the dark colouration of the stone, a vertical yellow stripe was painted along the central line of the wall, allowing the survey monitoring points to be more recognisable.

Once completed, due to uncertainties regarding the wall's stability, it was not backfilled with the skid steer loader. Instead, a large excavator was used to deposit the backfill in incremental layers without incurring any additional plant loads. The backfill was introduced up to the same height used for walls 1 to 4 (2.2m).

(a) (b)

Figure 6-30: Wall 5: Internal configuration

Figure 6-31: Wall 5: Limestone / slate boundary

6.6.2 Test procedure

Wall 5 was not tested until the 11th of March 2009, leaving the wall standing fully backfilled but unloaded for almost three months. During this time, the instrumentation was left running, recording information regarding the platform loads and draw wire measurements every 15 minutes to monitor any movements or changes of the wall.

Figure 6-32: Wall 5: Prior to testing

The testing again consisted of an initial raise of the platform by 50mm followed by surcharging until collapse. However, the entire test was conducted over the course of one day. The course of the surcharging was much more rapid than for previous walls, as the deformations increased rapidly in response to the applied loads. A peak load of 60kN was applied, however unlike previous walls this could not be maintained, and immediately began to decrease (fig. 6-33). 40 minutes after the surcharging began, the maximum applied load had reduced to 24kN, which then rapidly dropped off to zero where failure occurred.

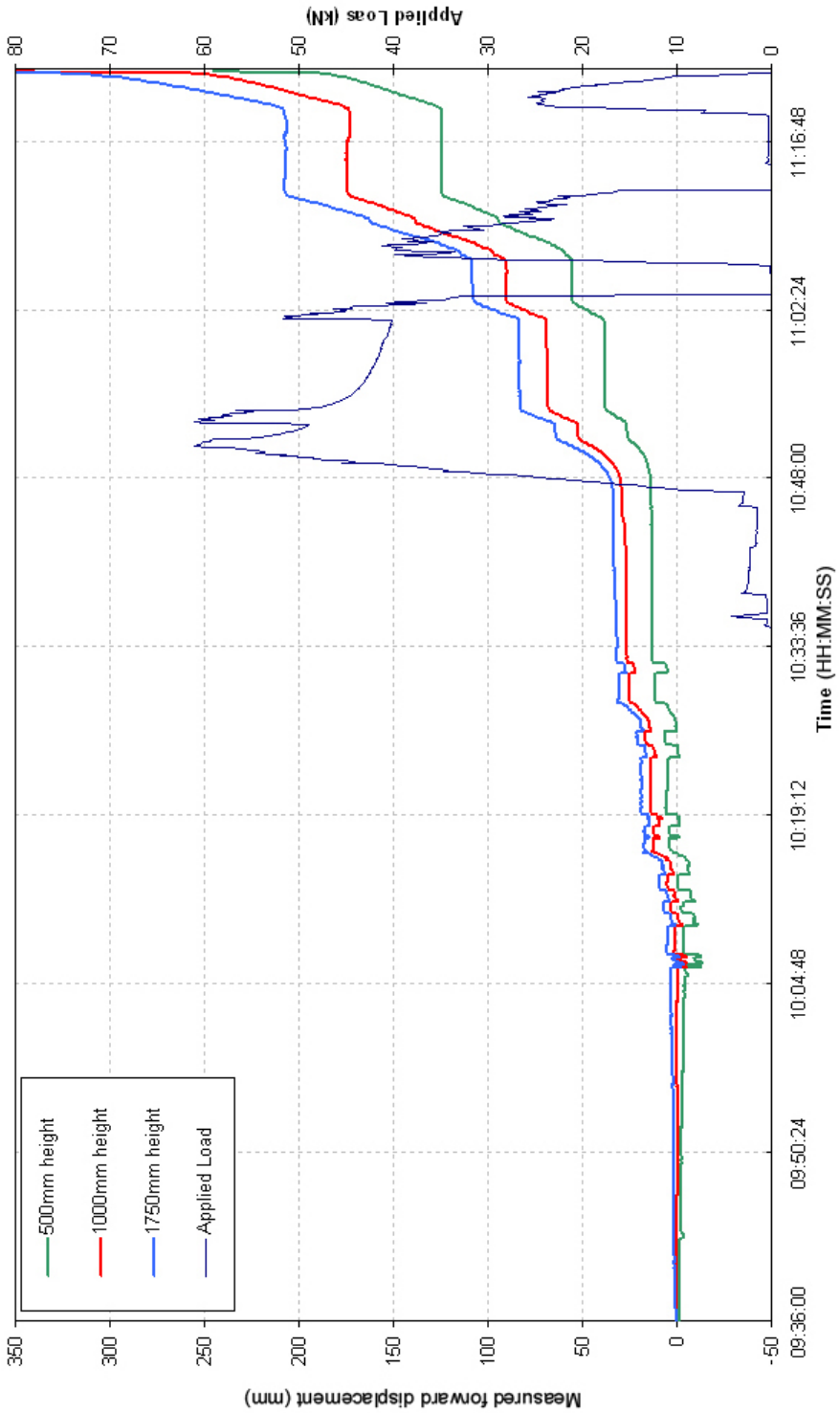

Figure 6-33: Wall 5: Applied surcharge vs wall displacements

6.6.3 Recorded data & observations

In addition to surveying the external face of the wall during testing, full monitoring was conducted throughout the backfilling and prior to surcharging. The movements obtained in these periods were generally much larger than those recorded for walls 1 to 4. As figure 6-34 shows, backfilling of the wall caused a forward rotation of the wall, with a maximum recorded movement at the peak of the wall of 15mm.

Whereas walls 1 to 4 did not show any tendency to move without a surcharge (but fully backfilled), wall 5 moved substantially between the backfilling and the test day. In this three month period, the wall again moved forwards, with the movements varying linearly from the base to the coping. At the highest monitored point 2m above the base, a displacement of 61mm occurred, equating to approximately 0.7mm of movement each day.

Raising of the platform caused displacements larger than for any of the previous walls, with 18mm of movement at 300mm from the base, increasing to 32mm at a height of 2m. There was no evidence of a developing bulge, as above 300mm the movements increased linearly.

Surcharging continued the pattern of displacement seen during the platform raise, with the lowest 400mm of the wall moving 150mm prior to failure. Above this point, displacements were more gradual, increasing to 320mm at coping. The internal face of the wall also moved in a similar fashion to the external face. The deformations measured at two of the four locations were almost identical to the movements at the external face, giving changes in the thickness of the wall of 2mm and -4mm. At the highest monitored internal point (1.6m above the base), the wall thickness increased by 26mm following a forward movement of 300mm. The lowest monitored point moved only 29mm (260mm above the base). This gave an overall increase in the wall thickness of 55mm, which is again much lower than determined for walls 3 and 4.

Failure was via overturning, approximately three courses from the base. After sufficient forward translation of the wall, several of the lower stones were overhanging the stones below by a large enough amount that they became unstable. Upon the failure of these stones, the entirety of the wall above also failed.

6.7 Behavioral overview

The general observations and data gathered in the tests described is compiled in table 6.1. As previously mentioned, photographic records and further data regarding specific movements and load changes in each of the walls are located on the CD included with this thesis.

Table 6.1 shows that wall 1 was the most stable wall, as it underwent the greatest deformations prior to failure, whilst being subject to the largest surcharge force. However, as will be discussed in chapter 7, this wall was subject to several

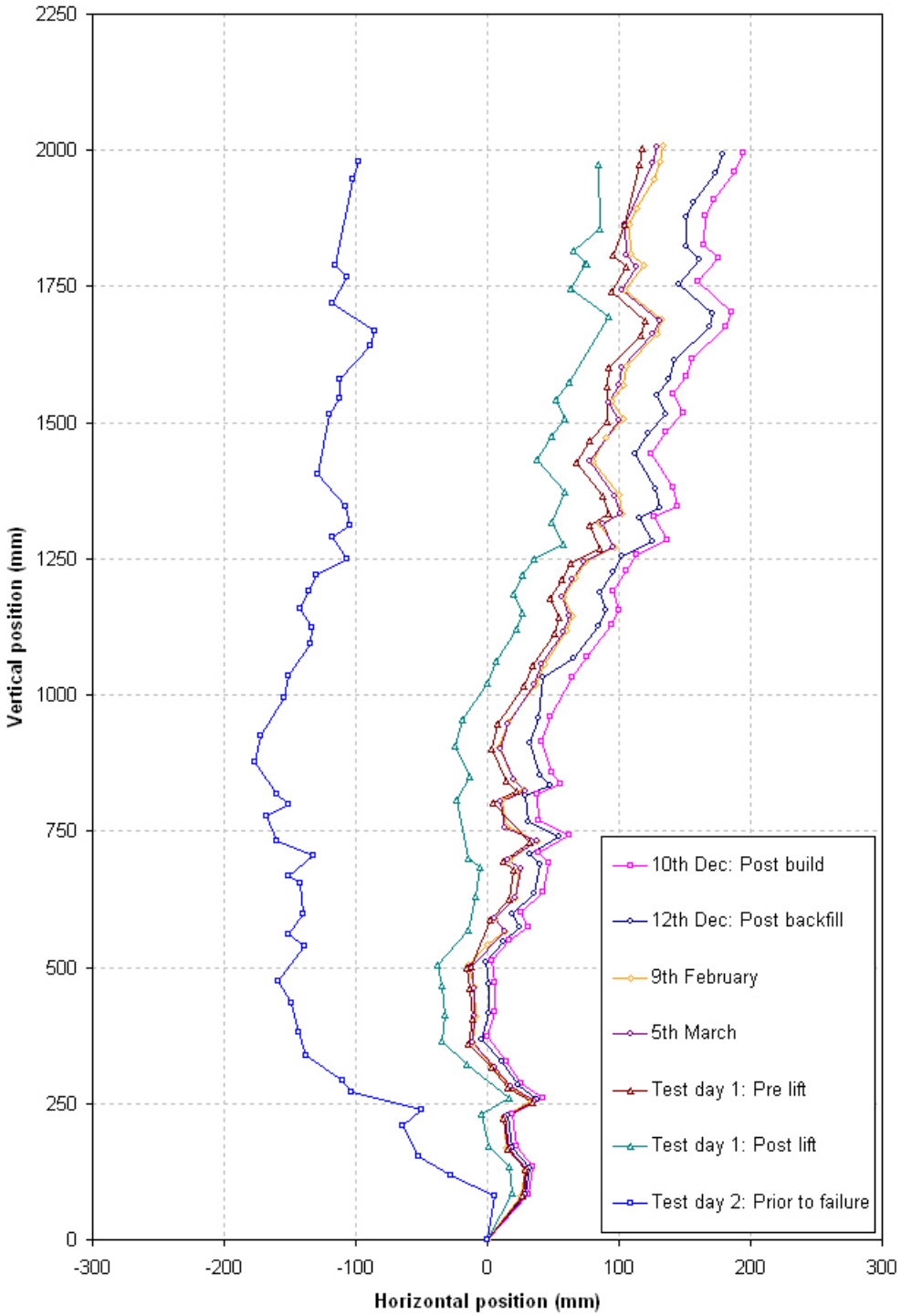

Figure 6-34: Wall 5: Measured displacements

factors which would aid stability (i.e., a compacted backfill and the ability to shed load to the wing walls). Walls 2, 3, 4 and 5 did not have these advantages, and so could not repeat deform to the same extent as wall 1.

With the exception of wall 1 (where the backfill was compacted) and wall

5 (where a different walling material was used), the peak surcharge loads were relatively consistent. This was due to the fact that the surcharge was mainly being used to drive the deformations by creating a failure plane within the backfill. The wedge of soil created by this failure plane was then forced towards the wall by the surcharge, hence causing the wall displacements. The peak load which was applied to the backfill was then partially governed by the amount of force required to move the mass of the wall and soil wedge. As walls 2, 3 and 4 all had roughly the same mass, and the wedges were each similar in size, so the loads required would be similar. The surcharge required for wall 5 would in part be less due to the lower frictional resistance of the slate. Where the limestone walls had a high internal angle of friction, this would resist the movements due to the surcharge force. Conversely in the slate wall, the friction angle was much lower, and therefore could not resist the forces to the same degree. Hence, a smaller force was required to drive the deformations.

Table 6.1: Summary of full-scale test walls 1 - 5

	Wall 1	Wall 2	Wall 3	Wall 4	Wall 5
Material	Limestone	Limestone	Limestone	Limestone	Slate
Wall height	2.5m	2.5m	2.5m	2.5m	2.5m
External batter	5.0^o	3.4^o	4.2^o	8.5^o	5.5^o
Base thickness	600mm	500mm	600mm	700mm	670mm
Test procedure	Wall raised Wall rotated Surcharge	Wall raised Surcharge	Wall raised Surcharge	Wall raised Surcharge	Wall raised Surcharge
Platform raise Max related movement	18mm 10mm	40mm 20mm	40mm 29mm	50mm 28mm	50mm 32mm
Platform tilt	3.1^o	NA	NA	NA	NA
Max surcharge	110kN	75kN	80kN	85kN	60kN
Final surcharge	40kN	47kN	45kN	61kN	24kN
Deformation	Rotation	Rotation	Bulging & Rotation	Bulging & Rotation	Sliding
Max deformation position Magnitude(relative to toe)	Coping 425mm	Coping 150mm	1.2m 350mm	1.1m 250mm	Coping 175mm
Failure mode	Overturning	Overturning	Bursting & Overturning	Bursting & Overturning	Overturning

Chapter 7

Analysis

7.1 Introduction

This chapter discusses the data obtained from the full-scale and laboratory testing as well as the use of the limit equilibrium program described in chapter 4. The mechanisms which instigate wall behaviour such as toppling, sliding and bulging are investigated, as well as the final failure modes of the five full-scale walls. These analyses of the wall tests relate to both the data and observations given in chapter 6, and also to the additional data found on the data CD included in this thesis.

7.2 Wall 1

7.2.1 Analysis of observed behaviour

The first test wall failed purely by toppling, with very little additional deformation. This was due to a combination of the rotation as a result of the platform tilting and from initial surcharging too close to the wall. The surcharging load was initially applied only 500mm away from the internal face of the wall. This position was based on the assumption that the load would spread out in a 1:2 ratio, and the surcharge would begin to affect the wall at roughly mid height (the area affected by the surcharge would spread out 1m for every 2m of depth below of the loading plate), however the wall's response to the loading was indicating that the spread was much more rapid in response to the high friction angle. Non-linear movements were recorded, with 15mm of deformation at a height of 2m, whilst only 4mm was observed at 1m above the base. The compaction of the backfill could have had some impact of this. As described in section 6.2.1, the fill was placed in layers approximately 300mm deep and then compacted using a 1kN vibrating plate compactor. It is likely that several of the layers were placed thicker than this, and due to the stiff nature of the backfill the compactor was not able to provide a uniform level of compaction throughout the backfill. This could cause the load from the surcharging plate to spread out much more rapidly as it passes through

thin bands of alternately loose and dense backfill, and affect the wall much sooner than otherwise anticipated.

An additional reason for moving the plate back from the face of the wall is due to the complex interaction that occurs between a flexible wall and a retained backfill. As the structure deforms in response to the surcharge, its geometry changes, altering the magnitude of the loads affecting the wall. In addition, the backfill will also be altered, and display different properties where the deformations have occurred, causing difficulties in accurately calculating the loads being applied to the wall. To attempt to negate this phenomenon, the surcharge was moved further away from the internal face, somewhat reducing the impact that the inherent flexibility of the wall has on the behaviour of the applied loads.

From the readings given by the load cells attached to the platform, the changes in the overall thrust of the wall and backfill can be observed. As the surcharge was applied, the loads on both the front jacks and the radial arms increased. The rear jacks also initially increased in response to the surcharge, although by a lesser amount. As the wall neared failure and the thrust moved further forwards, the load on the rear jacks began to decrease, while the front jacks were still increasing. Overall stability was undermined, causing a danger of toppling, with the thrust moving further and further forwards, hence increasing the loads upon the front of the platform and decreasing at the rear. However, it is difficult to assess the exact position of the line of thrust or the bearing pressures applied at the base from this data. This is partly due to the fact that the distribution of load is not necessarily linear due to the unbonded nature of the wall. In addition, it is unknown precisely what volume of wall is bearing directly on the platform, as some of the load is undoubtedly being supported by the concrete foundations adjacent. The magnitude of the lateral loads measured by the radial arms are also not precise, as the contact points where the transition beams meet the concrete foundations will generate friction. However, efforts were made to eliminate this by using greased plates under the contact points.

It was noted that during the initial raising of the platform, the tension forces in the radial arms increased by a proportionally larger amount than the loads on either the front or rear pairs of jacks (fig. 6-8). This could potentially be explained by the way the radial arms were connected to the platform. As the platform moves up, the radial arms will swing upwards in an arc. Although the radial arm itself will not change its length, the horizontal distance between the platform and the concrete anchor beam (to which the other end of the radial arm is attached) will be reduced very slightly. As a result the whole wall will be pulled backwards slightly, attempting to move it further into the backfill. This shortening could therefore explain the increase in load upon the radial arm, as the pressure of the backfill increases in an attempt to resist the slight rearward movement of the wall.

7.2.2 Limit equilibrium analysis of wall 1

The limit equilibrium program has been used to recreate each of the walls at the various stages of the test as measured with the total station. The data for wall 1 are summarised in table 7.1. The data relate to the walls in their unloaded state, with only the active pressures from the backfill and the self weight of the wall in effect.

Table 7.1: Summary of LE program output for wall 1

Date		9/07/07		13/07/07		
Time		11:00	14:00	12:25	14:25	14:50
Event		Pre test	Wall raised	Surcharge	Surcharge	Surcharge
Base thickness	(mm)	600	600	600	600	600
Wall height	(mm)	2500	2500	2500	2500	2500
External batter	(deg)	6.8				
Internal better	(deg)	0.0				
Wall voidage	(%)	28	28	28	28	28
Limestone unit weight	(kN/m^3)	24.5	24.5	24.5	24.5	24.5
Limestone friction	(deg)	37.4	37.4	37.4	37.4	37.4
Backfill unit weight	(kN/m^3)	13.7	13.7	13.7	13.7	13.7
Backfill friction	(deg)	51	51	51	51	51
Backfill height	(mm)	2200	2200	2200	2000	1900
Horizontal force	(kN)	3.33	3.24	2.91	2.51	2.51
Vertical force	(kN)	24.7	24.28	20.95	21.03	21.04
Eccentricity from toe	(mm)	281	283	101	64	-49
Overturning safety		3.84	3.94	2.16	1.85	0.73
Sliding safety		5.39	5.42	5.23	6.10	6.00

At 14:50 on the 13th of July, the analysis suggests that the wall should have already collapsed, in that the overturning safety factor is less than one. However, the program analyses the wall purely in two dimensions, whereas the observed behaviour is suggestive of three-dimensional effects. This was first indicated during the rotation of the platform. Each time the front jacks were lowered, all of the platform loads decreased. For this to occur, the wall must be transferring load from the central section into the wing walls, where the concrete foundations will assume an increased load. The tilting movement caused the wall to drop in height relative to the wing walls. As the build quality was very high and the individual blocks tightly fitted, this relative movement caused an increase in the degree of interlock between the stones, allowing some of the weight of the wall to be carried in tension laterally along the wall (shown by fig. 7-1, as well as arching between the ends of the platform. Had the wall been looser in construction, it is likely that this phenomenon would have been reduced or possibly not occur, as the individual blocks would have the freedom to rotate, hence not generating the same tension along the bedding places and supporting the central section.

The generation of increased amount of friction between the courses also explains

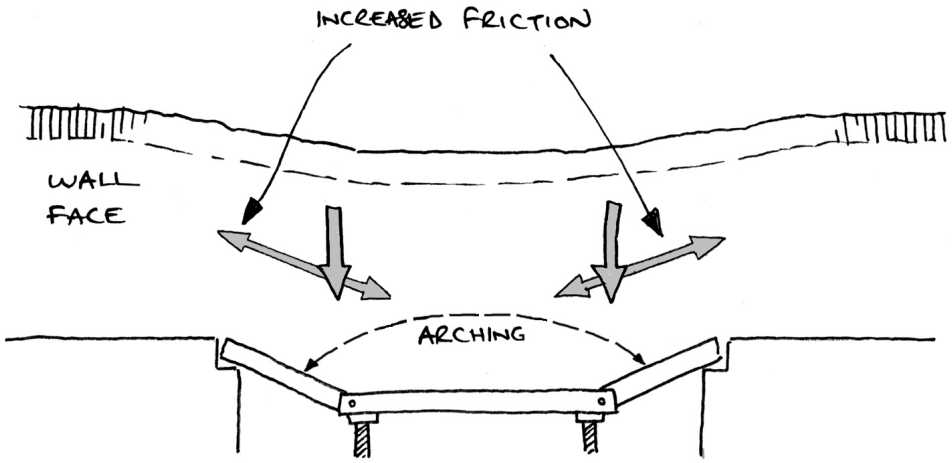

Figure 7-1: Load readjustment due to platform tilting

why the wall was still stable when the program indicated that failure should have previously occurred. As the wall became distorted and the central section moved forwards, the tension force which was partially supporting the wall would also act to resist an overturning failure, as shown in figure 7-2.

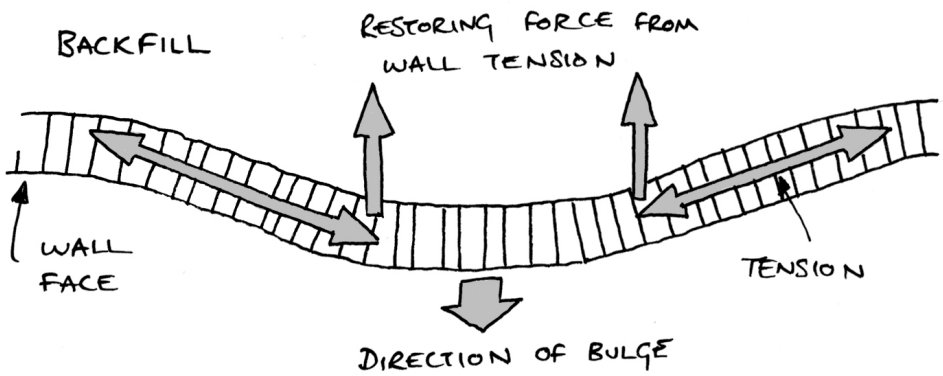

Figure 7-2: Wall stabilisation due to block friction

To be able to support the central section, it is critical for the wing walls to be largely uncracked. For drystone walls, it is difficult to identify precisely crack propagation due to the unbonded nature of construction. However, in response to large deformations, long cracks may appear and widen rapidly - usually at points of weakness; e.g., along running joints. In the case of wall 1, even prior to failure when the wall was heavily distorted, the wall was minimally cracked (fig. 7-3). There was a large crack along the centreline of the wall, with smaller fissuring near the wing

walls, however the face was relatively undisturbed, with a particularly important uncracked band running along the crest of the wall where the deformations were highest.

Figure 7-3: Crack propagation of wall 1 prior to failure

The factor of safety for sliding given in table 7.1 is based on the assumption that the bedding planes remain horizontal. However, from photographic records, it can be observed that the face stones do not remain horizontal. Figure 7-4 shows a profile of the wall prior to failure, with targets attached for the Particle Image Velocimetry (PIV) tests conducted at Southampton University. From these targets, it is possible to ascertain the angle of the stones they are attached to. Whilst this angle may hold true only for the face stone, the safety factor against sliding at this inclination was also checked using the limit equilibrium program. At failure, the lowermost block fitted with a target (200mm above the base) was inclined forward at 18.9^o. Should the whole bedding plane be inclined thus, the factor of safety against sliding drops to 2.1 (although at this point the thrust line is almost certainly only passing through the blocks at the face). However, as this is still above 1, failure by sliding should not occur. This was borne out by the test observations, with the wall failing purely by rotation about the toe.

7.2.3 Test progression

Although wall 1 exhibited large deformations prior to failure, they were primarily due to a linear topple about the toe. To encourage flexibility in the wall 2, it was made 100mm thinner, with a rougher finish. This would give a wall which was

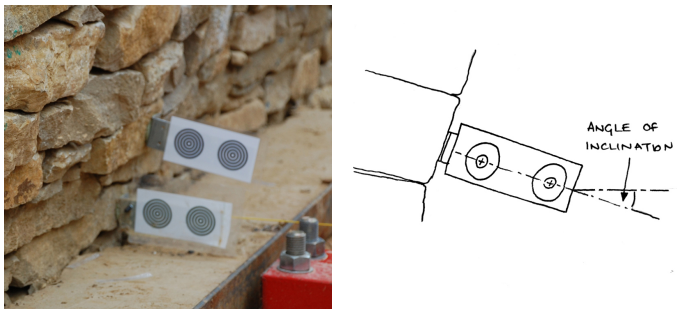

(a) (b)

Figure 7-4: Block rotation of wall 1 prior to failure

still stable upon fully backfilling, but with a more marginal factor of safety. To inhibit the spread of load to the wing walls, vertical running joints would also be purposefully built into the wall. This would make the analysis of the behaviour much simpler, as it is similar to the two-dimensional approach of the analytical approaches adopted and the limit equilibrium program.

To discourage failure via toppling, the tilting of the platform was removed from the test procedure. It was also done to give clarity during analysis, as any deformations would be purely due to the surcharge load and not a combination of factors.

7.3 Wall 2

7.3.1 Analysis of observed behaviour

As wall 2 incorporated the use of draw wire transducers, the movements of the external face were recorded in real time, and linked with the data from the load cells. To better understand the data, a visual representation of the wall was created using a Microsoft Excel spreadsheet. This combined the surveying data, the draw wire data and the load cell readings to produce a profile of the wall which could be viewed at any stage of the test (fig. 7-5). In addition to the diagrammatic representation of the wall, the data can be displayed numerically, simultaneously giving the deformations at the monitored points, the rate of movement and the applied load at any time. With the data in this format the physical effects of the test procedures are more easily identified, in particular showing where along the face of the wall the movements are greatest.

A drawback of the draw wire data is that there was no ability to monitor the rotations of the monitored blocks, however this data was ascertainable from photographic records. In addition, the draw wires required fixed mounting points to be drilled into the face of the wall. Once the test had begun, it was unsafe to change the mounting points of the draw wires. As a consequence, the limited number of draw wires meant that should the deformations occur in positions not

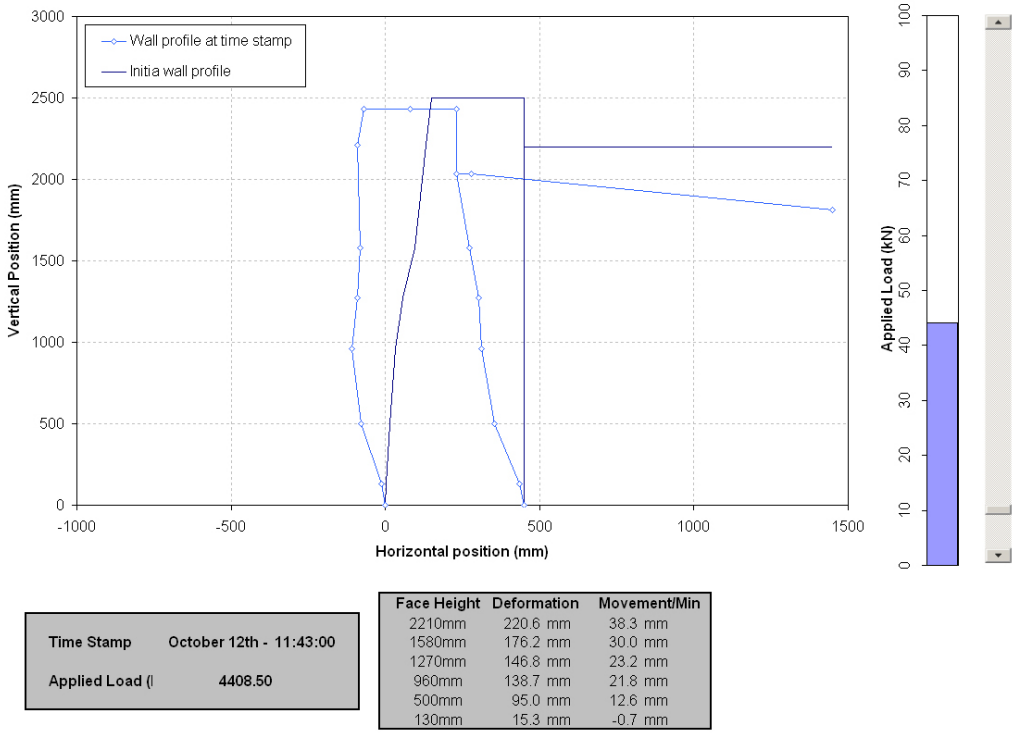

Figure 7-5: Visual representation of draw wire data from wall 2

covered by the transducers, the equipment could not be modified to suit. For this reason, the use of the Total Station was still critical for monitoring during the test, ensuring that the entire profile of the wall was captured at regular intervals.

The uncompacted nature of the backfill was also beneficial to the data obtained from the second test. Primarily the aggregate was not compacted to give an angle of friction which was more comparable to the granular fills found behind most retaining walls. Plate loading tests indicated an angle of friction of 39^o, which was much more realistic than the value of 51^o as measured behind the first wall. A second reason was to give a more uniform unit weight throughout the backfill. As described in section 7.2, the use of the vibrating plate compactor gave alternating layers of dense and loose gravel, which affected both the behaviour of the surcharge and the loads recorded by the buried pressure cells. To overcome any localised compaction of the gravel by the skid steer loader, large timber boards were placed over the backfill, spreading the tyre load over a much greater area and lessening its impact.

The behaviour of this wall under loading was different to that of wall 1. As described in chapter 6, the lower half of the wall moved rapidly in response to the load, with the upper portion remaining relatively upright and undisturbed. The geometry of the wall and the block selection were a critical reason for this behaviour. As with wall 1, the stones used were deep and slab-like, with each protruding a relatively long way into the wall. Higher up, the thickness of the wall

was much reduced, however the stone sizes remained the same, giving a reduced block depth/wall thickness ratio at this point. As the wall was surcharged, the additional load encouraged the blocks to move and rotate as with the first test wall. This was more possible lower down in the wall, where the forces were higher and the stones had some room to shift and move. However, higher up the wall, a larger percentage of the wall's self weight would be spread across the stones due to their increased relative size, holding them more firmly in place. This would be accompanied by much lower active pressures from the soil, further reducing the potential for movement.

Although the overall deformations were smaller than wall 1, the cracks exhibited prior to failure were much wider and longer (fig. 7-6). The running joints purposefully created by the masons became points of weakness for the wall, and spread almost the entire height of the wall. The fact that the cracks continued up to the coping is also important, as this prohibited a large proportion of the load spread to the wing walls, which was found to affect the results in the first test.

Figure 7-6: Crack propagation of wall 2 prior to failure

7.3.2 Limit equilibrium analysis of wall 2

As per wall 1, the limit equilibrium program has been used to recreate the wall during construction and testing, and summarised in table 7.2.

From the final eccentricity, it is clear that this wall is on the verge of collapse. However, although this was the last recorded position prior to failure, it was probably not quite as close as this output suggests, as it still required a substantial load

Table 7.2: Summary of LE program output for wall 2

Date		04/09/07	10/09/07	10/10/07	12/10/07
Time				15:30	12:05
Event		Partially built	Fully built	Wall raised	Surcharge
Base thickness	(mm)	500	500	500	500
Wall height	(mm)	1100	2500	2500	2500
External batter	(deg)	4.6			
Internal better	(deg)	0.0			
Wall voidage	(%)	23	23	23	23
Limestone unit weight	(kN/m^3)	24.5	24.5	24.5	24.5
Limestone internal friction	(deg)	37.4	37.4	37.4	37.4
Backfill unit weight	(kN/m^3)	13.7	13.7	13.7	13.7
Backfill friction	(deg)	39	39	39	39
Backfill height	(mm)	1100	2200	2200	2000
Horizontal force	(kN)	2.49	5.78	5.52	4.60
Vertical force	(kN)	18.42	22.37	21.86	22.18
Eccentricity from toe	(mm)	175	102	109	2
Overturning safety factor		3.05	1.56	1.60	1.02
Sliding safety factor		5.38	2.81	2.89	3.51

to initiate the collapse mechanism. It is difficult to ascertain if the wall is supported in any way by the wing walls, which would in this case be a potential reason for the wall being slightly more stable than otherwise indicated. It is likely that the large running joints have prevented most of the load being transferred, although a small amount of additional stability may be given through block friction.

By analysing the position and orientation of the individual stones before collapse, the major factors which instigated the wall failure may be determined. The observed failure mechanism again appeared to be a toppling failure about the toe. However, by examining the photographic records and combining this data with the limit equilibrium program, it is shown to be slightly more complex. As with wall 1, failure by sliding may be ruled out by examining the PIV targets. The target attached to a block of the fourth course from the base was observed to rotate by 21.4^o. If this inclination were to continue through the whole wall, the safety factor against sliding would still be 1.21, allowing no overall failure by this mechanism. Collapse instead occurs due to the failure of stones critical to the stability of the wall, located near the base. Figure 7-7 shows the lower stones prior to failure. Due to the large relative movement between the courses, several of the blocks are overhanging those directly beneath them. A relative movement of 37mm was recorded along the surveyed centreline, although this number may have been greater elsewhere.

Using surveying data to recreate the final wall position in the limit equilibrium program, the stability of the individual overhanging blocks can checked. The block geometry can be estimated from photographs of both the internal wall during

Figure 7-7: Overhanging blocks prior to failure

construction and of the face once completed. This information can then be used together to give the theoretical safety factor of the blocks at these points. Even should the overall thrust of the wall be behind the toe, the combination of the thrust, the overhang and the geometry of the blocks is enough to cause them to rotate and fail. Since virtually the entire weight of the wall is passing through these critical stones, once the forces are enough to cause this failure the wall above will collapse in tandem as its support is undermined. The calculated safety factor for a block 50mm high and spanning 200mm into the wall at this point is 0.95, indicating that a failure should already have occurred at this point. However, as this assumes that this section of wall was unsupported by the wing walls, this is likely to be conservative.

7.3.3 Test progression

Although the collapse mechanism of wall 2 was not purely by overturning as for wall 1, the belly bulges commonly found in many drystone walls was not exhibited. Partly the reason for this was that although the wall was built to a slightly lower standard than the first, the voidage of the wall was also lower. This was due to the fact that the stones were the same size as those used in the first wall, whilst the overall profile was thinner. These comparatively large stones reduced the space for fill and hence gave smaller voids within the wall. The subsequent movements of the individual blocks and the wall were therefore limited by the lack of sufficient voids.

The geometry of the wall itself was an issue which hindered the development of a

stable bulge. As the wall was thinner in profile, it was immediately more susceptible to overturning than the previous wall. It was intended that this would impart some flexibility into the structure, however the increased tendency for overturning combined with the decreased voidage resulted in a reduction in both its capacity as a retaining structure and its ability to deform.

The ability for the stones to rotate had by this point been identified as a key factor in potential bulge development. To this end, the third wall was made to a very rough standard, with few pins used and the core material placed with little regard for its orientation and fit. To further encourage rolling of the stones during testing, the stones chosen for the wall were generally smaller, with a smaller height to depth ratio. This would mean that the wall had a higher number of individual stones than previous walls, and these would be able to move relatively easily in response to any loads. As a consequence of the rough construction, combined with the use of smaller block elements, the wall was expected to have a much higher percentage of internal voids, giving the individual blocks more space in which to move and rotate.

The anticipated effect of these changes was to create a wall which was similar in nature to a much older wall. Over time, an in situ drystone wall will become weathered and have many of the pins and material washed out, giving a much rougher wall with stones susceptible to movement. By building the wall rapidly and without many of the stabilising pins and wedges, a much older wall is recreated without the necessity of weathering and decay.

The wall was also increased in base width to 600mm, as per the first wall. As the overturning occurs at or near the toe, by making the wall wider it is more stable against such failures. In this way it was reasoned that even should failure again be via overturning, the wall would have sufficient opportunity to fully develop any bulges and deformations prior to collapse.

7.4 Walls 3 & 4

7.4.1 Analysis of observed behaviour

Upon completion, it was obvious that wall 3 was visibly rougher than walls 1 or 2. Figure 7-8 shows sections of both walls 1 and 3 to highlight these differences. Despite the apparently lower quality of construction, the wall was left fully back-filled for several months with no signs of distress before testing. The voidages for walls 3 and 4 were obtained based on the internal-external void relationship given in section 3.4.4. Photos of the walls taken before the tests began were analysed and the internal voids determined. Walls 3 and 4 were estimated to have 44% and 46% voids respectively.

On the first day of testing when the third wall was raised, the initial bulging was much more pronounced than for any of the previous walls, with the central

(a) Wall 3 (b) Wall 1

Figure 7-8: Comparison of walls 1 and 3

portion deforming up to 29mm. Moreover, this was the first time during the course of the testing that any wall had exhibited a larger movement at the mid point than at the coping.

The approximate centre of the bulge was relatively high for wall 3, coinciding with other observations from the surveying and draw-wire data and the inclinometers within the backfill. From figure 6-22, the centre of the bulge is shown to be at about 1.2m. Also shown on this diagram is an apparent slip at approximately 600mm from the base. This is likely due to a particularly weak plane within the wall, unaided by either through stones or blocks of any significant depth to resist movements. The development of this weak plane is also indicated by the data given by the inclinometers. The readings obtained show a failure plane developing within the backfill, initiating behind the surcharging plate, and terminating approximately at the wall at a height of 600mm above the base. It may therefore be assumed that the location of the failure plane of the backfill was predominantly determined by the weak plane within the wall. This in turn caused the bulging to occur much higher up the wall. Figure 6-25 shows the wall during failure. From this image, it is obvious that failure is by bursting, and that the failure is not originating at the base of the wall. The ends of the failure shown in the image appear to originate at a course just above the first row of through-stones, which would place this height at 550mm - 600mm above the base. This again further supports the theory of the weak-plane development.

Examining the readings from the instrumentation underneath the platform for the third test, there is still some evidence of load being transferred to the relatively unloaded sections adjacent to the central area of the wall. It would be expected that as the wall becomes more unstable, the loads under the platform would change. This would occur as the line of thrust moves further forwards, simultaneously increasing the load on the front jacks, and reducing the load on the rear. However,

as figure 7-9 shows, whilst the loads on the rear jacks do reduce, the front jacks remain fairly constant. As the total load upon the platform should be consistent, and the front jacks are not showing an increase as the rear jacks are unloaded, it suggests that the load is being restrained elsewhere. The logical place for this transferral would be to the adjacent concrete foundations, indicative of the wing walls again providing some measure of support to the central section. Although at failure the wall is showing significant cracking, the general direction of several of the major cracks in the lower portion of the wall appear to be following a curve, arching between the concrete supports.

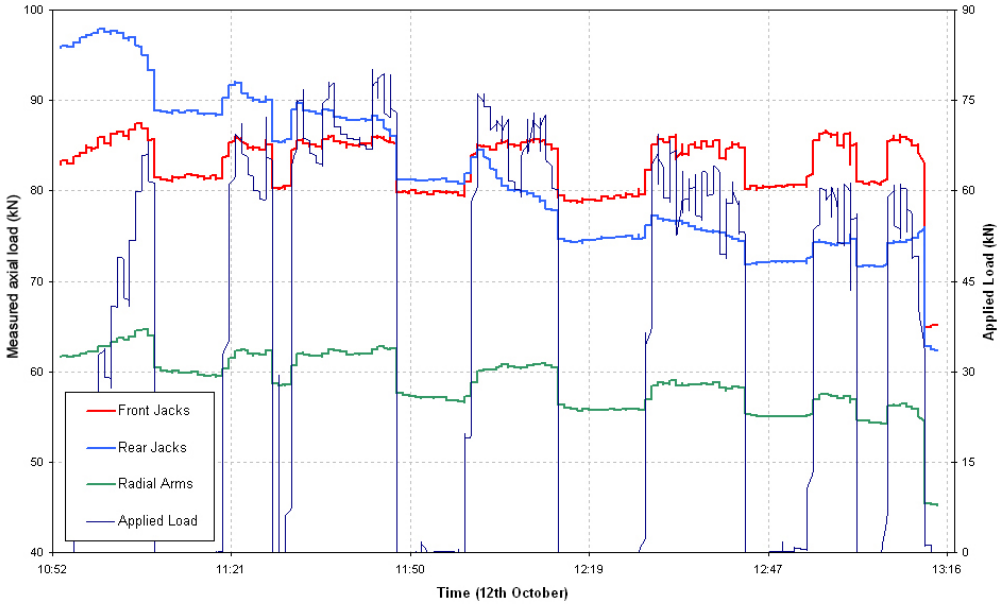

Figure 7-9: Wall 3: Applied load vs platform readings

Due to the specific characteristics of the internal make-up of the third wall, a stable bulge had been developed during testing. This was followed by a bursting failure, rather than an overturning failure as observed for walls 1 and 2. As these phenomena are specific to drystone walls, the mechanics of their development is of great importance to the project described within this thesis. In order to prove the repeatability of these results, the fourth wall was intended to be as identical as possible to wall 3. Although wall 4 had a similar build quality and overall appearance to wall 3, it was inadvertently 100mm wider at the base, giving an overall base thickness of 700mm. However, the internal face of the wall was not vertical from this point, instead narrowing by approximately 50mm almost directly above the base (fig. 7-10). From this point, the internal face is predominantly vertical. Although the limit equilibrium program automatically accounts for the centre of mass based on the individual layers, any simpler analyses must account for this, as it has the twofold effect of reducing the weight of the wall and shortening the distance between the centre of mass and the toe.

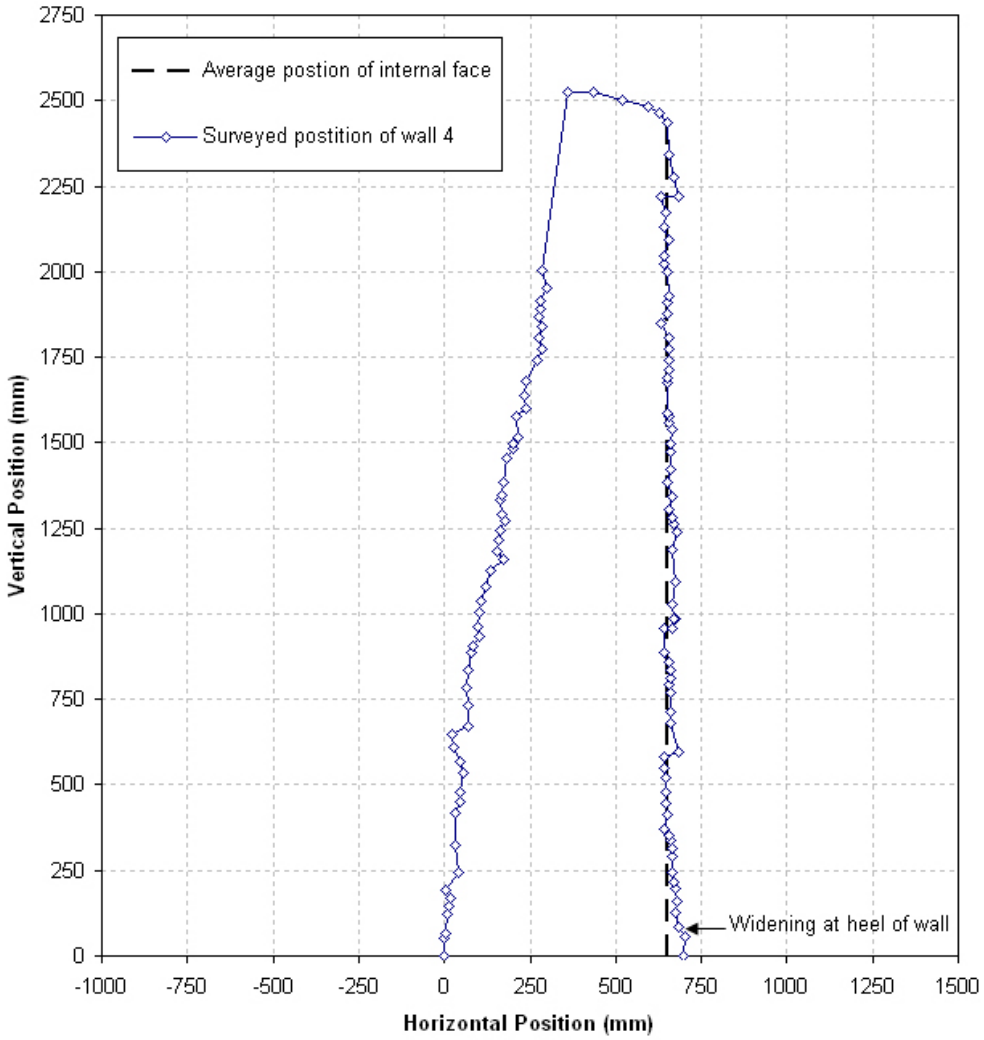

Figure 7-10: Wall 4: Overall surveyed geometry prior to testing

Although walls 3 and 4 both displayed significant bulges prior to failure, the apparent centre of bulging for the fourth wall was lower than for the third. As previously discussed, the reason for the high bulge of the third wall was due to a plane of significant weakness at a height of approximately 600mm. The fourth wall did not show evidence of such a slip, and the inclinometers indicate that the failure wedge intercepted the wall much lower down. Despite this, the overall behaviour is identical, with the bulge developing in the same manner.

With any wall, without any intrusive tests or obvious indications of weak planes within a drystone wall, it is almost impossible to determine at what height a bulge will occur. However, it is very likely that the plane identified in wall 3 was due to a particular orientation of stones which allowed excessive deformations. For wider walls such as wall 4, it would be more difficult (but not impossible) for these planes to develop due to the random nature of the wall. The thicker the wall, the higher

the chance that enough blocks will be placed such that they resist the development of a failure plane, by virtue of higher interlock with the adjacent courses.

7.4.2 Limit equilibrium analysis of walls 3 and 4

The limit equilibrium analyses for walls 3 and 4 are given in tables 7.3 and 7.4. These both show that in the final stages of the tests, the walls are approaching an overturning failure, however they have much higher factors of safety against this than for walls 1 and 2. This is not unexpected, as the walls did not fail strictly by overturning.

Table 7.3: Summary of LE program output for wall 3

Date		30/04/08	10/10/08	12/10/08	
Time			12:30	11:45	12:45
Event		Pre test	Wall raised	Surcharge	Surcharge
Base thickness	(mm)	600	600	600	600
Wall height	(mm)	2500	2500	2500	2500
External batter	(deg)	6.8			
Internal better	(deg)	0.0			
Wall voidage	(%)	44	44	44	44
Limestone unit weight	(kN/m^3)	24.5	24.5	24.5	24.5
Limestone internal friction	(deg)	37.4	37.4	37.4	37.4
Backfill unit weight	(kN/m^3)	13.7	13.7	13.7	13.7
Backfill friction	(deg)	39	39	39	39
Backfill height	(mm)	2200	2200	2000	1900
Horizontal force	(kN)	5.37	5.39	4.43	3.98
Vertical force	(kN)	20.19	20.23	19.52	19.07
Eccentricity from toe	(mm)	171	159	150	58
Overturning safety factor		1.91	1.85	1.99	1.46
Sliding safety factor		2.73	2.73	3.21	3.48

The bursting failure which was exhibited by both walls would be encouraged by means which are not necessarily identified by the limit equilibrium program, which nonetheless act towards destabilising the structure. This mainly originates from the upper sections of the walls, which lie above the centre of the bulges. The program assumes that the wall mass acts only in a vertical fashion, and that the entire weight of the wall counters the overturning moment. When considering overturning about the toe, this is generally a valid assumption, however at the centre of the bulge this may not hold true. From the surveying measurements, it is apparent that the upper half of both walls are inclined backwards. These angles of inclination are approximately 6.6^o and 6.4^o for walls 3 and 4 respectively. Therefore, at the centre of each of the bulges, the load from the mass of wall above is actually inclined from the vertical, which in turn causes a horizontal destabilising force to be applied. The magnitude of these forces have been estimated based on the volume of wall above the bulge and the inclination of the face. Wall 3 in theory

Table 7.4: Summary of LE program output for wall 4

Date		28/10/08		29/10/08	
Time		9:30	15:00	15:25	16:40
Event		Pre test	Wall raised	Surcharge	Surcharge
Base thickness	(mm)	600	600	600	600
Wall height	(mm)	2500	2500	2500	2500
External batter	(deg)	6.8			
Internal better	(deg)	0.0			
Wall voidage	(%)	46	46	46	46
Limestone unit weight	(kN/m^3)	24.5	24.5	24.5	24.5
Limestone internal friction	(deg)	37.4	37.4	37.4	37.4
Backfill unit weight	(kN/m^3)	13.7	13.7	13.7	13.7
Backfill friction	(deg)	39	39	39	39
Backfill height	(mm)	2200	2200	2100	2000
Horizontal force	(kN)	4.95	5.01	5.02	5.01
Vertical force	(kN)	20.41	19.75	18.17	18.21
Eccentricity from toe	(mm)	289	247	39	38
Overturning safety factor		2.76	2.41	1.21	1.21
Sliding safety factor		3.15	3.01	2.77	2.77

was subject to an additional force of approximately 0.65kN at a height of 1.2m, whilst wall 4 had an additional 0.85kN at a height of 1m (per metre length of wall). Whilst not exceptionally large forces, they are not insignificant when compared to the total forces being applied to the wall from the backfill. Therefore, it is highly likely that the eventual bursting failures occurred due to the general instabilities from the excessive bulging, combined with the horizontal forces from the upper portions of the walls. This caused the bulged areas to be forced further out, and resulted in the bursting failures as observed.

7.4.3 Test progression

Originally, the program scope included only four full-scale tests. However, following a donation of slate from the Coombe Sydenham Country Park, a fifth wall was scheduled to test this material. One of the primary reasons was to give physical test data related to a completely different material, hence broadening the scope and applicability of the tests. In addition, it allows further verification of the theories and analysis techniques which have been developed throughout the project, checking their applicability to materials other than limestone. It was predicted that due to the low frictional resistance of the slate that sliding would dominate the wall behaviour and be the eventual collapse trigger.

7.5 Wall 5

7.5.1 Analysis of observed behaviour

As described in chapter 6, the slate was inclined to fracture, and easily broke into shards and thin slabs of slate. As such, the wall consisted of many more layers than would be found in a limestone wall of the same size. Each of the limestone walls consisted of approximately 35 courses through the central region, whereas the slate wall had approximately 44 (these values may change slightly depending on where the count is made). In addition, due to the difficulties in working the slate, only basic changes could be made to the individual stone geometries, forcing the masons to place the majority of stones unworked. The consequence of this is that many of the stones spanned a large distance into the wall, giving an internal configuration similar to that of the first and second wall.

As discussed in chapter 6, the movements of wall 5 were purely driven by sliding, with almost not evidence of rotation at any point. As this was the case, the bulging as seen by walls 3 and 4 did not occur. Figure 7-11 highlights this by showing the lower courses of both walls 4 and 5. Figure 7-11(a) shows wall 4 prior to failure, and figure 7-11(b) shows wall 5. The targets used for Particle Image Velocimetry (PIV) are heavily rotated for the fourth wall, but remain horizontal for the fifth wall despite significant displacements. The individual block geometry was also a further restriction on any rotation or bulge development. The fact that the stones spanned much deeper into the wall meant that a much larger shift in the internal structure would be required before a rotation was possible. Even in walls 1 and 2 where many of the blocks were of a similar nature, there were still enough smaller, rounder stones so that some rotation could occur. In wall 5 however, almost every stone was thin and plate-like, hence there were no opportunities for rotation of any kind.

From figure 6-34, the movements are shown to be as expected given the properties of the slate. The majority of the movements occur in the bottom 500mm of the wall, with the rest of the wall remaining relatively undisturbed. As the horizontal pressures from the backfill will be highest at the base of the wall, in this region the forces are enough to cause sliding to occur - particularly when supplemented by the surcharging load. Above this point, the friction is able to resist the applied loads, and as no other forms of deformation are possible, remains unchanged. Instead, this part of the wall simply translates as the section below carries it forwards.

7.5.2 Limit equilibrium analysis of wall 5

The limit equilibrium output for wall 5 is given in table 7.5. Examining the various factors of safety gives an insight as to the influences upon the wall. Initially, sliding is the major issue, as the sliding safety is well below the other walls even while assuming horizontal bedding planes. As the wall continues to displace, the

(a) Wall 4

(b) Wall 5

Figure 7-11: Comparison of movements with wall 4

overturning factor also begins to reduce, as the centre of gravity moves closer to the toe.

In the final stages of the wall, the sliding safety rises, whilst the overturning force reduces dramatically. This is due to the continuing deformations which have been focused on the lower 500mm of the wall. By this point, the translations are so pronounced that the internal face of the wall is heavily inclined forwards at the base, which allows a much larger mass of soil to be applied in a vertical manner. This in turn resists the sliding right at the base, which is where the results of table 7.5 are obtained from. Conversely, the new geometry has a centre of mass which is much closer to the toe, and hence overturning is now a risk.

The final failure mode was by individual block rotation. Table 7.5 shows that although the wall is not particularly stable, it should not be in immediate danger of

Table 7.5: Summary of LE program output for wall 5

Date		20/12/08	11/03/09		
Time		14:00	9:00	10:30	11:15
Event		Wall built	Pre-raise	Post-raise	Surcharge
Base thickness	(mm)	630	630	630	630
Wall height	(mm)	2500	2500	2500	2500
External batter	(deg)	6.8			
Internal better	(deg)	0.0			
Wall voidage	(%)	30	30	30	30
Limestone unit weight	(kN/m^3)	25.7	25.7	25.7	25.7
Limestone internal friction	(deg)	17.5	17.5	17.5	17.5
Backfill unit weight	(kN/m^3)	13.7	13.7	13.7	13.7
Backfill friction	(deg)	39	39	39	39
Backfill height	(mm)	2200	2200	2200	1800
Horizontal force	(kN)	4.78	4.80	5.19	3.86
Vertical force	(kN)	23.67	23.75	24.73	23.30
Eccentricity from toe	(mm)	212	183	174	70
Overturning safety factor		2.62	2.40	2.23	1.72
Sliding safety factor		1.56	1.56	1.50	1.90

collapse. However, if we examine the photographic records of the base of the wall, it is possible to see where the failure originates. Figure 7-12 shows three images of the base of the wall leading up to the failure. Using the two lowermost PIV targets as reference points, the movement of the corresponding stones may be identified. In the final image, taken moments before failure, the lowermost target is almost fully obscured from view, after being initially almost directly in line with the adjacent target. The relative movement required to produce this is in excess of 100mm, and given the size of the stones visible at this point that is likely to be a large percentage of the depth of the overhanging stones at this point. Despite having an overturning safety factor greater than 1, once these stones were pushed far enough, one would undoubtedly fall out of the wall. As the eccentricity of the wall was then passing near to the external face, the sudden absence of this stone would cause the thrust to be outside the boundaries of the wall at this point, initiating a failure by overturning (Note: this is not the same as a failure by overturning at the base).

7.6 Parametric studies

Several previous studies have investigated the effects and relative importance of the various material properties involved in drystone walls (e.g., Walker et. al.[11], Claxton et. al.[7] and Harkness et. al.[8]). A distinct advantage of a simple limit-equilibrium analysis program used in this thesis is the ability to generate instantaneous results. This allows for a great deal of experimentation into wall deformation and the influence which individual parameters have upon stability.

(a) (b) (c)

Figure 7-12: Block sliding of wall 5

7.6.1 Geometry

As proved by Burgoyne, wall geometry has an enormous influence on wall stability. Each test wall has the same volume of stone, and yet the walls have vastly different retaining capacities; Walls 'A' and 'D' both have similar wall thicknesses, and yet wall A comfortably retains almost a 1m height of extra fill. There are several reasons behind this, one of the obvious factors being that wall 'A' has a longer lever arm from toe to centroid (in the horizontal plane), creating a larger restoring moment against overturning. In addition, the sloped backface decreases the forces from the soil - both horizontal and vertical. The restoring moment is somewhat reduced, however the majority of the load comes from the self-weight of the wall. By comparison, the overturning moment is dependent solely on the horizontal force applied through the backfill, therefore having a greater effect on the overall stability.

Walls 'B' and 'C' further reinforce the importance of the backface slope, due to their mirror-image nature. Wall 'C' is inferior to 'B' firstly by virtue of a shorter lever arm from toe to centroid, as was seen with walls 'D' when compared to 'A'. In addition, the sloped backface for wall 'C' in this instance is detrimental to wall stability. Conversely to wall 'A', wall 'C' has a positively sloped backface ($\alpha > 90^o$), which increases both vertical and horizontal loads. Again, whilst the increased vertical force is beneficial, the increased horizontal force has the greater effect, lowering the stability of the structure.

7.6.2 Loading conditions

It is intuitive that the backfill height directly affects wall stability, and that in many cases if no soil is retained then the structure is perfectly stable. However, it may not be quite as obvious exactly how great the effect of even small increases in backfill height can be. With regards to overturning and equilibrium, the major reason is found when deriving the resultant force P_a, from a block of soil behind a wall (equation 4.2). As shown in this equation, the height H, of the backfill is squared. The consequence of this is that overturning failures may occur very

rapidly with seemingly insignificant increases in retention height, and must be carefully considered.

Theoretically, the thrust line of a wall is little affected by an applied surcharge - a fact highlighted by the hand-calculations found in chapter 3.4.1, where a $1m^2$ behind the wall has $10kNm^{-2}$ load applied to it. Due to the load spreading out in all directions, after only 1m of soil depth, the load has reduced to $2.5kNm^2$, with only minimal effects to the wall. To have a substantial effect on the thrust within the wall, large areas loaded with considerable surcharges must be employed, similar to a structure retaining a foundation, or a wheel load from a fully-laden heavy goods vehicle. Although it may appear from the various load against displacement graphs that the walls move even with very low applied loads, it must be remembered that due to the size of the plate (0.6m x 0.5m), the applied pressures are much greater. For example, in test wall 3 when the surcharge was initially applied, a load of 30kN produced a movement of 3mm at the coping height. However, due to the relatively small plate, the pressure applied by this 30kN load is $100kNm^{-2}$.

Due to the way the test rig was designed, it was not possible to apply a constant surcharge load to the wall. Therefore, it should be remembered that the peak loads applied do not correspond with an ultimate resistance for the wall. Movements were always observed before reaching the peak applied load, and from these tests it is not possible to determine what maximum static load could be applied before collapse occurred. However, as discussed in section 5.4.3, it should be remembered that in these wall tests, the surcharge is used only to drive the displacements of the wall, rather than measure their strength. The tests were more concerned with understanding the mechanisms involved in drystone wall behaviour, rather than the limits of the whole structure.

7.6.3 Material properties

Within the program, various properties of the stone and soil were tested by individually modifying one whilst holding the others constant in a given wall geometry. It was found that modifying the densities of the soil and stone is of minor importance to stability. In most instances weight of stone and soil are generally fairly close - especially when dealing with well compacted earth - and require a vast difference to produce a major effect; i.e., a loose soil fill behind a well-constructed granite wall.

By comparison, the angle of friction for the soil and the soil/stone interface have a comparatively large impact on wall stability. The friction angle ϕ, determines the stable 'angle of repose' for the soil; i.e., the angle at which it would rest if subjected to no other forces except gravity. In terms of the limit equilibrium analysis, a lower soil friction angle will create a larger coefficient of active earth pressure (K_a), causing an increased resultant force against the back of the wall.

The soil/stone friction interface δ is developed by friction on the backface, with

larger angles being associated with rougher walls. The friction angle determines the way in which the backfill affects the wall; a comparatively rough wall surface will take more of the resultant force as a vertical stress acting down the backface, creating a larger restoring moment and reducing the horizontal forces. This is of particular importance for drystone walls, as the structure generally has an uneven surface, generating large friction angles. Greater amounts of friction are often generated due to the fact that the backface is typically of a poorer construction than the front.

7.7 Stable and progressive bulge development

As previously discussed, although bulging is a commonly observed phenomenon of drystone walls, very little work has been undertaken in an attempt to understand its formation. It may be misconceived that the bulge is a result of blocks sliding over one another. Through the observations during the full-scale tests, combined with the laboratory data acquired, it has been shown that in the observed limestone walls it is due to block rotation rather than sliding. This section discusses these data and observations, describing the factors and mechanisms which contribute to the formation of stable and unstable bulges.

The initial platform raise during testing caused bulging to occur in all four of the limestone walls; these were not visible to the naked eye, but easily identifiable with the resolution offered by the Total Station. The scale of these bulges varied from an outward movement of 10mm (recorded for the first wall) to 29mm (for the third wall), with the location of the maximum movement always occurring between 0.8m to 1.1m from the base.

Despite deforming, the wall may be more stable after these initial bulges. In part, this is due to the new profile. Tables 7.1 and 7.2 give the stability prior to, and after the vertical movement of the platform. From these tables, it is shown that the factors of safety can increase for sliding and overturning, based purely on the new geometries.

The importance of the friction angle between the wall and backfill is discussed in section 7.6. It is demonstrated that a higher value allows a larger amount of the active pressure to be applied vertically to the internal face of the wall, hence increasing the stability by virtue of giving a larger restoring moment. Conversely, the effect of a lower friction angle has the effect of giving higher horizontal loads, and lower vertical loads, reducing stability. Before the platform was raised, it was impossible to determine precisely the value of this friction angle, however it is unlikely to be at its maximum value. Therefore, although it is difficult to precisely know the exact forces applied to the backfill before the vertical lift, the forces after this event would undoubtedly be highly beneficial to the wall's stability. As previously discussed in section 5.4.2, this also allows a much better understanding

from this point in the test onwards, as this crucial friction angle can now be safely assumed.

Although the raising of the platform is not a naturally occurring phenomenon, it successfully represents the inverse; i.e., settlement of the backfill. Due to the increased friction angle that is generated, it is likely that in-situ drystone walls will actually become more stable over time as settlement occurs. This is also accompanied by bulging of the wall, which the limit equilibrium program has determined will further increase the stability. As the deformations observed during the tests were clearly a response to the movement and did not continue after the event, this simple action has been proved to induce a stable bulge, albeit one which is relatively small.

Stable bulge development may continue even during localised surcharging, as found whilst testing walls 3 and 4. In these tests, the surcharging caused the wall to respond by further developing the already formed bulge. The movements only occurred during the surcharging, and once stopped, the bulge also ceased to move. As will be discussed in section 7.7.1, the developed bulge may actually aid stability, but only up to a certain point. If the applied surcharge loads exceed (and are continuously applied) beyond the limits of the structures, the bulge will quickly move beyond the initial beneficial geometry. At this point, each subsequent movement will decrease the wall's stability even without the surcharge, and the wall will move towards either a bursting, toppling or sliding failure. In the two full-scale tests, wall 3 failed almost exclusively via bursting, as the central bulge was pushed out until instability occurred. In wall 4 a bulge quickly developed in response to the loading, however as the loads were continuously applied this was turned into a predominant failure via overturning. The bulge was still present in the final wall profile, however the failure mode was predominantly a rotation originating near the toe. This test highlights the complex behaviour of these structures, disallowing the simple assumption that they will always fail purely in one mode or another.

Through a comparison of all four limestone walls, the major factors which determine how a wall will react to any applied loads may be ascertained. In particular, walls 1 and 3 should be examined, as they had the same profiles, but with different internal geometries (fig 7-13). Although the test procedure varied slightly (the first test included some platform rotation), these internal differences are the predominant reason for the difference in the deformations. By varying the internal geometry from those shown by walls 1 to wall 3, there are two main effects; the wall unit weight is lowered and individual block rotation is encouraged.

As discussed in section 7.6, the wall unit weight must be substantially altered before significant changes are effected on a wall's stability. However, through the much rougher construction, wall 3 is estimated to be 17% less dense than wall 1, and as such has a measurable effect on wall stability. Were wall 1's unit weight to be reduced to the same value as wall 3, the overall safety against overturning

(a) Wall 1 (b) Wall 3

Figure 7-13: Comparison of the internal structure of walls 1 and 3

would be reduced by 18%, or 0.7 in terms of its numerical safety factor (although it should be noted that the thrust of the wall is still within the middle third range).

Despite the lowering of the unit weight of wall 3, it still proves to be more stable than wall 2, which had the highest unit weight of all 4 walls (due to having the lowest voidage), but was 100mm thinner in profile. This is not due to the larger volume of wall 3, as wall 2 has a higher mass per metre along its length despite its narrower width. Critically, the smaller base width of wall 2 substantially reduces the distance of the eccentricity to the toe when compared to wall 3, resulting in the described outcome.

The second effect of the internal differences between walls 1 and 3 - an increase in the rotational freedom of the individual stones - has a much larger impact on wall behaviour than alteration of the unit weight. The block rotation is encouraged by two factors; individual block geometry and voidage. As discussed in chapter 6, the geometry of the blocks for wall 3 was much more rounded than wall 1, which tended to employ flatter, plate-like blocks at the faces. These rounder blocks had a much closer height:depth ratio, and as such required much lower horizontal forces before any rolling would occur (fig. 7-14). What is also evident from this figure is that for the geometries sketched, sliding would more readily occur than rolling in the flatter wall block.

(a) Wall 1 (b) Wall 3

Figure 7-14: Comparison of the individual blocks of walls 1 and 3

For the block depicted in figure 7-14(a), the width of the stone also discourages any movements due to the increased top surface. This larger area would allow more stones above to rest upon it, giving more contact points to hold it in place, along with a comparatively larger normal force. These both combine to ensure that rotations are far more difficult than for the block depicted in figure 7-14(b). Wall 1 also had a significantly larger number of pins and wedges than wall 3. This would further ensure than many contact points existed between each stone and the adjacent blocks, further restricting their movements.

Finally, the comparatively large amount of voids within wall 3 also allow greater block rotations. For drystone structures of a tightly-packed nature like the first wall, even should the block geometries lend themselves to rotation (see fig. 7-14(b)), the proximity of the adjacent stones would disallow any movement. With the more rapid construction of wall 3, the individual blocks are not necessarily in immediate contact with the neighboring stones. With this separation, many of the stones may rotate a certain degree before encountering any resisting stones.

Observations of the external faces of walls 3 and 4 give further evidence that bulging is linked to block rotation rather than course sliding. Aided by the targets used to provide the PIV monitoring of the walls, the inclination of the face stones can be ascertained, as shown previously by figure 7-4. It is shown by these observations that to form the bulges of wall 3 and 4, the stones of the wall have rotated, with the external faces of each block resting parallel to the curvature at that level. Furthermore, the faces are relatively continuous, without the stepped profile that would be visible if the deformations were a result of sliding.

7.7.1 Limit equilibrium assessment of bulge development

Bulging begins when the loads behind the wall cause blocks or entire sections of wall to move, and the resulting movement causes both the forces acting on the wall and the equilibrium of its own mass to change, such that a new equilibrium position is found. Were this not the case, the wall would continue to move, resulting in collapse. Once a bulge is formed, the pressures acting upon the wall must change in response to the new geometry. A section of a typically bulged wall is shown in figure 7-15, highlighting the common features. Above the bulge, the wall is leaning back somewhat, having a twofold effect. Firstly, it stabilises the wall by moving its centre of gravity away from the toe of the wall, which is usually the overturning point. Secondly, it reduces the magnitude of the forces applied to the wall by the backfill.

Below the bulge, the wall is leaning forwards, causing the active pressures within the backfill to have a much greater effect upon this portion of the wall. The magnitude of the force will be greater, but the downwards component will be most increased, so increasing the stability of this portion of the wall, provided that the face has not moved so far forwards that individual blocks are no longer

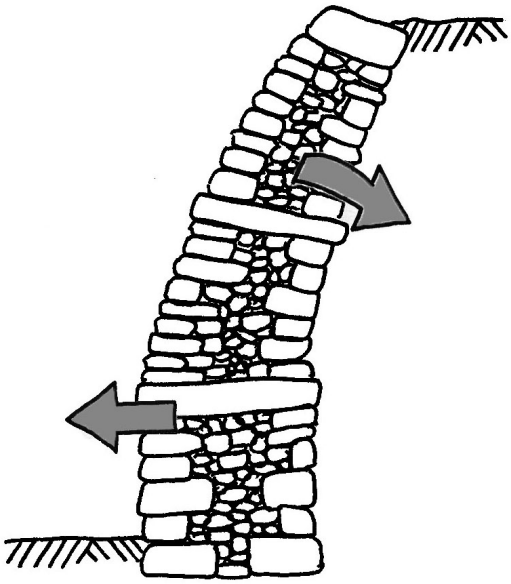

Figure 7-15: Typically bulged drystone wall

supported. Overall, these changes tend to be in favour of increasing wall stability, and walls have commonly remained perfectly safe for years whilst displaying this type of bulge without any detrimental effects.

To prove this theoretically, the limit equilibrium program was used to deform a wall into a bulged profile, and the effects on the thrust line observed. The initial geometry was based on an idealised section similar to Burgoyne's full-scale tests, i.e. 6m in height, with base and crest widths of 1m respectively. The bulge was formed by moving the wall out at 2m ($\frac{1}{3}^{rd}$ of the height), with a respective tilt backwards above this point. As the bulge was created the overall thrust remained approximately in its initial position. The bulge was then progressed to the point at which further movement would cause an overall loss in stability from the initial factor of safety. A comparison of the initial and final outputs are shown in table 7.6, with the final geometry shown in figure 7-16.

From table 7.6, it is shown that the combination of the new geometry and the active pressures now being applied upon inclined surfaces results in a net change in the thrust line of 0mm. Up to this point, the safety has not been compromised by the progressing bulge, despite an outward movement of 156mm. Although the stability is in part ensured by the mass of the upper half of the wall being behind the overall centre of gravity, this is not unreasonable to suggest. As the wall begins to move outwards at the centre of the bulge, the backfill material will fill up the space previously occupied by the wall. If this is done by the material immediately above this point falling down, this will create a void in this space. Whilst this in turn will elicit further material to fall down from above this point, it may also

Table 7.6: Comparison of bulged and non-bulged profiles

Height (m)	Width (m)	Wall movement Δ (mm)	Thrust change Δ (mm)	Vertical Force Δ (kN)	Horizontal Force Δ (kN)
6.0	1.02	-300	N/A	0	0
5.7	1.02	-263	273	0.13	0.00
5.4	1.02	-228	255	0.26	0.00
5.1	1.02	-192	237	0.39	0.00
4.8	1.02	-156	219	0.52	0.00
4.5	1.02	-108	198	0.69	0.00
4.2	1.02	-72	178	0.81	0.00
3.9	1.02	-36	158	0.94	-0.01
3.6	1.02	0	138	1.01	-0.01
3.3	1.02	24	119	1.14	-0.01
3.0	1.02	48	102	1.22	-0.02
2.7	1.02	72	85	1.30	-0.02
2.4	1.02	96	69	1.38	-0.02
2.1	1.02	132	53	1.50	-0.03
1.8	1.02	156	38	1.57	-0.03
1.5	1.02	132	24	1.50	-0.02
1.2	1.02	108	15	1.42	-0.02
0.9	1.02	84	7	1.35	-0.01
0.6	1.02	60	3	1.28	0.00
0.3	1.02	36	0	1.20	0.00
0.0	1.02	0	0	1.10	0.01

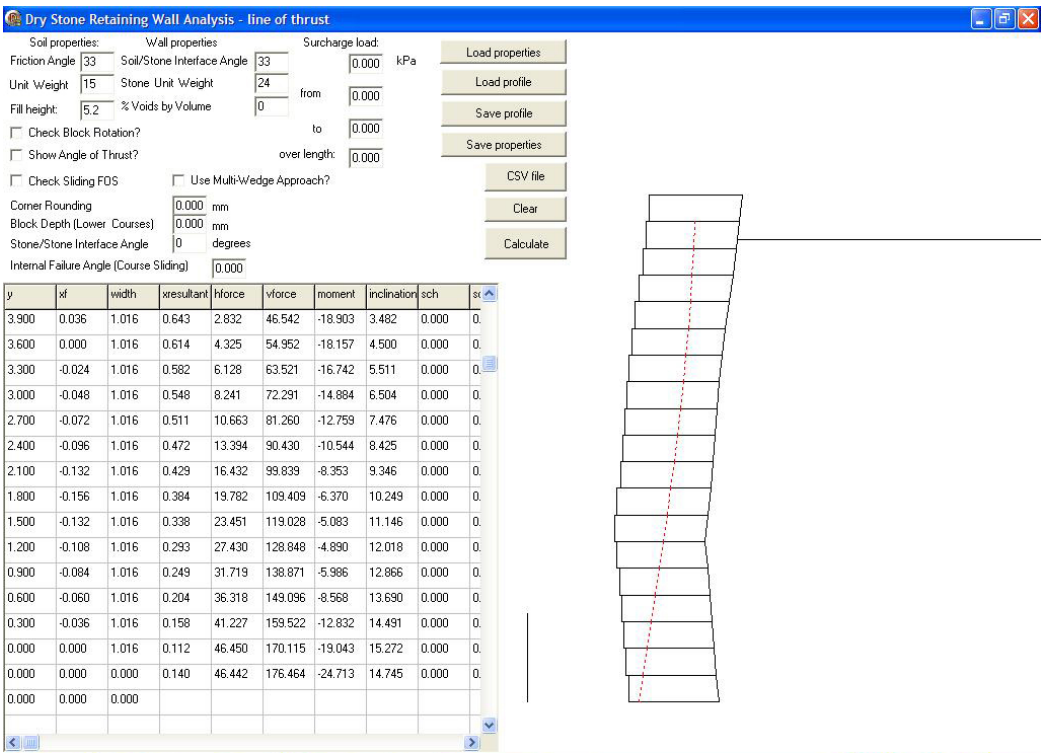

Figure 7-16: Program output for bulged wall profile

allow the wall to relax backwards due to the reduced passive pressure, which would normally prevent movements of this nature. Hence the wall above the bulge may be allowed to gradually relax backwards, even as the outward movement progresses. This will eventually reach a critical point where the safety of the wall is impinged, and the buckling may accelerate into what would be considered to be a bursting failure at the extreme point of the bulge.

7.8 Comparison studies

Several local in-situ walls have been examined over the course of this project, both drystone and mortared in nature. The three main locations are Atworth, Crudwell and Bradford upon Avon, in Wiltshire, UK. All three locations were brought to the attention of the project team after localised collapses of sections of retaining walls. Each wall extended much further than the limits of the collapsed sections, and many of these other areas exhibited bulges or deformations.

7.8.1 Bradford upon Avon, Wiltshire

The Bradford upon Avon walls which were examined all had mortared joints, and as such would not be expected to behave in entirely the same manner as unmortared drystone walls. The collapsed section, shown was approximately 2.5m tall and 0.5m thick where visible. Total Station surveying measurements were made in an adjacent section which remained upright and undamaged following the partial collapse of the wall. In addition, the local authorities advised the project team of a second location where the wall was known to be leaning and its stability in question. This wall was again mortared, but no section of this stretch had as yet failed. Total Station surveying measurements of this section were also taken. Both sets of readings are given in figure 7-17.

As the walls have infilled joints, they are much less flexible, and hence are deforming by relatively small amounts and in a purely linear manner. The weepholes also evidenced some blockages, which would encourage the build up of water pressures in the slope, and potentially initiate the toppling failure which was observed.

7.8.2 Atworth, Wiltshire

In December 2007, a 3m stretch of a drystone retaining wall collapsed in Atworth, Wiltshire. This wall was approximately 2.3m in height and 700mm to 800mm in width at the base. The retained fill is approximately 1.5m high and consists of a root-filled soil, with several large trees directly behind the failed section (fig. 7-18).

No equipment was available to take precise measurements of these walls, however the photographs themselves provide several clues as to the causes of the failure. Primarily, the vegetation behind the wall should be considered. As the backfill

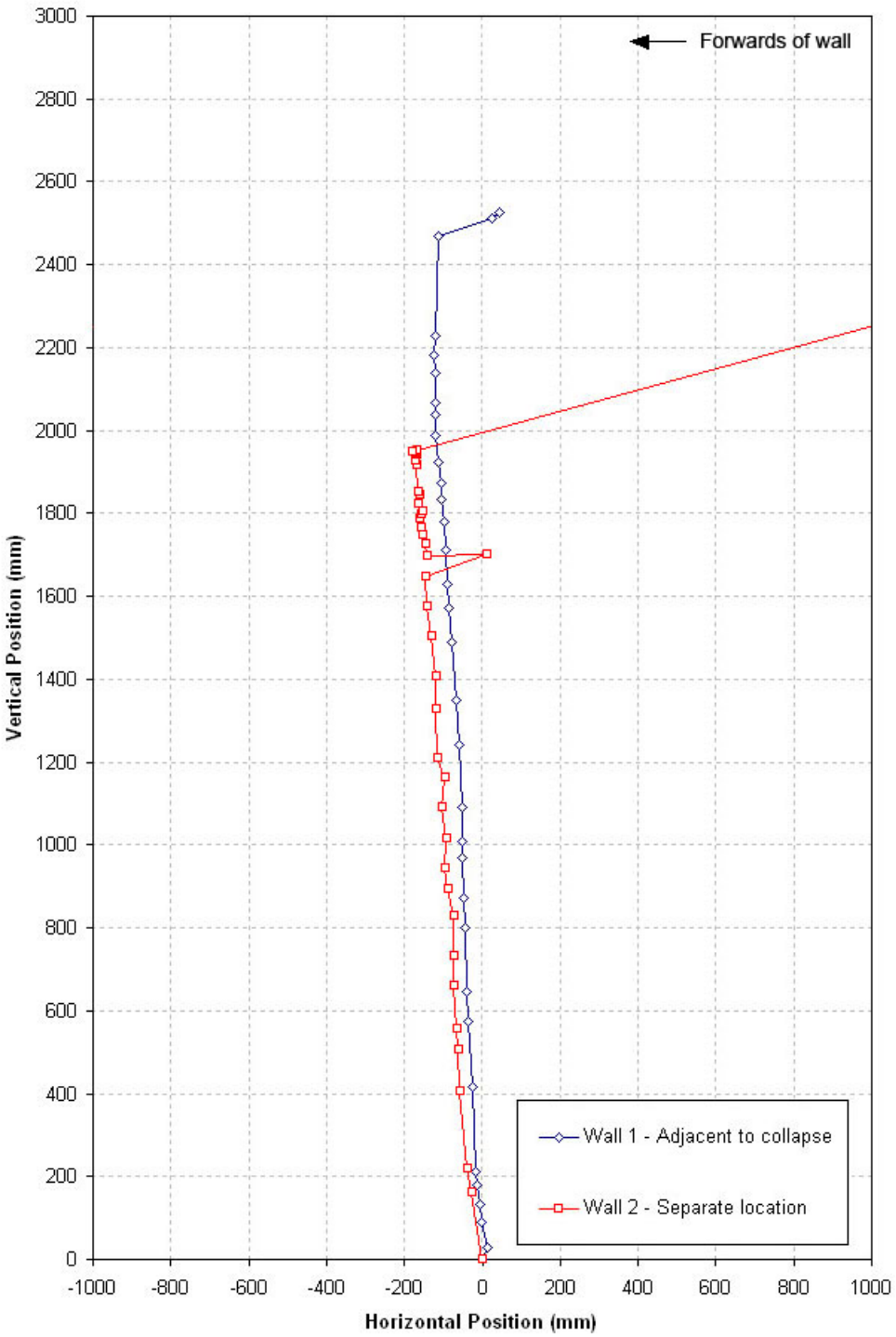

Figure 7-17: Measurements of wall sections in Bradford upon Avon, Wiltshire

Figure 7-18: Collapsed wall section in Atworth, Wiltshire

height is not particularly excessive, it is unlikely that soil pressure alone could generate the forces required to collapse the section of wall. It should also be noted that the majority of the wall does not appear to be in danger of collapse or show any excessive movements. However, figure 7-18 shows several large trees in the vicinity of the collapsed section, including one near the centre of the failed section which had to be given additional support after the collapse. Figure 7-19 more clearly shows the proximity of the tree to the wall, in addition to the cross section of the wall.

Even with the proximity of the tree, there are still several factors which may contribute to the overall failure. The additional loads from both the tree and root growth would undoubtedly cause the wall to deform and bulge. This is also apparent in figure 7-19, as shown by the sloped nature of the courses in the bottom half of the wall. Secondly, there is evidence that the majority of the joints had become infilled with soil (and potentially roots), which would lower the bedding friction, as discussed by Walker et. al.[25]. This evidence stems from close inspections of the walls, but also from photographic evidence showing vegetation growing in some of the wall joints. With the additional pressure from the tree and roots, combined with the sloped and soil-infilled joints, a failure would be much more likely in this area. The factor of safety would likely be worst after a heavy rainfall, when the soil in the joints would become saturated. It should be noted that there appears to be no subsidence or other movements of the foundations directly under the failed

Figure 7-19: Cross section of collapsed wall section in Atworth, Wiltshire

section, and that the failure originated several courses above the base level.

7.8.3 Crudwell, Wiltshire

Figure 7-20 shows the failed section of wall in Crudwell, Wiltshire, which occurred in July 2008. The image shows the wall after the debris and foundations had been removed, and the collapsed backfill has been squared off using plant machinery. However, the failure width remains the same, there being a distance of 5m between the intact ends of coping either side of the collapse.

This wall is of particular interest to this project as the construction quality and wall geometry are very similar to the full-scale test walls described in this thesis. The walls were appromately 2m high, and 0.6m wide through the base, and retained a soil backfill up to a height of 1.8m. Figure 7-21 shows the internal

Figure 7-20: Collapsed wall section in Crudwell, Wiltshire

make-up of the wall, consisting of both an internal and external face, a rubble infill and through stones.

Although only one section of the wall had collapsed, many other parts of the wall displayed visible deformations and cracks. These took a wide variety of forms, as various failures over the lifespan of the wall have been repaired in different ways. Figure 7-22 shows the relative locations of these cracked or deformed areas, with dotted lines indicative of bulged areas, and solid lines showing cracks.

Both ends of the failed section were measured using the Total Station, along with three other areas showing the greatest deformations. These investigated sections are those marked A, F and G on figure 7-22, with C(a) and C(b) being the surveying runs adjacent to the failure zone. These results are plotted in figure 7-23. From this figure, it is shown that runs A, C(a) and F are all showing significant bulges through the central region. Sections C(a) and G both show linear displacements, with G being much more pronounced.

The displacements shown by the Crudwell walls are not uncommon, and show many interesting results. Section G, which was mortared, displayed both the greatest displacements and a linear deformation. This is not unexpected, as the mortared joints would be unable to give the same degree of flexibility as the unmortared areas. The lack of weepholes also is a cause for concern in this region, perhaps explaining the larger deformations. Whilst mainly unnecessary in the rest of the wall, the localised barrier to moisture would potentially allow a build up of water pressure in the retained fill at this point, reducing soil-suction and increasing the

Figure 7-21: Section through collapsed wall section in Crudwell, Wiltshire

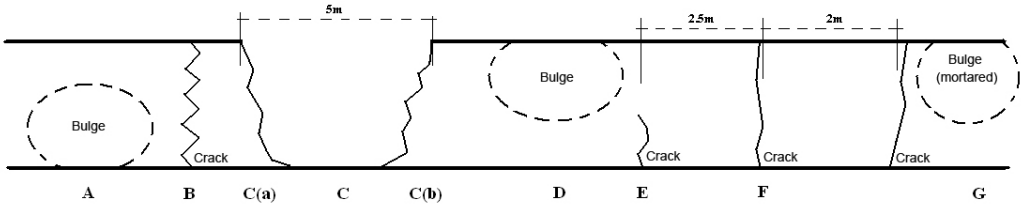

Figure 7-22: Relative locations of deformed and cracked areas of Crudwell wall

horizontal loads.

As previously mentioned, many sections of this wall have been subject to repairs, and the effectiveness of these repairs may be clearly observed. Although the standard procedure for many masons is to 'stitch' a rebuilt section into the existing wall and blend the two together, in this instance the repair the masons have simply inserted a new rectangular section of masonry which is not tied into the existing structure. The reasoning for this is unknown, however as a result there exist full-length running joints at either side of the rebuilt section, allowing no amount of load sharing to the original wall. Consequently, the rebuilt section has deformed precisely within these boundaries, showing evidence of both bulging and in-plane

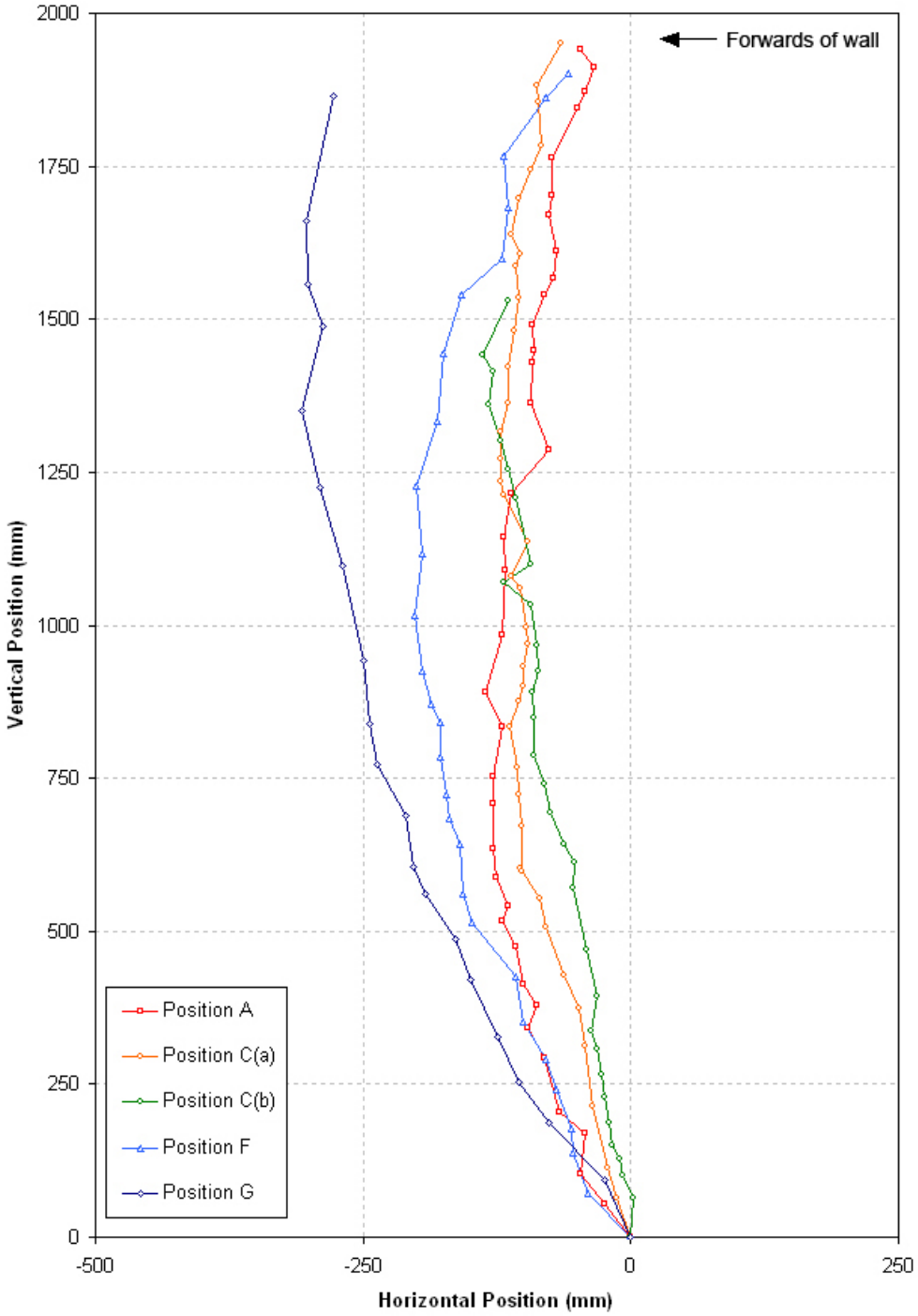

Figure 7-23: Measurements of wall sections in Crudwell, Wiltshire

sliding (fig. 7-24. Had these sections been stitched into the existing wall, it is likely that the deformations would have been much reduced.

(a) (b)

Figure 7-24: Movements at boundaries of repaired sections

As these walls were relatively similar to the full-scale test walls of this project, a comparison study was carried out. This involved examining the surveying measurements of the Crudwell walls and comparing them to those of the project walls prior to collapse. Figure 7-25 shows the same five full-scale wall tests prior to failure at an identical scale to figure 7-23 so that a direct comparison may be made.

From this comparison, it may be observed that there is excellent correlation between the in-situ walls and the project tests. Therefore, the methods being applied to test the full-scale tests are recreating not only the same type of deformations, but also movements of a similar scale. What should also be noted is that the different backfill materials do not appear to alter the behaviour of the wall (the Crudwell wall was backfilled with soil, as opposed to the gravel backfill of the project tests). This is particularly encouraging, allowing confidence in transferring the theories and observations from the full-scale tests to in-situ walls.

7.9 Conclusions

This chapter has examined the observations from the full-scale tests, and explained them using data from a variety of sources, including the testing instrumentation, laboratory tests and the limit equilibrium package. By doing so, it has been possible to explain the underlying reasons as to why particular deformation patterns occur, using existing methods and theories.

The limit equilibrium package has been utilised not only to assess the full-scale wall tests, but also to investigate wall behaviour in a more general sense. A

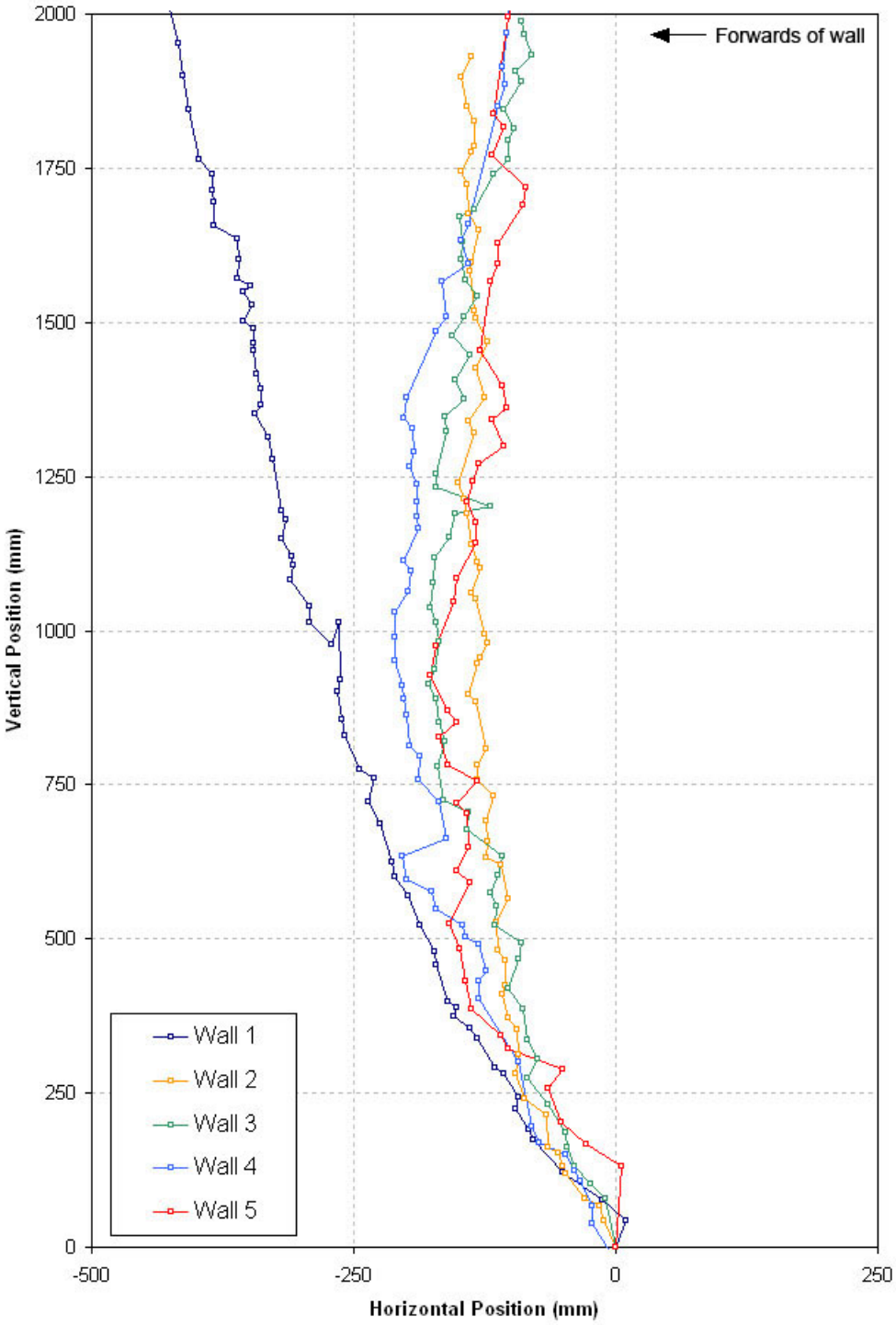

Figure 7-25: Comparison of Crudwell wall measurements with project data

parametric study highlighted several important criteria for wall stability, as well as those factors which are not so crucial. Following this, the process of bulging was investigated, allowing its explanation in terms of the geometry, self weight and application of the applied loads.

Finally, some local drystone wall collapses were discussed, using photographic evidence and surveying measurements where available. Of particular interest was the wall at Crudwell, where the geometries of the still standing sections of wall matched the bulged profiles of the full-scale tests of this project. This agreement indicates that the full-scale tests have indeed been replicating the real behaviour of existing in-situ walls, and so allows the theories developed to be applied to walls other than those of this project.

Chapter 8

Discussion and application of results

8.1 Introduction

During the course of the full-scale tests described in this thesis, a great deal of data has been gathered regarding many aspects of drystone wall behaviour. This chapter discusses the implications of this work, and its relevance to the engineers attempting to assess existing drystone walls with unknown safety margins.

8.2 Limit equilibrium analyses

The limit equilibrium program has vast potential for practicing engineers. Its flexibility allows analysis of any size of structure comprised of any material. The generation of the backfill is similarly versatile, giving the user the freedom to analyse the effects of a fill of any height and friction angle. These factors combined with the ability to deform the walls and create bulges within the structure means that the analysis is far more straightforward than the comparative hand calculations.

Despite the fact that the analysis is more rigorous than the potentially aforementioned hand calculations, the basic engine of the program is straightforward and based upon well-established principles. The ability to alter all of the variables and see the results practically instantaneously also means that the user quickly gets a complete grasp of the structure, and is able to better understand what the critical factors are. This is perhaps more true than for the respective numerical packages (such as UDEC), which may require significant run-time before a result is generated. In these instances, unless the package is being used specifically to perform a parametric analysis of some kind, a user would likely be unlikely to fully investigate the relative importance of the different variables.

The interface for the package has been laid out in a way that is easy to use and understand, with numerical and graphical outputs. The graphical output gives the

user an instant summary of the structure in one image, with the line of thrust and any extra required checks clearly shown in one image. For a more precise analysis, the information is also tabulated on the page, in addition to giving the safety factor as a numeric and listing the forces acting in the system. Similarly, there is equal flexibility in the manipulation of a generated wall. The geometry may be altered precisely in the tabulated data, or alternatively the user may directly change the visual representation of the wall, and 'drag and drop' the blocks' new locations. Either method causes the line of thrust to be immediately recalculated, showing the stability for the new geometry. This combination of a user-friendly interface and almost instantaneous results also means that it is very cost-effective for use as an analysis package; very little time is required for its use and generation of results, meaning that it may potentially be used for very small projects where there are budgetary constraints.

Another significant advantage of the program is that it can run with very few known variables. Once the profile is known, the wall geometry may be estimated and entered along with either the specific material properties derived from laboratory tests or from standard values from various geological studies. Where the geometry is not entirely known, it may be possible to estimate it based upon the visible sections of wall. Adjacent or nearby walls of similar sizes that have collapsed or have visible end sections may be used, or the simple assumption that the wall has a vertical internal face from the coping may also be adopted if no other information is available. The properties of the backfill may be quickly ascertained ideally from borehole data, or a simple site investigation may suffice in some circumstances. It should be noted that the condition and nature of the backfill obviously has a major influence on the behaviour of the wall, and as such should be investigated as thoroughly as possible. Once these basic data are all entered into the program, a stability analysis may be conducted. Parameters which are unknown may be conservatively estimated, although the higher the number of known quantities the more accurate the stability analysis will be. In this way, a rough approximation of the stability of a wall with very few known quantities may be carried out. In these cases, the program has significant advantages over hand calculations and numerical studies, as the hand calculations are more laborious and potentially not as accurate, whilst the numerical studies generally require many more known variables before they become feasible.

Verification of the program has revealed that it gives generally very close agreement to the observed failures of the available physical test data. In addition, these failure modes are not limited to simple overturning failures, but also more complicated collapse modes such as sliding along inclined planes or the rotational failure of individual stones. It is important to note, however, that drystone walls are entirely bespoke structures, and that no two are alike. For this reason, the program should be used to give a general overview of a structure's stability. It should not be

assumed that because a structure has an adequate safety factor against a certain failure mode that it will not happen; the wall may contain unforeseen weaknesses which may instigate a collapse. The program is best used to give an overview of the of a structure, identifying the most likely failure modes in its current state. A similar observation may be made about the material properties which are used to represent a structure. As previously described in section 7.6, some parameters are difficult to determine, and yet have large implications for the overall stability of the wall (e.g., the angle of friction δ which occurs at the interface between the wall and the backfill). Small alterations of these variables may significantly change the predicted stability of a wall, potentially leading to an underestimation of the various factors of safety. Despite this, the program is perhaps better suited to dealing with these unknowns than a more complicated numerical study. For any given variable, the values used may be quickly made more conservative, allowing for a worst-case scenario. However, as previously mentioned, for numerical packages, these variables are still just as important, however the same changes and their outcomes take much longer to effect.

There are some aspects regarding the stability of drystone retaining structures which are currently not modeled by the limit equilibrium program. There is no ability to assess the bearing pressures in the foundation, or model local and overall settlements. These are complicated processes, especially given the unmortared nature of the walls, which would not necessarily fail due to these movements, but would undoubtedly undergo a shift in their structure and load distribution. Similarly, the saturation of the backfill by water cannot currently be modeled. This is potentially a vast drawback, as the build up of water pressures may undermine the stability of a wall quickly and without warning. A build up of water pressures behind a wall also has implications for the strength of the soil, which will lose any soil suction when saturated. This is a complex process, and as such was not in the initial scope of the program. Instead, it was intended that this phenomenon would be examined by the numerical package being developed by John Harkness et. al. at Southampton University, who are working in partnership with the project team based at the University of Bath. The goals of this work are to produce a three-dimensional numerical package, capable of recreating a drystone retaining wall comprised of a random assortment of stones as found within a real wall, rather than a repeating pattern of interlocked blocks. This work is still currently in development, and so no results are presented in this thesis.

Despite the aforementioned drawbacks of the limit equilibrium program, the program is coded in an open-source manner so that it may be easily altered to include additional methods of analysis and check for other modes of failure. In this way, should additional data become available which is not represented accurately by the program, the appropriate changes may be made relatively quickly and easily.

8.3 Visual inspections of in-situ walls

For the analysis of any existing wall, a primary tool should always be monitoring and observation of the structure in question. As discussed in section 2.5, there are no specific codes of practice for the assessment of drystone walls. Instead, there are some documents which give some guidance, e.g. the recently published CIRIA guide[1]. Much of the guidance available is based on empirical data, as scientific drystone test data is scarce. Given the observations and analysis of the full-scale tests and the laboratory data conducted throughout this project, this guidance may be further supported and expanded upon.

8.3.1 Cracking and settlement

Many of the important phenomena relating to drystone wall stability are highlighted by documents such as the CIRIA guide[1]. Several of these are specific to drystone walls, or must be dealt with in a different manner to other structures. For example, crack propagation is an obvious indication that the stresses within a structure are increasing. However, in a drystone wall, the whole structure is unmortared, allowing the potential for cracks to be mistakenly identified throughout the structure. In terms of drystone walls, a crack must be a joint which has been identified to have moved or still be moving in a given time-frame, otherwise the perceived crack may simply be a badly constructed section or similar. In such cases a pre-existing crack may have no effect on the stability of the structure, although it may become a weakness if the conditions change.

If there is a suspicion of a developing crack or instability, there are often several other indications which may also occur. The line of cracking will generally follow the jointing of the wall, as this is obviously the path of least resistance. However, should a wall stone bisecting the suspected crack path have split, this is a definite indication that the crack has formed or is still forming. Other symptoms such as localised settlement may be visible; this can occur and the top of the wall (as in the Kwun Lung Lau wall[32]), or it may be a movement at or near the foundations. Settlement of the foundations may sometimes be difficult to identify, especially if the area has been covered in Tarmac etc. In these cases there may instead be evidence of cracking on the surface of the foundation, which should also be carefully monitored.

To monitor the crack development, there are several possible options. Simple 'telltales' may be attached and periodically inspected, determining the distance between adjacent stones. These may be replaced with more sophisticated displacement equipment or with the use of DEMEC gauges, however this is not always necessary. Dated photographic records of the wall are extremely useful, ideally with some means of scaling within the image. These may be used not only to monitor the propagation of a crack, but also may highlight other movements not

previously identified.

8.3.2 Bulging and deformation

Many in-situ drystone walls exhibit either bulges or other deformations. For any engineer attempting to determine if these deformations are impinging on the stability of the wall, several factors must be considered. Again, similar to the monitoring of cracks, it must be identified whether the deformations are progressing over time. It may be the case that the deformations are occurring in addition to cracking or settlement, and so similar monitoring techniques may be used (photographic records, telltales, etc.). Where possible, the location and size of the deformations should be recorded and documented in a sketch or similar, as it is often difficult to gauge the extent of a three dimensional movement from a photographic image. The ideal tool for determining the profile of a deformed structure is through the use of surveying equipment, e.g., the Leica Total Station used for this project.

As discussed in section 7.7, it should be understood that the formation of a bulge does not necessarily indicate that the wall is becoming more unstable. It is likely that the bulges found in many of the existing walls today occurred relatively soon after they were constructed, as they and their retained fill gradually settled. For walls which exhibit bulging but no identifiable movements, simple assessment techniques such as the limit equilibrium program may be sufficient to determine the general stability - particularly if the wall is subject to ongoing monitoring and inspections.

Where the movements are progressive, it is likely that the wall is becoming more unstable, and will eventually reach a point where collapse will occur. Again, tools such as the limit equilibrium package may be used to assess the identified movements and their impact on stability. Analyses such as these can be very useful to determine the next step which must be taken; if the wall is on the verge of collapse then it must be dealt with immediately. However, if the wall is showing only a slow progression of movements and still retains a high degree of stability, then monitoring may continue for a time whilst the possible solutions to the situation are considered.

For linear deformations, i.e., the wall is toppling about the toe, the situation is potentially more dangerous. A bulging wall is ductile, and may possibly deform by a large extent before failing. Conversely, a wall which is exhibiting linear deformations may be indicative of a wall which is behaving monolithically. This may be due to either a tightly-knit structure, or a wall which has been pointed or grouted, hence reducing its flexibility. In either case, the wall may be liable to collapse suddenly and without any seeming warnings. In such cases where even a small progressive linear topple has been identified, steps must be taken immediately to stabilise the wall.

There may be many clues which indicate that a bulge is forming. If a local

bulge or deformation is occurring, it will generally be accompanied by movements of the courses within the wall. If the courses of the wall are generally not level or straight, this may be difficult to identify. If the wall is generally constructed of straight, level and even courses however, and one section appears to be deviating from this practice, this may give the first indication that deformations of some sort are taking place. Individual block rotations must also be observed carefully; as demonstrated by the limit equilibrium program, a block which is overhanging or has rotated may be forced out of the wall by the forces acting upon it (particularly near the base of the wall). Should the majority of the wall's thrust be passing through this stone this individual failure would lead to a total wall collapse.

8.3.3 Vegetation and water effects

Vegetation and tree growth may have a large effect of the behaviour of a drystone wall. The root growth of trees is of particular concern, and may lead to the bulging or toppling failures previously described. Vegetation growing in between the joints may also be a cause for concern, as this indicates that the joints have become infilled with soil to allow such plants to grow. As discussed by Walker et. al.[25], soil infilled joints could potentially have much weaker friction angles, particularly when saturated with water.

Due to the theoretically free-draining nature of drystone walls, the build up of water pressures should not occur behind these structures. Even should the joints become saturated, provided there the contact is stone upon stone, there will be little or no difference to the friction angle. The presence of water only becomes problematic should the joints become infilled and a barrier is created to the water behind the wall. This may be due to a gradual soil infilling as previously described, or it may be due to a remedial measure such as pointing or grouting. In either case, there is the necessity for weepholes, to ensure that the water may effectively drain away before any pressures may build up. Over time, these weepholes will undoubtedly become infilled with soil and debris in the same manner as the joints, and so must be periodically inspected.

If water pressures are suspected to be building up, they may be accompanied by various phenomena. The seepage of water between cracks in the joints may start, particularly after heavy rainfall. Alternatively, patches of the wall may become wet to the touch, occurring in areas where the wall is impermeable. This may spread to a larger area as the water pressure builds up. Anecdotal evidence of this behaviour was seen at the Kwun Lung Lau wall failure[32]. In either case, the wall may be experiencing temporary increases in loads due to a build up of water pressure, which may be worsened by a respective lowering in the strength of the backfill. Walls such as these should ideally be temporarily shored and stabilised while more permanent measures are taken, e.g., the installation or clearing of weepholes, clearing of the wall joints or stabilisation of the retained fill.

8.3.4 Age, construction quality, weathering and voidage

Aging and weathering are not generally factors which are considered during the analysis of a structure. Despite this, they will likely affect how the wall will respond to the applied loads. The weathering of the wall is unavoidable, and as a consequence the individual stones will become eroded and their contact points reduced. The pins and wedges used to stabilise the wall blocks may also be washed away, further loosening the wall. It was identified through the full-scale tests of this project that this was a major cause of bulging, and so should be carefully considered for in-situ walls. Test walls 3 and 4 were built specifically to represent a wall which had undergone several years of weathering and aging. Therefore, they may be used as a direct comparison with walls such as test wall 1, which was built with much more care and attention, representative of a much newer wall which had not yet been subject to decay of any sort.

A consequence of aging and weathering in a wall is that the blocks are more rounded, and hence rotate much easier. In addition, the wall would have a much higher percentage of voids in the internal structure of the wall. These combine to allow the bulging deformations which we have often identified, as the stones roll and rotated to accommodate the loading conditions. Conversely a new wall may not contain stones with the ability to rotate, thereby disallowing bulging and instead causing more linear deformations. As the same effects were purposefully built into the test walls of this project, it should be noted that some in-situ walls may also display a similar level of workmanship so that these effects may also be identified much newer walls.

By studying this aspect of a wall, the mode of deformation and potential failure may be estimated. From the parametric study conducted in section 7.6, it is shown that the voidage on a wall has little effect on its theoretical stability. Therefore, an aged, weathered or more roughly built wall is not necessarily any less able to resist a particular load or retained height of fill than a much tightly constructed structure. Should both walls be loaded to their capacity, whilst the peak loads could be the same, the walls would respond in a different manner; the newer wall would likely topple linearly with potentially little warning, whilst the rougher wall would be much more ductile prior to failure. This ductile behaviour of the rougher wall is a distinct advantage for the inspection if in-situ walls, as the very small movements of the more monolithic walls are often very difficult to detect.

There is currently no proven non-destructive method for ascertaining the internal voidage of a wall. It is possible to take core samples of a wall, however this is not ideal for walls of questionable stability as the disruption could potentially instigate a collapse. The work described in section 3.4.4 is a potential avenue of exploration, as it allows an estimation of the internal voidage of a wall based on the condition of the external face. This work has some potential, although it would require a great deal more data before it could be properly validated. The initial

study conducted shows that there is correlation between the internal and external voidages for the samples tested. As discussed in section 3.4.4, this could be used for estimation purposes only, as there is the potential for a wall to have a well crafted external face masking a rougher and poorly built wall. Similarly, there would be issues in applying this correlation to a single faced wall, as it will likely not be representative.

Other non-destructive techniques for assessing the voidage of walls have yet to be thoroughly tested, although it may be possible to ascertain the internal geometry of a wall using temperature or radar-based technology to differentiate between the solid walling material and the voids.

8.4 Continuation of research

Despite the research which has been conducted to date, the understanding of drystone retaining walls is still incomplete. The relatively recent work recreating these walls either in physical or numerical tests has undoubtedly pushed the understanding forwards, however there are still no codes of practice for either drystone construction or repair. If the construction of new-build drystone walls are to be encouraged, and the repairs of walls suspected of instability are to be successfully carried out, these codes must be put in place, with more research conducted where necessary.

8.4.1 New build structures

For the construction of new build structures, there is now sufficient information available to justify a suitable code of practice. Currently, there are several approved documents which give detailed instructions for the construction of any size of structure (e.g., 'Pierre Seche'[13] and 'Dry stone walling: a practical handbook'[2]). In addition there are several bodies such as the Drystone Walling Association of Great Britain (DSWA), which have approved masons and further guidance on the construction of drystone walls. The limit equilibrium analysis package discussed in chapter 4 also has use in this respect, as it could allow the safety margins of a new build wall to be quickly assessed prior to construction. For larger or more critical structures, numerical work similar to that conducted by Harkness et. al.[8], Powrie. et. al.[23] or Walker et. al.[11] could be applied, giving sufficient data to ensure the stability of the construction. These existing guidelines and analysis methods could feasibly be combined to form a document which details the specifications for any new build.

As the construction industry becomes more responsible with regard to environmental concerns, the use of the drystone wall should be more often considered; these walls are an environmentally friendly construction form, and may also be comparatively cheap should the material be readily available. Certainly the current research

- such as that described in this thesis - demonstrates that these structures can be subject to analyses similar to any other construction form, and so can also be built in compliance with modern codes of practice with little difficulty.

Much of the work to date has focussed on the construction of limestone drystone walls, using roughly rectangular blocks. This project conducted a final full-scale wall using slate, yielding much different results to the limestone walls. Work of this nature should be continued, with walls of other materials and walling styles tested in a similarly thorough manner. This would be most profitable for the construction industry if the tests utilised commonly found drystone walling materials (such as other slates or granite), and varying walling styles such as herringbone or polygonal (as shown in figure 1-3).

8.4.2 Remedial works

The current methods available for attempting to repair or stabilise drystone walls are discussed in section 2.5.3. Each method has benefits and drawbacks, and it must be ensured that the correct procedure is chosen for each situation.

Although pointing or grouting of walls is a commonplace repair technique, its effectiveness must be questioned. It is often used as it is the quickest, cheapest and easiest method available, and in the short term may indeed halt any movements that have been noted. However in many cases, this will not be a permanent solution. The water pressure issues already mentioned will become problems which must be dealt with, and will require the additional task of installing weepholes. The issue of halting the deformations may also only be temporary, especially if the movements were instigated by gradually increasing load conditions (e.g., vegetation growth). The stresses in the structure will increase, and rather than deform and give indications of these pressures, the wall will remain in place until the collapse occurs suddenly and without warning.

Techniques such as nailing or anchoring through the wall may be effective in stabilising the whole structure. These methods are currently advertised by some companies for use with drystone walls (e.g., Cintec reinforcement anchors), although no full-scale tests under scientific conditions similar to those of this project have been reported.

A potential solution which is often overlooked is a simple reconstruction of the deformed section. By rebuilding the wall, no new material is required for the wall, and it may be the case that all is required is the elimination of a previously existing flaw. The wall geometry may also be altered if required, potentially making the wall thicker if the original stability was questionable. Alternatively, the fill being the wall could be stabilised using a variety of soil reinforcement techniques, with the wall being built mainly as a facing to this embankment. Again, the combination of these construction styles has not been tested, but they could offer long-term stability for a relatively low cost.

The recent Ciria guide guide written by O'Reilly and Perry[1] may be a useful document in terms of appraisal and repair as it discusses many of the factors which may be problematic within drystone walls. However, this focusses on collating the advice given by any relevant standards or codes of practice. There contains no specific guidance on the methodologies which should be adopted, and simply lists some of the options which may be applicable.

To further the use and sympathetic repair of existing drystone retaining walls, the various methods outlined in section 2.5.3 must be tested under scientific conditions. Ideally, these tests would be conducted in the same conditions as those described in this thesis. This would not only provide the required data regarding their effectiveness, but also allow a direct comparison against unstabilised walls. The existence of the outdoor drystone wall laboratory at the University of Bath would therefore be the ideal place to continue such experiments, as the site and equipment required are already in place.

The tests could potentially involve building the walls with the remedial works included when the wall is undeformed and unloaded. This would allow a direct comparison with the already conducted tests, and their effectiveness qualifiedly quantified. A perhaps more realistic series of tests could involve directly building off the procedures and results conducted as part of this thesis. As the in-situ walls in question are often deformed and bulged by the time that repairs and stabilisation are required, the initial stages of the wall tests described in chapter 6 could be repeated. In this way, a wall could be built in a traditional manner, then loaded until a bulged or deformed profile is induced. At this point the repair techniques could be attempted, and their effectiveness monitored. Such tests could then be directly compared with the wall tests of this thesis.

When repairing a drystone wall, the methodology for conducting the repairs may be as critical as the stabilisation technique itself. Introducing anchors or nails to a wall is a potentially disruptive technique, and if the stability is already in question, some method of resisting collapse during installation is required. This is further complicated by the presence of any bulges or deformation, rendering standard formwork and shoring to be inoperable, as they often require flat surfaces to be effective. To this end, this particular aspect of the repair must also be attended to, so as to ensure stability and safety during the repair as well as after.

8.4.3 Theoretical and numerical analyses

Despite the apparent longevity of drystone construction, the assessment of these structures using modern analysis techniques may often lead to their stability being questioned. However, as discussed in previous chapters, this is not necessarily due to an incorrect analysis method. For most of the assessments made throughout this thesis, a static equilibrium approach has been used to identify and understand much of the observed wall behaviour. Despite this, these same basic principles may

lead to similar in-situ walls being classified as structurally unsafe by practicing engineers. This is partly due to the application of excessive safety factors, particularly when compared to those likely used when the wall was originally constructed. It may also be due to a lack of understanding regarding the critical parameters relating to wall stability. An engineer may have detailed knowledge regarding the unit weight of the structure, but little or no information relating to the backfill. Crucial information - such as the angle of friction of the backfill and the interface friction between the wall and the fill - may be assumed rather than tested, leading to large inaccuracies as to the overall stability of the structure.

With more physical data now available to prove the effectiveness of any theories or methodologies, more efficient and realistic analysis techniques may be employed. However, there is still a need for the continuation of a full-scale drystone test program, covering other walling materials and investigating the effectiveness of the remedial measures previously identified. With this work, so must the development of analysis and assessment techniques also be continued. Whilst tools such as the limit equilibrium program (chapter 4) or the numerical tools such as UDEC are extremely useful, they still have room for improvement. In particular, the three-dimensional aspects of the wall have been shown to effect the overall behaviour, but are not fully explored by either of the existing packages.

A particular drawback of the limit equilibrium package is that it cannot automatically predict the movements that will occur in response to a given load. This is a potential avenue of continuation research which would greatly benefit the use and applications of the program. In a similar vein, further work is also required of the available numerical packages, creating more realistic wall models, incorporating not just the large, blocky elements but also the voids that exist between them, and potentially some of the pins which hold the blocks in place. These factors are also being investigated by the three-dimensional numerical package under development by John Harkness (as mentioned in section 8.2).

As more physical testing is conducted, it is important that the simple static equilibrium and the more complex numerical packages both progress in tandem. As previously discussed, each is extremely useful for design and analysis applications, with the correct tool being chosen for each situation as size, scale and importance of the structure dictates.

Chapter 9

Conclusions

The main aims of this project were to gain an understanding of the behaviour of drystone retaining walls, specifically regarding those phenomena which relate purely to this construction medium (e.g., bulging and block sliding). These were to be achieved through a series of four full-scale tests, conducted in a bespoke outdoor laboratory. A series of additional tests were scheduled to gather the data necessary to fully investigate these structures. From this research would stem new methods of analysis, which would be verified against the physical data generated. These methods were aimed at being applicable for drystone walls of any shape, size, material or age, and so had to be flexible and quicker to use than the current available numerical packages. These goals were all met and in some cases exceeded.

9.1 Chapter 3: Laboratory testing

Throughout the thesis, various laboratory studies have been conducted, described in chapter 3. These include measurements of the various materials' properties, the interaction between a wall and backfill, and investigations into the voids within typical drystone walls. Also detailed were a series of small-scale tests which attempted to recreate the behaviour of the full-scale walls.

The initial tests obtained the mechanical properties of the limestone, slate and the aggregate for the backfill. The results obtained where within the generally within the expected standard ranges of values for each material, with the exception of the Mort slate. The Mort slate had a particularly low compressive strength, being in the range of values normally associated with a shale. The interaction between a limestone face and an aggregate backfill was recreated in a 300mm x 300mm shearbox, giving a peak friction angle for this interface. Despite being difficult to measure for in-situ walls, this angle of friction is particularly critical, as it determines how the forces from the backfill will affect a wall. From this laboratory test, much greater confidence could be given in the subsequent analyses of the full-scale tests.

From a series of wall sections built by the project masons, a range of possible values for the percentage of internal voids was obtained. The data indicated that this could vary by a large amount, given the construction quality and age of a wall. However, repeat testing indicated that a minimum value for the percentage of these voids was approximately 21% - a much higher value than originally anticipated by the project masons. This could increase to over 50%, given a sufficiently loose material with little consideration given to the interlock of the blocks. Again, this information is difficult to obtain for in-situ walls, and would normally require intrusive testing. To attempt to reconcile this data with the external quality of any given wall, the percentage of visible cracks and joint spaces on the face of each of the sections tested was measured, and correlated with their internal voidages. For these data, it was found that there was indeed a linear correlation between the percentage of joint space visible on the external face and the internal voidage. It should be noted that this only holds true for the limestone walls tested, and may not always be accurate depending on the style of the wall (see section 3.4.4). However, with further testing this method could potentially be a useful tool for engineers, as it would allow an estimation to be made on the internal voidage of a wall with very little difficulty. As previous explained in section 7.6, the voidage of a wall requires a large change to affect the stability of a wall, and so an estimation of this parameter may often be sufficient.

A series of small-scale tests, consisting of concrete wall blocks and a backfill comprised of small lead pellets was conducted with mixed success. The tests themselves were successful, and were particularly useful in validating the limit equilibrium program (section 4.8). However, as the small-scale walls were heavily simplified, mechanisms such as bulging and bursting were not easily reproduced, instead tending towards overturning failures as a primary means of collapse.

9.2 Chapter 4: Limit equilibrium program development and verification

Chapter 4 introduced the limit equilibrium program and outlined its use. This tool allows almost instantaneous evaluation of any wall geometry, constructed and backfilled with any material. In line with the project goals, this program is extremely flexible and simple to use, being ideal for use even when assessing small walls or structures. The program was initially validated using previous physical test results from a broad variety of sources, including the small-scale tests described in section 3.3.

As it was primarily developed to allow the rapid appraisal of a wall, it did not always give perfect agreement with the observed behaviour, although the error was within an acceptable margin in all instances. It should be noted that due to the bespoke nature of drystone walls, an analysis tool which could perfectly predict the

behaviour of any wall would have to correctly model each block, pin and wedge, and would be wholly impractical. The limit equilibrium program makes several generalisations, however the important criteria are represented as accurately as possible. This allows not only the correct prediction of the maximum backfill height for the wall geometry entered, but also the manner in which a wall will fail.

As discussed in chapter 8, the program could potentially be adjusted to incorporate three-dimensional effects, thereby increasing its accuracy and decreasing its conservativeness. Other factors such as pore water effects could potentially be included, as the program was written with the intention of allowing such modifications.

9.3 Chapter 5: Design and development of full-scale test laboratory

The outdoor test laboratory was successfully designed and constructed, incorporating all of the required functionality and flexibility (imitation of foundation settlement, localised surcharging etc). As the test procedure and requirements of the latter tests were not fully determined until after the completion of the first walls, the laboratory required the flexibility to ensure that should much larger walls or surcharges be required, they could be tested safely. This was done by initially designing the site to accommodate walls and surcharges much much larger than anticipated (i.e., wall thickness of 1m and surcharges up to 200kN). As the tests did not eventually require such measures there was a relatively large degree of redundancy in the capacity of the site. However, this ensured that there was never any danger of the components failing unexpectedly, and also gives a large amount of flexibility for any future tests which may utilise the test laboratory.

The instrumentation used to monitor each test also progressed along with the walls themselves. The methods initially used to gather data from the tests were quickly superseded, as the best use of instruments such as the draw wire transducers became understood. The final tests gave large quantities of useful data, as each piece of equipment was placed in the most efficient manner. In particular, the use of buried ball bearings within the backfill was replaced by simple flexible pipes, which could be used with a mandrel to locate the presence of a failure plane. Draw wire transducers were also used heavily in later walls, allowing the instantaneous measurement of the wall profile without excessive danger of damage to the equipment. This superseded the use of the Total station in many respects, although the draw wires were not used to obtain any vertical movements of the external face, hence both were used throughout the later tests.

In terms of the costing of this particular project, it was important that it did not exceed the original budget as raised by the EPSRC. This aspect of the project was also successful, as the total cost of the project was within the budget, in addition

to incorporating an extra full-scale test.

9.4 Chapter 6: Full-scale test proceedings

The tests themselves explored many of the particular characteristics of in-situ wall behaviour, and as new understanding was gained from the deformation and collapse of each wall, the following test was adjusted accordingly. The first test wall failed almost purely by toppling from the base, and the large deformations were due to the structure rotating rather than bulging. In addition, the wall was not acting in a two-dimensional manner, as the wing walls were evidenced to be supporting the central section to some degree.

In an attempt to create a more flexible structure, the second wall was much thinner, and subsequently had a lower factor of safety prior to the application of the surcharging force. The deformations during testing were much different to the first wall, and although the failure was eventually rotational, it was due to a different mechanism, whereby one or more stones above the base level had shifted to a point where they were no longer stable and fell out of the wall. At the time the wall as a whole was stable (although only marginally), and the failure of these individual stones caused the rest of the structure to collapse as the foundations for the upper sections became undermined.

The limestone full-scale tests culminated in the third wall, which successfully demonstrated a stable bulge before collapsing via bursting. This was done by reverting to a wall of the same proportions as the first, but with a much looser internal configuration to encourage the rotation and movement of individual stones. To ensure that this was a repeatable phenomenon, the fourth wall was a repeat of the third wall, and again a stable bulge was developed.

Overall, the progression of the individual limestone walls highlighted the general progression of the understanding regarding drystone construction. The initial failure was one which could be observed in any monolithic gravity retaining wall, which was followed by a wall test which partially bulged and collapsed in a slightly more complicated manner. The third and fourth tests were based the accumulated data at that point, including the full-scale tests and also the laboratory tests. The voidage tests indicated that drystone walls could contain much higher voids than originally anticipated, whilst information from the second test highlighted the importance of block rotation in wall behaviour. These were combined, and the walls were built of a geometry which would better resist overturning (i.e., wider at the base), but with a rough build quality with an internal configuration which would promote individual block rotation. The resulting bulges of walls 3 and 4 proved the validity of these assumptions.

As there was the available time, materials and funding available, an additional fifth test was conducted. This utilised slate for the central section of the wall, and

was predicted to behave in a different manner due to its mechanical properties. By contrast to the limestone walls, wall 5 was built of a material which was inherently more likely to fail by sliding, as well as having individual geometries less amenable to rotation (the slates were flat and plate-like, as opposed to the much rounder and taller limestone blocks). The results were as predicted, and the wall failed almost purely by sliding, with very little observed block rotation.

9.5 Chapter 7: Analysis of full-scale tests

Chapter 7 analysed the data obtained from each of the full-scale tests in conjunction with both the laboratory tests and the limit equilibrium program. The underlying reasons behind the deformations for each of the walls were explained using these data, as well as comparing the results with the predicted failure modes from the limit equilibrium program. The results were remarkably close, with the correct modes of failures given in each case.

In addition to using the limit equilibrium program to assess the stability of the full-scale wall tests, it was also used to conduct a parametric study to highlight which parameters are critical to wall stability. It was determined that whilst changes in factors such as the unit weight of the backfill or wall will not have a large effect on overall stability. Conversely, the angle of friction of the backfill and the associated friction angle between the wall and fill can have substantial effects on the stability of the wall with only minor alterations.

A further use for the program was to investigate the mechanism of bulging from a theoretical point of view. It was proven using the limit equilibrium package that a bulged profile does not necessarily reduce the overall stability. Whilst excessive bulging will undoubtedly reduce a wall's stability, it has been proven that a bulge to a certain extent may even in some cases increase the safety factor against collapse. This has many implications for existing walls, as currently, bulges are regarded as deficiencies in a structure, even should no movements be recorded in their recent history.

Finally, the bulged profiles of the full-scale tests were compared to deformed in-situ walls of similar heights and thicknesses, which were measured using the project Total Station. It was found that the bulges demonstrated by the test walls were almost identical to the in-situ walls, proving that the behaviour of the project walls was indeed representative of existing walls. This gives confidence in the results of the tests themselves, but also in the theories and analyses which have been drawn out of them.

9.6 Chapter 8: Discussion of results

Chapter 8 is a summation of the findings from this project and their relevance to the construction industry. This includes the use of the limit equilibrium package for analyses of in-situ walls, and an appraisal of the current methodologies which may be adopted for their inspection and repair. The guidance for inspections includes identification of those phenomena usually advocated for drystone walls, i.e., cracking and settlement, bulging, weathering and the growth of vegetation. In addition, the data from the full-scale and laboratory tests, as well as historical reports, are used to explain the underlying reasons for the importance of identifying these occurrences.

An outline for continuation studies are also given, as further work is required before drystone construction may be fully understood. This consists of more full-scale tests in addition to advancing the theoretical methods already established. As the mechanisms behind commonly-observed behaviour such as bulging are now better understood and can be recreated in physical tests, the repair and stabilisation of substandard walls must be investigated. In tandem with this, analysis tools such as the limit equilibrium program and the available numerical packages should be further explored and refined, allowing them to incorporate more factors such as three-dimensional effects, as well as potentially assessing the effectiveness of various repair techniques (to be verified with the proposed full-scale tests).

9.7 Summary of objectives

In chapter 1, a series of objectives were set out. Each of these objectives were met and in many cases exceeded, as detailed in the following summary:

- Design and build a bespoke test facility with capable of housing full scale drystone walls and a retained fill. The laboratory should be designed to allow a variety of tests to be performed, allowing flexibility in the testing regime. Future use of the test laboratory beyond the scope of this project should also be considered.

The test facility was constructed with the capability to house the required full-scale test walls and the relevant test procedures. When required, the test procedure was able to be modified without being restricted by any site constraints. The site was constructed within the proposed budget, allowing for the purchasing of additional materials and equipment.

- Conduct four full-scale tests, recreating commonly observed phenomena relating to drystone retaining walls (e.g., bulging, sliding, bursting etc.).

The four programmed full-scale tests were completed within the time-frame of the project, with the each progressive test demonstrating a greater understanding

of drystone wall behaviour. Drystone-specific behaviour such as stable bulging was exhibited, followed by progressive loading until failure occurred.

Due to the site construction phase being under-budget, there was funding available to conduct a fifth wall. This fifth test utilised slate as a primary building material, and as such effectively expanded the overall scope of the project.

- Carry out laboratory testing in parallel to the full-scale testing. This should focus on the material properties relevant to the full-scale tests (e.g., material densities, friction angles etc.).

Several laboratory tests were conducted, giving many of the critical parameters required for the effective analysis of a drystone wall. Additional experiments that were not included within the initial scope of works were also conducted. These included the voidage test blocks, the stone/backfill interface shearbox tests and the voidage determination via external face photographs. These experimental avenues were a result of either observations during testing or from later analyses, and each gave substantial insights into drystone behaviour.

- Develop an analysis package to allow stability assessments of drystone retaining walls. This will likely be based on the code originally written by McCombie as part of the work reported by Walker et. al.[11]. This program is intended to be used by design engineers to carry out rapid stability analyses of in-situ walls, and so should be flexible and easy to use. This program is to be updated and validated as the full-scale tests progress, incorporating any observed phenomena where possible.

The limit equilibrium package was developed throughout the course of the project, incorporating several new sub-routines. These mainly stemmed from observed full-scale behaviour, allowing the model to be much more realistic and account for several phenomena specific to drystone walls. This includes the ability to chamfer the wall segments (indicative of an aged and weathered wall), as well as check the stability of individual blocks on the external face. The program was modified to output specific factors of safety against overturning and sliding at each level, with the option of inclining the bedding planes to assess its impact. Different surcharge models were also tested, again comparing the program output with the observed wall behaviour.

The overall validity of the package was given by recreating the physical test data available within the program environment. It was found that the program would successfully indicate failure in line with the observed physical tests, as well as in many cases predicting the correct mode of failure.

As initially stated within the objectives, the program was to be rapid and user-friendly. The package remains a Delphi-coded program, and provides results almost instantaneously. Walls of any size, material and geometry may be entered, with

any unknown parameters set to default values, allowing the program to run even with only basic information provided. The output is both numerical and graphical, allowing the user to ascertain the overall stability and the critical factors in quickly and easily.

- Combine each of the above objectives to further understanding of the behaviour of drystone walls. This should draw upon data and observations gathered throughout the various tests, as well as using the validated analysis package to confirm these findings. This should include investigating the mechanisms behind the phenomena particular to drystone walls (e.g., bulging and bursting), as well as the important criteria that should be considered when investigating the stability of these structures.

Through the analysis of the gathered data, the mechanisms behind many aspects of drystone wall behaviour have been assessed. Out of this work, new methods for analysing these structures have been proposed. These incorporate the data from the full-scale tests and the laboratory data, also using the limit equilibrium package where appropriate. The phenomenon of bulging has been linked to block rotation and the build quality of the wall, giving a much greater insight as to why some walls will exhibit substantial deformations and others will not. Other analyses have provided the data to determine which aspects of a wall and its retained fill are critical, such as the wall/backfill friction angle, or the friction angle of the backfill itself.

The gathered data has also been used to assess the practicality and effectiveness of current inspection and repair techniques. As each of the test walls approached its collapse condition, several visible phenomena were evident. These included crack propagation, block rotation, bulging, sliding and backfill settlement. Having documented these occurrences, should they be identified along in-situ walls, their relative importance are now better understood. More importantly, much more is known regarding the mechanisms that cause such actions to take place, potentially allowing the overall stability to be assessed with more certainty. The importance of determining whether or not the movements or cracks are progressive was also highlighted. This is a factor which may cause many stable walls to be unnecessarily replaced; It has been found that newly built drystone walls will often deform and move when they are first loaded. This has proved not to be indicative of failure, but more an initial 'settling in' period, after which it is possible that the wall will not exhibit any further movements. Therefore, the presence of a distinct bulge or rotation may not necessarily be indicative of an imminent failure. However, these should not be ignored, but rather monitored to assess if such movements are continuing or have long since ceased.

In terms of current repair techniques, methods such as pointing or grouting may achieve short-term stability, however the risk of a build up of water pressures

cannot be ignored. The use of drainage may help to prevent this, although these measures are likely to become fouled over time, requiring additional maintenance. Soil nailing or ground anchors are also sometimes used to stabilise potentially unsafe walls, although due to a lack of testing in conjunction with drystone walls, the effectiveness of these are uncertain. Despite these, these are undoubtedly potentially viable solutions, giving support to the retained fill in addition to anchoring the wall itself.

9.8 Concluding remarks

It may be concluded that this work clearly demonstrates that these structures can be accurately analysed using simple, well established theories. Drystone walls are often misconceived to be existing on the point of collapse, but with the correct approaches their stability can be determined just as for any other structure. Found throughout the UK and all over the world, these walls are a visible part of our heritage. As such, this traditional building material should not be lost but revitalised, with new builds and sympathetic restorative techniques being encouraged. This may only happen once the correct guidance is in place, which in turn requires that the knowledge gained from this project is expanded upon and the work continued. To date, the research conducted regarding drystone walls has focussed almost entirely upon analysing stability and assessing the mechanisms behind their failure. The attention must now shift towards the various retrofitting and investigative techniques. The causes of the deformations and collapse modes are better understood, however the correct responses to these movements must be determined. Given the knowledge obtained from the project data, and the presence of a suitable site already developed to test full-scale walls, this work is now at a stage where it can commence, given the appropriate funding. Once this has been achieved, drystone walling will then potentially be in a position where it may be reintegrated back into the modern construction industry.

References

[1] M. O'Reilly and J. Perry, "Drystone retaining walls and their modifications - condition appraisal and remedial treatment," 2009.

[2] A. Brooks, S. Adcock, and E. Agate, "Dry stone walling: a practical handbook," 1999.

[3] G. Timmins, "Techniques of easing road gradients during the industrial revolution: a case study of textile lancashire," *Industrial archaeology review*, vol. 25, no. 2, pp. 97–117, 2003.

[4] T. Aitken, *Road making and mainteinance*. Charles Griffin and Company, Ltd., 1900.

[5] M. O'Reilly and D. B. adm K.C. Brady amd W. Powrie, "The stability of drystone retaining walls on highways," *Proc. Instn. Civ. Engrs. Mun. Engr.*, vol. 133, no. June, pp. 101–107, 1999.

[6] C. Jones, "The maintenance of old masonry retaining walls," in *Proceedings of the conference of retaining structures*, 1993.

[7] M. Claxton, R. Hart, P. McCombie, and P. Walker, "Rigid block distinct-element modelling of drystone retaining walls in plane strain," *ASCE*, vol. 131, no. 3, pp. 381–389, 2005.

[8] R. Harkness, W. Powrie, X. Zhang, K. Brady, and M. O'Reilly, "Numerical modelling of full-scale tests of drystone masonry retaining walls," *Geotechnique*, vol. 50, no. 2, pp. 165–179, 2000.

[9] C. Jones, "Current practice in designing earth retaining structures," *Ground Engineering*, vol. 12, no. 6, pp. 40–45, 1979.

[10] M. O'Reilly, K. Brady, and D. Bush, "Research on masonry-faced retaining walls," in *Second European road research conference*, 1999.

[11] P. Walker, P. McCombie, and M. Claxton, "Plane strain numerical model for drystone retaining walls," *Geotechnical engineering*, vol. 159, no. GEI, pp. 1–7, 2006.

[12] J. Burgoyne, "Revetments or retaining walls," *Corps of royal engineers*, vol. 3, pp. 154–159, 1853.

[13] CAPEB, ABPS, M. de Provence, CBPS, C. 84, and ENTPE, *Pierre Seche - guide de bonnes practiques de construction de murs de soutenement*. ENTPE, 2008.

[14] B. Villemus, J. Morel, and C. Boutin, "Experimental assessment of drystone retaining wall stability on a rigid foundation," *Engineering structures*, vol. 29, pp. 2124–2132, 2007.

[15] A. Colas, J. Morel, and D. Garnier, "Yield design of dry-stone masonry retaining structures-comparisns with analytical, numerical, and experimental data," *International journal for numerical and analytical methods in geomechanics*, vol. 32, pp. 1817–1832, 2008.

[16] C. Constable, "Retaining walls-an attempt to reconcile theory with practice," *American society of civil engineers*, vol. 3, pp. 67–75, 1875.

[17] C. Coulomb, "Essai sur une application des regles des maximis et minimis a quelquels problemesde statique relatifs, a la architecture," *Memoirs Divers Savants, Academie Science*, vol. 7, 1776.

[18] M. Cooper, "Deflections and failure modes in drystone retaining walls," *Ground engineering*, vol. 19, no. 8, pp. 28–33, 1986.

[19] A. Arya and V. Gupta, "Retaining wall for hill roads," in *Journal of Indian road congress*, pp. 291–326, 1983.

[20] C. Mundell, "Limit equilibrium analysis of drystone retaining walls," MEng final year dissertation, University of Bath, 2006.

[21] P. Cundall, "A computer model for simulating progressive, large-scale movements in blocky rock systems," in *Symposium soc. internat. mecanique des roches*, 1971.

[22] J. Dickens and P. Walker, "Use of distinct element model to simulate behaviour of drystone walls," *Structural engineering review*, vol. 8, no. 2/3, pp. 187–199, 1996.

[23] W. Powrie, R. Harkness, X. Zhang, and D. Bush, "Deformation and failure modes of drystone retaining walls," *Geotechnique*, vol. 52, no. 6, pp. 435–446, 2002.

[24] X. Zhang, N. Koutsabeloulis, S. Hope, and A. Pearce, "A finite element analysis for the stability of drystone masonry retaining walls," *Geotechnique*, vol. 54, no. 1, pp. 57–60, 2004.

[25] P. Walker and J. Dickens, "Stability of medieval drystone walls in Zimbabwe," *Geotechnique*, vol. 45, no. 1, pp. 141–147, 1995.

[26] G. Molesworth, *Useful formulae & Memoranda*. E & F N, 1876.

[27] J. Trautwine, *The civil engineers pocket-book*. John Wiley & Sons, 1895.

[28] R. Tufnell, *Building and repairing dry stone walls*. Dry Stone Walling Association, 2004.

[29] British standards institution(BSI), *Grounds maintenance - recommendations for the maintenance of hard areas*, 1994.

[30] Roads Liaison Group, *Management of highway structures*, 2005.

[31] The Highways Agency, *Inspection manual for highways structures*, 2007.

[32] H. Wong and K. Ho, "The 23 July 1994 landslide at Kwun Lung Lau, Hong Kong," *Canadian geotechnical journal*, vol. 34, pp. 825–840, 1997.

[33] P. Whyley, "Soil nailing - a practical solution," *Construction repair*, pp. 8–11, September/October 1996.

[34] Cotswold natural stone Ltd., "http://www.cotswoldnaturalstone.co.uk," 2009.

[35] B. Villemus, *Etude des murs de soutenement en maconnerie de pierres seches*. PhD thesis, L'Institut National des Sciences Appliquees de Lyon, 2004.

[36] P. Atwell and I. Farmer, "Principles of engineering geology," 1976.

[37] G. Readshaw, "Determining shear behaviour of dense gravel," MEng final year dissertation, University of Bath, 2008.

[38] C. Bailey, "Model tests of drystone retaining walls," MEng final year dissertation, University of Bath, 2008.

[39] British standards institution(BSI), *Code of practice for strengthened/reinforced soils and other fills*, 1995.

[40] M. Bolton, "Geotechnical stress analysis for bridge abutment design," 1991.

[41] British standards institution(BSI), *Code of practice for earth retaining structures*, 1994.

[42] J. Corte, "Reinforced earth retaining walls under strip load: Discussion," *Canadian geotechnical journal*, vol. 18, pp. 324–326, 1981.

[43] J. Boussinesq, *Application des potentials à l'étude de l'équilibre et du mouvement des solids elastiques*. Gauthier-Villars, 1885.

[44] K. Terzaghi, *Theoretical soil mechanics.* John Wiley and sons, New York, 1943.

[45] G. Barnes, *Soil mechanics: principle and practice.* Macmillan Press ltd, 1995.

[46] B. Hansen, "A revised and extended formula for bearing capacity," *Danish Geotechnical Institute, Copenhagen*, no. Bulletin No. 28, pp. 5–11, 1970.

Appendix A

Limit equilibrium analysis verification

Variables:

$\alpha = 90^o$
$\phi = 28^o$
$\delta = 30^o$
$\beta = 0^o$
$\gamma_{soil} = 18kN$
$\gamma_{stone} = 20kN$

Coefficient of active pressure, K_a:

$$K_a = \left[\frac{\sin(\alpha - \phi)/\sin(\alpha)}{\sqrt{\sin(\alpha + \delta)} + \sqrt{\frac{\sin(\phi+\delta)\sin(\phi)}{\sin(\alpha)}}} \right]^2$$

$$K_a = \left[\frac{\sin(90 - 28)/\sin(90)}{\sqrt{\sin(90 + 30)} + \sqrt{\frac{\sin(28+30)\sin(28)}{\sin(90)}}} \right]^2 = 0.32$$

Forces on the wall due to active soil pressures:

$$P_a = 0.5\gamma_{soil} K_a H^2$$

$$P_a = 0.5 \times 18 \times 0.32 \times 2^2 = 11.52kN$$

$$P_{a_H} = 11.52 \cos 30 = 10.0kN$$

$$P_{a_V} = 11.52 \sin 30 = 5.8kN$$

Moments due to active pressures:

$$Overturning = 10 \times 2 \times \frac{1}{3} = 6.7kNm$$

$$Restoring = 5.8 \times 0.5 = -2.9kNm$$

Forces and moments due to self weight:

$$Self weight = 2 \times 0.5 \times 20 = 20kN$$

$$Restoring moment = 20 \times \frac{0.5}{2} = -5kNm$$

Loads and moments due to surcharging:

At 1m depth, surcharge area has spread from 1m x 1m square to a 2m x 2m square.

$$P_1 = \frac{10}{2 \times 2} = 2.5kNm^{-2}$$

$$F_{H1} = 2.5 \times 0.32 \times \cos 30 = 0.69kN$$

$$F_{V1} = 2.5 \times 0.32 \times \sin 30 = 0.40kN$$

At 2m depth, surcharge would have naturally spread to a 3m x 3m square. However as the area has intruded into the wall by 0.5m, the area spread is 3 x 2.5m.

$$P_2 = \frac{10}{3 \times 2.5} = 1.33 kNm^{-2}$$

$$F_{H2} = 1.33 \times 0.32 \times \cos 30 = 0.37 kN$$

$$F_{V2} = 1.33 \times 0.32 \times \sin 30 = 0.21 kN$$

The horizontal, vertical and moment forces are then calculated and summated:

$$\sum F_H = (0.37 \times 1) + [(0.69 - 0.37) \times 1 \times 0.5] = 0.53 kN$$

$$\sum M_H = (0.37 \times 1 \times 0.5) + [(0.69 - 0.37) \times 1 \times 0.5 \times 0.67] = -0.29 kNm$$

$$\sum F_V = (0.21 \times 1) + [(0.40 - 0.21) \times 1 \times 0.5] = 0.30 kN$$

$$\sum M_V = (0.21 \times 1 \times 0.5) + [(0.40 - 0.21) \times 1 \times 0.5 \times 0.5] = -0.15 kNm$$

Summation of all forces

$$\sum M = 6.7 + 0.29 - 2.9 - 5 - 0.15 = -1.08 kNm$$

$$\sum V = 5.8 + 20 + 0.30 = 25.90 kN$$

$$\sum H = 10 + 0.53 = 10.53 kN$$

Location of the eccentricity at the base height:

$$x = \frac{-\sum M}{\sum V} = \frac{1.08}{25.9} = 0.042m$$

Appendix B

Test site design & construction

B.1 Groundworks and rammed earth wall construction

Figure B-1: Test site prior to construction

Figure B-2: Initial groundworks

Figure B-3: Construction of drystone retaining wall using excavated material

Figure B-4: Completed drystone retaining wall

Figure B-5: Secondary groundworks and formwork erection

Figure B-6: Formwork and reinforcement cage

Figure B-7: Reinforcement cage for radial beam

Figure B-8: Formwork for radial beam

Figure B-9: Concrete pour via pump truck

Figure B-10: Finished concrete pour

B.2 Rammed earth wall construction

Figure B-11: Erection of shuttering for rammed earth construction

Figure B-12: Shuttering corner detail

Figure B-13: Completed section of shuttering

Figure B-14: Deposition of material for compaction

Figure B-15: Earth compaction using pneumatic rammer

Figure B-16: Completed section of rammed earth wall

Figure B-17: Rammed earth wall with lime mortar coping

Figure B-18: Erection of surcharging frame

Figure B-19: Formwork for platform seating area

Figure B-20: Completed concrete works (view 1)

Figure B-21: Completed concrete works (view 2)

Figure B-22: Completed concrete works (view 3)

B.3 Platform installation

Figure B-23: Transfer of platform to site

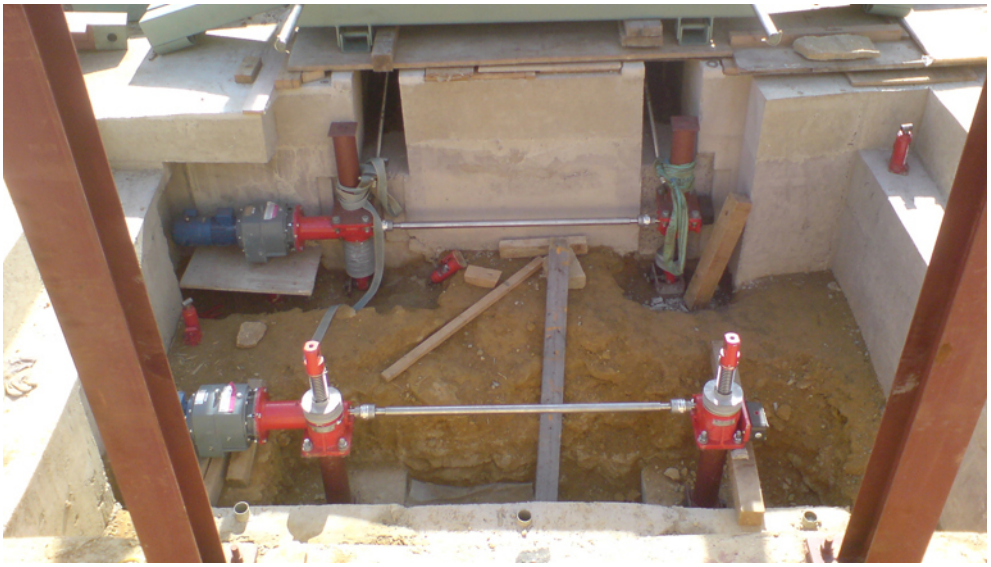

Figure B-24: Jack and motor setup

Figure B-25: Platform placement using chain pulleys

Figure B-26: Platform positioned and attached

Figure B-27: Platform with rubber seals and steel grid flooring